RELEVANCE OF SURVIVIN ACETYLATION FOR ITS BIOLOGICAL FUNCTION

Dissertation

zur Erlangung des Doktorgrades

Dr. rer. nat. der Fakultät für Biologie

an der Universität Duisburg-Essen

vorgelegt von

Britta Unruhe

aus Dortmund

Oktober 2014

Die der vorliegenden Arbeit zugrunde liegenden Experimente wurden am Zentrum für medizinische Biotechnologie in der Abteilung für Molekularbiologie II der Universität Duisburg-Essen durchgeführt.

1. Gutachter: Prof. Dr. Shirley Knauer

2. Gutachter: Prof. Dr. Peter Bayer

3. Gutachter: -

Vorsitzender des Prüfungsausschusses: Prof. Dr. Michael Ehrmann

Tag der mündlichen Prüfung: 04.12.2014

Table of Contents

List of Abbreviations

µ	micro
A	Ampere
aa	Amino acid
AcK	Acetylated lysine
AIF	Apoptosis-inducing factor
Ang-1	Angiopoietin 1
APAF-1	Apoptotic protease activating factor 1
APC/C	Anaphase-promoting complex/cyclosome
approx.	approximately
APS	Ammonium persulfate
ASEB	Acetylation set enrichment-based
ATM	Ataxia telangiectasia mutated
ATP	Adenosine triphosphate
ATR	Ataxia telangiectasia and Rad3-related protein
AurB	Aurora kinase B
BIR	Baculovirus IAP repeat
BRCA1/2	Breast cancer type 1/2 susceptibility protein
BSA	Bovine serum albumin
BUB1	Budding uninhibited by benzimidazoles 1
c	centi
c-IAP	Cellular inhibitor of apoptosis protein
CAK	CDK-activating kinase
Carb	Carbenicillin
CARD	Caspase recruitment domain
CBP	CREB-binding protein

CD ..... Circular dichroism
CDC2 ..... Cell division control protein 2 homolog
CDC6 ..... Cell division cycle 6
CDK1 ..... Cyclin-dependent kinase 1
CDKI ..... CDK inhibitor
Chk ..... Checkpoint kinase 1
CHMP4 ..... Charged multivesicular body protein 4C
CK2 ..... Casein kinase 2
Co-IP ..... Co-immunoprecipitation
CRM1 ..... Chromosome region maintenance 1
CSF-1 ..... Colony stimulating factor 1
CTD1 ..... Chromatin licensing and DNA replication factor 1
CXCL12 ..... C-X-C motif chemokine 12
Da ..... Dalton
deg ..... Degree
DIABLO ..... Direct IAP-binding protein with low pI
DMEM ..... Dulbecco's Modified Eagle Medium
DNA ..... Deoxyribonucleic acid
DNMT1 ..... DNA (cytosine-5)-methyltransferase 1
dNTP ..... Deoxynucleotide triphosphate
DPBS ..... Dulbecco's Phosphate-Buffered Saline
dsDNA ..... Double stranded desoxyribonucleic acid
DTT ..... Dithiothreitol
ECM ..... Extracellular matrix
ECT2 ..... Epithelial cell-transforming 2
EDTA ..... Ethylenediaminetetraacetic acid
EGF ..... Epidermal growth factor
EGFR ..... Epidermal growth factor receptor
ER ..... Endoplasmic reticulum
FCS ..... Fetal calf serum
FGF2 ..... Fibroblast growth factor 2
G ..... Gap
GAPDH ..... Glyceraldehyde-3-phosphate dehydrogenase
Gcn5 ..... General control of amino acid synthesis protein 5

GFP ..... Green fluorescent protein
GNAT ..... GCN5-related N-acetyltransferase
GSH ..... Glutathione
GST ..... Glutathione S-transferase
h ..... hour
HA ..... Hemagglutinin
HBXIP ..... Hepatitis B X-interacting protein
Hda1 ..... Histone deacetylase 1
HDAC1 ..... Histone deacetylase 1
HEAT ..... Huntingtin, elongation factor 3, protein phosphatase 2A, and the yeast kinase target of rapamycin kinase 1
HeLa K ..... HeLa Kyoto
hFAM ..... Fat facets in mammals
HGF ..... Hepatocyte growth factor
Hh ..... Hedgehog
HP1 ..... Heterochromatin protein 1
HRP ..... Horseradish peroxidase
Hsp ..... Heat shock protein
IBM ..... IAP-binding motif
IL-1β ..... Interleukin 1β
ILP2 ..... Inhibitor of apoptosis-like protein 2
INCENP ..... Inner centromere protein
INM ..... Inner nuclear membrane
IP ..... Immunoprecipitation
IPTG ..... Isopropyl β-D-1-thiogalactopyranoside
k ..... kilo
Kan ..... Kanamycin
KMN KNL1-MIS12-NDC80
KNL1 ..... Kinetochore-null protein 1
L ..... liter
LB ..... Luria-Bertani
LC ..... Liquid chromatography
LMB ..... Leptomycin B
M ..... Mitosis

M ..... mol/liter
m ..... meter
m ..... milli
MAD ..... Mitotic arrest deficient 1-like protein
MCAK ..... Mitotic centromere-associated kinesin
MCC ..... Mitotic checkpoint complex
MCM ..... Mini-chromosome maintenance
MEM ..... Minimal essential medium
MgcRacGAP ... Male germ cell RacGAP
MIS12 ..... Mum2p-Ime4p-Slz1p
MKLP2 ..... Mitotic kinesin-like protein 2
MMP-9 ..... Matrix metalloproteinase-9
MPS1 ..... Metallopan-stimulin 1
MYST ..... Moz, Ybf2/Sas3, Sas2 and Tip60
n ..... nano
NAD ..... Nicotinamide adenine dinucleotide
NAIP ..... Neuronal apoptosis inhibitory protein
NCBI ..... National Center for Biotechnology Information
NDC80 ..... Nuclear division cycle 80
NE ..... Nuclear envelope
NEBD ..... Nuclear envelope break down
NES ..... Nuclear export signal
NLS ..... Nuclear localization signal
NP40 ..... Nonidet P40
NPC ..... Nuclear pore complex
Nup ..... Nucleoporin
ONM ..... Outer nuclear membrane
ORC ..... Origin recognition complex
PAGE ..... Polyacrylamide gel electrophoresis
PBS ..... Phosphate-buffered saline
PCR ..... Polymerase chain reaction
PDGF ..... Platelet-derived growth factor
PEI ..... Polyethylenimine
pH ..... Potentia Hydrogenii

PI3K Phosphatidylinositol-4,5-bisphosphate 3-kinase
PKA ..... Protein kinase A
PLK1 ..... Polo-like kinase 1
PMSF ..... Phenylmethanesulfonylfluoride
PP1 ..... Protein phosphatase 1
pRb ..... Retinoblastoma protein
PreIC ..... Pre-initiation complex
PreRC ..... Pre-replicative complex
PTM ..... Post-translational modification
R point ..... Restriction point
RCC1 ..... Regulator of chromosome condensation 1
RhoA ..... Ras homolog family member A
RING ..... Really interesting new gene
RIPA ..... Radioimmunoprecipitation assay buffer
RNA ..... Ribonucleic acid
Rpd3 ..... Reduced potassium dependency 3
RT ..... Room temperature
S ..... Synthesis
s.d. ..... Standard deviation
SAC ..... Spindle assembly checkpoint
SDS ..... Sodium dodecylsulfate
Sir2 ..... Silent information regulator 2
Smac ..... Second mitochondria-derived activator of caspase
SNP ..... Single nucleotide polymorphism
SOE ..... Splice overlap extension
STAT3 ..... Signal transducer and activator of transcription 3
Surv ..... Survivin
TAE ..... Tris-acetate-EDTA
TBS ..... Tris-buffered saline
TBST ..... Tris-buffered saline/Tween
TE ..... Tris-EDTA buffer
TEMED ..... N,N,N',N'-Tetramethylethylenediamine
TGF-α ..... Transforming growth factor α
Tris ..... Tris(hydroxymethyl)aminomethane

Tris-HCl	Tris hydrochloride
TSA	Trichostatin A
UFD1	Ubiquitin fusion degradation protein
UV	ultraviolet
V	Volt
VEGF	Vascular endothelial growth factor
wt	Wildtype
XAF1	XIAP-associated factor 1
XIAP	X-linked inhibitor of apoptosis protein
Zn	Zinc
℃	degree Celsius

Amino acids

A	Alanine
C	Cysteine
D	Aspartate
E	Glutamate
F	Phenylalanine
G	Glycine
H	Histidine
I	Isoleucine
K	Lysine
L	Leucine
M	Methionine
N	Asparagine
P	Proline
Q	Glutamine
R	Arginine
S	Serine
T	Threonine
V	Valine
W	Tryptophan
Y	Tyrosine

List of Figures

List of Tables

SUMMARY

Survivin belongs to the inhibitor of apoptosis protein family and is also a regulator of mitosis as it is a member of the chromosomal passenger complex (CPC). While it is not expressed in differentiated adult tissue (Adida *et al.*, 1998), it was found to be up-regulated in virtually all types of human cancers (Ambrosini *et al.*, 1997; Adida *et al.*, 2000). Its overexpression is associated with resistance of tumors against chemo- and radiotherapy, frequent recurrences and decreased patient survival (Engels *et al.*, 2007; Capalbo *et al.*, 2007; Xu *et al.*, 2014; Chen *et al.*, 2014). Thus, Survivin is a potential target for cancer therapy. In order to develop strategies for the therapeutic inhibition of Survivin, the mechanisms underlying its dual role have to be clarified in detail. While Survivin fulfills some of its cellular tasks as a homodimer (Pavlyukov *et al.*, 2011), other functions require the monomer (Jeyaprakash *et al.*, 2007). A further layer of complexity is introduced by the fact that Survivin shuttles between the nucleus and the cytoplasm as it is able to passively diffuse into the nucleus and is actively exported by the soluble receptor CRM1 (Rodriguez *et al.*, 2002; Knauer *et al.*, 2006). The mechanisms regulating Survivin's functions, its localization as well as its dimerization state are still not completely resolved and a matter of scientific disagreement. Recently, Wang *et al.* (2010b) reported that acetylation of Survivin at lysine 129 facilitates its dimerization, thus causing an accumulation of the protein in the nucleus as only the monomer is able to interact with CRM1 for nuclear export. As lysine acetylation has emerged as a major post-translational modification capable of altering the functions and interactions of proteins, it is conceivable that Survivin's function might be regulated by the acetylation of any of its 16 lysine residues.

Thus, as a preliminary work to our study, which aimed to identify further acetylation sites in Survivin and the effect of a potential acetylation on some of Survivin's functions, we first set out to verify the findings obtained by Wang *et al.* (2010b). Accordingly, we cloned the four SurvK129 mutants investigated in their study and characterized them performing comprehensive molecular and structural analyses. Wang *et al.* (2010b) reported a facilitated nuclear export and a reduced tendency to form dimers for the

SurvK129E mutant, which they refered to as a mimicking mutant for Survivin unmodified at K129. They also claimed that this mutant was comparable to the SurvK129R mutant bearing a lysine to arginine mutation typically introduced to mimic an unmodified lysine. In contrast to their results, we found that SurvK129E is unique among the analyzed SurvK129 mutants and not comparable to SurvK129R. Taken together, our results suggest that the effects observed for SurvK129E are not caused by the lack of acetylation at K129, but might be due to the emergence of a potential high-affinity export signal by the exchange of a positively charged lysine with a negatively charged glutamate at position 129. Moreover, our findings indicate that acetylation of Survivin at K129 impairs dimerization rather than facilitating it.

Furthermore, we wanted to find out whether Survivin acetylated at K129 is involved in mitosis. Our analyses indeed indicate that acetylated Survivin might be incorporated into the CPC.

Finally, potential further acetylation sites within the Survivin protein were identified by *in situ* acetylation prediction. Fifteen Survivin mutants were cloned in which probably acetylated lysine residues were either mutated to arginine or to glutamine in order to mimic an unmodified or an acetylated lysine residue. These mutants were analyzed accordingly to the SurvK129 mutants in order to reveal potential effects on Survivin's cellular and mitotic localization as well as on its dimerization. However, the characterization of the mutants could not identify lysine residues potentially involved in Survivin regulation. Nevertheless, we could show that, although K90 is located within Survivin's classical export signal, its acetylation is unlikely to affect the protein's dimerization.

In summary, our results indicate that further comprehensive studies are required in order to understand the complex regulation of Survivin's various functions and the role that lysine acetylation plays in it.

ZUSAMMENFASSUNG

Survivin gehört zur Proteinfamilie der Apoptose-Inhibitoren, ist aber als Mitglied des chromosomalen Passenger-Complexes (CPC) ebenso an der Regulation der Mitose beteiligt. Während es in differenziertem, adulten Gewebe nicht exprimiert wird (Adida *et al.*, 1998), wurde eine Hochregulation in nahezu allen humanen Krebsarten nachgewiesen (Ambrosini *et al.*, 1997; Adida *et al.*, 2000). Seine Überexpression steht in Verbindung mit der Resistenz von Tumoren gegen Chemo- und Strahlentherapie, einem häufigen Wiederauftreten von Tumoren und einer verringerten Überlebenszeit der Patienten (Engels *et al.*, 2007; Capalbo *et al.*, 2007; Xu *et al.*, 2014; Chen *et al.*, 2014). Demzufolge stellt Survivin ein mögliches Angriffsziel für die Krebstherapie dar. Die Entwicklung von Strategien zur therapeutischen Inhibition von Survivin setzt jedoch ein grundlegendes Verständnis der molekularen Mechanismen, die seiner Doppelfunktion zugrunde liegen, voraus. Seine duale Rolle führt Survivin innerhalb der Zelle teilweise als Monomer, zum Teil aber auch als Homodimer aus. Survivin ist zudem in der Lage, zwischen Zellkern und Cytoplasma hin und her zu wandern, indem der durch den Exportrezeptor CRM1 vermittelte, aktive Export aus dem Kern der passiven Diffusion entgegenwirkt (Rodriguez *et al.*, 2002; Knauer *et al.*, 2006). Die Mechanismen, welche die Funktion, Lokalisation und Dimerisierung von Survivin regulieren, konnten bisher nicht vollständig aufgeklärt werden und sind Gegenstand kontroverser wissenschaftlicher Diskussionen. Einer Studie von Wang *et al.* (2010b) zufolge fördert die Acetylierung von Survivin an Lysin 129 dessen Dimerisierung. Dies führt zu einer Ansammlung des Proteins im Zellkern, da nur das Survivin-Monomer an den Exportrezeptor CRM1 binden kann. Da die Lysin-Acetylierung zudem als eine bedeutende post-translationale Modifikation gilt, welche die Funktionen und Interaktionen von Proteinen beeinflussen kann, ist eine Regulation von Survivin durch die Acetylierung einiger seiner 16 Lysin-Reste durchaus denkbar.

Zunächst wurden zur Verifizierung der Ergebnisse von Wang *et al.* (2010b) die dort verwendeten vier SurvK129-Mutanten kloniert und mittels umfassender molekularer

und struktureller Analysen charakterisiert. Wang *et al.* (2010b) beschreiben einen erleichterten Kernexport sowie eine verringerte Dimerisierungstendenz der SurvK129E-Mutante, welche in dieser Studie als an Lysin 129 nicht modifizierbar charakterisiert wird. Auch sei diese Mutante vergleichbar mit der SurvK129R-Mutante, die eine Lysin-zu-Arginin-Mutation trägt, welche typischerweise zur Nachahmung eines unmodifizierten Lysins eingeführt wird. Im Gegensatz zu Wang *et al.* (2010b) konnten wir zeigen, dass SurvK129E einzigartig unter den betrachteten SurvK129-Mutanten und nicht vergleichbar mit SurvK129R ist. Insgesamt weisen unsere Ergebnisse darauf hin, dass die Effekte, die für die SurvK129E-Mutante beobachtet wurden, nicht durch die fehlende Acetylierung an K129, sondern durch die Entstehung eines möglichen Exportsignals mit einer hohen Affinität zu CRM1 hervorgerufen werden könnten. Die Erhöhung der Affinität des möglicherweise bestehenden, schwachen Exportsignals käme dabei durch den Austausch des positiv geladenen Lysins an Position 129 durch ein negativ geladenes Glutamat zustande. Darüberhinaus deuten unsere Erkenntnisse eher auf eine Beeinträchtigung als auf eine Begünstigung der Dimerisierung durch die Acetylierung an K129 hin.

Im Rahmen unserer Untersuchungen zur Rolle von acetyliertem Survivin in der Mitose deutete sich weiterhin an, dass im CPC gebundenes Survivin acetyliert vorliegen könnte.

Weitere mögliche Acetylierungsstellen innerhalb von Survivin wurden durch eine *in situ* Acetylierungsvorhersage identifiziert. Darauf basierend wurden 15 Survivin-Mutanten kloniert, in welchen mit hoher Wahrscheinlichkeit acetylierte Lysin-Reste zu Arginin oder Glutamin mutiert wurden, um entweder ein unmodifiziertes oder ein acetyliertes Lysin zu imitieren. Diese Mutanten wurden analog zu den SurvK129-Mutanten analysiert, um mögliche Effekte auf die zelluläre und mitotische Lokalisation sowie die Dimerisierung von Survivin nachzuweisen. Anhand dieser Untersuchungen konnten allerdings keine Lysin-Reste identifiziert werden, welche eine tragende Rolle in dessen Regulation spielen. Allerdings ist davon auszugehen, dass eine Beeinträchtigung der Dimerisierung durch die Acetylierung von Lysin 90 unwahrscheinlich ist, obwohl sich dieses innerhalb des klassischen Exportsignals von Survivin befindet.

Zusammenfassend implizieren unsere Ergebnisse, dass weitere umfassende Studien nötig sind, um die komplexe Regulation der verschiedenen Funktionen von Survivin und insbesondere die Rolle der Lysin-Acetylierung im Detail zu verstehen.

1 Introduction

1.1 Cancer

Cancer is the second most common cause of death in Germany following diseases of the circulatory system. In 2012, 222,000 people died from cancer, which corresponds to 25.5 % of all cases of death (Federal Statistical Office Germany, 2014). According to estimates, approx. 252,000 men and 225,000 women were newly diagnosed with cancer in 2010 (Robert Koch Institute and the Association of Population-based Cancer Registries in Germany, 2014). While the most frequently occurring cancer types in men were prostate (26.1 %), lung (13.9 %) and colorectal cancer (13.4 %), in women almost one third of new cancer cases were caused by breast cancer, followed by colorectal (12.7 %) and lung cancer (7.6 %) (Figure 1.1).

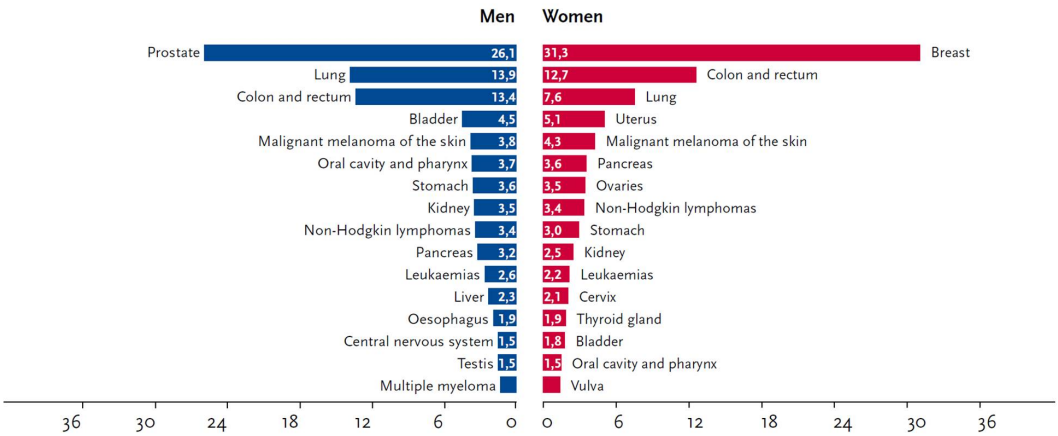

Figure 1.1: Estimated incidence of different tumor types in Germany 2010. Most frequent tumor sites as a percentage of all new cancer cases. (Robert Koch Institute and the Association of Population-based Cancer Registries in Germany, 2014).

With 24.9 % lung cancer is the major cause of cancer death cases in men, whereas

breast cancer causes the highest mortality in women (17.4 %) (Figure 1.2). The probability to develop cancer rises with increasing age. The median age at which cancer is diagnosed is 69 years for both sexes. Today, every second man and 43 % of all women have to expect to develop cancer in the course of their life.

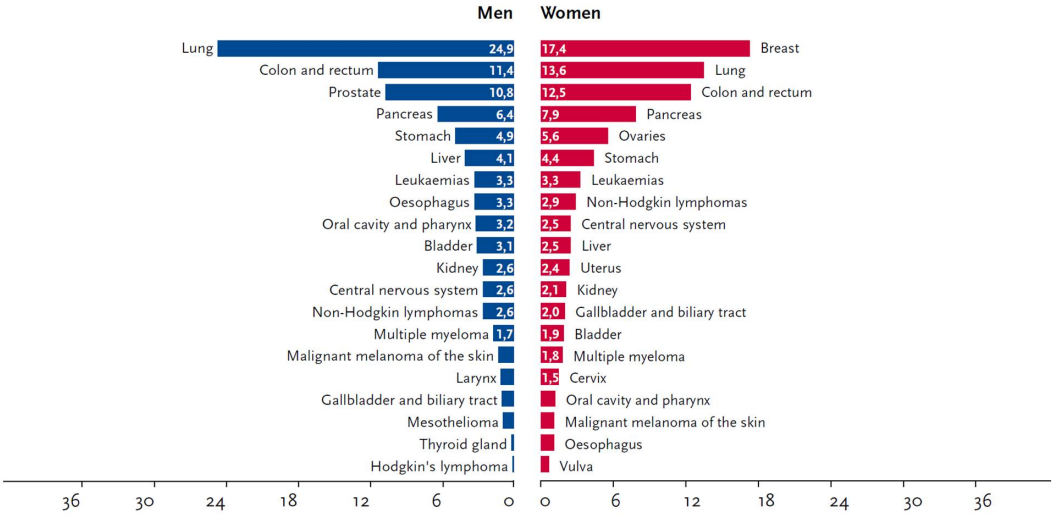

Figure 1.2: Estimated mortality of different tumor types in Germany 2010. Most frequent tumor sites as a percentage of all cases of death caused by cancer. (Robert Koch Institute and the Association of Population-based Cancer Registries in Germany, 2014).

1.1.1 Carcinogenesis

The term "cancer" is a generic term used for all malignant tumors. A tumor is defined as an abnormal growth of new tissue (neoplasia), which can be benign or malignant. In contrast to a benign tumor, which only ousts the surrounding tissue, but stays localized, cells of a malignant tumor can breach the basal membrane and invade adjacent tissue. Furthermore, they are capable of forming metastases in other parts of the body, distant from the primary tumor (Weinberg, 2013). The ability of malignant tumors to invade and metastasize is one of the six "hallmarks of cancer" proposed by Hanahan and Weinberg in 2000 describing the biological capabilities of malignant tumors acquired during their multistep development. As further hallmarks, the ability of cancers to enable replicative immortality, induce angiogenesis, resist cell death, sustain proliferative signaling as well as to evade growth suppressors were suggested. In 2011, Hanahan and Weinberg have revisited and expanded their concept of cancer hallmarks due to new insights in cancer research (Figure 1.3). The capability to deregulate cellular energetics and to

avoid destruction by the immune system were added to the list as emerging hallmarks, which have to be validated by further research. Genome instability and mutations as well as a tumor-promoting inflammation were described as characteristics enabling a tumor to become malignant.

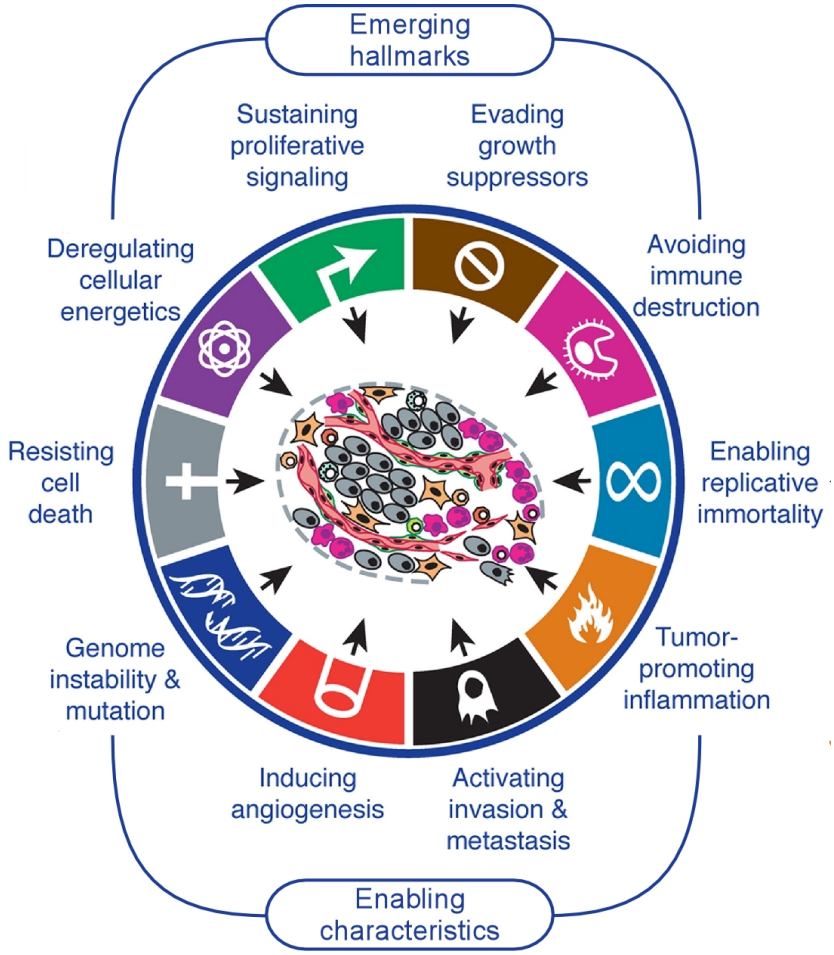

Figure 1.3: The hallmarks of cancer. Acquired capabilities of malignant cancer cells (modified after Hanahan and Weinberg, 2011).

As mentioned before, carcinogenesis is a multistep process. It is characterized by the successive accumulation of genomic alterations caused by inherited and/or spontaneous mutations, chromosomal rearrangements and epigenetic changes (Hanahan and Weinberg, 2011). Alterations in different types of genes have been shown to contribute to cancer development. Tumor suppressor genes (TSGs), also called "gatekeepers" (Kinzler and Vogelstein, 1997), are genes whose products govern cell proliferation, promote differentiation or induce apoptosis (Weinberg, 2013). Their inactivation (loss of function), for example by point mutation, chromosomal deletion or promotor methylation, enables a defective cell to override these control mechanisms and further prolifer-

ate, thus increasing the probability that the cell will undergo neoplastic transformation. The loss of function phenotype is usually recessive, implying that it only occurs when both alleles have become inactivated. The most prominent and initially identified TSGs are tumor protein 53 (*TP53*) (Finlay *et al.*, 1989; Levine *et al.*, 2004) and retinoblastoma 1 (*RB1*) (Lee, 1989).

Another group of genes behaving similar to TSGs are the genome maintenance genes, also known as "caretakers" (Kinzler and Vogelstein, 1997). Their gene products are involved in sensing DNA damage and activating the repair machinery (e.g. breast cancer type 1/2 susceptibility protein (BRCA1/2)), or they directly repair DNA lesions or inactivate mutagenic molecules, thus sustaining genomic integrity (Hanahan and Weinberg, 2011).

Oncogenes, a third type of genes contributing to carcinogenesis, are former normal cellular genes (proto-oncogenes) which have been activated by mutations, chromosomal translocations or amplifications, or transcriptionally by a virus. Consequences of the activation of a proto-oncogene are the overexpression of the gene product or the expression of a protein with altered function (Weinberg, 2013). Most oncogenes code for proteins involved in mitogenic signaling pathways, for example growth factors (e.g. transforming growth factor α (TGF-α)), their receptors (e.g. epidermal growth factor receptor (EGFR)), GTPases (e.g. hRas), or transcription factors (e.g. Myc).

In addition to genome instability outlined above, the second characteristic enabling normal cells to become malignant is the tumor-promoting inflammation (Hanahan and Weinberg, 2011). It has been observed that many tumors are infiltrated by immune cells, already in early stages of neoplasia (Dvorak, 1986). Such immune responses, reflecting the attempt of the immune system to eradicate tumors, paradoxically, not always lead to the destruction of the tumors, but can even promote tumorigenesis by helping incipient neoplasms to acquire hallmark capabilities. Tumor-promoting inflammatory cells, like macrophages, mast cells, neutrophils as well as B and T lymphocytes, contribute to the transformation of neoplastic cells in several ways, for example by supplying growth or survival factors (e.g. epidermal growth factor (EGF), vascular endothelial growth factor (VEGF)), which facilitate proliferation and prevent apoptosis, or by secreting extracellular matrix (ECM)-modifying enzymes (e.g. matrix metalloproteinase-9 (MMP-9)) fostering invasion and angiogenesis. They can also release mutagenic reactive oxygen species, which increase the rate of genomic alterations in the tumor cells (Colotta *et al.*, 2009; Grivennikov *et al.*, 2010; DeNardo *et al.*, 2010).

The definition of the tumor-promoting inflammation as an enabling characteristic of cancer development is due to a new understanding of cancer. While earlier a tumor

was considered to be nothing more than an accumulation of cancer cells, it is now clear that all cell types surrounding the cancer cells play a crucial role in carcinogenesis. Among these are the already mentioned cells of the immune system, but also other mesenchymal cells like endothelial cells, pericytes and cancer-associated fibroblasts, forming the tumor stroma (Figure 1.4A). A complex heterotypic signaling occurs in the tumor microenvironment, in which reciprocal interactions between tumor and stroma cells promote the transformation of normal tissue to cancer (Figure 1.4B) (Hu and Polyak, 2008; Goubran *et al.*, 2014; Landskron *et al.*, 2014).

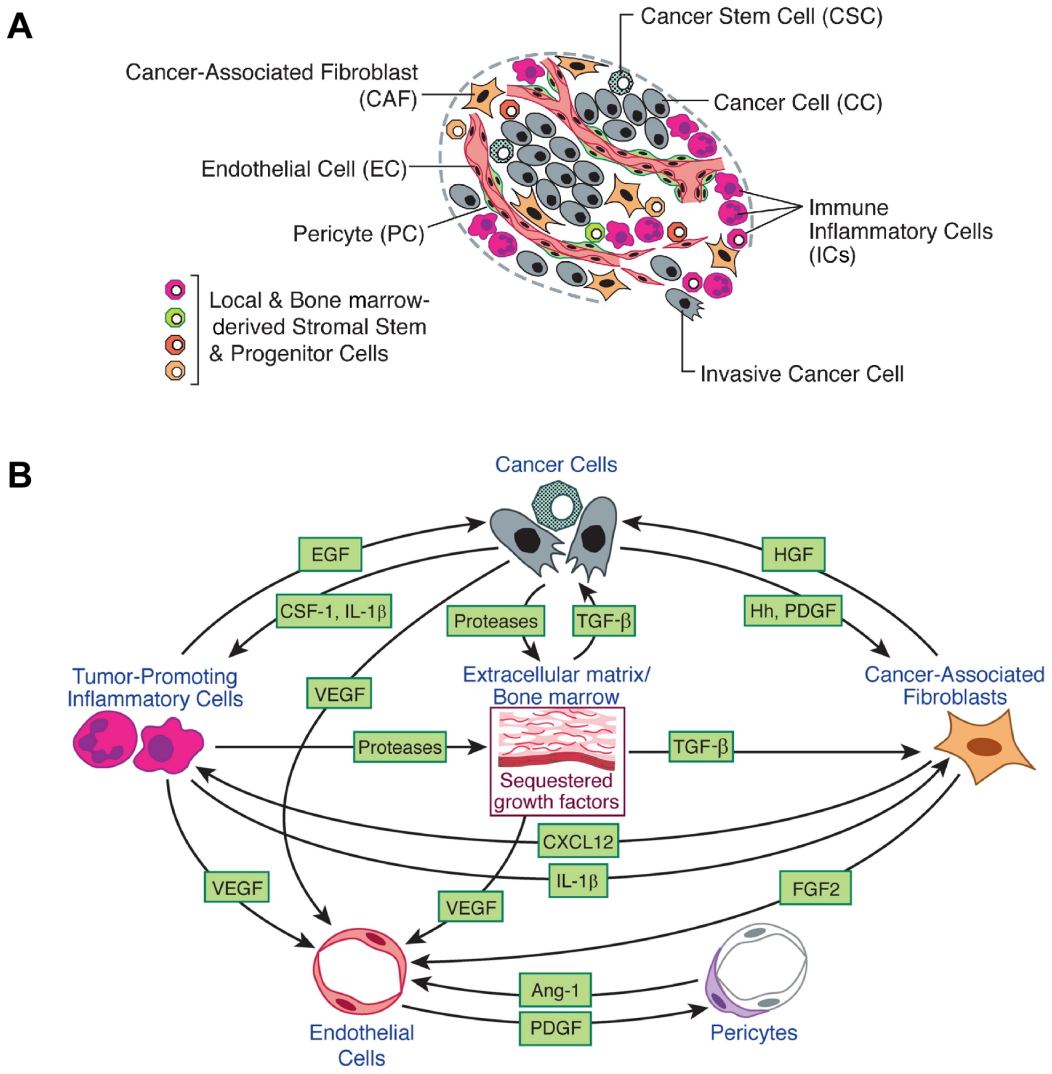

Figure 1.4: The tumor microenvironment. A) Cell types constituting the tumor microenvironment of most solid tumors. B) Examples of reciprocal heterotypic signaling interactions in the tumor microenvironment (modified after Hanahan and Weinberg, 2011). EGF: epidermal growth factor, CSF-1: colony stimulating factor 1, IL-1β: interleukin 1β, VEGF: vascular endothelial growth factor, TGF-β: transforming growth factor β, CXCL12: C-X-C motif chemokine 12, Ang-1: angiopoietin 1, PDGF: platelet-derived growth factor, HGF: hepatocyte growth factor, Hh: hedgehog, FGF2: fibroblast growth factor 2.

1.2 Survivin

Survivin, with 16.5 kDa the smallest member of the inhibitor of apoptosis protein (IAP) family and a member of the chromosomal passenger complex (CPC), is up-regulated in various human cancers (Ambrosini *et al.*, 1997; Adida *et al.*, 2000). Its overexpression is associated with resistance of tumors against chemo- and radiotherapy, frequent recurrences and decreased patient survival (Engels *et al.*, 2007; Capalbo *et al.*, 2007; Xu *et al.*, 2014; Chen *et al.*, 2014). Besides its up-regulation in cancer cells, Survivin is highly expressed during embryonic and fetal development, but absent in differentiated adult tissue (Adida *et al.*, 1998).

The gene coding for Survivin, *BIRC5* (baculoviral IAP repeat containing 5), contains four exons and three introns and is located on chromosome 17q25 (Ambrosini *et al.*, 1997). Alternative splicing of the pre-mRNA gives rise to five different transcripts: Survivin, SurvivinΔEx3, Survivin3B, Survivin2B and Survivin2α. In normal dividing cells, *BIRC5* expression is tightly regulated in a cell cycle-dependent manner peaking at the G_2/M transition of the cell cycle (Li *et al.*, 1998). Also epigenetic regulation through DNA (cytosine-5)-methyltransferase 1 (DNMT1) or histone deacetylase 1 (HDAC1) as well as post-transcriptional control by microRNAs has been reported (Smallwood *et al.*, 2007; Alajez *et al.*, 2011; Ma *et al.*, 2013). Survivin overexpression in cancer is due to mutations in its promotor (Xu *et al.*, 2004; Boidot *et al.*, 2010), gene duplication (Tajiri *et al.*, 2001) or deregulation of its related transcription factors. Among them are several known as products of TSGs, such as the retinoblastoma protein (pRb) and p53, as well as oncogenes, for example Myc (Jiang *et al.*, 2004; Hoffman *et al.*, 2002; Mirza *et al.*, 2002; Cosgrave *et al.*, 2006). Hence, in many tumors Survivin is found not only in dividing, but also in interphase cells (Engels *et al.*, 2007).

The gene product of *BIRC5*, the Survivin protein, has a unique structure (Figure 1.5). The monomer contains three regions enabling the protein to interact with other proteins and conduct its various functions. The N-terminal BIR domain (amino acid (aa) 15-88) characterizes Survivin as a member of the IAP family as this domain is common to all IAPs. It is a globular zinc finger domain stabilized by the tetrahedral coordination of a Zn^{2+} ion by the amino acids C57, C60, H77 and C84. Survivin's long C-terminal α-helix (aa 99-142) extends out and away from the BIR domain. Hydrogen bonds as well as hydrophobic contacts between the BIR domain and the first turns of the helix stabilize it and fix its direction. It contains a cluster of hydrophobic amino acids between F124 and L138 which functions as an adaptor for protein-protein interactions. Between the BIR domain and Survivin's C-terminal helix, a linker region is located containing two overlapping, functionally important features: the nuclear export signal (NES)(aa 89-98),

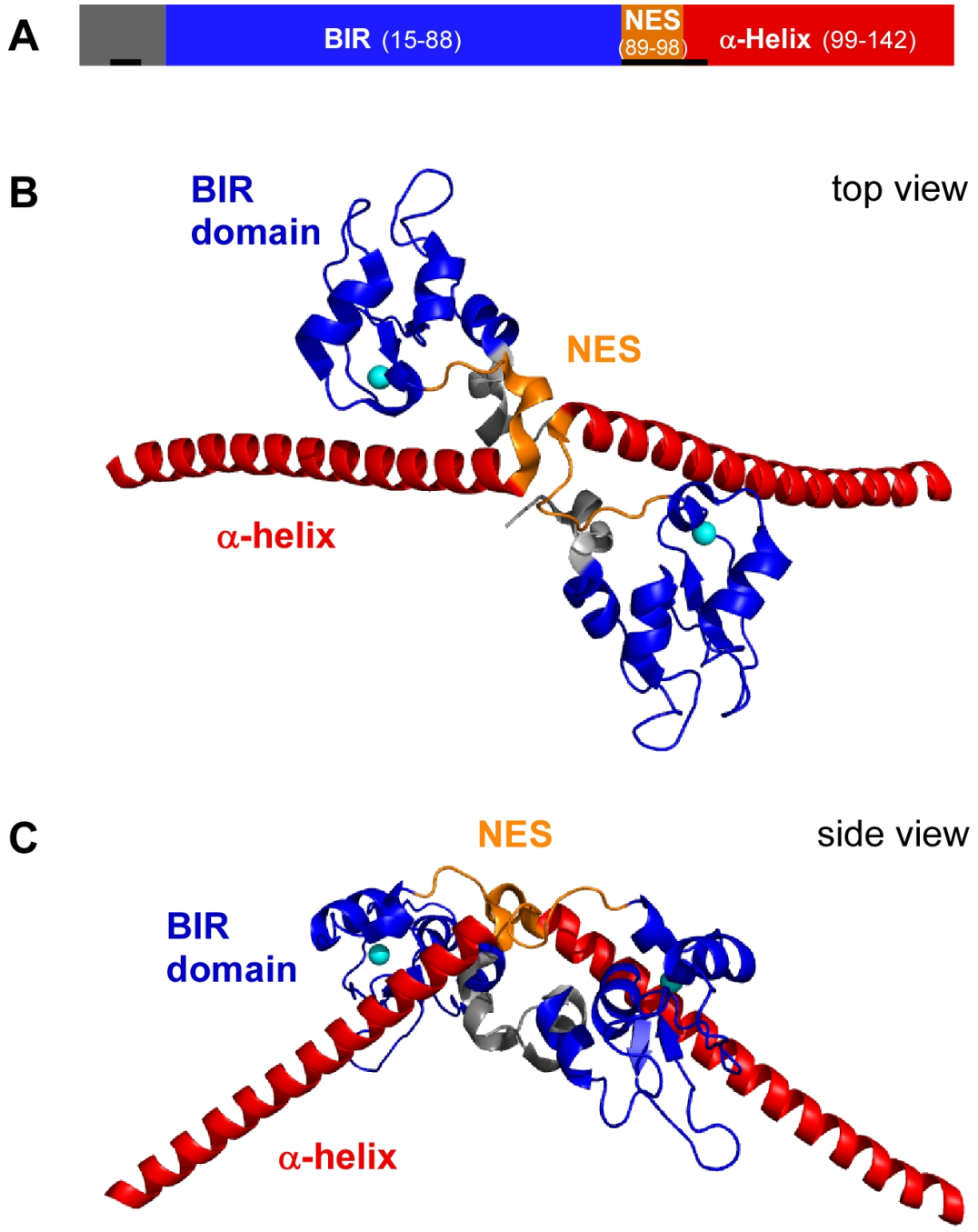

Figure 1.5: Structure of the Survivin protein. A) Domain organization of Survivin. B) Ribbon representation of the Survivin homodimer (Chantalat *et al.*, 2000; PDB ID: 1E31). C) The view in B rotated by 90° around the horizontal axis. The N-terminal BIR domain is depicted in blue, the NES in orange and the C-terminal α-helix in red. The dimer interface is indicated by a black bar. The Zn^{2+}ion is shown as a cyan sphere.

which serves as the binding site for the nuclear export receptor chromosome region maintenance 1 (CRM1), and one part of the dimer interface (aa 6-10 and 89-102). The dimer interface is formed by hydrophobic contacts of L98 from one monomer with a hydrophobic pocket composed of L6, W10, F93, F101 and F102 of the other monomer. The Survivin homodimer formed in solution has a bow tie shape with the C-terminal α-helices forming a 110° angle (Chantalat *et al.*, 2000; Verdecia *et al.*, 2000).

In addition to the transcriptional control of *BIRC5*, Survivin is also regulated on the protein level by post-translational modifications (PTMs). The stability of the protein is regulated by proteasomal degradation dependent on the cell cycle. Increased degradation due to K48-linked ubiquitination has been observed at the end of mitosis (Zhao *et al.*, 2000). It has also been reported that XIAP-associated factor 1 (XAF1), a pro-apoptotic factor that can bind to X-linked inhibitor of apoptosis protein (XIAP) and inhibit its anti-caspase function, induces Survivin ubiquitination and the subsequent proteasomal degradation by activating XIAP's E3 ubiquitin ligase activity (Arora *et al.*, 2007). The interaction of Survivin with the chaperones Hsp60 and Hsp90 (heat shock proteins 60 and 90), in contrast, retains its stability against degradation by the proteasome (Fortugno *et al.*, 2003; Ghosh *et al.*, 2008). Further PTMs, such as phosphorylation and acetylation, have been found to regulate Survivin (Figure 1.6). These are discussed in detail below, according to their function.

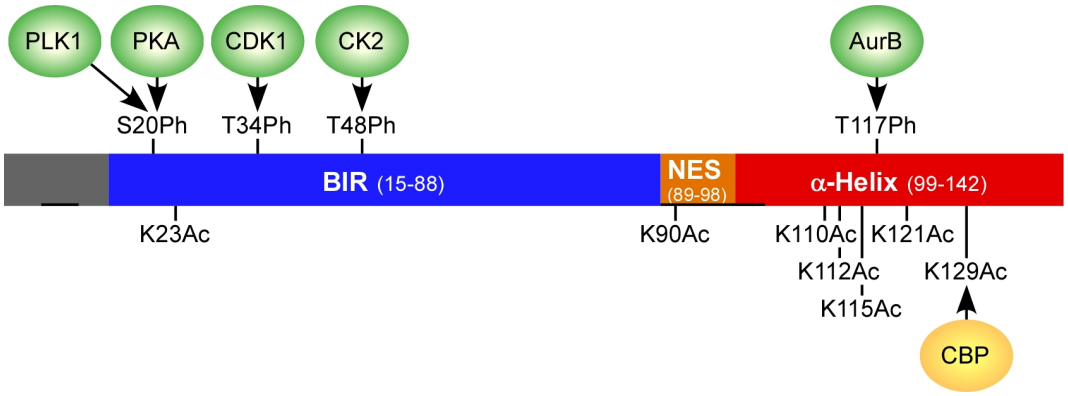

Figure 1.6: Post-translational modifications regulating Survivin. Schematic representation of Survivin's domain structure indicating sites of known post-translational modifications. While phosphorylation occurs at amino acids within the BIR domain (blue), acetylated residues are mainly located in Survivin's α-helix (red) and the NES (orange). Ubiquitination is not depicted as the targeted positions have not yet been identified. Kinases are indicated as green spheres, acetyltransferases as yellow spheres (O'Connor *et al.*, 2000a; Wheatley *et al.*, 2004; Dohi *et al.*, 2007; Colnaghi and Wheatley, 2010; Wang *et al.*, 2010b; Barrett *et al.*, 2011). BIR: baculoviral IAP repeat, NES: nuclear export signal, PLK1: polo-like kinase 1, PKA: protein kinase A, CDK1: cyclin-dependent kinase 1, CK2: casein kinase 2, AurB: Aurora B, CBP: CREB-binding protein.

As mentioned above, Survivin belongs to the inhibitor of apoptosis protein family since it contains a baculoviral IAP repeat (BIR) domain. The human IAP family consists of eight proteins: Apollon, inhibitor of apoptosis-like protein 2 (ILP2), Livin, Survivin, neuronal apoptosis inhibitory protein (NAIP), cellular inhibitor of apoptosis proteins 1 and 2 (c-IAP1/2) and XIAP (Riedl and Shi, 2004) (Figure 1.7). Unlike the seven other IAPs, Survivin contains only one BIR domain and no further protein domains like CARD (caspase recruitment domain) or RING (really interesting new gene) domains.

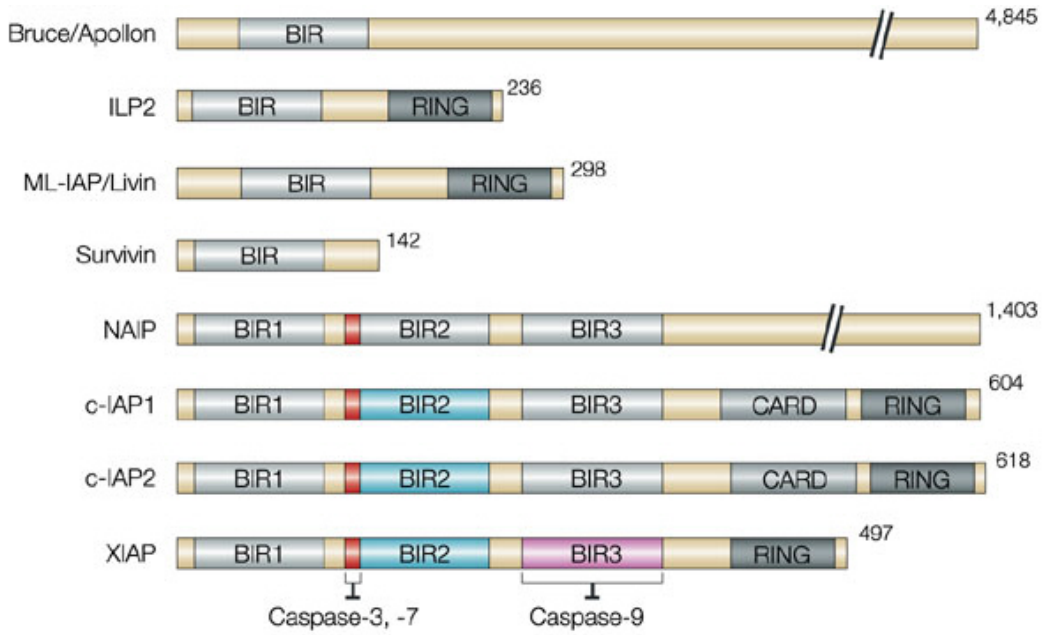

Figure 1.7: The human members of the IAP family. Schematic representation of the human inhibitor of apoptosis proteins including Apollon, ILP2, Livin, Survivin, NAIP, c-IAP1, c-IAP2 and XIAP. A conserved linker peptide that precedes the BIR2 domain of XIAP, c-IAP1 and c-IAP2 and is responsible for inhibiting caspases-3 and -7 is indicated in red (modified after Riedl and Shi, 2004). NAIP: neuronal apoptosis inhibitory protein, c-IAP1/2: cellular inhibitor of apoptosis proteins 1/2, XIAP: X-linked inhibitor of apoptosis protein, BIR: baculoviral IAP repeat, RING: really interesting new gene, CARD: caspase recruitment domain.

BIR domains mediate protein recognition and protein-protein interactions (Altieri, 2010). XIAP, c-IAP1 and c-IAP2, for example, bind proteins containing an IAP-binding motif (IBM) via one of their BIR domains. IBMs are present in caspases as well as in certain apoptosis inducers for instance second mitochondria-derived activator of caspase/direct IAP-binding protein with low pI (Smac/DIABLO). Caspase inhibition by direct interaction was originally proposed for all IAPs including Survivin (Deveraux and Reed, 1999; Tamm *et al.*, 1998; Shin *et al.*, 2001). Recent studies, however, revealed that only XIAP can directly interact with caspases *in vivo* (Eckelman *et al.*, 2006;

Srinivasula and Ashwell, 2008). For Survivin, various modes of indirect inhibition of caspase-dependent cell death have been reported. Survivin can form a complex with XIAP resulting in an increased stability of XIAP against proteasomal degradation. This complex, but not Survivin alone, is able to suppress caspase-9 activity. Phosphorylation of Survivin at S20 by protein kinase A (PKA) disrupts the interaction of Survivin with XIAP (Dohi *et al.*, 2004, 2007). A similar function has been shown for a Survivin-HBXIP (hepatitis B X-interacting protein) complex, which precludes pro-caspase-9 recruitment to activated apoptotic protease activating factor 1 (APAF-1), thus preventing the formation of the apoptosome (Marusawa *et al.*, 2003). Song *et al.* (2003) have reported that Survivin binds to the pro-apoptotic factor Smac/DIABLO in the cytosol. Consequently, XIAP is released from an inhibiting complex with Smac/DIABLO and can conduct its anti-apoptotic function. In addition, mitochondrial Survivin, which can be released from mitochondria upon apoptotic stimuli, has been described as a regulator of Smac/DIABLO release from mitochondria as it can sequester the pro-apoptotic factor in the intermembrane space (Ceballos-Cancino *et al.*, 2007). Barrett *et al.* (2011) have demonstrated that the phosphorylation of cytoplasmic Survivin at T48 by casein kinase 2 (CK2) is also required to inhibit caspases. Besides abrogating caspase-dependent apoptosis, Survivin is also involved in the inhibition of caspase-independent cell death. A study by Pavlyukov *et al.* (2011) revealed that Survivin prevents the release of apoptosis-inducing factor (AIF), a marker for caspase-independent apoptosis, from mitochondria. Survivin's cytoprotective activity conferring therapy resistance to tumor cells is assumed to be conducted by cytoplasmic Survivin, whereas nuclear Survivin seems to be involved in regulating cell division (Lippert *et al.*, 2007). However, it has been shown that Survivin phosphorylated at T34 by cyclin-dependent kinase 1 (CDK1) is able to protect cells from cell death by inhibiting caspase-9 during mitosis (O'Connor *et al.*, 2000a; Barrett *et al.*, 2009).

As aforementioned, Survivin has a dual role. Besides its anti-apoptotic function as an IAP, it is also a key regulator of cell division as a member of the chromosomal passenger complex (see subsection 1.3.4). During mitosis, the CPC regulates chromosome condensation, correction of erroneous kinetochore-microtubule attachments as well as the activation of the spindle assembly checkpoint (SAC). In cytokinesis, it controls the formation and function of the contractile ring that drives the abscission of the two daughter cells (Carmena *et al.*, 2012). The CPC is composed of a localization module and a kinase module linked together by the central region of the inner centromere protein (INCENP). The localization module, which comprises INCENP's N-terminus, Borealin and Survivin, targets the CPC first to centromeres, later to the mitotic spindle, and last to the midbody. All three proteins contain stretched α-helices which interact with each other to form a stable three-helical bundle, the core of the CPC (Figure 1.8)

(Jeyaprakash *et al.*, 2007). The kinase module consisting of Aurora B kinase and the C-terminus of INCENP provides the enzymatic activity of the complex (Adams *et al.*, 2000). Together, both modules allow spatially restricted phosphorylation of Aurora B substrates via dynamic changes in the localization of the CPC during mitosis and cytokinesis.

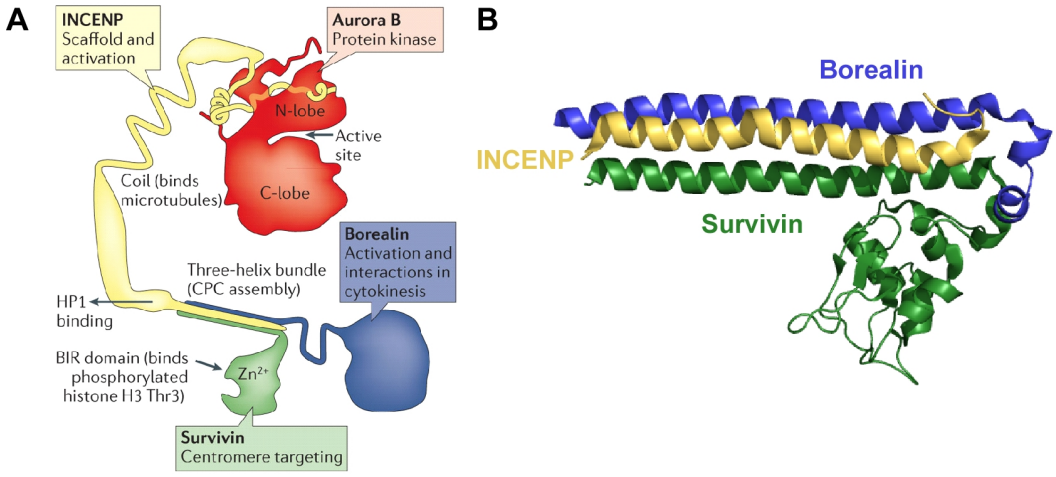

Figure 1.8: Structure of the chromosomal passenger complex. A) Schematic representation of the CPC (modified after Carmena *et al.*, 2012). The domains and functions of the CPC members are indicated. B) Ribbon representation of the three-helical bundle forming the core of the CPC (Jeyaprakash *et al.*, 2007; PDB ID: 2QFA). Survivin is shown in green, Borealin in blue and INCENP in yellow. HP1: heterochromatin protein 1, CPC: chromosomal passenger complex.

Survivin is responsible for targeting the CPC to centromers in early prophase. Its BIR domain has been shown to directly bind the N-terminus of histone H3 phosphorylated at T3 (H3T3Ph), a mitosis-specific phosphorylation mark most prominent at the inner centromer (Jeyaprakash *et al.*, 2011; Carmena *et al.*, 2012). Additionally, it has been demonstrated that the interaction of the nuclear export receptor CRM1 with Survivin's NES (aa 89-98) is important for tethering the CPC to centromeres as well as for CPC function, but not for its assembly (Knauer *et al.*, 2006). For the association of Survivin to centromeres, furthermore, its ubiquitination through K63 ubiquitin linkages by ubiquitin fusion degradation protein 1 (UFD1) is necessary, while its deubiquitination by hFAM (fat facets in mammals) is required for its dissociation (Vong *et al.*, 2005). Besides Survivin's function in CPC localization, its phosphorylation at S20 by polo-like kinase 1 (PLK1) is required for accurate chromosome alignment since it causes a complete activation of Aurora B (Colnaghi and Wheatley, 2010; Chu *et al.*, 2011). The phosphorylation of Survivin at T117 by Aurora B during mitosis has been reported to

regulate localization and stability of the CPC, and its dephosphorylation is crucial for progression to anaphase (Wheatley *et al.*, 2004, 2007; Delacour-Larose *et al.*, 2007). In general, Survivin inhibition results in mitotic defects for instance cell cycle arrest at prometaphase, abberant spindle formation, cytokinesis failure and multinucleated cells (Conte and Altieri, 2006). Aside from Survivin which is part of the CPC, there is another pool of the protein conducting a critical role in mitosis: Survivin bound to polymerized microtubules has been shown to depress microtubule dynamics, sustain their stability, and thus, support the assembly of mitotic spindles (Altieri, 2006).

In addition to its roles in apoptosis and mitosis, several other functions have recently been indicated for Survivin. Capalbo *et al.* (2010) and Reichert *et al.* (2011) reported that Survivin is linked to DNA repair as it rapidly accumulates in nuclear foci after irradiation and forms complexes with members of the DNA double strand break repair machinery. Survivin has also been related to inhibiting autophagy and promoting angiogenesis (Niu *et al.*, 2010; Wang *et al.*, 2011; O'Connor *et al.*, 2000b; Tran *et al.*, 2002).

While originally only the Survivin homodimer was considered to be functionally active (Muchmore *et al.*, 2000; Song *et al.*, 2004), recent studies have demonstrated that the dimer as well as the monomer play distinct roles in critical cellular processes. It has been shown that only the Survivin monomer can be part of the CPC (Jeyaprakash *et al.*, 2007), and interact with CRM1 for its nuclear export (Engelsma *et al.*, 2007). Moreover, Pavlyukov *et al.* (2011) found that monomeric Survivin prevents caspase-dependent apoptosis by interacting with Smac/DIABLO and XIAP, and that it can also inhibit caspase-independent cell death by preventing AIF release from mitochondria. They could also show that only the Survivin dimer is able to stabilize microtubules. A further function attributed to the Survivin homodimer is the inhibition of signal transducer and activator of transcription 3 (STAT3) transactivation (Wang *et al.*, 2010b). Wang *et al.* (2010b) suggested that acetylation of Survivin at K129 in the nucleus functions as a switch between the momoneric and dimeric state of the protein: while CREB-binding protein (CBP)-mediated acetylation facilitates Survivin homodimerization and inhibits its interaction with the export receptor CRM1, its deacetylation by HDAC6 favors the monomeric state of Survivin which shows enhanced binding to CRM1, and consequently, is exported to the cytoplasm (Wang *et al.*, 2010b; Riolo *et al.*, 2012).

It has been demonstrated before that the homodimerization of Survivin antagonizes its nuclear export (Engelsma *et al.*, 2007; Jeyaprakash *et al.*, 2007). This is due to the overlap of a classical leucine-rich nuclear export signal (^{89}VKKQFEELTL^{98}) identified by Knauer *et al.* (2006) with one part of Survivin's dimer interface. The NES is recognized by the soluble export receptor CRM1, which mediates active export of Survivin

from the nucleus. However, as mentioned above, the NES is not only required for Survivin's nuclear export, but also for its targeting to centromeres in mitosis. Survivin lacking the NES, or containing a NES in which two critical hydrophobic residues (L96 and L98) are mutated to alanine, does not localize to centromeres, thus impairing the correct localization and function of the CPC. Inhibition of the Survivin-CRM1 interaction by leptomycin B (LMB) also leads to mislocalization of Survivin and other CPC members (Knauer *et al.*, 2006). In addition to the classical NES, Rodriguez *et al.* (2002) proposed a non-classical CRM1-dependent export motif in the α-helix of Survivin. Their study revealed that Surv119-142, like the NES-containing fragment Surv89-136, predominantly localized to the cytoplasm and relocated to the nucleus upon CRM1 inhibition by LMB. However, the exact sequence of this export motif has not been further defined. They speculated that CRM1-dependent export of Survivin via this motif could be mediated by a NES-containing adapter protein, rather than via direct interaction.

1.3 The cell cycle

The cell cycle, a process in which cells undergo the replication of their DNA, the division of their nucleus, and last, the division of their cytoplasm, is the mechanism by which all living cells reproduce. The cell cycle of eukaryotic cells is divided into four phases: G_1 (gap 1), S (synthesis), G_2 (gap 2) and M (mitosis) (Figure 1.9). G_1, S and G_2 together are named interphase. In many types of cultured mammalian cells, G_1 lasts 12-15 h, S phase 6-8 h, G_2 3-5 h and M phase only 1 h (Weinberg, 2013). In G_1 and G_2 phase, the cell prepares for the upcoming critical phases of the cell cycle, S and M phase, and monitors whether the extra- and intracellular conditions are favorable, before it proceeds with the cell cycle. In S phase, the DNA is replicated yielding duplicated chromosomes. The M phase is divided into two processes: mitosis, in which the duplicated chromosomes are segregated, and cytokinesis, the partitioning of the cytoplasm, which finally results in the formation of two daughter cells.

1.3.1 Regulation of the cell cycle

The cell cycle is a highly complex process which is tightly regulated, and controlled by a series of checkpoints preventing cells from entering a new phase until they have successfully completed the previous one. The central players that drive the cell cycle are the cyclin-dependent kinases CDK1, CDK2, CDK4 and CDK6. These serine/threonine kinases require binding to their regulatory subunits, the cyclins, to become catalytically

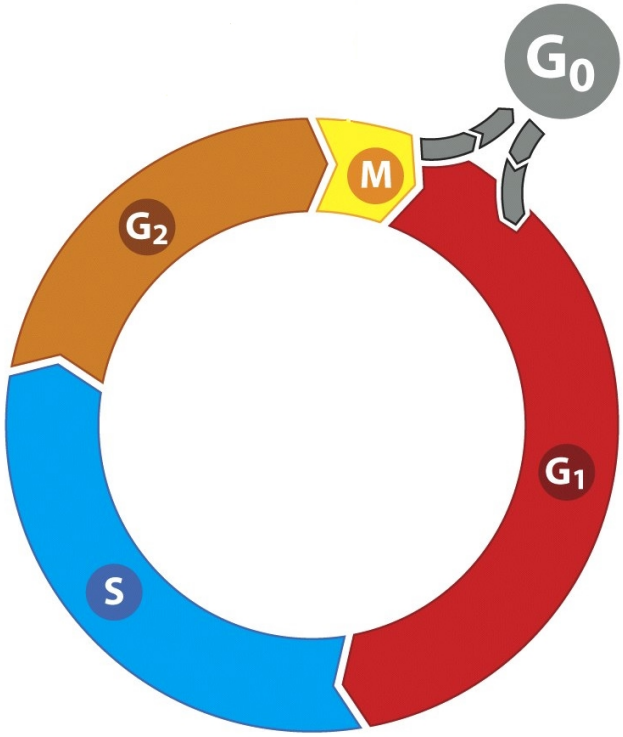

Figure 1.9: The cell cycle. The eukaryotic cell cycle is divided into four phases: G_1, S, G_2 and M. Cells can also exit the cell cycle to reach a quiescent, non-proliferating state (G_0), from which they can re-enter the cell cycle at a later time point (modified after Weinberg, 2013).

active and recognize their substrates (Murray, 2004; Massagué, 2004). In addition, CDK activity is also regulated by phosphorylation. The CDK-activating kinase (CAK) provides activating CDK phosphorylation, while the phosphorylation by Wee1 kinase has an inhibitory effect (Malumbres and Barbacid, 2001). A third mode of CDK regulation is by CDK inhibitors (CDKIs). The strictly regulated timing and extend of CDK-cyclin complex activity drives the progression of the cell cycle from one phase to the next (Figure 1.10A).

In early and mid G_1, CDK4 and CDK6 bind to D-type cyclins. After the restriction point (R point) (see below) CDK2 associates with E-type cyclins to enable the phosphorylation of substrates required for S phase entry. In early S phase, E cyclins are replaced by A cyclins as binding partners of CDK2, which leads to the progression of S phase. Later in S phase and during G_2, A cyclins are bound to CDK1. Finally, at the onset of M phase, CDK1-cyclin B complexes form triggering the events in all phases of mitosis (Weinberg, 2013). While the levels of most CDKs are constant, the levels of cyclins fluctuate dramatically during the different phases of the cell cycle (Figure 1.10B). Cyclin D expression is dependent on extracellular mitogenic signaling, for example on the hRas or phosphatidylinositol-4,5-bisphosphate 3-kinase (PI3K) pathways, and its nuclear level is regulated by export from the nucleus after G_1/S transition. The levels of

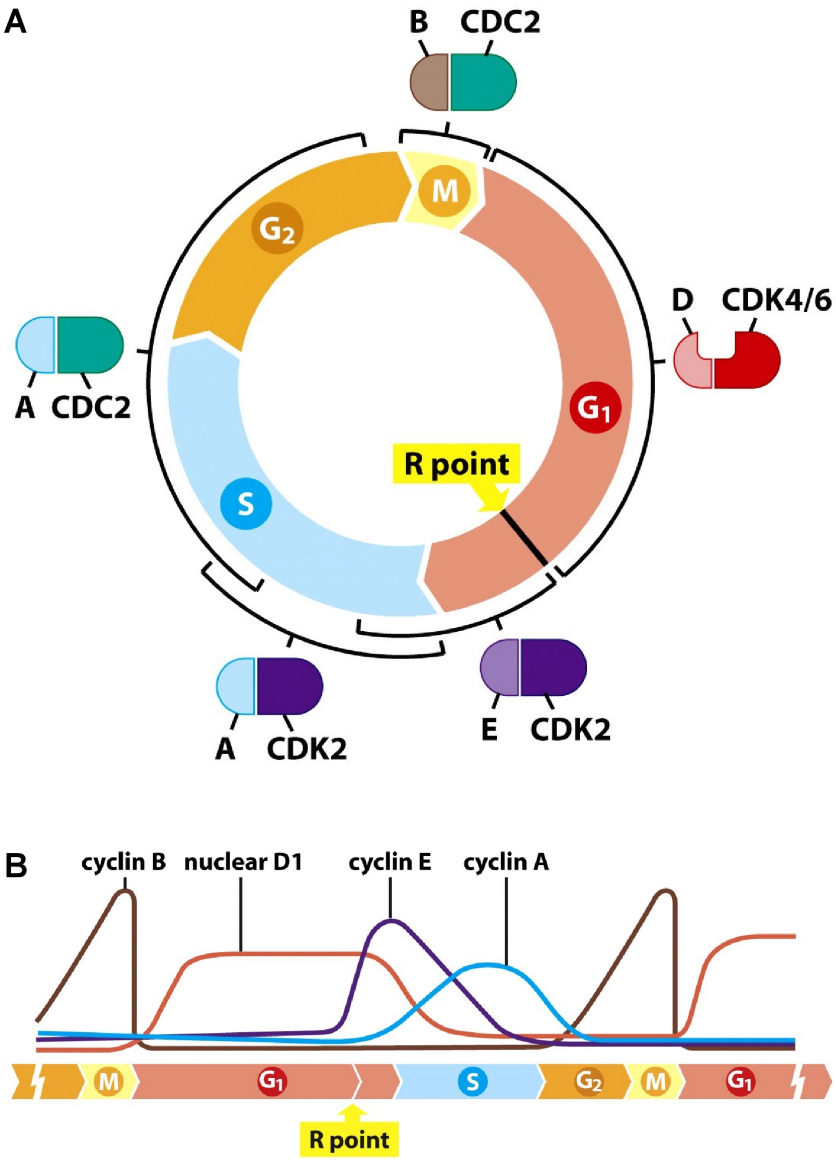

Figure 1.10: Regulation of the cell cycle by CDK-cyclin complexes. Cell cycle progress is driven by the activity of various CDK-cyclin complexes in different phases of the cell cycle. A) The period of activity of each CDK-cyclin complex. B) The fluctuating levels of cyclins during the cell cycle regulating CDK activation (modified after Weinberg, 2013). CDC2: cell division control protein 2 homolog (also known as CDK1), CDK: cyclin-dependent kinase, R point: restriction point.

the other cyclins, however, are independent from the cell's environment and are tightly coordinated with the advance of the cell cycle. Their rapid decrease at specific points is due to ubiquitination, and subsequent proteasomal degradation.

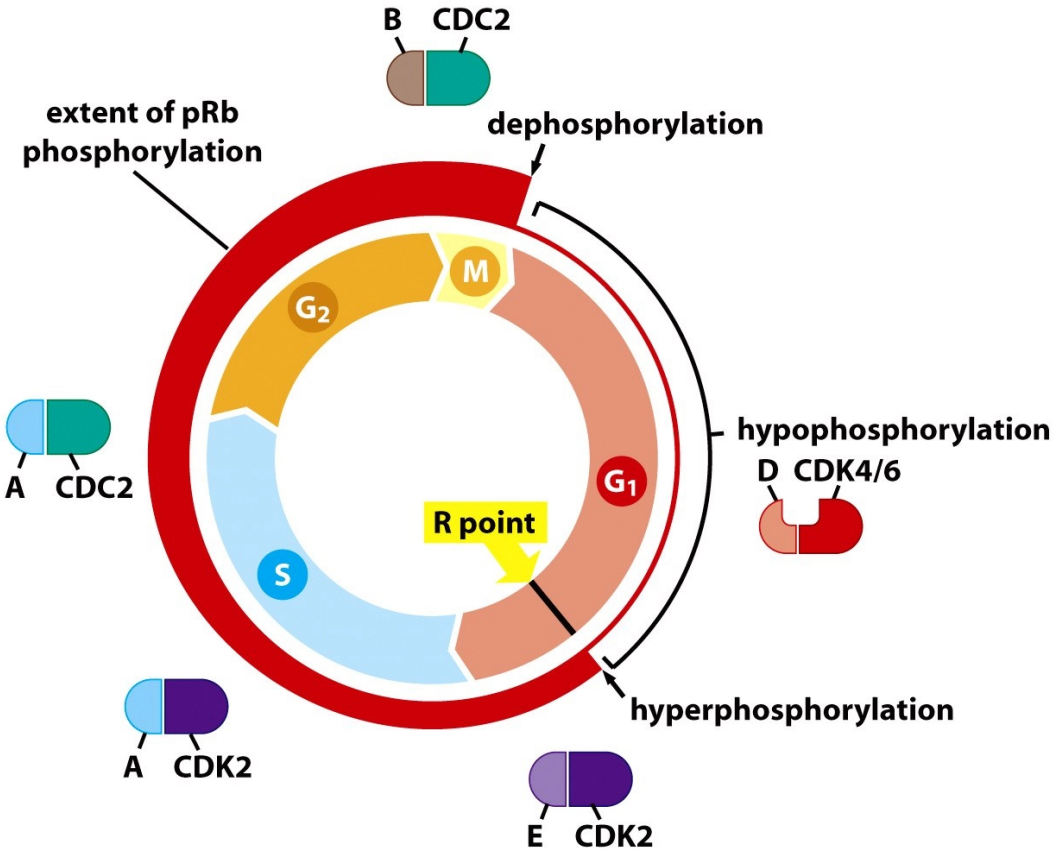

Figure 1.11: Cell cycle-dependent phosphorylation of pRb. The phosphorylation state of pRb (red circle) is controlled by CDK-cyclin complexes and increases throughout the cell cycle from G_1 to M phase. Its dephosphorylation is conducted by PP1 at the end of mitosis (modified after Weinberg, 2013). pRb: retinoblastoma protein, CDC2: cell division control protein 2 homolog (also known as CDK1), CDK: cyclin-dependent kinase, R point: restriction point, PP1: protein phosphatase 1.

An important substrate of CDK-cyclin complexes is the retinoblastoma protein (pRb), a master regulator of the cell cycle. pRb becomes hypophosphorylated by CDK4/6-cyclin D complexes in early and mid G_1. In its unphosphorylated or hypophosphorylated state, it binds to E2F transcription factors, hence repressing the transcription of E2F-controlled genes. When CDK2-cyclin E is activated in late G_1, it further phosphorylates pRb (Figure 1.11). In its hyperphosphorylated state, pRb releases E2F and allows expression of the repressed genes, whose products, for instance proteins involved in DNA replication, guide the cell into S phase. The hyperphosphorylation of pRb is maintained throughout the remaining cell cycle, until it is dephosphorylated at

the end of mitosis by protein phosphatase 1 (PP1) (Sears and Nevins, 2002; Stevaux and Dyson, 2002; Kolupaeva and Janssens, 2013).

Five checkpoints are integrated in the cell cycle that monitor the conditions required for proceeding to the next phase, and can halt the cell cycle when necessary. The first checkpoint, G_1 checkpoint or R point, occurs in late G_1. At this point, the cell decides whether to stay in G_1, proceed to S phase, or even exit from the cell cycle and reach a quiescent state (G_0) (Malumbres and Barbacid, 2001; Massagué, 2004). This decision is based on the integration of intra- and extracellular signals providing information on the cell's metabolic state, stress and the availability of nutrients and growth factors. The R point is a "point of no return" as once the cell has decided to enter S phase, this decision cannot be reversed. The transition from G_1 to S phase is controlled by the G_1/S checkpoint, which deters the cell from replicating its DNA in case of DNA damage. The next checkpoint occurs in S phase. Here, the ongoing DNA synthesis is slowed down or halted if DNA damage is sensed. The G_2/M checkpoint at the transition from G_2 to M phase deters the cell from initiating mitosis in case of DNA lesions. All three DNA damage checkpoints are controlled by the ATM (ataxia telangiectasia mutated)/ATR (ataxia telangiectasia and Rad3-related protein)-Chk1/Chk2 (checkpoint kinase 1/2) pathway (Kastan and Bartek, 2004). The spindle assembly checkpoint, occurring at the metaphase-to-anaphase transition, blocks anaphase onset if mitotic chromosomes are not properly attached to spindle microtubules (see subsection 1.3.4).

1.3.2 Interphase

In both gap phases, the cell grows and produces components required to conduct DNA replication or mitosis, for example nucleotides, RNA and proteins. It also has to increase the amount or size of organelles and cytosol, in order to establish two daughter cells.

In S phase, the chromosomes are duplicated. DNA replication begins at multiple origins of replication, special regions on the chromosomes on which replication is initiated. The initiation of replication is divided into two steps. Already at the end of mitosis of the previous cell cycle, and in early G_1 when CDK activity is low, the replication origins are loaded with the pre-replicative complex (preRC), which consists of the origin recognition complex (ORC), cell division cycle 6 (CDC6) kinase, chromatin licensing and DNA replication factor 1 (CTD1) and mini-chromosome maintenance (MCM) proteins (Massagué, 2004). At S phase onset, activated CDK2 phosphorylates MCM proteins, thus initiating the recruitment of DNA helicases, primases and polymerases to the preRCs to form even larger protein complexes, the pre-initiation complexes (preICs) (Costa *et al.*,

2013). They unwind the DNA double helix and initiate DNA synthesis. Simultaneously to the initiation of replication, CDK2 triggers the disassembly of the PRC by phosphorylating ORC and CDC6. Hence, preRC re-assembly is inhibited at the newly replicated origin until CDK activity drops at the end of mitosis (Kelly and Brown, 2000; Prasanth *et al.*, 2004). Chromosome duplication not only requires replication of the DNA, but also the duplication of chromatin proteins and their proper assembly on the DNA. The synthesis of chromatin proteins increases during S phase, and CDK2-cyclin E complexes have been shown to stimulate expression of the four histone subunits (Kelly and Brown, 2000). At the end of S phase, each duplicated chromosome consists of two identical sister chromatids held together along their chomosome arms by cohesin protein complexes. This sister-chromatid cohesion is required for successful mitosis as it facilitates attachment of the chromatids to the spindles (Zou, 2011).

1.3.3 Mitosis and cytokinesis

In mitosis, the duplicated sister chromatids are segregated and packed into two new daughter nuclei. This process is divided into five phases: prophase, prometaphase, metaphase, anaphase, and telophase (Figure 1.12). In prophase, the chromosomes condense yielding the mitotic chromosome structure, and the mitotic spindle begins to assemble. Prometaphase begins with nuclear envelope break down (NEBD). Subsequently, the chromosomes attach to spindles via their kinetochores. In metaphase, the chromosomes align at the spindle equator, and their kinetochores achieve a bi-polar attachment to kinetochore microtubules. In anaphase, the formation of central spindles occurs, and the sister chromatids are pulled to opposite spindle poles. Telophase is characterized by the decondensation of the segregated chromosomes and the reassembly of the nuclear envelope.

Mitosis is regulated by the cell cycle machinery in two major steps. The abrupt increase of CDK1-cyclin B activity at the G_2/M transition induces the events of early mitosis, while activation of the anaphase-promoting complex/cyclosome (APC/C) facilitates the processes from metaphase-to-anaphase transition onward.

At the G_2/M transition, the CDK1-cyclin B complex is activated. It phosphorylates condensin, a protein complex involved in chromosome condensation and sister chromatid resolution, which facilitates the re-organization of the chromosomes to gain their mitotic structure (Ono *et al.*, 2003). Parallel with chromosome restructuring, CDK1-cyclin B induces spindle assembly. The centrosome duplication, however, already begins when the cell enters S phase triggered by CDK2-cyclin E (Winey, 1999). The mitotic spindle apparatus is a bipolar array of microtubules, which spread between the two spin-

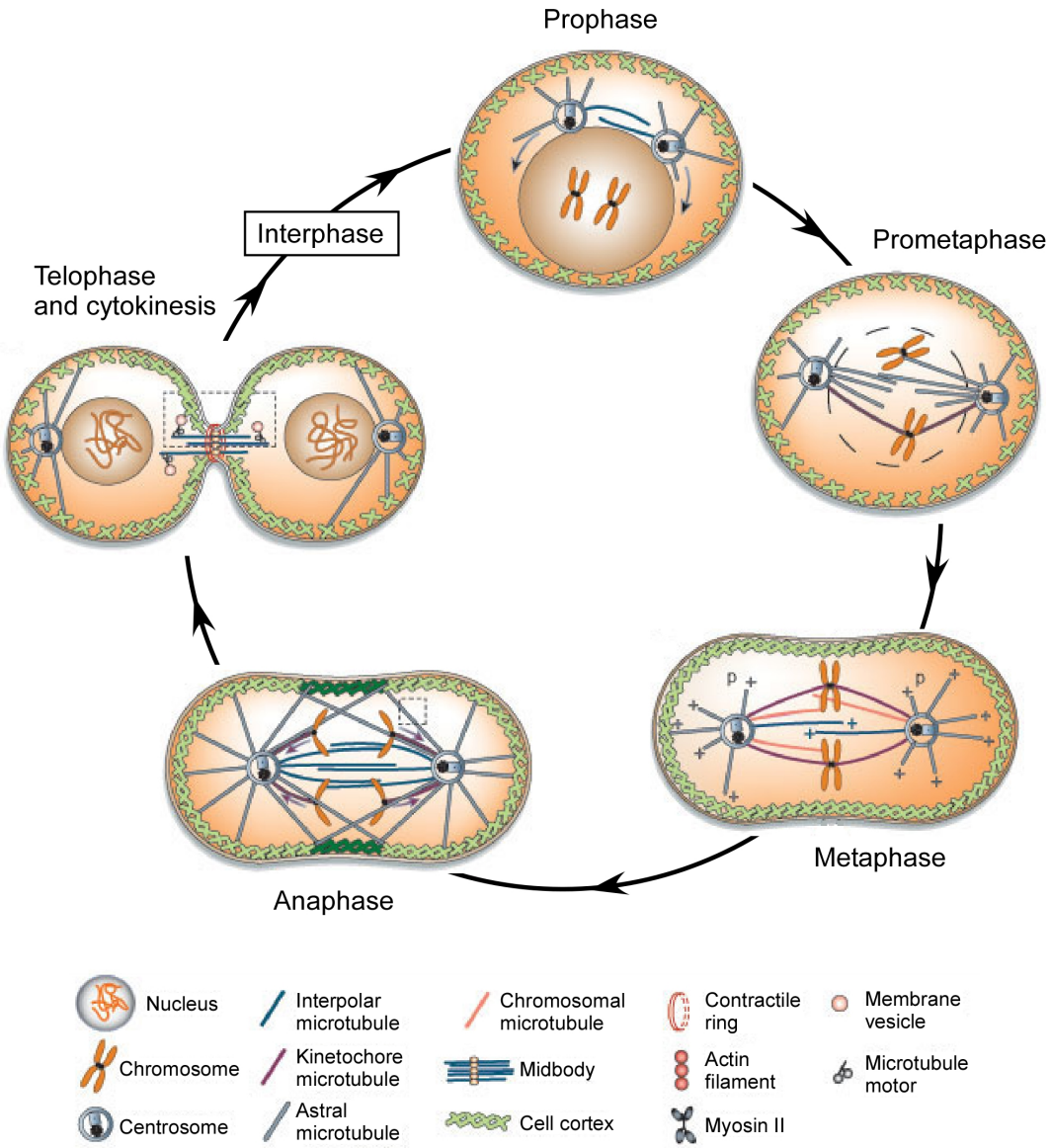

Figure 1.12: The phases of mitosis. Mitosis, the division of the nucleus containing the duplicated DNA, occurs in five subsequent steps: prophase, prometaphase, metaphase, anaphase and telophase. Shortly after the end of telophase, cytokinesis, the partitioning of the cytoplasm, is completed yielding two new daughter cells (modified after Scholey *et al.*, 2003).

dle poles organized by centrosomes. Three types of microtubules emanate from the spindle poles where they are anchored with their minus ends: interpolar microtubules interacting with microtubules from the opposite pole, kinetochore microtubules, which attach to the kinetochores of the metaphase chromosomes, and astral microtubules radiating outward to contact the cell cortex. The assembly and function of spindles depend on microtubule-dependent motor proteins, for example kinesins and dyneins (Glotzer, 2009).

As centrosomes and microtubules are located in the cytoplasm, the attachment of spindles to the chromosomes in prometaphase requires the disassembly of the nuclear envelope. NEBD is initiated by the phosphorylation of subunits of the nuclear pore complexes and the nuclear lamina by CDK1-cyclin B (Alvarez-Fernández and Malumbres, 2014). During prometa- and metaphase, the stability of microtubules decreases, while the ability of centrosomes to nucleate new microtubules increases, creating a dense and dynamic array of spindles. These changes are also induced by CDK1-cyclin B phosphorylation of motor proteins and microtubule-associated proteins (Glotzer, 2009). The attachment of microtubules to kinetochores is conducted by a search-and-capture mechanism. Stable attachment occurs when the kinetochores of each sister chromatid bind to spindles from opposite spindle poles (bipolar or amphitelic attachment). Incorrect attachments, such as syntelic (both kinetochores bind to microtubules emanating from the same pole) and merotelic (a single kinetochore binds to microtubules from both spindle poles) attachments, are not stabilized (Ruchaud *et al.*, 2007; Cheerambathur and Desai, 2014; Pavin and Tolić-Nørrelykke, 2014).

Sensing and correction of erroneous microtubule-kinetochore attachments occurs at the spindle assembly checkpoint in metaphase. The mitotic kinase Aurora B, the enzymatic subunit of the chromosomal passenger complex (see subsection 1.3.4), senses proper attachments via the presence of tension at the kinetochore. In the absence of tension, Aurora B phosphorylates components of the microtubule attachments sites on kinetochores, thus decreasing the sites' affinity for microtubule plus ends. The SAC also blocks the APC/C until all chromosomes have achieved a correct bi-orientation (Foley and Kapoor, 2013). Once all chromosomes are attached correctly, chromosome congression can take place: the chromosomes are positioned at the spindle equator forming the metaphase plate, and the cell can progress to anaphase.

Anaphase begins with the sudden disruption of sister chromatid cohesion induced by the APC/C, which is also activated by CDK1-cyclin B. The APC/C targets securin, an inhibitor of the protease separase, for degradation allowing separase-mediated cohesin cleavage. In addition, the APC/C mediates degradation of cyclins A and B, thus inactivating CDKs. Anaphase proceeds in two steps: in anaphase A, the chromatids move

polewards, accompanied by the shortening of kinetochore microtubules. In anaphase B, the spindle poles are separated. Completion of anaphase requires dephosphorylation of CDK substrates resulting from the APC/C-dependent degradation of cyclins (Kim and Yu, 2011).

In telophase, the mitotic spindle disassembles and the nuclear envelope is rebuilt. First, fragments of the nuclear membrane associate with the chromosomes, then fuse to form a continuous membrane. Nuclear pore complexes are incorporated, and last, the nuclear lamina is re-assembled. The chromosomes decondense to allow gene transcription. For these processes, also the APC/C-induced dephosphorylation of CDK substrates is necessary (Schooley *et al.*, 2012).

Cytokinesis, the division of the cytoplasm, already begins in anaphase and is completed shortly after telophase. During chromosome segregation in anaphase, actin and myosin filaments as well as various structural and regulatory proteins dynamically assemble to form a contractile ring at the equatorial cell cortex. After anaphase is completed, the ring contracts gradually, while intracellular vesicles fuse with the plasma membrane adjacent to the ring promoting cleavage furrow ingression. When cleavage is completed, the plasma membrane of the cleavage furrow forms the midbody. It also contains remains of the central spindle and functions as an intercellular bridge between the two daughter cells until they are completely separated by abscission. The assembly and function of the contractile ring is controlled by the small GTPase ras homolog family member A (RhoA), which in turn is regulated by the CPC (Carmena *et al.*, 2012; Agromayor and Martin-Serrano, 2013; Chircop, 2014).

1.3.4 The CPC in mitosis and cytokinesis

As mentioned above, the CPC regulates crucial events in mitosis and cytokinesis, for instance the correction of kinetochore-microtubule attachment errors, the activation of the SAC as well as the formation and function of the contractile ring (Carmena *et al.*, 2012) (Figure 1.13). It consists of a kinase module comprising Aurora B and the C-terminus of INCENP, and a localization module consisting of Survivin, Borealin and INCENP's N-terminus which form a stable three-helical bundle (Jeyaprakash *et al.*, 2007) (Figure 1.8).

Aurora B, together with Aurora A, which functions at the spindle poles, and Aurora C, which regulates meiosis and mitosis in early development, belongs to a family of highly conserved serine/threonine kinases (Glover *et al.*, 1995; Carmena *et al.*, 2009). It requires INCENP binding to become activated, a mechanism similar to the activation of

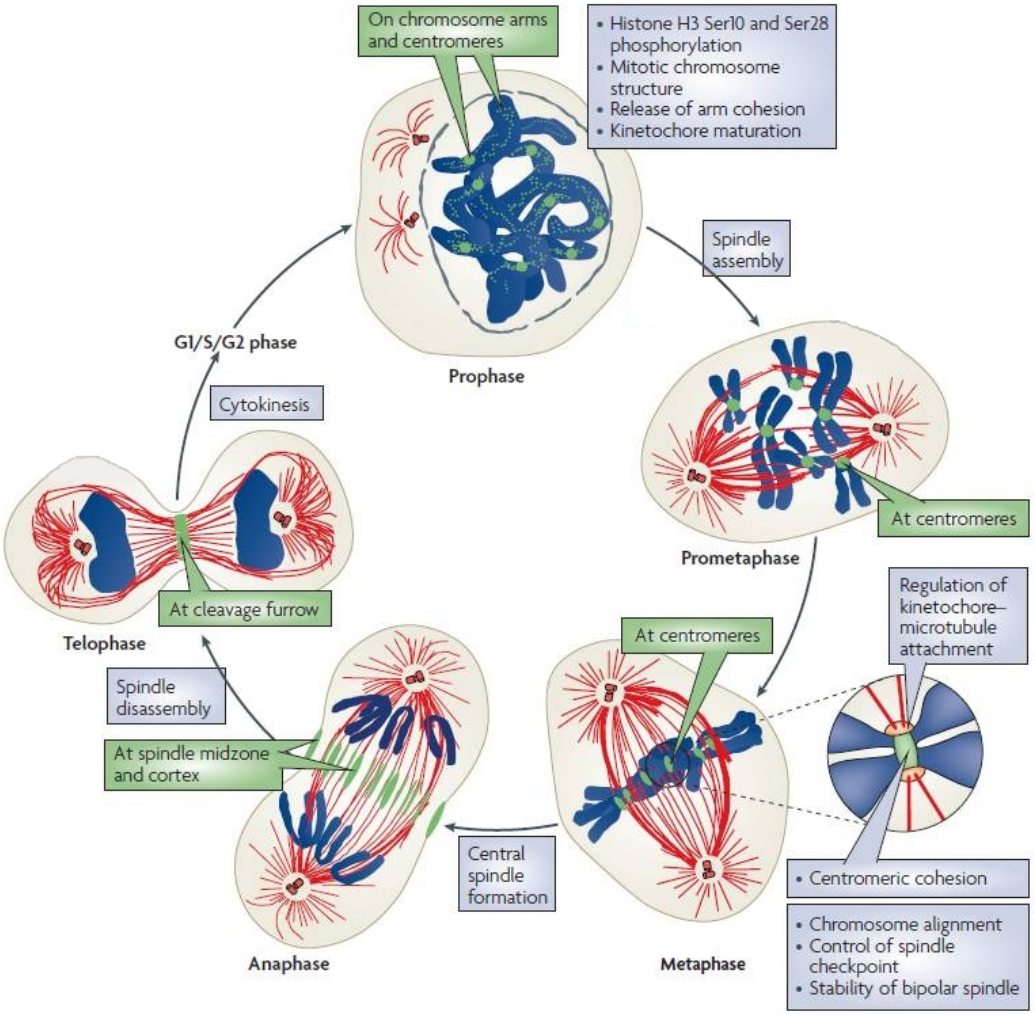

Figure 1.13: Localization and function of the CPC during mitosis. The CPC (green) is localized to chromosome arms and centromeres in prophase. In prometaphase, it concentrates at centromeres, where it remains during metaphase. The relocalization of the CPC to the spindle midzone and the cell cortex occurs in anaphase. In telophase, the CPC localizes to the cleavage furrow. The functions of the CPC during the different phases of mitosis are indicated in blue boxes. Tubulin is depicted in red, chromosomes are shown in blue (modified after Ruchaud *et al.*, 2007).

CDKs by cyclins. Besides being a regulator of Aurora B activity, INCENP also serves as a scaffold for CPC assembly, and is required for proper localization of the CPC together with Survivin and Borealin (Ainsztein *et al.*, 1998; Jeyaprakash *et al.*, 2007). The activation of Aurora B is a complex multistep process. Once the CPC has assembled, Aurora B is partially active due to its binding to INCENP's C-terminus. This enables Aurora B to phosphorylate INCENP's TSS motif and T232 in the T-loop of its kinase domain in *trans* resulting in further Aurora B activation (Bishop and Schumacher, 2002; Sessa *et al.*, 2005). The necessity of a second CPC for Aurora B activation explains its density-dependent activation at inner centromers and the spindle midzone (Kelly *et al.*, 2007; Fuller *et al.*, 2008) (Figure 1.14). Complete activation of Aurora B requires its phosphorylation by Chk1 and phosphorylation of Survivin at S20 by PLK1 (Petsalaki *et al.*, 2011; Chu *et al.*, 2011). In early mitosis, Aurora B phosphorylates multiple substrates at the kinetochore to destabilize and correct erroneous kinetochore-microtubule attachments. To gain stable attachments, which are required in prometaphase and transition to anaphase, the phosphorylation has to be removed from Aurora B substrates. This is achieved by the recruitment of antagonistic phosphatases like PP1 or PP2A (Meadows *et al.*, 2011; Foley *et al.*, 2011). It has been proposed that the concentrations of Aurora B and its counteracting phosphatases are spatially regulated: upon the formation of a bipolar kinetochore-microtubule attachment, tension is generated which stretches the kinetochore. Hence, Aurora B substrates are pulled away from the inner centromer where Aurora B activity is high (Lampson and Cheeseman, 2011).

In interphase, the CPC localizes to heterochromatin via the interaction of INCENP with heterochromatin protein 1 (HP1). HP1 directly binds to histone H3 tri-methylated at K9 (H3K9Me3), which is a typical histone modification found in transcriptionally silenced heterochromatin (Ainsztein *et al.*, 1998; Zeng *et al.*, 2010). At onset of mitosis, Aurora B phosphorylates H3 at the adjacent S10, which causes dissociation of HP1 from H3 (Hirota *et al.*, 2005). The following enrichment of the CPC at centromeres is achieved by direct and indirect binding to mitosis-specific phosphorylation marks: Haspin kinase, located at the inner centromer, phosphorylates histone H3 at T3, which is recognized and bound by Survivin's BIR domain. Additionally, the kinetochore-associated kinase budding uninhibited by benzimidazoles 1 (BUB1) phosphorylates histone H2A at T120 (H2AT120Ph). Subsequently, Shugoshin 1 (Sgo1) and Shugoshin 2 (Sgo2) are recruited to H2AT120Ph and interact with Borealin that has been phosphorylated by CDK1 (Yamagishi *et al.*, 2010; Kawashima *et al.*, 2007) (Figure 1.15). In addition, a recent study by Liu *et al.* (2014) has revealed that Borealin can directly bind to HP1α and that this interaction is required for targeting the CPC to centromeres.

One proposed role of the CPC in prophase is the regulation of chromosome conden-

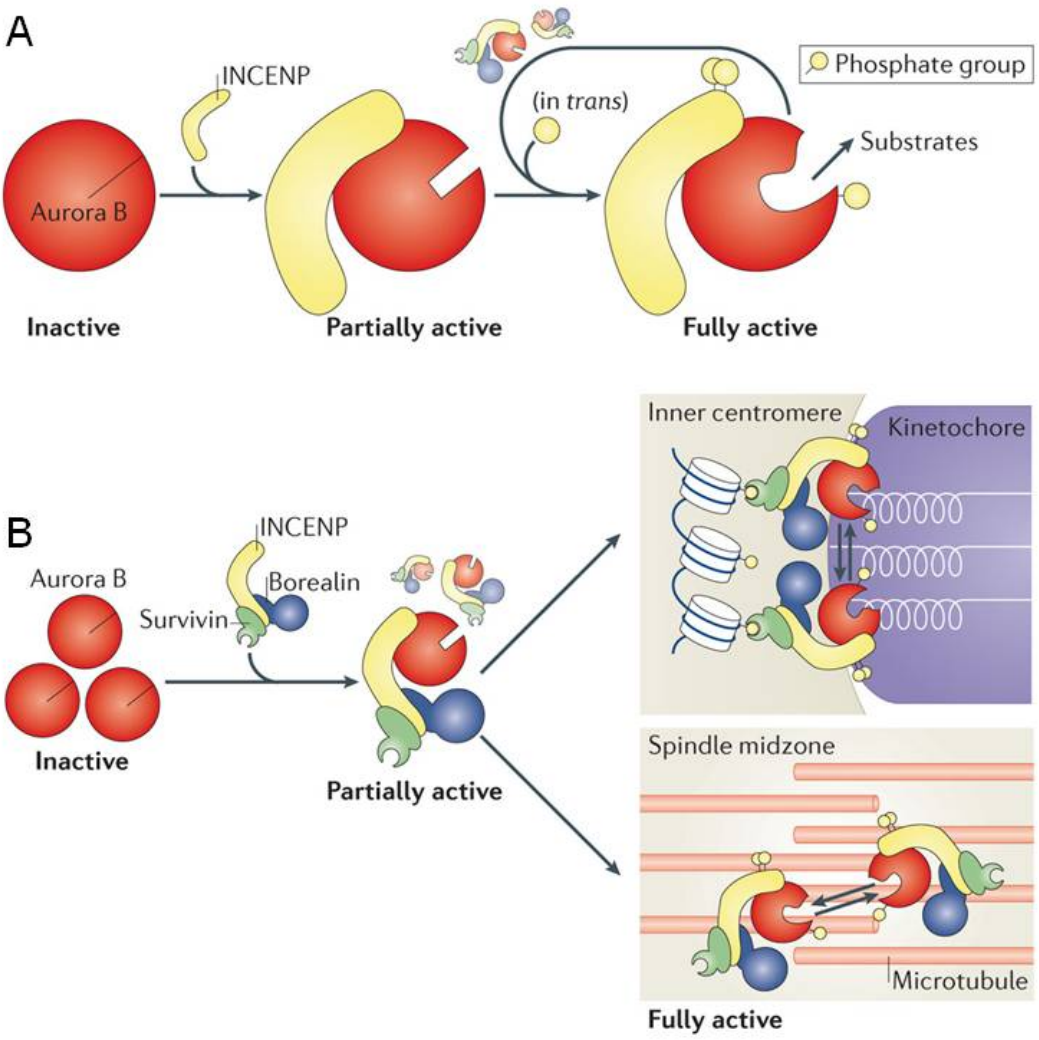

Figure 1.14: Aurora B kinase activation. Activation of Aurora B is coupled to CPC formation and function. A) Aurora B requires binding to INCENP to become partially activated. Subsequently, it phosphorylates INCENP and itself to gain full activity. Both phosphorylation events are catalyzed in *trans*. B) Autophosphorylation of Aurora B requires a second CPC. This prerequisite is fulfilled at sites of high CPC density like the inner centromere and the spindle midzone (modified after Carmena *et al.*, 2012).

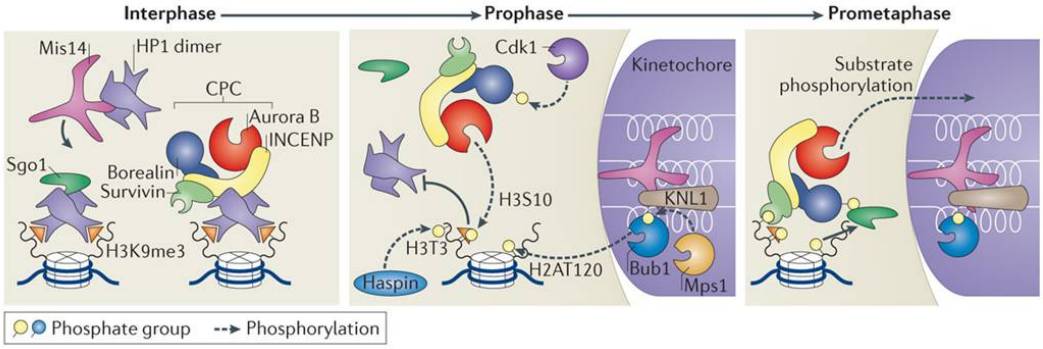

Figure 1.15: Recruitment of the CPC to centromeres in early mitosis. In interphase, the CPC is recruited to heterochromatin via the interaction of INCENP with HP1. In prophase, phosphorylation of centromeric histone tails by the mitotic kinases Aurora B, Haspin and BUB1 induces displacement of HP1, and the recruitment of the CPC to inner centromers via the interaction of Survivin with H3T3Ph by prophase (modified after Carmena *et al.*, 2012). MIS14: Mum2p-Ime4p-Slz1p protein 14, HP1: heterochromatin protein 1, CPC: chromosomal passenger complex, SGO1: Shugoshin 1, H3K9me3: histone H3 tri-methylated at lysine 9, CDK1: cyclin-dependent kinase 1, H3S10: histone H3 serine 10, H3T3: histone H3 threonine 3, H2AT120: histone H2A threonine 120, KNL1: kinetochore-null protein 1, BUB1: budding uninhibited by benzimidazoles 1 kinase, MPS1: metallopan-stimulin 1.

sation by targeting condensin (Collette *et al.*, 2011). As mentioned above, in prometaphase, the function of the CPC is to destabilize and correct erroneous kinetochore-microtubule attachments. The KMN (KNL1-MIS12-NDC80) network, a microtubule-binding module of the outer kinetochore comprising the KNL1 (kinetochore-null protein 1), MIS12 (named after the yeast proteins Mum2p, Ime4p and Slz1p) and NDC80 (nuclear division cycle 80) complexes, captures plus-ends of dynamic microtubules. Aurora B weakens its affinity for microtubules by phosphorylating the N-terminus of NDC80 at multiple sites (Powers *et al.*, 2009; DeLuca *et al.*, 2006; Cheeseman *et al.*, 2006). It also regulates other microtubule stabilizing or destabilizing proteins at the kinetochore, for example the mitotic centromere-associated kinesin (MCAK) (Lan *et al.*, 2004).

In metaphase, the CPC controls the spindle assembly checkpoint. A proposed mechanism for SAC activation by Aurora B is the recruitment of SAC proteins, for instance mitotic arrest deficient 1-like proteins 1 and 2 (MAD1/2), to kinetochores in the absence of bipolar attachments (Ditchfield *et al.*, 2003; Vigneron *et al.*, 2004; Saurin *et al.*, 2011). The interaction of these two proteins at kinetochores results in the binding of MAD2 to the APC/C activator CDC20, thus preventing it from activating the APC/C. The accumulation of further proteins results in the formation of the mitotic checkpoint complex (MCC), which additionally blocks the APC/C (Musacchio and Salmon, 2007; Luo and Yu, 2008). Once a bipolar kinetochore-microtubule attachment is achieved, Aurora B activity decreases at kinetochores, while PP1 is recruited (Welburn *et al.*, 2010; Liu and

Mitchell, 2010). PP1 promotes SAC silencing in different ways, for example it reverses the Aurora B-dependent phosphorylation of several SAC proteins releasing them from kinetochores. One result is the activation of the APC/C by CDC20 and the subsequent ubiquitination of its targets cyclin B and securin (Peters, 2006). This indicates that the spatial regulation of phosphorylation/dephosphorylation is essential for SAC activation and silencing.

During metaphase-to-anaphase transition, the CPC leaves the inner centromere to relocate to the spindle midzone, and subsequently to the equatorial cortex (Figure 1.16A). The relocation is initiated by the APC/C-mediated decrease of CDK1 activity and driven by three different processes: the termination of CPC targeting to centromeres, its active removal from chromosomes, and its targeting to the central spindle (Carmena *et al.*, 2012). The centromeric localization of the CPC is abrogated by the dephosphorylation of H3T3Ph by PP1 (Qian *et al.*, 2011). Its active removal from chromosomes upon ubiquitination is conducted by the AAA^+ ATPase p97. This process also facilitates chromosome decondensation as well as nuclear reformation in telophase (Ramadan *et al.*, 2007; Dobrynin *et al.*, 2011). The targeting to the central spindle requires interaction of INCENP and Aurora B with mitotic kinesin-like protein 2 (MKLP2), which binds to microtubules at the central spindle only during anaphase, when CDK1-mediated inhibitory phosphorylation is removed (Hümmer and Mayer, 2009). Central spindle formation is facilitated by the CPC by recruiting the protein complex centralspindlin. Phosphorylation of a centralspindlin component by Aurora B increases its microtubule-bundling activity, thus stabilizing the central spindle (Kaitna *et al.*, 2000; Douglas *et al.*, 2010).

During cytokinesis, the CPC contributes to the maturation and constriction of the contractile ring by indirectly regulating the small GTPase RhoA via centralspindlin recruitment to the spindle midzone (Figure 1.16B). RhoA fosters actin polymerization and myosin activation (Nishimura and Yonemura, 2006; Touré *et al.*, 2008). Another role of the CPC in contractile ring constriction is the phosphorylation of intermediate filament components which facilitates their disassembly (Kawajiri *et al.*, 2003). During abscission, the final step of cytokinesis, Aurora B is involved in the abscission checkpoint, which delays the separation of the daughter cells in case lagging chromatin is present in the intercellular bridge (Steigemann *et al.*, 2009). The CPC can possibly also inhibit components of the ESCRT-III complex, which mediates membrane fission at the end of cytokinesis, thus deferring premature cytokinesis (Capalbo *et al.*, 2012; Carlton *et al.*, 2012).

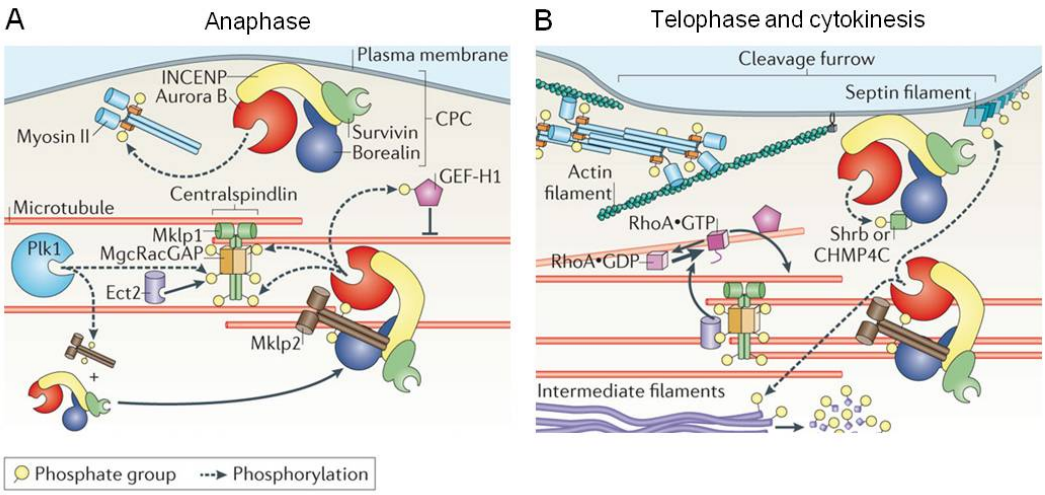

Figure 1.16: Localization and function of the CPC in late mitosis. At anaphase onset, the CPC relocalizes from chromosomes to the spindle midzone, and subsequently to the cell cortex. In telophase and cytokinesis, the CPC is found at the cleavage furrow. A) CPC targeting to the central spindle in anaphase requires its interaction with MKLP2. Central spindle formation is promoted by the CPC as it recruits centralspindlin to the spindle midzone. B) During telophase and cytokinesis, the CPC contributes to the maturation and constriction of the contractile ring as it indirectly regulates RhoA via the recruitment of centralspindlin. It also mediates intermediate filament phosphorylation, thus facilitating their disassembly (modified after Carmena *et al.*, 2012). PLK1: polo-like kinase 1, MKLP1/2: mitotic kinesin-like protein 1/2, MgcRacGAP: male germ cell RacGAP, ECT2: epithelial cell-transforming 2, CPC: chromosomal passenger complex, GEF-H1: guanine nucleotide exchange factor H1, CHMP4C: charged multivesicular body protein 4C.

1.4 Nucleo-cytoplasmic transport

The cell nucleus is separated from the cytoplasm by the nuclear envelope (NE). It is formed of the outer nuclear membrane (ONM), which is continuous with the endoplasmic reticulum (ER), and the inner nuclear membrane (INM) separated from the ONM by a luminal space. Nuclear pore complexes (NPCs) are distributed throughout the NE at fusion sites between the outer and inner nuclear membrane (Schooley *et al.*, 2012; Grossman *et al.*, 2012). The NPCs contribute to the function of the NE as a selective physical barrier. They allow free diffusion of all small molecules up to a size of 20 kDa, for example water, ions, metabolites and small proteins. Dependent on their surface properties, even larger molecules up to a size of approx. 60 kDa can passively diffuse through NPCs. Despite the possibility to passively diffuse into the nucleus, proteins with a molecular weight between 20 and 60 kDa mostly undergo active transport as it is more efficient and can be regulated by the cell. Molecules larger than 60 kDa like proteins or RNAs must be actively transported through the pore with the assistance of soluble transport receptors (Yoneda, 2000).

The NPC is a large cylindrical protein complex with octagonal symmetry comprising approx. thirty different nucleoporin proteins (Nups), which are present in multiple copies (Figure 1.17). Its core scaffold consists of two inner and outer rings of Nups. Two transmembrane rings connected to the core scaffold anchor the NPC to the nuclear envelope. Attached to the inside of this scaffold are linker Nups which, together with the inner ring, serve as attachment sites for Nups with phenylalanine-glycine repeats (FG Nups). A gel-like matrix of FG Nups inside the central tube of the NPC serves as a mechanical barrier and mediates translocation of transport receptor-cargo complexes. Eight large filaments protrude into the cytoplasm, whereas a basket structure is attached to the nuclear face of the central core. Both structures mediate transport receptor-cargo docking to the NPC (Wente and Rout, 2010; Turner *et al.*, 2012).

Active transport of a cargo protein through the NPC requires three prerequisites: existence of a localization signal, binding to a transport receptor, and energy (Figure 1.18). For the import into the nucleus, a nuclear localization signal (NLS) is needed. The classical NLS is a cluster of basic amino acids and can be mono- or bipartite (Goldfarb *et al.*, 1986; Hodel *et al.*, 2001). Proteins undergoing nuclear export contain a nuclear export signal (NES), a leucine-rich stretch of hydrophobic amino acids (Kutay and Güttinger, 2005). Some proteins shuttling between nucleus and cytoplasm possess NLSs as well as NESs which can also function in a cooperative manner. Most of the transport receptors are karyopherins. Except for NLS-mediated import, which often requires cargo recognition by an adapter protein, for example Importin-α, the karyopherins di-

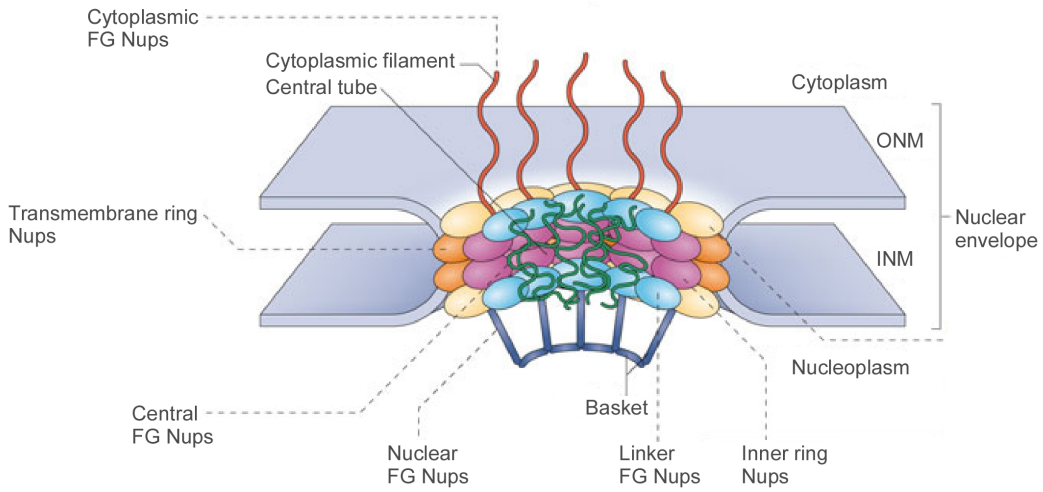

Figure 1.17: Structure of the nuclear pore complex. The NPC is a cylindrical, octagonal protein complex comprised of specialized nucleoporins that form distinct structures. The FG Nups of the cytoplasmic filaments, the nuclear basket and those filling the central tube mediate the selective passage of transport receptor-cargo complexes through the NPC (modified after Strambio-De-Castillia *et al.*, 2010). NPC: nuclear pore complex, Nup: nucleoporin, FG: phenylalanine-glycine, ONM: outer nuclear membrane, INM: inner nuclear membrane.

rectly bind to their cargo proteins. In addition, they interact with the small GTPase Ran, which produces the energy necessary for the transport. The different concentrations of GTP-bound Ran (RanGTP) – high in the nucleus and low in the cytoplasm – form the RanGTP gradient driving transport via the NPC. The gradient is maintained by the nuclear Ran guanine nucleotide exchange factor (RanGEF) regulator of chromosome condensation 1 (RCC1) , which is tethered to chromatin, and the cytoplasmic Ran GTPase activating protein (RanGAP) RanGAP1 (Fung and Chook, 2014). To be imported, a cargo protein must be recognized by its specific import receptor, e.g. Importin-β, which mediates docking and passage through the NPC. In the nucleus, dissociation of the complex is stimulated by RanGTP. Subsequently, the RanGTP-bound import receptor is recycled to the cytoplasm and released from RanGTP following RanGAP1-induced GTP hydrolysis. For export, a specific export receptor, for example CRM1 (also known as Exportin1), binds its cargo protein in the presence of RanGTP. This trimeric complex can then pass the central channel of the NPC to reach the cytoplasm. Here, RanGAP1 activates Ran to hydrolyze GTP to GDP resulting in the dissociation of the complex. The cargo is released and the export receptor as well as RanGDP are recycled back to the nucleus, where RCC1 exchanges GDP by GTP (Turner *et al.*, 2012; Tran *et al.*, 2014; Mor *et al.*, 2014).

The docking and passage of transport receptor-cargo complexes through the NPC is mediated by interactions of the FG repeats of FG Nups inside the NPC and HEAT

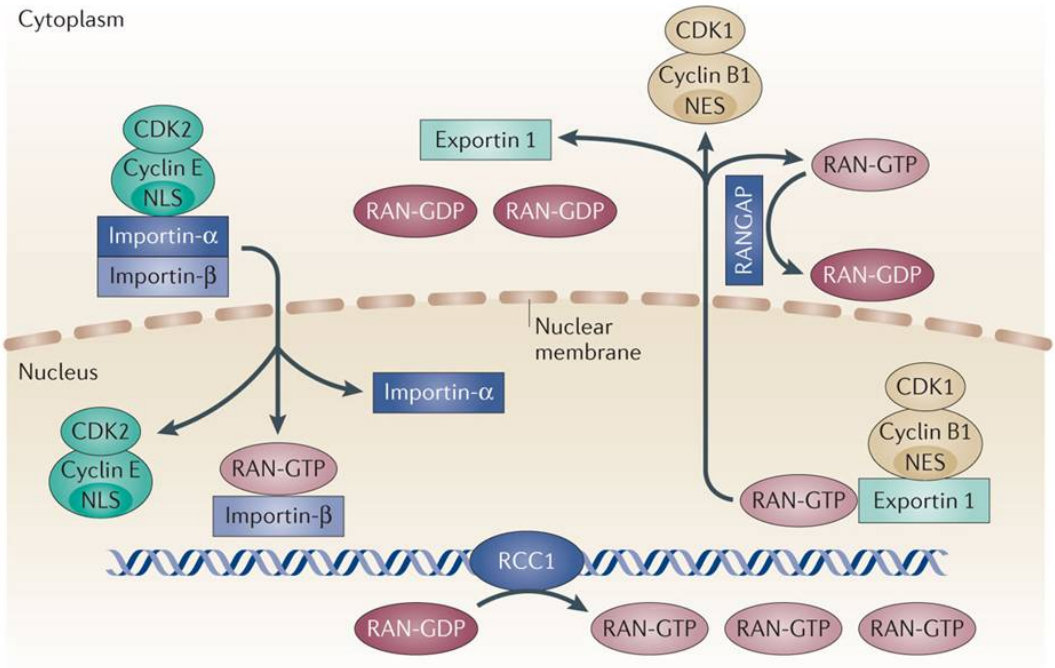

Figure 1.18: Nucleo-cytoplasmic transport. Schematic representation of the export of NES-containing proteins and the import of NLS-containing proteins. Cargo proteins (here exemplarily CDK-cyclin complexes) bind to their transport receptors, Exportin 1 (or CRM1) for export and a complex of Importin-α and Importin-β for import, which mediate passage through the nuclear pore. Transport is driven by a Ran-GTP gradient, which is maintained by the cytoplasmic GAP RanGAP1 and the nuclear GEF RCC1 (modified after Moore, 2013). CDK: cyclin-dependent kinase, NLS: nuclear localization signal, NES: nuclear export signal, GTP: guanosine triphosphate, GDP: guanosine diphosphate, GAP: GTPase activating protein, GEF: guanine nucleotide exchange factor.

repeat domains (named after the proteins Huntingtin, elongation factor 3, protein phosphatase 2A, and the yeast kinase target of rapamycin kinase 1) of the receptors. The FG repeat regions of FG Nups are disordered and form a dense mesh of filaments that fills the central tube and serves as a barrier for larger molecules. Karyopherins overcome this barrier by binding to the FG Nups and passing from one Nup to the next. Several models have been proposed describing how passage might occur. The hydrogel model is based on crosslinks of FG repeats forming a dense hydrophobic gel. Transport receptors can pass through the gel by binding the FG repeats, therefore transiently and locally dissolving the crosslinks (Frey *et al.*, 2006). In the brush model FG Nups are understood as polymer brushes: by rapid diffusion-driven movements their filaments sweep away macromolecules, but transport receptors can overcome this by binding to FG Nups (Lim *et al.*, 2007).

In addition to its role as a highly selective, bidirectional transporter, the NPC, or its components, are also involved in other processes. In mitosis, for instance, Nups are important for kinetochore function (Roux and Burke, 2006). In interphase, Mad pro-

teins, which are involved in the spindle assembly checkpoint, are docked to the NPC, but are released in mitosis (Iouk *et al.*, 2002; Lee *et al.*, 2008).

1.4.1 CRM1

CRM1 (also known as Exportin 1) is an ubiquitous nuclear export receptor for NES-containing proteins (Fornerod *et al.*, 1997; Daelemans *et al.*, 2005). It consists of 21 HEAT repeats arranged in a distorted toroid structure. RanGTP is enclosed in the ring and stabilizes it. Cargo proteins bind to the exterior of the toroid at a hydrophobic cleft whose accessibility for the cargo is regulated by RanGTP binding (Monecke *et al.*, 2009). The components of the export complex – CRM1, RanGTP and the cargo protein – interact with positive cooperativity: the affinity of CRM1 to either RanGTP or a NES protein is weak. However, when both proteins bind to CRM1, the affinity for both increases by 500-1000 fold (Turner *et al.*, 2012).

In addition to its role as an export receptor in interphase, CRM1 also has crucial functions during mitosis. Arnaoutov *et al.* (2005) have reported that CRM1-RanGTP complexes localize to kinetochores in mitosis, and that this localization is essential for the formation of stable kinetochore fibers as well as for proper chromosome segregation during anaphase. Moreover, as shown by Knauer *et al.* (2006), the interaction of CRM1 with its cargo Survivin is required for the correct localization and function of the CPC.

1.5 Post-translational modifications

The post-translational modification (PTM) of proteins allows eukaryotic cells to rapidly alter the functions of existing proteins by transmitting chemical signals across divers cellular pathways. Prominent PTMs are the phosphorylation of serine, threonine and tyrosine residues, proline isomerization, arginine and lysine methylation as well as ubiquitination, sumoylation and acetylation also occurring at lysine residues. Hence, the lysine side chain is a target of different PTMs which are mutually exclusive on the same lysine residue (Yang and Seto, 2008; Arif *et al.*, 2010).

1.5.1 Acetylation

In addition to phosphorylation, the acetylation of the ε-amino group of lysine residues has emerged as a major PTM in eukaryotes. Like phosphorylation, acetylation is able to

influence various protein functions for instance protein-DNA and protein-protein interactions, activation or inactivation of enzymes as well as protein localization and stability (Arif *et al.*, 2010). Lysine acetylation has originally been associated with the regulation of gene transcription as it was first identified in nuclear core histones in the 1960s (Allfrey *et al.*, 1964). The acetylation of histone tails of promotor-proximal nucleosomes results in a lower binding affinity of histones to DNA. Thus, the chromatin packaging is loosened and DNA becomes accessible for transcription factors and coactivators. Only the development of Tubulin as the first cytoplasmic target of lysine acetylation in 1985 revealed that this modification is not restricted to the nucleus (L'Hernault and Rosenbaum, 1985).

Acetylation neutralizes the positive charge of the lysine side chain, thus inhibiting the formation of ionic interactions with other amino acids, and additionally impairs the ability of the lysine side chain to form hydrogen bonds (Figure 1.19). The functional impact of lysine acetylation is context-dependent and varies from protein to protein. Three modes of acetylation events have been identified so far: first, acetylation occurs at one or a few lysine residues and functions as an on/off switch. Second, acetylation occurs at multiple residues within lysine clusters that form charged patches. The third mechanism describes the interplay of acetylation with other PTMs in a site-specific manner, for example acetylation of H3K9 crosstalks with phosphorylation of H3S10 (Yang and Seto, 2008).

Lysine acetylation is a reversible process (Figure 1.19). The transfer of an acetyl group from acetyl-CoA to a lysine residue is catalyzed by lysine acetyltransferases (KATs). KATs are classified into three families according to their homology with yeast proteins: the general control of amino acid synthesis protein 5 (Gcn5)-related N-acetyltransferase (GNAT) family containing for example the human KATs GCN5 and PCAF, the p300/CBP family and the MYST family (named after monocytic leukemia zinc finger protein, Ybf2/Sas3 (something about silencing protein 3), Sas2 and 60 kDa Tat-interactive protein). Although most KATs are predominantly localized in the nucleus, recent studies demonstrated that some of them, for example PCAF and GCN5, undergo nucleo-cytoplasmic transport (Sadoul *et al.*, 2011). Deacetylation is carried out by lysine deacetylases (KDACs), which are divided into four classes according to their relation to yeast proteins. The class I (similar to Rpd3 (reduced potassium dependency 3)), class II (related to Hda1 (histone deacetylase 1)) and class IV KDACs belong to the classical family of Zn^{2+}-dependent KDACs, whereas class III KDACs, also called sirtuins (homologs of Sir2 (silent information regulator 2)), require the cofactor NAD^+ for their activity. Many KDACs contain NES as well as NLS sequences enabling them to shuttle between nucleus and cytoplasm. As KATs and KDACs are acetylated themselves, they are able to

regulate each other's activity by a direct interplay, thus controling the dynamic acetylation state of their target proteins (Yang and Seto, 2008; Peserico and Simone, 2011; Sadoul *et al.*, 2011).

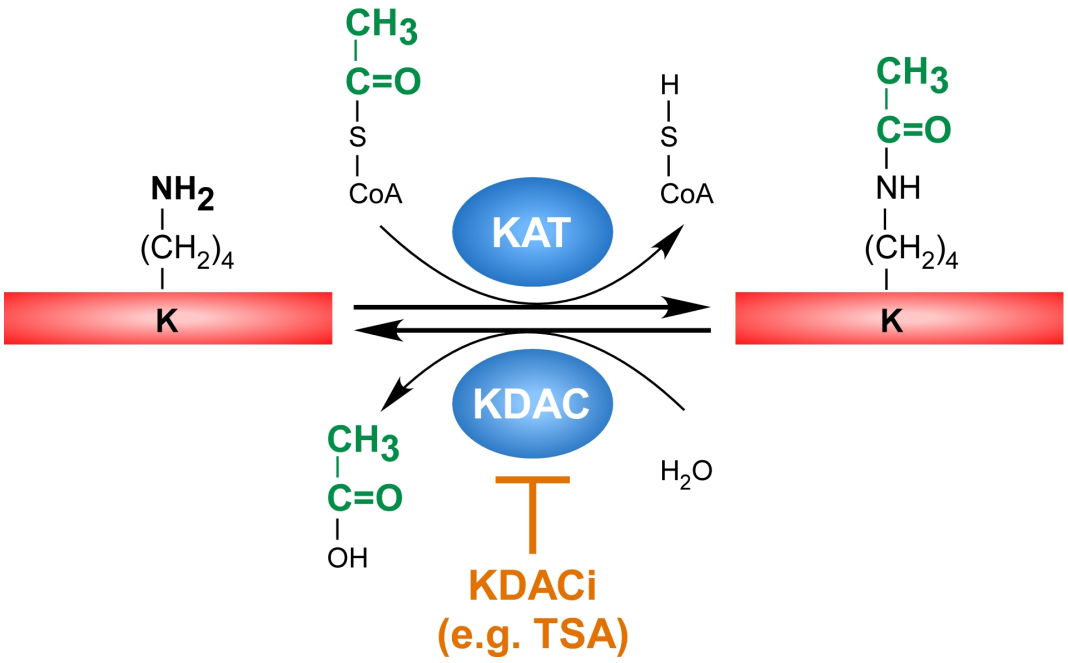

Figure 1.19: Lysine acetylation/deacetylation. Schematic representation of lysine acetylation by KATs and its deacetylation by KDACs. A target protein containing a lysine residue is indicated in red. The KAT and the KDAC are shown as blue spheres. The transferred acetyl group is depicted in green. Deacetylase activity can be inhibited by KDAC inhibitors, such as trichostatin A. K: lysine, KAT: lysine acetyltransferase, KDAC: lysine deacetylase, KDACi: KDAC inhibitor, TSA: trichostatin A.

1.6 Aims of the thesis

Survivin is up-regulated in various human cancers (Ambrosini *et al.*, 1997; Adida *et al.*, 2000). Due to its dual role as an inhibitor of apoptosis and a member of the chromosomal passenger complex, Survivin on the one hand is able to protect tumor cells from therapy-induced apoptosis, and on the other hand provides a proliferative advantage (Engels *et al.*, 2007; Capalbo *et al.*, 2007; Xu *et al.*, 2014; Chen *et al.*, 2014). This makes Survivin an interesting therapeutic target. In order to develop strategies for the therapeutic inhibition of Survivin, the mechanisms underlying the different functions of the protein have to be understood in detail. In case of Survivin this is complicated as some of its functions are conducted by the homodimer (Wang *et al.*, 2010b; Pavlyukov

et al., 2011), while other roles critically rely on the monomer (Jeyaprakash *et al.*, 2007; Engelsma *et al.*, 2007; Pavlyukov *et al.*, 2011). In addition, Survivin's functions are spatially controlled as it is able to shuttle between nucleus and cytoplasm (Rodriguez *et al.*, 2002; Knauer *et al.*, 2006). However, the mechanisms by which Survivin's functions, its localization as well as its dimerization state are regulated are still not clarified in detail. Recently, Wang *et al.* (2010b) reported that acetylation of Survivin at lysine 129 functions as a switch between its monomeric and dimeric state, and that it also regulates Survivin's interaction with the export receptor CRM1.

In this study, we first aimed to verify the results of Wang *et al.* (2010b) concerning the influence of SurvK129 acetylation on Survivin's dimerization and nuclear export. Therefore, the four SurvK129 mutants also used in this study should be cloned and their properties analyzed by means of immunofluorescence stainings, immunoprecipitation, gel filtration as well as CD spectroscopy. Furthermore, we aimed to investigate the role of Survivin acetylated at K129 in mitosis.

In order to gain further insight into the complex regulation of Survivin, we intended to find out whether other lysine residues in Survivin might be subjected to acetylation, and thus to examine the effects of a potential acetylation on Survivin's divers functions. Therefore, the lysine residues most likely to be acetylated should be identified and mutated to arginine or glutamine in order to mimic unmodified or acetylated lysine, respectively. The properties of the mutants should then be analyzed accordingly to the analysis of the SurvK129 mutants.

2 Materials & Methods

2.1 Materials

2.1.1 Chemicals

The chemicals and reagents used in this thesis are listed in Table 2.1.

Table 2.1: Chemicals and reagents.

Chemical/ Reagent	Manufacturer
Acetic acid	Applichem GmbH, Darmstadt
Acrylamide solution (30 %) - Mix 37.5:1	Applichem GmbH, Darmstadt
Agarose	Applichem GmbH, Darmstadt
Ammonium persulfate (APS)	Applichem GmbH, Darmstadt
Ampicillin sodium salt	Applichem GmbH, Darmstadt
Antibiotic-Antimycotic	Life Technologies GmbH, Darmstadt
Bovine serum albumin (BSA)	Applichem GmbH, Darmstadt
Bromophenol blue sodium salt	Applichem GmbH, Darmstadt
Carbenicillin disodium salt	Applichem GmbH, Darmstadt
Chloramphenicol	Applichem GmbH, Darmstadt
Coomassie Brilliant Blue G-250	Applichem GmbH, Darmstadt
Deoxynucleotide (dNTP) Solution Mix	New England BioLabs GmbH, Frankfurt am Main
Disodium hydrogen phosphate dihydrate	Applichem GmbH, Darmstadt

Table 2.1 continued

Chemical/ Reagent	**Manufacturer**
Dithiothreitol (DTT)	Applichem GmbH, Darmstadt
DNA Loading Dye (6x)	Thermo Fisher Scientific, Waltham
Dulbecco's Modified Eagle Medium (DMEM), high glucose, GlutaMax supplement	Life Technologies GmbH, Darmstadt
Dulbecco's Phosphate-Buffered Saline (DPBS)	Life Technologies GmbH, Darmstadt
Ethylenediaminotetraacetic acid (EDTA) disodium salt dihydrate	Applichem GmbH, Darmstadt
Ethanol	VWR International GmbH, Darmstadt
Ethanol technical grade	Applichem GmbH, Darmstadt
Fetal calf serum (FCS)	Life Technologies GmbH, Darmstadt
GelRed	Biotium Inc, Hayward
Glutathione Sepharose 4B	GE Healthcare Life Sciences, Freiburg
Glycerol 87 %	Applichem GmbH, Darmstadt
Glycine	Applichem GmbH, Darmstadt
Hoechst 33342	Applichem GmbH, Darmstadt
Hydrochloric acid 1 M	Applichem GmbH, Darmstadt
Hydrochloric acid 37 %	Applichem GmbH, Darmstadt
Isopropanol	Applichem GmbH, Darmstadt
Isopropanol technical grade	Applichem GmbH, Darmstadt
Isopropyl β-D-1-thiogalactopyranoside (IPTG)	Applichem GmbH, Darmstadt
Kanamycin sulfate	Applichem GmbH, Darmstadt
Luria-Bertani (LB)-Agar powder	Applichem GmbH, Darmstadt
LB-Medium powder	Applichem GmbH, Darmstadt
Leptomycin B (LMB)	Enzo Life Sciences, Lörrach
Lipofectamine 2000	Life Technologies GmbH, Darmstadt
Magnesium chloride hexahydrate	Applichem GmbH, Darmstadt

Table 2.1 continued

Chemical/ Reagent	Manufacturer
β-Mercaptoethanol	Applichem GmbH, Darmstadt
Methanol	Applichem GmbH, Darmstadt
Methanol technical grade	Applichem GmbH, Darmstadt
Milk powder	Applichem GmbH, Darmstadt
Nocodazole	Enzo Life Sciences, Lörrach
Nonidet P40 (NP40)	Applichem GmbH, Darmstadt
Normal goat serum (NGS)	Dako Deutschland GmbH, Hamburg
Opti-MEM	Life Technologies GmbH, Darmstadt
Phenylmethanesulfonylfluoride (PMSF)	Applichem GmbH, Darmstadt
Polyethylenimine (PEI)	Sigma-Aldrich Chemie Gmbh, Munich
Potassium chloride	Applichem GmbH, Darmstadt
Potassium dihydrogen phosphate	Applichem GmbH, Darmstadt
Protease inhibitor cocktail tablets Complete	Roche, Mannheim
Roti-Histofix 4 %	Carl Roth GmbH & Co. KG, Karlsruhe
Sodium azide	Applichem GmbH, Darmstadt
Sodium chloride	Carl Roth GmbH & Co. KG, Karlsruhe
Sodium deoxycholate	Applichem GmbH, Darmstadt
Sodium dihydrogen phosphate monohydrate	Carl Roth GmbH & Co. KG, Karlsruhe
Sodium dodecyl sulfate (SDS)	Applichem GmbH, Darmstadt
Sodium hydroxide pellets	Applichem GmbH, Darmstadt
Sodium sulfate anhydrous	Applichem GmbH, Darmstadt
N,N,N',N'-Tetramethyl-ethylenediamine (TEMED)	Applichem GmbH, Darmstadt
Trichostatin A (TSA)	Sigma-Aldrich Chemie Gmbh, Munich

Table 2.1 continued

Chemical/ Reagent	Manufacturer
Tris(hydroxymethyl)aminomethane (Tris)	Applichem GmbH, Darmstadt
Tris acetate	Applichem GmbH, Darmstadt
Tris hydrochloride	Applichem GmbH, Darmstadt
Triton X-100	Applichem GmbH, Darmstadt
TrypLE Express	Life Technologies GmbH, Darmstadt
Tween 20	Applichem GmbH, Darmstadt
Zinc sulfate heptahydrate	Applichem GmbH, Darmstadt

2.1.2 Buffers, solutions and media

The buffers, solutions and media used in this thesis are listed in Table 2.2. Unless otherwise stated, the ingredients were dissolved in ultra-pure water (ddH_2O).

Table 2.2: Buffers, solutions and media.

Buffer/Solution/ Medium	Ingredients	Final concentration
Acetylation IP lysis buffer	Tris-HCl	50 mM
	Sodium chloride	150 mM
	EDTA	1 mM
	SDS	1 % (w/v)
	Sodium deoxycholate	1 % (w/v)
	Triton X-100	1 % (v/v)
	DTT	1 mM
	PMSF	1 mM
	Protease inhibitor cocktail tablet Complete	1x
	TSA	1 µM
		pH 6.8
APS		10 % (w/v)
Antibody dilution buffer	BSA	1 % (w/v)

Table 2.2 continued

Buffer/Solution/ Medium	**Ingredients**	**Final concentration**
	Triton X-100	0.3 % (v/v) in PBS
Carbenicillin		100 mg/mL
CD buffer	Sodium dihydrogen phosphate Sodium sulfate Zinc sulfate	20 mM 20 mM 10 mM pH 7.7
Cleavage buffer	Tris-HCl Sodium chloride DTT EDTA	50 mM 150 mM 1 mM 1mM pH 7.5
Coomassie destaining solution	Ethanol Acetic acid	40 % 10 % (v/v)
Coomassie staining solution	Coomassie brilliant blue G250 Ethanol Acetic acid	0.1 % (w/v) 40 % (v/v) 10 % (v/v)
DMEM++	FCS Antibiotic-Antimycotic	10 % (v/v) 1x in DMEM, high glucose, GlutaMax supplement
Gel filtration buffer	β-Mercaptoethanol	2.5 mM in PBS
Hoechst solution	Hoechst 33342 Ethanol	1 mg/ml 25 % (v/v) in PBS

Table 2.2 continued

Buffer/Solution/ Medium	**Ingredients**	**Final concentration**
IF blocking buffer	Normal goat serum Triton X-100	5 % (v/v) 0.3 % (v/v) in PBS
Interaction IP lysis buffer	Tris Sodium chloride EDTA NP40 DTT PMSF Protease inhibitor cocktail tablet Complete	50 mM 150 mM 5 mM 0.5 % (v/v) 1 mM 1 mM 1x pH 8
IPTG		1 M
Kanamycin		50 mg/mL
LB-Agar	LB-Agar powder	40 g/L pH 7.5
LB-Medium	LB-Medium powder	25 g/L pH 7.5
Lysis buffer	Tris-HCl Sodium chloride DTT PMSF	50 mM 150 mM 1 mM 1 mM pH 7.5
Magnesium chloride		1 M
Nocodazole		1 mg/mL in DMSO
PBS	Sodium chloride Potassium chloride Disodium hydrogen phosphate	137 mM 2.7 mM 10 mM

Table 2.2 continued

Buffer/Solution/ Medium	Ingredients	Final concentration
	Potassium dihydrogen phosphate	2 mM pH 7.4
PEI		10 mM pH 6.8
RIPA buffer	Tris-HCl Sodium chloride EDTA NP40 Sodium deoxycholate DTT Protease inhibitor cocktail tablet Complete PMSF	50 mM 150 mM 5 mM 1 % (v/v) 1 % (w/v) 1 mM 1x 1 mM
SDS-PAGE running buffer	Tris Glycine SDS	25 mM 192 mM 0.1 % (w/v)
SDS sample buffer (5x)	EDTA Glycerol Tris-HCl SDS β-Mercaptoethanol Bromophenol blue	5 mM 30 % (v/v) 60 mM 15 % (w/v) 7.5 % (v/v) 0.1 % (w/v) pH 6.8
Separating gel buffer (4x)	Tris SDS	1.5 M 0.8 % pH 8.8
Sodium azide		0.1 % (w/v) in PBS
Stacking gel buffer (4x)	Tris-HCl SDS	0.5 M 0.8 % pH 6.8

Table 2.2 continued

Buffer/Solution/ Medium	Ingredients	Final concentration
TAE buffer	Tris acetate EDTA	40 mM 1 mM pH 8.3
TBS	Tris-HCl Sodium chloride	50 mM 150 mM pH 7.4
TBST	Tris-HCl Sodium chloride Tween 20	50 mM 150 mM 0.1 % pH 7.4
TE	Tris-HCl EDTA	10 mM 1 mM pH 8
Transfer buffer	Tris Glycine SDS Methanol	25 mM 192 mM 0.01 % (w/v) 20 % (v/v) pH 8.3
WB blocking buffer	Milk powder	5 % (w/v) in TBST

2.1.3 Protein and DNA standards

The protein and DNA standards used in this thesis are listed in Table 2.3.

Table 2.3: Protein and DNA standards.

Size standard	Manufacturer
GeneRuler 1 kb DNA Ladder	Thermo Fisher Scientific, Waltham
GeneRuler 100 bp DNA Ladder	Thermo Fisher Scientific, Waltham

Table 2.3 continued

Size standard	Manufacturer
Spectra Multicolor Broad Range Protein Ladder	Thermo Fisher Scientific, Waltham

2.1.4 Enzymes

The enzymes used in this thesis are listed in Table 2.4.

Table 2.4: Enzymes.

Enzyme class	Enzyme	Manufacturer/Received from
Endonucleases	ApaI	New England BioLabs GmbH, Frankfurt am Main
	BamHI-HF	New England BioLabs GmbH, Frankfurt am Main
	DNase I	Applichem GmbH, Darmstadt
	EcoRI-HF	New England BioLabs GmbH, Frankfurt am Main
	HindIII-HF	New England BioLabs GmbH, Frankfurt am Main
	KpnI-HF	New England BioLabs GmbH, Frankfurt am Main
	NcoI-HF	New England BioLabs GmbH, Frankfurt am Main
	NdeI	New England BioLabs GmbH, Frankfurt am Main
	NheI-HF	New England BioLabs GmbH, Frankfurt am Main
	SacII	New England BioLabs GmbH, Frankfurt am Main

Table 2.4 continued

Enzyme class	Enzyme	Manufacturer/Received from
Proteases	Lysozyme	Applichem GmbH, Darmstadt
	PreScission Protease	Bayer group, University of Duisburg-Essen

2.1.5 Antibodies

The primary and secondary antibodies used in this thesis are listed in Table 2.5 and Table 2.6, respectively.

Table 2.5: Primary antibodies.

Antigen	Host	Dilution WB	Dilution IF	Manufacturer
Acetylated lysine	Rabbit	1:1,000		Cell Signaling Technology Europe, Leiden
Acetylated SurvivinK129	Rabbit	1:1,000	1:400	Novus Biologicals Ltd, Cambridge
Aurora B	Mouse		1:500	BD Transduction Laboratories, Heidelberg
Aurora B	Rabbit	1:2,000		Sigma-Aldrich Chemie Gmbh, Munich
Borealin	Mouse		1:200	MBL International, Woburn
CRM1	Rabbit	1:10,000		Novus Biologicals Ltd, Cambridge
Flag	Mouse	1:2,000		Sigma-Aldrich Chemie Gmbh, Munich
GAPDH	Mouse	1:1,000		Santa Cruz Biotechnology Inc, Heidelberg
GFP	Rabbit	1:2,000		Santa Cruz Biotechnology Inc, Heidelberg
HA	Mouse	1:1,000		Covance Inc, Munster

Table 2.5 continued

Antigen	Host	Dilution WB	Dilution IF	Manufacturer
INCENP	Mouse		1:150	Life Technologies GmbH, Darmstadt
Myc	Mouse	1:1,000	1:1,500	Cell Signaling Technology Europe, Leiden
Survivin	Rabbit	1:1,000	1:500	Novus Biologicals Ltd, Cambridge
α-Tubulin	Mouse	1:8,000	1:4,000	Sigma-Aldrich Chemie Gmbh, Munich

Table 2.6: Secondary antibodies.

Antibody	Host	Dilution WB	Dilution IF	Manufacturer
Anti-mouse IgG-Alexa Fluor 488	Goat		1:1,000	Life Technologies GmbH, Darmstadt
Anti-rabbit IgG-Alexa Fluor 568	Goat		1:1,000	Life Technologies GmbH, Darmstadt
Anti-mouse IgG-HRP	Sheep	1:10,000		GE Healthcare Life Sciences, Freiburg
Anti-rabbit IgG-HRP	Donkey	1:10,000		GE Healthcare Life Sciences, Freiburg

2.1.6 Plasmids

The plasmids used in this thesis are listed in Table 2.7 to Table 2.9. Vector maps for pc3-Survivin-GFP (Figure A.1), pc3-myc-Survivin (Figure A.2) and pET41-PreSc-GST-Survivin (Figure A.3) can be found in the appendix.

Table 2.7: Cloning vectors.

Vector	Description	Received from
pc3-SDSurvivinVL N-term-myc	Eukaryotic expression vector, amp^r, used for cloning Survivin mutants with C-terminal myc tag	Stauber group, University Medical Center Mainz
pc3-myc-TFIIA-GFP	Eukaryotic expression vector, amp^r, used for cloning Survivin mutants with N-terminal myc tag	Stauber group, University Medical Center Mainz
pc3-DDX3 N-term-HA	Eukaryotic expression vector, amp^r, used for cloning Survivin mutants with C-terminal HA tag	Stauber group, University Medical Center Mainz
pET41-GST-PreSc	Empty prokaryotic expression vector, kan^r, used for cloning Survivin mutants with N-terminal GST tag and PreScisson protease cleavage site	Bayer group, University of Duisburg-Essen

Table 2.8: Eukaryotic expression vectors.

Vector	Description	Received from/ Supplier/Reference
pc3-Aurora B-GFP	Aurora B C-terminally fused with GFP	Stauber group, University Medical Center Mainz
pc3-Borealin-GFP	Borealin C-terminally fused with GFP	Stauber group, University Medical Center Mainz
pc3-CRM1-HA	CRM1 C-terminally fused with HA	Stauber group, University Medical Center Mainz
pc3-Flag-GCN5	GCN5 N-terminally fused with Flag	PhD thesis Carolin Bier

Table 2.8 continued

Vector	Description	Received from/ Supplier/Reference
pc3-GFP	GFP	Stauber group, University Medical Center Mainz
pc3-HA-p300	p300 N-terminally fused with HA	PhD thesis Carolin Bier
pc3-myc-Survivin F101AL102A	Dimerization-deficient SurvivinF101AL102A mutant N-terminally fused with myc	Master's thesis Cecilia Vallet
pc3-myc-SurvivinK78Q	SurvivinK78Q mutant N-terminally fused with myc	This thesis
pc3-myc-SurvivinK78R	SurvivinK78R mutant N-terminally fused with myc	This thesis
pc3-myc-SurvivinK90E	SurvivinK90E mutant N-terminally fused with myc	This thesis
pc3-myc-SurvivinK90Q	SurvivinK90Q mutant N-terminally fused with myc	This thesis
pc3-myc-SurvivinK90R	SurvivinK90R mutant N-terminally fused with myc	This thesis
pc3-myc-SurvivinK90,91R	SurvivinK90,91R mutant N-terminally fused with myc	This thesis
pc3-myc-Survivin K110,112,115Q	SurvivinK110,112,115Q mutant N-terminally fused with myc	This thesis
pc3-myc-Survivin K110,112,115R	SurvivinK110,112,115R mutant N-terminally fused with myc	This thesis
pc3-myc-SurvivinK112Q	SurvivinK112Q mutant N-terminally fused with myc	This thesis
pc3-myc-SurvivinK112R	SurvivinK112R mutant N-terminally fused with myc	This thesis
pc3-myc-SurvivinK115Q	SurvivinK115Q mutant N-terminally fused with myc	This thesis

Table 2.8 continued

Vector	Description	Received from/ Supplier/Reference
pc3-myc-SurvivinK115R	SurvivinK115R mutant N-terminally fused with myc	This thesis
pc3-myc-SurvivinK120-122Q	SurvivinK120-122Q mutant N-terminally fused with myc	This thesis
pc3-myc-SurvivinK120-122R	SurvivinK120-122R mutant N-terminally fused with myc	This thesis
pc3-myc-SurvivinK129R	SurvivinK129R mutant N-terminally fused with myc	This thesis
pc3-myc-SurvivinK129E	SurvivinK129E mutant N-terminally fused with myc	This thesis
pc3-myc-SurvivinK129Q	SurvivinK129Q mutant N-terminally fused with myc	This thesis
pc3-myc-SurvivinK129A	SurvivinK129A mutant N-terminally fused with myc	This thesis
pc3-myc-SurvivinK129,130R	SurvivinK129,130R mutant N-terminally fused with myc	This thesis
pc3-myc-Survivin wt	Survivin wildtype N-terminally fused with myc	This thesis
pc3-Survivin 1-119-GFP	truncated Survivin1-119 C-terminally fused with GFP	Stauber group, University Medical Center Mainz
pc3-SurvivinF101AL102A-GFP	Dimerization-deficient SurvivinF101AL102A mutant C-terminally fused with GFP	This thesis
pc3-SurvivinK129Q-GFP	SurvivinK129Q mutant C-terminally fused with GFP	This thesis
pc3-SurvivinK129R-GFP	SurvivinK129R mutant C-terminally fused with GFP	This thesis
pc3-SurvivinNESmut-GFP	CRM1 binding-deficient SurvivinNES mutant C-terminally fused with GFP	Stauber group, University Medical Center Mainz

Table 2.8 continued

Vector	Description	Received from/ Supplier/Reference
pc3-Survivin wt-GFP	Survivin wildtype C-terminally fused with GFP	Stauber group, University Medical Center Mainz
pc3-Survivin F101AL102A-HA	Dimerization-deficient SurvivinF101AL102A mutant C-terminally fused with HA	This thesis
pc3-SurvivinK129E-HA	SurvivinK129E mutant C-terminally fused with HA	This thesis
pc3-SurvivinK129Q-HA	SurvivinK129Q mutant C-terminally fused with HA	This thesis
pc3-SurvivinK129R-HA	SurvivinK129R mutant C-terminally fused with HA	This thesis
pc3-Survivin wt-HA	Survivin wildtype C-terminally fused with HA	This thesis
pc3-SurvivinK129Q-myc	SurvivinK129Q mutant C-terminally fused with myc	This thesis
pc3-SurvivinK129R-myc	SurvivinK129R mutant C-terminally fused with myc	This thesis
pc3-Survivin wt-myc	Survivin wildtype C-terminally fused with myc	This thesis
pcDNA3.1(+)	Used as empty vector in transfections	Life Technologies GmbH, Darmstadt
pcDNA3.1-INCENP-GFP	INCENP C-terminally fused with GFP	Schramm group, University Children's Hospital Essen
pcDNA3.1-myc-INCENP	INCENP N-terminally fused with myc	Meyer group, University of Duisburg-Essen
pCMV-CBP-Flag	CBP C-terminally fused with Flag	PhD thesis Carolin Bier

Table 2.8 continued

Vector	Description	Received from/ Supplier/Reference
pcX-Flag-PCAF	PCAF N-terminally fused with Flag	PhD thesis Carolin Bier

Table 2.9: Prokaryotic expression vectors.

Vector	Description	Reference
pET41-GST-PreSc-SurvivinF101AL102A	Dimerization-deficient SurvivinF101AL102A mutant N-terminally fused with GST and PreScisson protease cleavage site	This thesis
pET41-GST-PreSc-SurvivinK90Q	SurvivinK90Q mutant N-terminally fused with GST and PreScisson protease cleavage site	This thesis
pET41-GST-PreSc-SurvivinK90R	SurvivinK90R mutant N-terminally fused with GST and PreScisson protease cleavage site	This thesis
pET41-GST-PreSc-SurvivinK129A	SurvivinK129A mutant N-terminally fused with GST and PreScisson protease cleavage site	This thesis
pET41-GST-PreSc-SurvivinK129E	SurvivinK129E mutant N-terminally fused with GST and PreScisson protease cleavage site	This thesis
pET41-GST-PreSc-SurvivinK129Q	SurvivinK129Q mutant N-terminally fused with GST and PreScisson protease cleavage site	This thesis
pET41-GST-PreSc-SurvivinK129R	SurvivinK129R mutant N-terminally fused with GST and PreScisson protease cleavage site	This thesis
pET41-GST-PreSc-Survivin wt	Survivin wildtype N-terminally fused with GST and PreScisson protease cleavage site	This thesis

2.1.7 Oligonucleotides

The PCR primers used in this thesis were purchased from Eurofins Genomics (Ebersberg) and are listed in Table 2.10. The sequencing primers were provided by the corresponding sequencing company and are listed in Table 2.11.

Table 2.10: PCR primers.

Primer	Sequence (5'→3')
3'-EcoRI-Surv	TTTGAATTCTTAATCCATGGCAGCCAG
Apa-Surv for	AAAGGGCCCGGTGCCCCGACGTTGCCC
Bam-Surv rev	TTTGGATCCTTAATCCATGGCAGCCAG
Bam-Surv(ATG) for	TTTGGATCCACATGGGTGCCCCGACGTTG
Bam-Surv(-ATG) for	TTTGGATCCACGGTGCCCCGACGTTGCCCC
GFP5-Sequ-new	GTGGCATCGCCCTCGCCCTC
pc3-F-Sequ	GGAGGTCTATATAAGCAGAGCTC
pc3'-Sequ	CAACTAGAAGGCACAGTCGAG
Surv-Bam for	AAAGGATCCACATGGGTGCCCCGACGTTG
SurvF101AL102A-1P	GTCCAGTTTCGCAGCTTCACCAAG
SurvF101AL102A-2P	CTTGGTGAAGCTGCGAAACTGGAC
SurvK78Q-1P	CGAATGCTTTTGATGTTCCTC
SurvK78Q-2P	GAGGAACATCAAAAGCATTCG
SurvK78R-1P	CGAATGCTTTCTATGTTCCTC
SurvK78R-2P	GAGGAACATAGAAAGCATTCG
SurvK90E-1P	CAAACTGCTTCTCGACAGAAAG
SurvK90E-2P	CTTTCTGTCGAGAAGCAGTTTG
SurvK90Q-1P	CAAACTGCTTCTGGACAGAAAG
SurvK90Q-2P	CTTTCTGTCCAGAAGCAGTTTG
SurvK90R-1P	CAAACTGCTTCCTGACAGAAAG
SurvK90R-2P	CTTTCTGTCAGGAAGCAGTTTG
SurvK90,91R-1P	TTCTTCAAACTGCCTCCTGACAGAAAG
SurvK90,91R-2P	CTTTCTGTCAGGAGGCAGTTTGAAGAA
SurvK110,112,115Q-1P	GGTTTCCTGTGCAATTTGGTTCTGGGCTCT

Table 2.10 continued

Primer	**Sequence (5'→3')**
SurvK110,112,115Q-2P	AGAGCCCAGAACCAAATTGCACAGGAAACC
SurvK110,112,115R-1P	GGTTTCCCTTGCAATTCTGTTCCTGGCTCT
SurvK110,112,115R-2P	AGAGCCAGGAACAGAATTGCAAGGGAAACC
SurvK112Q-1P	CTTTGCAATTTGGTTCTTGGC
SurvK112Q-2P	GCCAAGAACCAAATTGCAAAG
SurvK112R-1P	CTTTGCAATTCTGTTCTTGGC
SurvK112R-2P	GCCAAGAACAGAATTGCAAAG
SurvK115Q-1P	GTTGGTTTCCTGTGCAATTTT
SurvK115Q-2P	AAAATTGCACAGGAAACCAAC
SurvK115R-1P	GTTGGTTTCCCTTGCAATTTT
SurvK115R-2P	AAAATTGCAAGGGAAACCAAC
SurvK120-122Q-1P	CTCAAATTCTTGCTGCTGATTGTTGGT
SurvK120-122Q-2P	ACCAACAATCAGCAGCAAGAATTTGAG
SurvK120-122R-1P	TTCCTCAAATTCTCTCCTCCTATTGTTGGT
SurvK120-122R-2P	ACCAACAATAGGAGGAGAGAATTTGAGGAA
SurvK129A-1P	GCGCACTTTTGCCGCAGTTTC
SurvK129A-2P	GAAACTGCGGCAAAAGTGCGC
SurvK129E-1P	GCGCACTTTCTCCGCAGTTTC
SurvK129E-2P	GAAACTGCGGAGAAAGTGCGC
SurvK129Q-1P	GCGCACTTTCTGCGCAGTTTC
SurvK129Q-2P	GAAACTGCGCAGAAAGTGCGC
SurvK129R-1P	GCGCACTTTCCTCGCAGTTTC
SurvK129R-2P	GAAACTGCGAGGAAAGTGCGC
SurvK129,130R-1P	GCGCACTCTCCTCGCAGTTTC
SurvK129,130R-2P	GAAACTGCGAGGAGAGTGCGC
Surv-Nhe rev	TTTGCTAGCATCCATGGCAGCCAGCTGC

Table 2.11: Sequencing primers.

Primer	Sequence (5'→3')	Sequencing company
T7	TAATACGACTCACTATAGGG	GATC Biotech AG, Konstanz
pcDNA3.1-FP	CTCTGGCTAACTAGAGAAC	GATC Biotech AG, Konstanz
CMV-F	CGCAAATGGGCGGTAGGCGTG	LGC Genomics GmbH, Berlin
T7term	GCTAGTTATTGCTCAGCGG	LGC Genomics GmbH, Berlin

2.1.8 Bacterial strains

The bacterial strains used in this thesis are listed in Table 2.12.

Table 2.12: Bacterial strains.

Strain	Genotype	Manufacturer
E. coli SoluBL21	F^- *ompT hsd SB* (rB^- mB^-) *gal dcm* (DE3) + further uncharacterized mutations	Genlantis, San Diego
E. coli XL2-Blue	*endA1 supE44 thi-1 hsdR17 recA1 gyrA96 relA1 lac* [F' *proAB* $lacI^qZ\Delta M15$ Tn*10* (Tet^r) Amy Cam^r]	Agilent Technologies, Waldbronn

2.1.9 Eukaryotic cell lines

The cell lines used in this thesis are listed in Table 2.13. All cell lines were cultivated in DMEM++.

Table 2.13: Eukaryotic cell lines.

Cell line	Origin	Growth property	ATCC number
293T	*H. sapiens*, fetal kidney	adherent	CRL-11268
HeLa	*H. sapiens*, cervical adenocarcinoma	adherent	CCL-2
HeLa Kyoto	*H. sapiens*, cervical adenocarcinoma	adherent	

2.1.10 Kits

The kits used in this thesis are listed in Table 2.14.

Table 2.14: Kits.

Kit	Manufacturer
Expand High Fidelity ^{PLUS} PCR System	Roche, Mannheim
Gel Filtration LMW Calibration kit	GE Healthcare Life Sciences, Freiburg
µMACS c-myc Isolation kit	Miltenyi Biotec GmbH, Bergisch-Gladbach
µMACS GFP Isolation kit	Miltenyi Biotec GmbH, Bergisch-Gladbach
µMACS HA Isolation kit	Miltenyi Biotec GmbH, Bergisch-Gladbach
NucleoBond Xtra Midi kit	Macherey-Nagel GmbH & Co. KG, Düren
NucleoSpin 8 Plasmid kit	Macherey-Nagel GmbH & Co. KG, Düren

Table 2.14 continued

Kit	Manufacturer
NucleoSpin Gel and PCR Clean-up kit	Macherey-Nagel GmbH & Co. KG, Düren
Pierce ECL plus Western blotting Substrate kit	Thermo Fisher Scientific, Waltham
Protein Assay Kit	Bio-Rad Laboratories GmbH, Munich
Takara DNA Ligation kit	Clontech, Saint-Germain-en-Laye

2.1.11 Consumables

The consumables used in this thesis are listed in Table 2.15.

Table 2.15: Consumables.

Item	Manufacturer
Beaker 50 mL	VWR International GmbH, Darmstadt
Cell culture dish 10 cm	Sarstedt AG & Co., Nümbrecht
Cell culture flask T-75	Sarstedt AG & Co., Nümbrecht
Cell scraper 25 cm	Sarstedt AG & Co., Nümbrecht
Erlenmeyer flask 25/50 mL	Technische Glaswerke Ilmenau GmbH, Ilmenau
Erlenmeyer flask 250/500 mL	DURAN Group GmbH, Wertheim
µ Column	Miltenyi Biotec GmbH, Bergisch-Gladbach
PCR tubes 0.2 mL	Bio-Rad Laboratories GmbH, Munich
Pipette tip 10/20/200/1250 µL	Sarstedt AG & Co., Nümbrecht
Poly-Prep chromatography column	Bio-Rad Laboratories GmbH, Munich
Polyvinylidene fluoride (PVDF) transfer membrane BioTrace	Pall GmbH, Dreieich
PVDF transfer membrane Amersham Hybond P 0.45	GE Healthcare Life Sciences, Freiburg
Semi-micro cuvette 10 x 4 mm	Sarstedt AG & Co., Nümbrecht

Table 2.15 continued

Item	Manufacturer
µ-Slide 8 well	ibidi GmbH, Planegg
Reaction tubes 1.5/2 mL	Sarstedt AG & Co., Nümbrecht
Reaction tubes 15/50 mL	Sarstedt AG & Co., Nümbrecht
Serological pipettes 2/5/10/25 mL	Sarstedt AG & Co., Nümbrecht
UV micro cuvette	Sarstedt AG & Co., Nümbrecht
Vacuum filter	Techno Plastic Products AG, Trasadingen

2.1.12 Instruments

The instruments and devices used in this thesis are listed in Table 2.16.

Table 2.16: Instruments and devices.

Instrument	Manufacturer
Agarose gel electrophoresis chamber	Peqlab Biotechnologie GmbH, Erlangen
BioPhotometer Plus	Eppendorf AG, Hamburg
CD spectropolarimeter J-715	Jasco Inc, Easton
Centrifuge 5417 C/R	Eppendorf AG, Hamburg
Centrifuge Allegra X-22	Beckman Coulter GmbH, Krefeld
Centrifuge ROTINA 380/380 R	Andreas Hettich GmbH & Co. KG, Tuttlingen
Chemistry pumping unit	Vacuubrand GmbH & Co. KG, Wertheim
Chromatography column Superdex 75 10/300 GL	GE Healthcare Life Sciences, Freiburg
CO_2 incubator	Binder GmbH, Tuttlingen
CO_2 incubator INC153	Memmert GmbH & Co. KG, Schwabach

Table 2.16 continued

Instrument	Manufacturer
Confocal laser scanning microscope (inverse) TCS SP5	Leica Microsystems GmbH, Mannheim
Epifluorescence microscope (inverse) Axio Observer Z.1	Carl Zeiss, Oberkochen
Epifluorescence microscope (inverse) CKX41	Olympus Europa SE & Co. KG, Hamburg
Film processor Cawomat 2000 IR	Cawo, Schrobenhausen
Freezer (-80 °C) Forma 900S-RIFS	Thermo Fisher Scientific, Waltham
Freezer (-20 °C) Liebherr Premium BioFresh	Liebherr GmbH, Biberach
Gel caster	Bio-Rad Laboratories GmbH, Munich
Gel documentation system E-Box VX2	Vilber Lourmat Deutschland GmbH, Eberhardzell
Heating plate	Gesellschaft für Labortechnik mbH, Burgwedel
Heating plate	Medax GmbH & Co. KG, Rendsburg
Liquid chromatography system ÄKTApurifier	GE Healthcare Life Sciences, Freiburg
µMACS separator	Miltenyi Biotec GmbH, Bergisch-Gladbach
Magnetic stirrer Hei-Mix L	Heidolph Instruments GmbH & Co. KG, Schwabach
Magnetic stirrer HI 180	Hanna Instruments Deutschland GmbH, Kehl
Microscope Primo Vert	Carl Zeiss, Oberkochen
Microwave	Severin Elektrogeräte GmbH, Sundern
Mini centrifuge Spectrafuge	Labnet International Inc, Edison
Multichannel Pipette Plus	Eppendorf AG, Hamburg
Orbital shaker Forma 420 series	Thermo Fisher Scientific, Waltham
Orbital shaker POS-300	Grant Instruments Ltd, Royston

Table 2.16 continued

Instrument	Manufacturer
Pipettes Research Plus	Eppendorf AG, Hamburg
Pipetting aid Pipetus	Hirschmann Laborgeräte GmbH & Co. KG, Eberstadt
pH meter	Hanna Instruments Deutschland GmbH, Kehl
Polyacrylamide gel electrophoresis chamber Mini-Protean Tetra Cell	Bio-Rad Laboratories GmbH, Munich
Power supply Peqpower 300	Peqlab Biotechnologie GmbH, Erlangen
Power supply PowerPac Basic	Bio-Rad Laboratories GmbH, Munich
Precision balance	Kern & Sohn GmbH, Balingen
Quarz glass cuvette (path length 1mm	Hellma Analytics, Müllheim
Refrigerator Liebherr Comfort	Liebherr GmbH, Biberach
Refrigerator Liebherr Medline	Liebherr GmbH, Biberach
Rotator PTR-30	Grant Instruments Ltd, Royston
Safety cabinet NuAire NU-437-400E	Integra Biosciences GmbH, Fernwald
Safety cabinets HERAsafe	Thermo Fisher Scientific, Waltham
Shaker ST5	neoLab Migge Laborbedarf-Vertriebs GmbH, Heidelberg
Spectrophotometer Nanodrop 1000	Thermo Fisher Scientific, Waltham
Thermal mixer ThermoMixer Comfort	Eppendorf AG, Hamburg
Thermal mixer MHR 11	HLC BioTech, Bovenden
Thermal printer DPU-414	Seiko Instruments GmbH, Neu-Isenburg
Thermal printer P95D	Mitsubishi Chemical Europe GmbH, Düsseldorf
Thermoblock	Eppendorf AG, Hamburg
Thermocycler TProfessional standard gradient 96	Biometra GmbH, Göttingen

Table 2.16 continued

Instrument	Manufacturer
Ultrasonic homogenizer mini20	Bandelin electronic GmbH & Co. KG, Berlin
Ultrasonic homogenizer Sonopuls HD2200	Bandelin electronic GmbH & Co. KG, Berlin
UV Sterilizing PCR Workstation	Peqlab Biotechnologie GmbH, Erlangen
Vacuum removal system AZ 02	HLC BioTech, Bovenden
Vortexer PV-1	Grant Instruments Ltd, Royston
Vortexer Vortex-Genie 2	Scientific Industries, Bohemia
Water bath 1002-1013	Gesellschaft für Labortechnik mbH, Burgwedel

2.1.13 Software

The software used in this thesis is listed in Table 2.17.

Table 2.17: Software.

Software	Manufacturer
Adobe Photoshop CC 2014	Adobe Systems GmbH, Munich
AxioVision	Carl Zeiss, Oberkochen
BioEdit 7.2.5	Ibis Biosciences, Carlsbad
Canvas 11	ACD Systems International Inc., Seattle
Gene Construction Kit 3.0	Textco BioSoftware, Inc, New Hampshire
Image Studio Lite 4.0	LI-COR Biosciences GmbH, Bad Homburg
Jasco Spectra Manager 2.0	Jasco Inc, Easton
Leica Application Suite Advanced Fluorescence	Leica Microsystems GmbH, Mannheim
PyMOL 1.3	Schrödinger LCC, Portland
Unicorn 5.20	GE Healthcare Life Sciences, Freiburg

2.2 Methods

2.2.1 Molecular biology

2.2.1.1 Polymerase chain reaction

Polymerase chain reaction (PCR) is used to amplify DNA sequences. In addition to the DNA template, also a sequence-specific pair of oligonucleotides (primer), deoxynucleotide triphosphates (dNTPs) as well as a temperature-resistant DNA polymerase are required. A PCR cycle contains three steps: denaturation of the double-stranded DNA template and the primers, annealing of the primers, and primer elongation. It is repeated 30 to 40 times in order to gain a sufficient amount of the template. Denaturation is performed at 94 °C. The annealing temperature should be 2 to 5 °C lower than the melting temperature of the used primers in order to allow specific hybridization of the primers with the template. The elongation step requires 72 °C as this is the optimal temperature for the used DNA polymerase. Its duration depends on the length of the template and the amplification rate of the polymerase.

Table 2.18 summarizes the ingredients of a 50 µL PCR reaction mixture using the Expand High Fidelity ^{PLUS} PCR System (Roche Diagnostics). The standard PCR program for Survivin cDNA amplification is displayed in Table 2.19. The PCR cycle was repeated 30 times.

Table 2.18: PCR reaction mixture.

Reagents	Volume [µL]
Buffer 2 (5x)	10.0
Primer 1 (10 µM)	2.0
Primer 2 (10 µM)	2.0
dNTPs (10 mM each)	1.0
DNA polymerase	0.5
DNA template (10 ng/µL)	2.0
H_2O	32.5

Table 2.19: Standard PCR program for Survivin amplification.

Step	Temperature	Duration	
Initial denaturation	94 °C	2 min	
Denaturation	94 °C	30 s	
Annealing	53-65 °C	30 s	30x
Elongation	72 °C	45 s	
Final elongation	72 °C	5 min	

2.2.1.2 Splice overlap extension PCR

For the site-directed mutagenesis of the Survivin cDNA, splice overlap extension (SOE) PCR was applied. This method allows the generation of point mutations as well as the deletion or insertion of nucleotides into a DNA sequence. A pair of complementary mutagenesis primers bearing the mutation and a pair of primers that flank the DNA template are required for the two-step PCR. In the first step of SOE PCR, the template is amplified in two separate reaction mixtures containing either the forward flanking primer and the reverse mutagenic primer, or the reverse flanking primer and the forward mutagenic primer. In the second step, both PCR products are mixed allowing their hybridization along the complementary regions derived from the mutagenic primers. Thus, each DNA strand serves as a template for the completion of the other one. The addition of the flanking primers then leads to the amplification of the mutated DNA strands.

SOE PCR was performed using the same reagents and PCR program as for standard PCR (see Table 2.18 and Table 2.19). The elongation time was increased to 1 min.

2.2.1.3 Agarose gel electrophoresis

Agarose gel electrophoresis is used to separate nucleic acids according to size. The method utilizes the fact that charged molecules migrate within an electric field dependent on their conformation, size, and charge density. As DNA is negatively charged it moves to the anode. In order to achieve a size-dependent separation, the DNA moves through an agarose gel that is placed in an electric field. Agarose is a polysaccharide which forms a polymer gel upon boiling. The agarose concentration determines the

pore size of the gel and, thus, its separation capability as small DNA fragments migrate faster through the pores than large fragments. After separation, DNA bands are visualized by fluorescent DNA-binding dyes.

For an analytic gel, 30 mL 1x TAE buffer containing 1 to 2 % (w/v) agarose were boiled. The DNA-staining dye GelRed (Biotium) was added (1:10,000), and the gel was poured. After polymerization, the gel was placed in the electrophoresis chamber. The samples were mixed with 6x DNA sample buffer and loaded on the gel. Electrophoresis was conducted at 100 to 120 V for 45 to 90 min in 1x TAE buffer. After that, the DNA bands were visualized with UV light using the gel documentation system E-Box VX2 (Vilber Lourmat). GeneRuler 1 kb DNA Ladder and GeneRuler 100 bp DNA Ladder (Thermo Fisher Scientific) were used as DNA size standards.

2.2.1.4 Purification of DNA fragments

To remove impurities like salts, enzymes and primers from PCR products, and to extract DNA from agarose gels, the NucleoSpin Gel and PCR Clean-up kit (Macherey-Nagel) was used according to the manufacturer's instructions. The mechanism is based on binding of DNA to a silica membrane followed by washing steps to remove contaminations and, finally, the elution of the purified DNA.

2.2.1.5 Photometric determination of DNA concentration

Double stranded DNA (dsDNA) exerts an absorption maximum at a wavelength of 260 nm due to the strong absorption of the aromatic purine and pyrimidine bases at this wavelength. Thus, applying Lambert-Beer's law (see Equation 2.1, page 72) the concentration of a dsDNA solution can be determined photometrically by measuring its absorbance at 260 nm (A_{260}). Measured at a neutral pH in a quartz cuvette of a path length of 1 cm the absorbance of 1.0 corresponds to a dsDNA concentration of 50 µg/mL. The A_{260}/A_{280} ratio provides information about the purity of the DNA. Pure DNA exhibits a ratio of 1.8 to 2.0. While lower values hint at contamination with proteins or phenol, higher values indicate RNA contamination. The A_{260}/A_{230} ratio informs about contamination with phenol or other organic substances. For pure DNA the value should be 2.0

For the photometric quantification of the DNA concentration, 1 µL DNA was mixed with 70 µL ddH_2O in a UV micro cuvette (Sarstedt) and the absorbance of the solution was measured with a BioPhotometer (Eppendorf).

2.2.1.6 Restriction of DNA

Restriction endonucleases are used to cut dsDNA at distinct sites as they catalyze the hydrolysis of phophodiester bonds within the sugar phosphate backbone of DNA. For molecular biological applications type II endonucleases are relevant as they cut dsDNA within or near their mostly palindromic recognition sites. Depending on the restriction enzyme the cleavage yields 3' or 5' cohesive ends, or blunt ends. The vector and the PCR product serving as an insert have to be digested with the same restriction enzymes in order to allow proper ligation.

For an analytic digest, 0,5 to 2 µL DNA were digested with suitable restriction enzymes (New England BioLabs) in a buffer recommended by the manufacturer. The 10 µL reaction mixture was incubated at 37 °C for 1 h. For a preparative digest, 4 µg DNA were digested in a total volume of 50 µL for 4 h at 37 °C.

2.2.1.7 Ligation of DNA

Ligases are used to join DNA strands together as they catalyze the formation of phosphodiester bonds of the sugar phosphate backbone of DNA. An enzyme commonly used to insert a DNA fragment into a linearized plasmid is the T4 DNA ligase derived from the bacteriophage T4. It can ligate cohesive as well as blunt ends and requires adenosine triphosphate (ATP) as a cofactor.

Ligation of an insert into a linearized plasmid was performed using the Takara DNA Ligation Kit, Version 2.1 (Clontech), which also utilizes T4 DNA ligase. 0,5 µL plasmid, 2 µL insert and 2,5 µL Solution I of the kit were mixed and incubated for 30 min at room temperature (RT). A negative control was also included in which the insert was exchanged by ddH_2O in order to test for re-ligation of the linearized plasmid.

2.2.1.8 Isolation of plasmids

Depending on the required amount of DNA a mini or midi preparation was performed in order to isolate plasmid DNA from *E.coli* cells in which the plasmids were amplified.

For the mini preparation of plasmids, overnight cultures of *E. coli* XL2-Blue (Agilent Technologies) containing positive clones were inoculated in 4 mL LB medium containing 100 µg/mL carbenicillin (Carb) or 50 µg/mL kanamycin (Kan) depending on the antibiotic resistance coded on the plasmid. The cultures were incubated for approx. 16 h

at 37 °C under constant shaking at 180 rpm. 3 mL of the bacterial cultures were centrifuged for 10 min at 1,000 x g and the plasmids were isolated from the pellets with the NucleoSpin 8 Plasmid kit (Macherey-Nagel) according to the manufacturer's instructions. The kit is based on the principle of alkaline lysis of the bacterial cells (Birnboim and Doly, 1979) and the subsequent loading of the neutralized, cleared lysate on a column containing a silica membrane. Plasmid DNA binds to the silica membrane in the presence of chaotropic salts. Contaminants are removed by several washing steps, and the purified plasmids are eluted with a low salt buffer.

For the midi preparation, 150 mL overnight cultures were inoculated in antibiotic-containing LB medium and incubated for 16 h at 37 °C under constant shaking at 120 rpm. After harvesting the cells by centrifugation for 15 min at 3,900 x g and 4 °C the the plasmids were isolated from the pellets using the NucleoBond Xtra Midi kit (Macherey-Nagel) according to the manufacturer's instructions. This kit is also based on the principle of alkaline lysis of the bacterial cells followed by binding of the plasmids to a silica resin under high salt conditions. However, elution of the plasmids is also conducted in the presence of a high salt concentration by a shift from neutral to acidic pH. Thus, the eluted plasmids have to be precipitated with isopropanol, and subsequently washed with ethanol in order to remove salts.

2.2.1.9 DNA sequencing and sequence analysis

Sequencing of purified plasmid DNA was carried out by GATC Biotech or LGC Genomics according to the chain termination method (Sanger and Coulson, 1975). To this end, 20 µL plasmid DNA with a concentration of 80 to 100 ng/µL were sent to the companies. Sequencing primers (see Table 2.11) were provided by the companies. The alignment of the sequences obtained from the sequencing companies with the virtual constructs was performed using the cloning software Gene Construction Kit (Textco BioSoftware) as well as the alignment software BioEdit (Ibis Biosciences).

2.2.2 Cell biology

2.2.2.1 Transformation of competent *E. coli* cells

Transformation describes the genetic alteration of cells due to the uptake of exogenous DNA. Cells that are capable of taking up naked DNA are called competent. Not all bacteria strains possess a natural competence. *E. coli*, for example, which is commonly

used to amplify recombinant plasmids, has to be made competent by chemical treatment. Competent cells can be forced to incorporate DNA either by electroporation or by a heat shock. Both methods cause the temporary appearance of pores in the cell membrane enabling the DNA to enter.

For a heat shock transformation of chemically competent *E. coli* XL2-Blue or *E. coli* SoluBL21 cells (Genlantis), 10 to 20 µL bacteria suspension were mixed with 1 to 2 µL of the ligation product or a purified plasmid, and incubated for 20 min on ice. Then, the mixture was incubated for 45 s at 42 °C and immediately placed on ice again where it was incubated for further 10 min. After the heat shock, the cells were resuspended in 200 µL LB medium. *E. coli* cells transformed with plasmids carrying an ampicillin resistance were directly resuspended in LB-Carb medium and plated on LB-Carb agar plates. *E. coli* cells transformed with plasmids carrying a kanamycin resistance were first resuspended in LB medium without antibiotics, and incubated for 1 h at 37 °C under shaking at 180 rpm in order to enable the expression of the resistance gene. After that, they were plated on LB-Kan agar plates. The plates were incubated over night at 37 °C

2.2.2.2 Heterologous expression of recombinant GST fusion proteins

The heterologous expression of recombinant proteins in *E. coli* offers protein production within a short time and with a high yield. The most commonly used expression system consisting of an expression vector and a suitable *E. coli* host strain is based on the bacteriophage T7. In this system, the expression vector containing the gene of interest cloned downstream of the T7 promotor is introduced into a T7 expression host strain. These host strains carry a chomosomal copy of the T7 RNA polymerase gene, the expression of which is controlled by the *lac* operon. The addition of an inducer, e.g. isopropyl β-D-1-thiogalactopyranoside (IPTG), leads to the expression of the RNA polymerase which, in turn, transcribes the gene of interest.

In this thesis, an expression system comprising the *E. coli* SoluBL21 strain and the pET41-GST-PreSc vector was used. In order to test the expression conditions for recombinant proteins, a protein mini expression was performed. To this end, overnight cultures of clones grown on LB agar plates were inoculated in 5 mL LB-Kan medium and incubated at 37 °C under shaking at 180 rpm. Each culture was splitted into four 1 mL aliquots and diluted with 4 mL LB-Kan medium and the cultures were again incubated for 1 h. 500 µL of the suspensions were taken as a negative control sample. IPTG was added to the remaining suspensions in varying concentrations (0,1 to 1 mM)

in order to induce protein expression, and the cultures were incubated at different temperatures for different durations in order to evaluate the best expression conditions. 500 µL of each culture were taken as a positive control. The samples were pelleted, and the pellets were resuspended in 50 µL 2x SDS (sodium dodecylsulfate) sample buffer. After sonication for 1 min with the ultrasonic homogenizer Sonopuls mini20 (Bandelin) the samples were heated to 95 °C for 5 min. 10 µL of the samples were analyzed by SDS polyacrylamide gel electrophoresis (subsubsection 2.2.3.5).

For a preparative protein maxi expression, 50 mL LB-Kan medium were inoculated with 50 µL of a 5 mL overnight culture and incubated overnight at 37 °C under shaking at 120 rpm. 20 mL of the pre-culture were diluted with 280 mL LB-Kan medium and the culture was grown until its absorbance at 600 nm reached a value around 0.6. Then, protein expression was induced by adding IPTG and was conducted under the conditions evaluated by mini expression.

2.2.2.3 Cultivation of mammalian cell lines

The cultivation of mammalian cells requires special conditions. In order to enable cell proliferation, cells are incubated at 37 °C and 5 % CO_2 in approx. 90 % relative humidity. In addition, the cells have to be continuously supplied with fresh growth medium, and the cell density has to be regulated by regular splitting and transfer of the cells to new culture vessels. The cultivation of the cells must be conducted under sterile conditions in order to prevent infections with viruses, bacterial and fungi.

The mammalian adherent cell lines used in this thesis (HeLa, HeLa Kyoto and 293T) were cultivated in DMEM++ growth medium in T-75 cell culture flasks. They were passaged twice or three times a week with a ratio of 1:10 to 1:20. To this end, old growth medium was aspirated and the cell layer was carefully rinsed with 5 mL DPBS to remove remaining fetal calf serum (FCS) which inhibits the enzymatic detachment of the cells from the bottom of the cell culture flask. This was done by adding 2 mL of the trypsin replacement TrypLE Express (Life Technologies), which cleaves the adhesion proteins on the cell surface, and incubating the cells on a heating plate until they were detached. 8 mL DMEM++ were added and the cells were resuspended. 0,5 to 1 mL of the cell suspension was transferred to a new culture flask which was filled with DMEM++ up to 10 mL.

2.2.2.4 Transient transfection of eukaryotic cells

Transient transfection describes the temporally introduction of nucleic acids into eukaryotic cells. Eukaryotic cells can be transfected chemically, for example by using cationic polymers like polyethylenimine (PEI) or liposomal transfection reagents like Lipofectamine 2000 (Life Technologies), to transport nucleic acids through the cell membrane. PEI forms complexes with negatively charged nucleic acids, which are taken up into cells via endocytosis. Lipofectamine 2000 forms liposomes around the nucleic acids, which are capable of fusing with the cell membrane. Another method to introduce nucleic acids into cells is by physical transfection, e.g. by means of electroporation or via particles. Irrespective of the transfection method used, the nucleic acids must enter the cell and, subsequently, the nucleus in order to be transcribed. As they are not integrated into the cell genome the are diluted upon cell division or degraded.

293T cells were used for the production of cell lysates and transfected with PEI. To this end, 0.8 to 1 mL of the cell suspension produced during cell passage was diluted with 9 mL DMEM++ and plated on a 10 cm cell culture dish. 24 h later, two solutions were prepared: solution A comprised 240 µL DPBS and 44 µL 10 mM PEI, solution B consisted of 240 µL DPBS and 15 µg plasmid DNA. The solutions were mixed together, centrifuged and the mixture was incubated for 5 min at RT. Then, the transfection mixture was applied to the cell layer in drops and the cells were incubated for 24 h.

For microscopic analyses, proteins were expressed in HeLa or HeLa Kyoto cells. Cells were plated in 8 well µ-slides (ibidi) and transfected with Lipofectamine 2000. For the transfection of one well, 20 to 25 µL of the cell suspension produced during cell passage were diluted with 300 µL DMEM++ and seeded. 24 h later, the transfection solutions were prepared: solution A comprised 12.5 µL Opti-MEM (Life Technologies) and 0.2 µL Lipofectamine 2000, solution B consisted of 12.5 µL Opti-MEM and 150 ng plasmid DNA. The solutions were mixed together, centrifuged and the mixture was incubated for 5 min at RT. Then, the transfection mixture was applied to the cell layer in drops and the cells were incubated for 24 h.

2.2.2.5 Inhibitor treatment of eukaryotic cells

Leptomycin B (LMB) is a secondary metabolite of the actinobacterium *Streptomyces spp*. While it was originally discovered as an anti-fungal antibiotic (Hamamoto *et al.*, 1983), Kudo *et al.* (1999) found that LMB irreversibly inhibits the nuclear export receptor CRM1 in eukaryotic cells.

HeLa or HeLa Kyoto cells were incubated with DMEM++ containing 10 nM LMB for 3.5 h in order to inhibit CRM1 and, thus, analyze whether the export of the expressed Survivin variants is CRM1-dependent.

Trichostatin A (TSA) is a metabolite of the actinobacterium *Streptomyces hygroscopicus* and was originally identified as an anti-fungal antibiotic (Tsuji *et al.*, 1976). In 1990, Yoshida *et al.* reported that TSA is capable of inhibiting lysine deacetylases. It is now known that it is a selective inhibitor of the mammalian class I and class II KDACs, but not of the sirtuins (class III KDACs).

In order to enhance the general acetylation level, thus, gaining a higher amount of acetylated Survivin, 293T cells were incubated in DMEM++ containing 100 nm TSA for 16 h.

Nocodazole was patented in 1972 by Gelder *et al.*. Soon is was discovered that it is a potent anti-cancer drug due to its ability to inhibit microtubule polymerization, thus preventing cell division (Atassi and Tagnon, 1975; Hoebeke *et al.*, 1976). In cell biology, nocodazole is used to synchronize the cell cycle of cells as treatment with nocodazole arrests them in prometaphase of mitosis.

In order to arrest 293T cells in prometaphase, thus gaining a higher amount of assembled CPCs in IP experiments, cells were treated with DMEM++ containing 50 ng/mL nocodazole for 16 h.

2.2.2.6 Immunofluorescence staining

Immunofluorescence (IF) stainings are performed to label proteins within samples, for example cells or tissues, with fluorescence dyes in order to allow the analysis of their distribution within the sample by fluorescence microscopy. The method is based on the specific recognition of an antigen by an appropriate antibody. In indirect immunofluorescence, the protein of interest is first recognized by a specific primary, non-fluorescing antibody which, in turn, is detected by a secondary antibody labeled with a fluorescence dye.

For IF stainings of HeLa or HeLa Kyoto cells plated in 8 well µ-slides, the medium was aspirated and the cells were fixed with 200 µL 4 % Roti-Histofix (Carl Roth) per well for 15 min at RT. The fixative was then aspirated and the cells were rinsed three times with PBS for 5 min each. Afterwards, the cells were incubated in 200 µL blocking buffer for 1 h. While blocking, the primary antibodies were diluted in antibody dilution buffer as indicted in Table 2.5. The blocking buffer was aspirated and the cells were incubated in 120 µL primary antibody dilution at 4 °C over night. After rinsing the cells three times

with PBS for 5 min each, 120 µL of the secondary antibody dilution (see Table 2.6) containing 1 µg/µL of the DNA staining dye Hoechst 33342 (AppliChem) were applied and incubated for 1 h at RT in the dark. Subsequently, the cells were rinsed again. For conservation, the PBS was exchanged with PBS containing 0.1 % (w/v) sodium azide and the samples were stored at 4 °C in the dark. In case another antigen was to be stained, the entire procedure was repeated using a primary antibody derived from a different species.

2.2.2.7 Fluorescence microscopy

Fluorescence microscopy takes advantage of the property of a fluorophore to enter an excited state when it absorbs light of a distinct wavelength, and, after a short time, emit light of a longer wavelength when returning to the ground state. With this method the localization of proteins either indirectly labeled with fluorophore-coupled antibodies during IF stainings (see subsubsection 2.2.2.6), or directly labeled via their fusion with fluorescent proteins, can be analyzed in cells or tissues using epifluorescence or confocal fluorescence microscopes.

In an epifluorescence microscope, the excitation light is reflected on the fluorophore-labeled specimen through the objective by a dichroic beamsplitter. In addition to guiding the excitation light from the light source to the specimen, the beamsplitter ensures that only the fluorescence light emitted by the specimen, but not the reflected excitation light are focused on the detector. An additional downstream emission filter prevents transmission of light with wavelengths different from the wavelength of the light emitted by the used fluorophore.

Epifluorescence microscopy was conducted using the inverted microscopes Axio Observer Z.1 (Carl Zeiss Microscopy) and CKX41 (Olympus) with filter sets for imaging the fluorophores Hoechst 33342, green fluorescent protein (GFP)/Alexa Fluor 488 (AF488) and AF568.

In epifluorescence microscopy a great volume of the specimen is excited as the excitation light can penetrate into the specimen, and light emitted by all planes of the specimen reaches the detector. In a confocal microscope, however, only one small focal volume within the specimen is excited and its emitted fluorescence is detected increasing the contrast as well as the lateral resolution in comparison to conventional fluorescence microscopy. This is achieved by two additional apertures, or pinholes, within the light path. The first pinhole is located between the light source and the beam splitter in order to create a point-like light source. The excitation light is focused to the

specimen via the objective and excites only on a small volume of the specimen in the focus plane. Fluorescence light emitted by the specimen passes the objective and the beam splitter and reaches a second pinhole. Only light emitted from the focus plane is focused on that pinhole, thus, passing the pinhole to reach the detector. Light emitted from planes above or below the focus plane is not focused on the pinhole and, thus, cannot reach the detector.

Localization and co-localization studies were conducted using the laser scanning microscope TCS SP5 (Leica Microsystems) controlled by the Leica Application Suite Advanced Fluorescence software. The samples were imaged by sequential scans at excitation wavelengths of 405 nm (Hoechst 33342), 488 nm (GFP or AF488) and 561 nm (AF568) with a scan speed of 100 Hz and a resolution of 1024 x 1024 pixels. For microscopy with the 63x water objective, the diameter of the pinhole was set to 111,4 µm.

2.2.3 Biochemistry

2.2.3.1 Purification of recombinant GST fusion proteins

Proteins tagged with glutathione S-transferase (GST) can be purified from bacterial lysates via affinity chromatography using an affinity medium, e.g. sepharose beads, coupled to the GST ligand glutathione (GSH). At low flow rates GST-tagged proteins bind to immobilized GSH, and impurities can be removed by several washing steps. The bound GST-fusion proteins are then either eluted from the GSH-beads by adding reduced glutathione or, in case a protease cleavage site is located between the tag and the protein, they can be released from the chromatography medium by proteolytic cleavage. The pET41-GST-PreSc vector used to express the recombinant Survivin variants contains a PreScission protease cleavage site. PreScission protease is a fusion protein consisting of human rhinovirus 3C protease and GST. It specifically cleaves between the Q and G residues of its recognition sequence (LEVLFQ/GP).

E. coli SoluBL21 cells expressing the GST-tagged Survivin variants (see subsubsection 2.2.2.2) were harvested in a 50 mL reaction tube by subsequent steps of centrifugation for 15 min at 3,900 x g and 4 °C. Then, the bacterial cells were lyzed. After freezing in liquid nitrogen and re-thawing on ice, the bacterial pellet was resuspended in 15 mL cold lysis buffer and incubated on ice for 10 min. 150 µL of 50 mg/mL Lysozyme were added and the suspension was incubated on ice for 20 min. Next, 75 µL of 10 mg/mL DNase I as well as 75 µL of 1 M magnesium chloride were added and the lysate was transferred to a 25 mL beaker placed on ice. The complete disruption of the cells was achieved by sonication (four times for 7 s and once for 10 s with a break of

90 s each) with the ultrasonic homogenizer Sonopuls HD2200 (Bandelin). The bacterial lysate was cleared by centrifugation for 45 min at 3,900 x g and 4 °C. The supernatant was transferred to a 15 mL reaction tube.

The GST-tagged Survivin proteins were purified from the supernatant with Glutathione Sepharose 4B beads (GE Healthcare Life Sciences). To this end, 1 mL of the GSH beads was transferred to a 15 mL reaction tube and the beads were washed twice by resuspension in 5 mL cold PBS and subsequent centrifugation for 5 min at 500 x g and 4 °C. The bacterial supernatant was mixed with the beads and binding occurred for 2 h at 4 °C on an overhead shaker. After binding, the beads were separated from the supernatant by centrifugation and washed twice with 5 mL cold cleavage buffer containing 1 % (v/v) Triton X-100 (AppliChem).

The GST tag was removed from the recombinant Survivin proteins by proteolytical cleavage with PreScission protease. The beads were resuspended in 500 µL cleavage buffer and transferred to a 2 mL reaction tube. 10 µL PreScission protease (10 mg/mL) were added, and cleavage occurred over night at 4 °C on an overhead shaker. In order to separate the tag-free Survivin proteins from the beads, the suspension was transferred to a Poly-Prep chromatography column (Bio-Rad), and the first fraction of eluted, tag-free protein was collected. Successively, the proteins were eluted twice with 400 and 300 µL of cleavage buffer, respectively.

2.2.3.2 Preparation of whole cell lysates from eukaryotic cells

Whole cell lysates of mammalian cells can be prepared in several ways. One commonly used method is the chemical lysis using RIPA buffer. RIPA buffer, which derives its name from the radio-immunoprecipitation assay for which it has originally been developed, lyses cells effectively as it contains different detergents.

In order to prepare cell extracts from 293T cells plated on 10 cm cell culture dishes, the dishes were placed on ice for 5 min. Then, the cells were detached with a cell scraper, and the cell suspension was transferred to a 15 mL reaction tube. Cells were pelleted by centrifugation for 5 min at 400 x g and 4 °C, resuspended in 1 mL cold PBS and transferred to an 1.5 mL reaction tube. After further centrifugation, the PBS was aspirated. The cells were lyzed by resuspending the cell pellet in 100 to 150 µL RIPA buffer followed by a 15 min incubation on ice. To remove cell debris, the lysate was centrifuged for 20 min at 20,000 x g and 4 °C. Finally, the supernatant was transferred to a fresh 1.5 mL reaction tube. For SDS-PAGE analysis, 40 µg of protein were made

up to 15 µL with ddH_2O and 3.8 µL 5x SDS sample buffer were added. The samples were denatured by boiling at 95 °C for 5 min.

2.2.3.3 Photometric determination of protein concentration

There are several methods to determine the protein concentration of samples, for example the Bradford assay or the measurement of the absorbance at 280 nm (A_{280}). All of these methods have certain advantages and disadvantages. The Bradford assay is rapid and sensitive (Bradford, 1976). It is based on the binding of the anionic triphenylmethane dye Coomassie brilliant blue G-250 to arginine, tryptophan, tyrosine, histidine and phenylalanine residues of proteins under acidic conditions causing a shift in its absorption maximum from 470 nm in the unbound state to 595 nm when it is bound to proteins. Thus, in order to determine the protein concentration of a sample, it is mixed with Coomassie brilliant blue G-250, and the absorbance at 595 nm is measured and compared to a standard curve.

The protein concentration of cell lysates was determined by the Bradford micro assay using the Bio-Rad Protein Assay Kit according to the manufacturer's instructions.

The measurement of the absorbance at 280 nm in order to determine protein concentration is quick, but error prone. It depends on the presence of the aromatic amino acids tyrosine and tryptophan in the protein, which absorb at 280 nm. Similar to the concentration determination of nucleic acids, the calculation of the protein concentration from the A_{280} value is conducted according to Lambert-Beer's law (Equation 2.1):

$$A_\lambda = lg(\frac{I_0}{I}) = \epsilon_\lambda \cdot c \cdot l \tag{2.1}$$

where A_λ is the absorbance at wavelength λ, I_0 is the intensity of the incident light, I is the intensity of the transmitted light, ε_λ is the molar absorption coefficient, c is the concentration and l is the path length. Thus, if the sample contains a purified protein with known absorption coefficient, this method yields reliable results. However, for the concentration determination of proteins with unknown absorption coefficients or protein mixtures, this is not the method of choice.

In order to determine the concentration of purified proteins, their absorption at 280 nm was measured with the spectrophotometer NanoDrop 1000 (Thermo Fisher Scientific). After entering the molar absorption coefficient as well as the molecular weight of the protein, the instrument was calibrated by measuring a ddH_2O sample. After that, 2 µL cleavage buffer were applied to the sample pedestal and measured as a blank followed by measurements of the purified proteins.

2.2.3.4 Immunoprecipitation

Immunoprecipitation (IP) is a method to precipitate a protein from a solution using a specific antibody. The technique requires that the antibody is coupled to a solid matrix, e.g. sepharose or magnetic beads, in order to separate the antigen-antibody precipitate from the solution by centrifugation or application of a magnetic field. Despite isolating a single protein, IP experiments are also performed to investigate protein-protein interactions by pulling on one member of a protein complex under conditions that prevent its dissociation. This is called co-immunoprecipitation (co-IP). In this thesis, tagged proteins were immunoprecipitated from 293T cell lysates using µMACS Isolation kits (Miltenyi Biotec). These kits provide magnetic micro beads coupled to an antibody specific for the respective expression tag. The micro beads are incubated with the lysate, and the mixture is loaded onto a µ column placed in a magnetic field. The magnetically-labeled proteins are retained on the column while unspecifically binding molecules are removed by several washing steps. The target proteins are then eluted from the column with a denaturing elution buffer.

For co-IPs from 293T cells plated on 10 cm cell culture dishes, cell lysates were prepared as described in subsubsection 2.2.3.2 using 1 mL interaction IP lysis buffer. The lysate was incubated for 20 min at 37 °C and 500 rpm and placed on ice. 60 µL of the lysate was mixed with 15 µL 5x SDS sample buffer and heated to 95 °C for 5 min to serve as the input sample for western blot analysis. The remaining lysate was mixed with 50 µL micro beads and incubated for 30 min on ice. A µ column was placed into the magnetic field of a µMACS separator and equilibrated with 200 µL IP lysis buffer. Then, the lysate-beads mixture was loaded to the column and allowed to flow through. After washing the column four times with 200 µL IP lysis buffer each, and once with 100 µL wash buffer 2, the precipitated proteins were eluted. To this end, first 20 µL, and after a 5 min incubation, further 50 µL of elution buffer heated to 95 °C were applied. The eluted samples were collected in 1.5 mL reaction tubes. 25 µL of the input and eluate samples, respectively, were analyzed by SDS-PAGE (see subsubsection 2.2.3.5) and, subsequently, by western blot (see subsubsection 2.2.3.7).

For acetylation IP, lysates were prepared using acetylation IP lysis buffer. Before clearing the lysates by centrifugation, they were sonicated four times for 10 s using the ultrasonic homogenizer Sonopuls mini20 (Bandelin) , and pressed through a 0.8 mm hollow needle five times. All buffers were supplemented with 1 µM TSA in order to prevent deacetylation. 25 µL of the input and 50 µL of the eluate samples were analyzed by SDS-PAGE and, subsequently, by western blot.

2.2.3.5 SDS-polyacrylamide gel electrophoresis

SDS-polyacrylamide gel electrophoresis (PAGE) is a technique that allows to separate denatured proteins according to their mass within an electric field. To this end, the protein samples are mixed with a sample buffer containing, among others, the anionic detergent SDS (Laemmli, 1970). Binding of SDS to proteins leads to the disruption of nearly all noncovalent inter- and intramolecular interactions and results in a linearized conformation. In addition, a net negative charge is imparted to the proteins which is approximately proportional to their molecular mass. This allows the electrophoretic separation of proteins with different masses within a polyacrylamide gel. The acrylamide concentration determines the pore size of the gel and, thus, its separation properties as small proteins migrate faster through the gel than large proteins. The use of a discontinuous system containing of a stacking and a separating gel with different acrylamide and ion concentrations leads to the formation of distinct protein bands.

First, the components of the separating gel were mixed according to Table 2.20 and poured between two glass plates separated by a 1 or 1.5 mm spacer. A layer of isopropanol was added in order to gain a separating gel with a straight upper edge. After polymerization, isopropanol was removed and the stacking gel was poured on top of the separating gel. A comb was inserted in order to create sample wells. After polymerization, the gel was transferred to a vertical electrophoresis chamber and the chamber was filled with 1x SDS-PAGE running buffer. After removing the comb, the samples as well as 7 µL of the Spectra Multicolor Broad Range protein ladder (Thermo Fisher Scientific) were loaded to the gel. Electrophoresis was started at 80 to 100 V. When the samples had passed the stacking gel, the voltage was increased to 120 to 200 V. Electrophoresis was stopped when a sufficient separation was achieved.

Table 2.20: SDS-gel compositions. All volumes are given in mL.

Separating gel 1 mm	**7.5 %**	**10.0 %**	**12.5 %**	**15.0 %**	**2 Stacking gels 1mm**	**4.0 %**
ddH_2O	2.4	2.0	1.6	1.2	ddH_2O	2.5
Separating gel buffer	1.3	1.3	1.3	1.3	Stacking gel buffer	1.35
Acrylamide (30 % (v/v))	1.2	1.6	2.1	2.5	Acrylamide (30 % (v/v))	0.65
APS (10 % (w/v))	0.05	0.05	0.05	0.05	APS (10 % (w/v))	0.05
TEMED	0.005	0.005	0.005	0.005	TEMED	0.005
Separating gel 1.5 mm	**7.5 %**	**10.0 %**	**12.5 %**	**15.0 %**	**2 Stacking gels 1.5 mm**	**4.0 %**
ddH_2O	4.3	3.6	2.9	2.0	ddH_2O	2.5
Separating gel buffer	2.4	2.4	2.4	2.4	Stacking gel buffer	1.35
Acrylamide (30 % (v/v))	2.3	3.0	3.7	4.4	Acrylamide (30 % (v/v))	0.65
APS (10 % (w/v))	0.096	0.096	0.096	0.096	APS (10 % (w/v))	0.05
TEMED	0.010	0.010	0.010	0.010	TEMED	0.005

2.2.3.6 Coomassie staining of polyacrylamide gels

The unspecific staining of proteins within polyacrylamide gels after electrophoretic separation by SDS PAGE is based on the binding of the triphenylmethane dye Coomassie brilliant blue G-250 to basic amino acids as explained in subsubsection 2.2.3.3.

Polyacrylamide gels were incubated in Coomassie staining solution over night at RT under shaking. After staining, the gels were rinsed with water several times and incubated in destaining solution for at least 3 h at RT under shaking in order to remove background staining, and were again rinsed with water.

2.2.3.7 Western blot

Western blotting (or immunoblotting) is a method used to electrophoretically transfer proteins that have been separated by SDS-PAGE to a membrane allowing their detection by specific antibodies. To this end, the polyacrylamide gel containing the separated proteins is placed in an electric field. As the proteins are negatively charged due to treatment with SDS they migrate to the anode. The membrane is placed between the gel and the anode of the western blotting chamber, thus, when migrating towards the anode, the proteins are immobilized on the membrane due to hydrophobic and electrostatic interactions. After transfer, the proteins are accessible for detection by specific primary antibodies. Primary antibodies are, in turn, detected by secondary antibodies. The secondary antibody is derived from a different species than the primary antibody and recognizes all antibodies derived from the same species by their identical Fc domain. Secondary antibodies are labeled, for instance with fluorescent dyes or enzymes catalyzing light or color reactions, in order to locate their position on the membrane. The proteins bands are then detected either by a fluorescence scanner, X-ray films, or directly on the membrane due to the appearance of colored bands.

Western blotting was performed using the tank blot technique. First, the PVDF membrane was activated in 100 % methanol for 15 s and, subsequently, equilibrated in 1x transfer buffer together with the polyacrylamide gel. Four sheets of filter paper as well as the pads of the blot cassette were also soaked with transfer buffer . The blot sandwich was assembled from the anode-facing side of the blot cassette to the cathode-facing side as follows: a pad, two sheets of filter paper, the membrane, the gel, another two sheets of filter paper and another pad. After inserting the blot cassette into the tank blot chamber, the chamber was filled with transfer buffer. Western blotting occurred for 350 to 400 mA for 90 to 120 min at 4 °C. When transfer was finished, the membrane was incubated in blocking buffer for 1 h at RT on a rocking shaker in order to block free binding sites on the membrane, thus preventing unspecific binding of the primary antibody. Primary antibodies were diluted in blocking buffer according to Table 2.5. Incubation of the membrane with the primary antibody dilution occurred for 1 h at RT or over night at 4 °C. After washing the membrane three times with TBST, the secondary antibody coupled to the enzyme horseradish peroxidase (HRP) was diluted in blocking buffer (see Table 2.6) and incubated on the membrane for 1 h at RT. The membrane was washed twice with TBST and once with TBS, before developing the blot with the Pierce ECL Plus western blotting substrate (Thermo Fisher Scientific). This reagent contains an acridan substrate that undergoes enzymatic oxidation by HRP to yield a chemiluminescent acridinium ester. The chemiluminescence was detected by an X-ray film which was developed using the film processor Cawomat 2000 IR (Cawo).

2.2.3.8 Analytical gel filtration

Gel filtration (or size exclusion chromatography) is a chromatography technique that separates molecules due to differences in their size as they pass through a gel filtration medium packed in a column. The medium is a matrix of porous beads which allows small molecules to enter the pores resulting in a long retention time. Larger molecules that cannot enter the pores migrate around the beads and are eluted earlier. Gel filtration is commonly applied to analyze the oligomerization state of native proteins.

The dimerization of the recombinant, purified Survivin variants was investigated using the Superdex 75 10/300 GL gel filtration column together with the liquid chromatography (LC) system ÄKTApurifier controlled by the Unicorn control software (all GE Healthcare Life Sciences). Before the column was equilibrated with cold gel filtration buffer, the buffer had to be sterile-filtered and degassed. The purified proteins were diluted with the buffer to a final concentration of 1 to 2 mg/mL and 80 to 100 µL of the samples were injected into the 500 µL sample loop of the LC system. The samples passed through the column with a flow rate of 0.4 mL/min. The elution of the proteins was monitored by measuring the absorbance at 280 nm. For calibration, a mixture of the globular proteins Conalbumin (75 kDa), Ovalbumin (44 kDa), Carbonic anhydrase (29 kDa), Ribonuclease A (13.7 kDa) and Aprotinin (6.5 kDa) as well as Blue Dextran 2000 (>2,000 kDa) was analyzed under the same conditions.

2.2.3.9 Circular dichroism spectroscopy

Circular dichroism (CD) spectroscopy is a technique to study chiral molecules by measuring their CD over a range of wavelengths. CD is the difference in the absorption of left-handed circularly polarised light and right-handed circularly polarised light and is a characteristic of molecules containing one or more chiral chromophores. A common application of CD spectroscopy is the analysis of the structure or conformation of macromolecules, in particular of proteins. Far-UV CD spectra recorded between 170 and 260 nm provide information on the conformation of the amide bonds within the protein backbone, thus allowing to identify secondary structure elements within a protein. While randomly coiled regions of a protein exhibit a positive peak of the CD or the ellipticity at 212 nm and a negative peak at 195 nm, in case of β-sheets the peaks are shifted to 218 and 196 nm, respectively. α-helical regions exhibit three peaks: a positive one at 192 nm and two negative ones at 209 and 222 nm.

The integrity of the secondary structure of the purified, recombinant Survivin variants was analyzed by measuring CD with a J-715 CD spectropolarimeter (Jasco). The pro-

teins were diluted to a final concentration of 0.2 mg/mL with sterile-filtered CD buffer and 200 µL of the dilutions were transferred to a quartz glass cuvette with a path lengths of 1 mm (Hellma Analytics). For recording the far-UV CD spectra between 190 and 260 nm, the data interval was set to 0.1 nm, the scanning speed to 100 nm/min, the response time to 0.5 s and the band width to 2 nm. 15 spectra were recorded of each sample at 20 °C and accumulated. From each protein spectrum a buffer spectrum was subtracted and the measured ellipticity was converted to specific ellipticity using path length and protein concentration according to Equation 2.2

$$\Psi_{spec} = \frac{\Psi}{l \cdot c} \tag{2.2}$$

where Ψ_{spec} is the specific ellipticity in deg · cm^3 · dm^{-1} per gram of amino acid, Ψ is the measured ellipticity in mdeg, l is the path length in cm and c is the concentration in mg/ml.

3 RESULTS

3.1 Relevance of Survivin acetylation for its dimerization and cellular localization

In 2010, Wang *et al.* reported that the acetylation of Survivin at lysine 129 determines whether the protein forms homodimers or binds to the nuclear export receptor CRM1, and thus, is also responsible for Survivin's cellular localization. In the study, four Survivin mutants were compared, two, which cannot be acetylated at lysine 129 (SurvK129R and SurvK129E), the others mimicking acetylation (SurvK129Q and SurvK129A). By immunofluorescence (IF) stainings of the Survivin variants expressed in HeLa cells they showed that myc-tagged SurvK129R and SurvK129E showed a more cytoplasmic localization while the mimicking mutants localized mainly in the nucleus like the wt protein. Furthermore, immunoprecipitation (IP) and Förster resonance energy transfer (FRET) analyses revealed that SurvK129E formed less stable homodimers and that its binding affinity to CRM1 was increased compared to Survivin wt.

Survivin consists of three regions determining its various functions. The N-terminal BIR domain (aa 15-88) is responsible for Survivin's anti-apoptotic function, as it can bind to, and thus, stabilize XIAP (Dohi *et al.*, 2004). Between the BIR domain and Survivin's C-terminal α-helix (aa 99-142), a linker region is located containing two overlapping, functionally important features: the nuclear export signal (aa 89-98) and one part of the dimer interface (aa 89-102). The NES is the binding site for the nuclear export receptor CRM1, thus mediating the nuclear export of Survivin. At the dimer interface, two Survivin monomers can interact to form the bow tie-shaped dimer depicted in Figure 3.1. For the long C-terminal α-helix, two functions have been described so far: first, it mediates the interaction of Survivin with microtubules (Li *et al.*, 1998), and second, it forms a stable helical bundle with helices of Borealin and INCENP to build up the core of the CPC (Jeyaprakash *et al.*, 2007). K129 is located within a hydrophobic cluster

in the last third of Survivin's C-terminal helix, a region which is likely to be involved in protein-protein interactions.

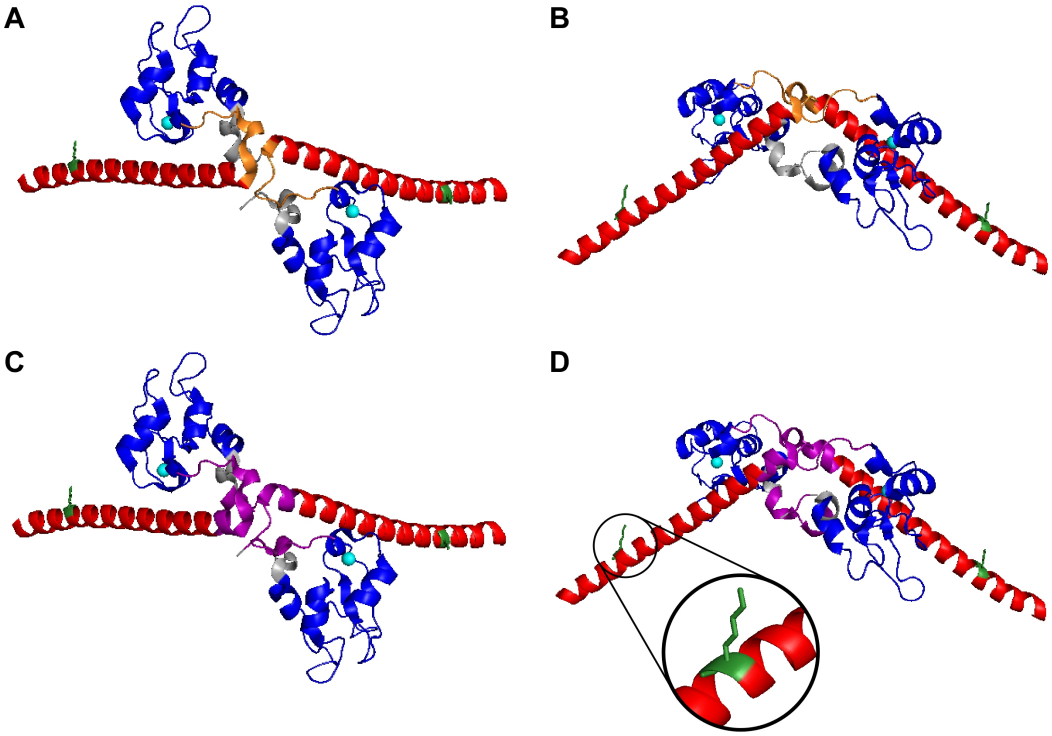

Figure 3.1: Schematic representation of acetylated lysine 129 in the Survivin homodimer. Ribbon representations of the bow tie-shaped Survivin homodimer (Chantalat *et al.*, 2000; PDB ID: 1E31). The N-terminal BIR domain is shown in blue and the C-terminal α-helix in red. K129 is depicted in green in stick representation. The Zn^{2+} ion is shown as a sphere in cyan. A) Bow tie-shaped Survivin dimer. The NES is depicted in orange. B) The view in A rotated by 90° around the horizontal axis. C) The same view as in A. The dimer interface is depicted in purple. D) The view in C rotated by 90° around the horizontal axis. The dimer interface is depicted in purple. The circle shows a close up view of K129.

It is noticeable about the abovementioned study by Wang *et al.* (2010b) that the results shown only included the SurvK129E mutant, which was described as unacetylatable, and thus, comparable to SurvK129R. For SurvK129R, however, except that it was mentioned that its cellular localization resembled that of SurvK129E, no results were shown at all. The SurvK129E mutant was chosen since a search in the NCBI single nucleotide polymorphism (SNP) database revealed a SNP in the Survivin gene changing lysine 129 to glutamate. Considering other studies analyzing protein acetylation, the substitution of lysine with glutamate is not the typical mutation to abolish acetylation. Conventionally, lysine is mutated to arginine on the one hand to inhibit acetylation and other post-translational modifications, and on the other hand to mimic the structural as well as biochemical properties of lysine.

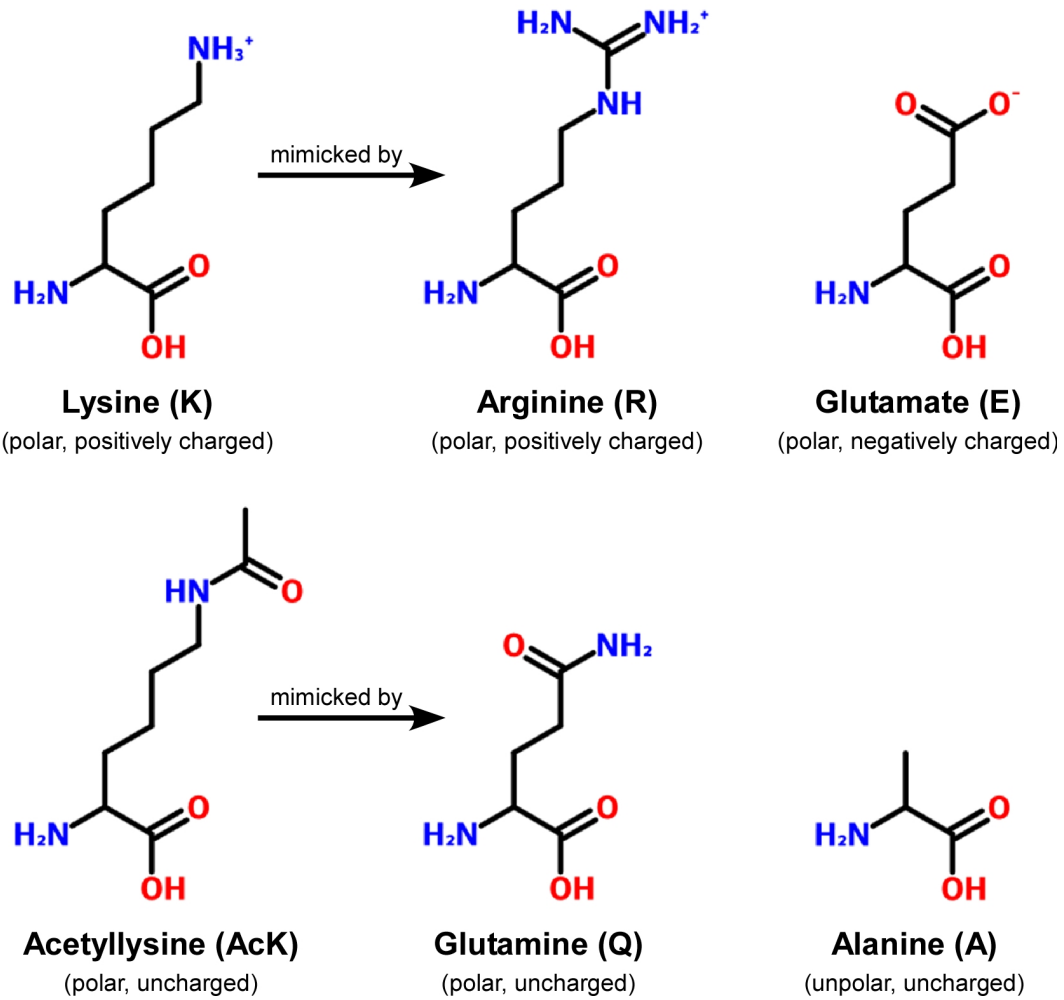

Figure 3.2: Chemical structures of the amino acids lysine and acetyllysine and the amino acids used for their substitution.

The side chain of lysine consists of four methylen groups followed by an amino group which makes lysine a basic, polar and positively charged amino acid at a neutral pH value (Figure 3.2). The side chain of arginine contains three methylen groups followed by a guanidino group which implicates that arginine is basic, polar and positively charged as well, and its side chain has a length comparable to that of lysine. Glutamate, however, besides having a shorter side chain, belongs to the acidic amino acids as its side chain ends with a negatively charged carboxyl group. This indicates that SurvK129E might not be comparable to Survivin wt not acetylated at K129 or to SurvK129R, and thus, might be inappropriate to gain information about the function of Survivin acetylation at K129. The acetylation of a lysine residue leads to the loss of its positive charge. Hence, an amino acid appropriate to mimic acetylated lysine must be polar and uncharged. For this purpose, glutamine is used as standard, although its side chain is shorter than that of lysine. The substitution of lysine with alanine is untypical for mimicking an acetylated lysine residue since alanine is unpolar and its side chain

consists only of one methyl group.

As a preliminary work to our studies, which were aimed at the identification of further acetylation sites in Survivin and the influence of the potential acetylation on Survivin's various functions, we first wanted to verify the findings observed by Wang *et al.* (2010b), and evaluate whether the results presented for the SurvK129E mutant allow to draw conclusions on the relevance of Survivin acetylation for its dimerization and cellular localization. Furthermore, we intended to analyze the effects of lysine 129 acetylation on Survivin's functions that were not addressed in the study, for example its role in mitosis.

3.2 Characterization of Survivin acetylation at lysine 129

3.2.1 Optimization of the conditions to analyze Survivin acetylation

As lysine to arginine and lysine to glutamine mutations are conventionally used to investigate protein acetylation, initially, the SurvK129R and SurvK129Q mutants were analyzed. To generate these mutants, the pc3-Survivin-GFP plasmid was used as a template for splice overlap extension PCR (subsubsection 2.2.1.2) with primers bearing the mutation of lysine 129 to arginine or glutamine, respectively. To first examine their general acetylation level, the Survivin variants were transiently expressed in 293T cells and immunoprecipitated from the lysates. Lysine acetylation was determined by western blot using an antibody specific for acetylated lysine (AcK) (Figure 3.3). For Survivin wt-GFP (43 kDa), a low acetylation level could be detected which did not increase upon treatment with the KDAC class I and II inhibitor trichostatin A (TSA) (Figure 3.3A). However, co-expression with the KATs p300 or CBP strongly enhanced the overall acetylation. The acetylation levels of SurvK129R and SurvK129Q were comparable to that of Survivin wt. Further analysis by IP including the isolated GFP tag (27 kDa) revealed that GFP also contains acetylated lysine residues (Figure 3.3B).

In order to investigate the cellular localization of the Survivin mutants, cDNAs coding for the GFP-tagged Survivin variants were transiently transfected into HeLa cells, and protein localization was assessed by IF staining (Figure 3.4). The wt protein and both mutants predominantly localized to the cytoplasm. A minor protein amount could also be detected in the nucleus.

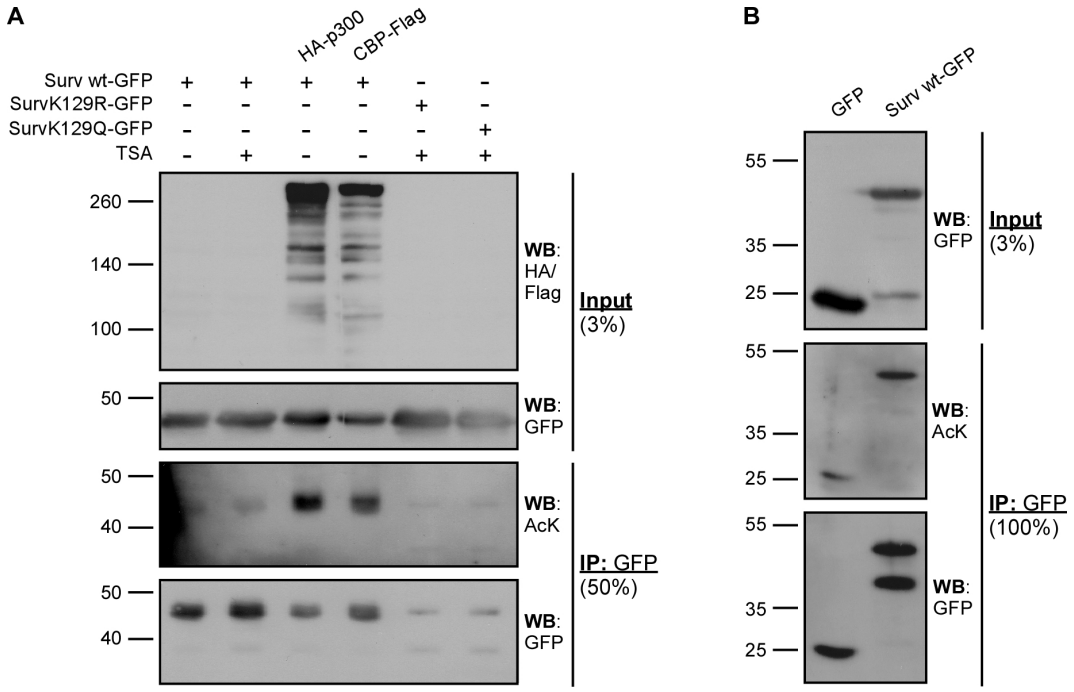

Figure 3.3: Acetylation of GFP-tagged Survivin by the KATs p300 and CBP. A) 293T cells were (co-)transfected with GFP-tagged Survivin variants, and the lysine acetyltransferases HA-p300 or CBP-Flag. Treatment with 100 nM trichostatine A (TSA) for 16 h was performed where indicated. Lysates were immunoprecipitated (IP) with magnetic beads coupled to a GFP-specific antibody using TSA-containing buffers and immunoblotted (WB). Membranes were probed with antibodies specific for HA, Flag, GFP, or AcK. B) 293T cells were transfected with cDNAs coding for GFP or Survivin wt-GFP. Lysates were immunoprecipitated with magnetic beads coupled to a GFP antibody using TSA-containing buffers and immunoblotted. Membranes were probed with antibodies specific for GFP or AcK.

Since GFP contains acetylated lysine residues, which was confirmed by the PAIL (Prediction of acetylation on internal lysines) online tool (http://bdmpail.biocuckoo.org/index.php, Li *et al.*, 2006), and a huge tag like GFP (27 kDa) fused to the C-terminus of Survivin (16.5 kDa) might prevent acetylation in the C-terminal region, Survivin wt and both mutants were cloned with smaller C-terminal expression tags (myc or HA). An acetylation prediction for the Survivin wt-myc sequence by PAIL revealed that although the myc tag contains a lysine residue, its acetylation is improbable. The HA tag does not contain lysine residues. The Survivin variants with smaller tags were expressed in HeLa cells and again, their cellular localization was analyzed microscopically (Figure 3.5 and data not shown). The results were comparable to that obtained for the GFP-tagged Survivin variants (Figure 3.4), with the only difference that more protein was present in the nucleus. In most cells, an intense membrane staining was observed.

Since no differences in the cellular localization of the C-terminally tagged mutants could be observed, Survivin wt and both mutants were finally cloned with an N-terminal myc tag in order to create the same conditions as reported by Wang *et al.* (2010b), although

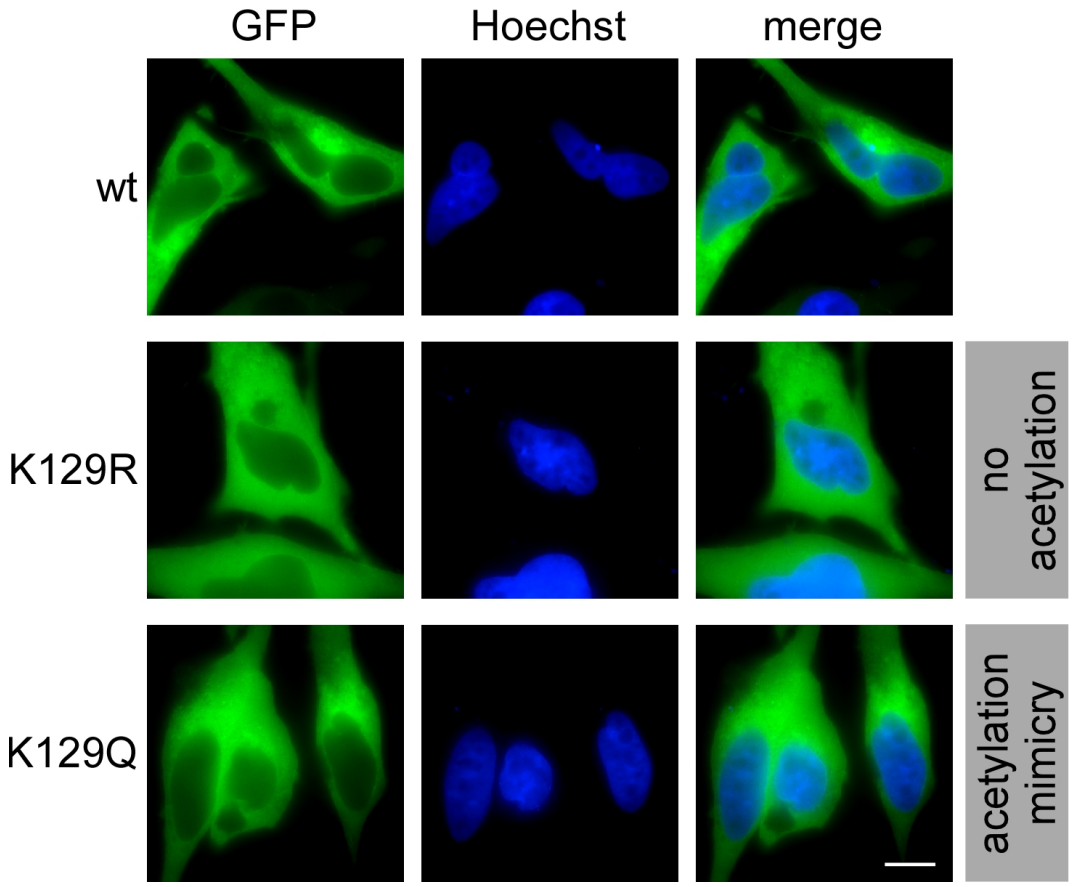

Figure 3.4: Cellular localization of GFP-tagged Survivin K129R/Q mutants. HeLa cells were transiently transfected with Survivin-GFP variants (green), fixed, and DNA was stained with Hoechst. Images were taken with a Zeiss AxioObserver fluorescence microscope. Scale bar, 10 µm.

PAIL prediction revealed that the lysine within the myc tag is likely to be acetylated if the tag is placed at the N-terminus of the protein. Also the unconventional SurvK129E and SurvK129A mutants were included in our study. Furthermore, a different strain of HeLa cells, HeLa Kyoto (HeLa K), was chosen for subsequent microscopic analyses as these cells have a larger cell body, they form an ordered monolayer, and no staining artifacts like membrane staining occur in IF experiments.

With Survivin wt and the four mutants available with an N-terminal myc tag, the different properties of the Survivin variants could be analyzed. The subcellular localization was assessed by IF stainings, while the dimerization was analyzed by IP as well as gel filtration experiments. IP was also used to investigate the interaction of the Survivin mutants with CRM1 and with members of the CPC. Their involvement in mitosis was additionally analyzed by IF staining, and CD spectra were recorded to survey the integrity of the proteins' secondary structure.

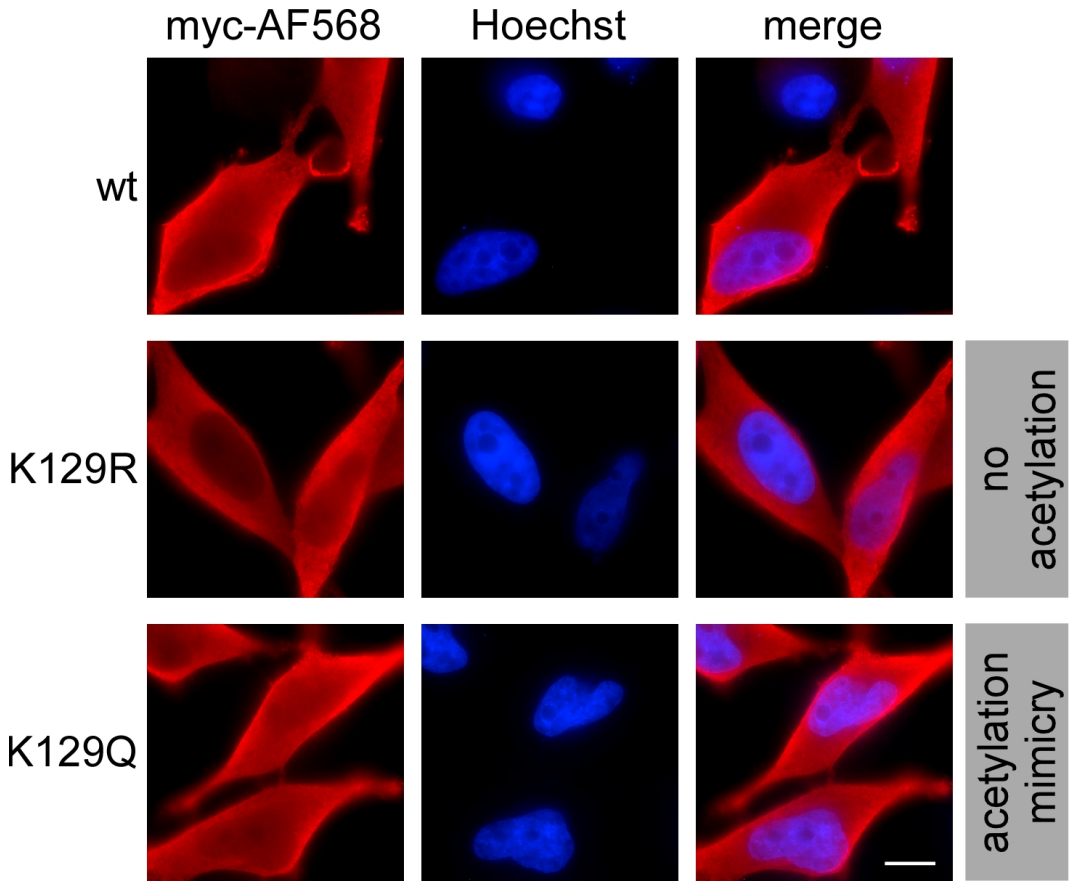

Figure 3.5: Cellular localization of myc-tagged Survivin K129R/Q mutants. HeLa cells were transiently transfected with Survivin-myc variants, fixed, and immunostained with a myc-specific antibody (red). DNA was stained with Hoechst (blue). Images were taken with a Zeiss AxioObserver fluorescence microscope. Scale bar, 10 µm.

3.2.2 Effect of Survivin acetylation on its cellular localization

In order to investigate their cellular localization, the myc-tagged Survivin variants were transiently expressed in HeLa K cells, and their localization was assessed by IF staining (Figure 3.6). The wt protein and both acetylation mimicking mutants, K129Q and K129A, localized primarily in the cytoplasm, but a minor amount of protein was also detectable in the nucleus. The same distribution was observed for the acetylation abolishing K129R mutant. SurvK129E, however, showed an altered subcellular localization as no protein could be detected in the nucleus.

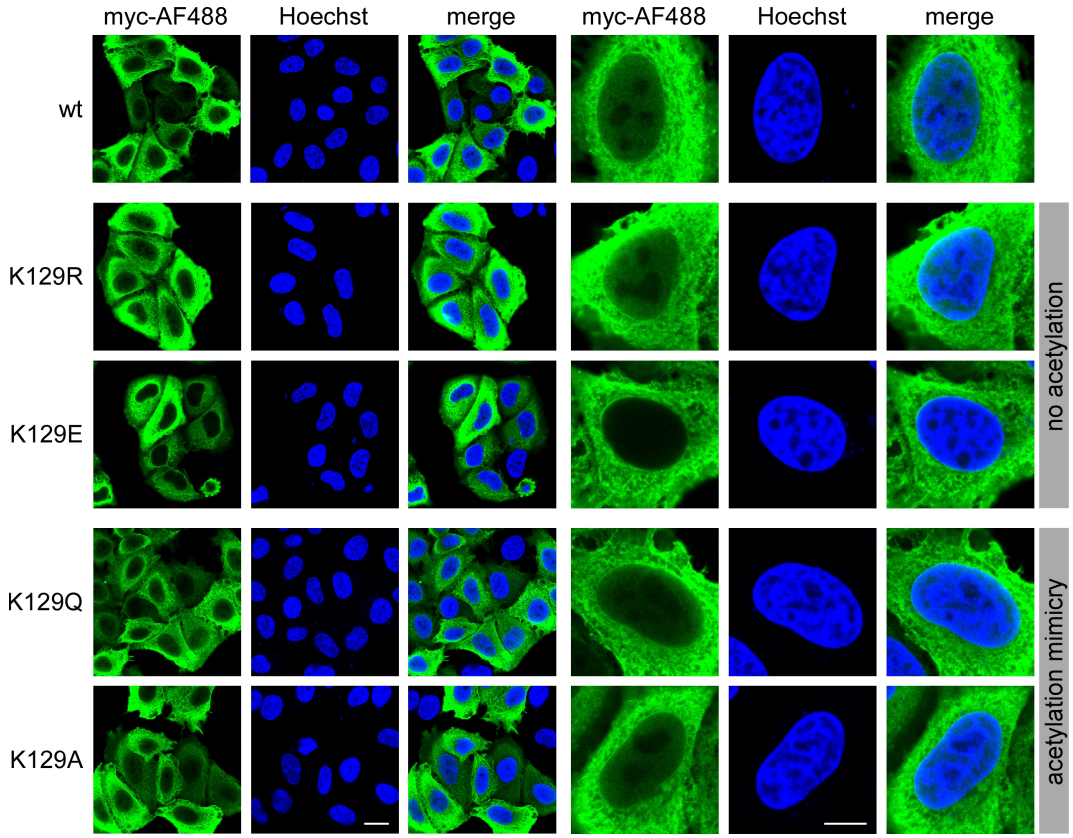

Figure 3.6: Cellular localization of myc-tagged Survivin K129 mutants. HeLa K cells were transiently transfected with myc-Survivin variants and fixed 24 h later. After permeabilization, they were immunostained with a myc-specific antibody (green). DNA was stained with Hoechst (blue). Images were taken with a Leica SP5 confocal microscope. Scale bar, 20 µm (overview) and 10 µm (zoom), respectively.

3.2.3 Effect of Survivin acetylation on its dimerization

As Wang *et al.* (2010b) argued that SurvK129E forms less stable dimers than wt Survivin, the homodimerization of the Survivin variants was investigated by IP experiments. 293T cells were co-transfected with myc-, HA- or GFP-tagged Survivin mutants and lysed. The lysates were incubated for 20 min at 37 °C before adding the microbeads coupled to an HA-specific antibody. HA-tagged Survivin was immunoprecipitated from the lysates, and the interaction of the different Survivin mutants was then analyzed by western blot (Figure 3.7). SurvF101AL102A, a dimerization deficient mutant described by Engelsma *et al.* (2007), was used as negative control.

No dimerization of SurvF101AL102A with Survivin wt or with itself could be detected. The non acetylatable SurvK129E mutant also preferentially existed as a monomer. The second mutant that cannot be acetylated, SurvK129R, however, showed a strong dimerization with Survivin wt similar to that of wt with wt protein. In comparison to that, the homodimerization of SurvK129R was reduced by 38 %. Also a different interaction

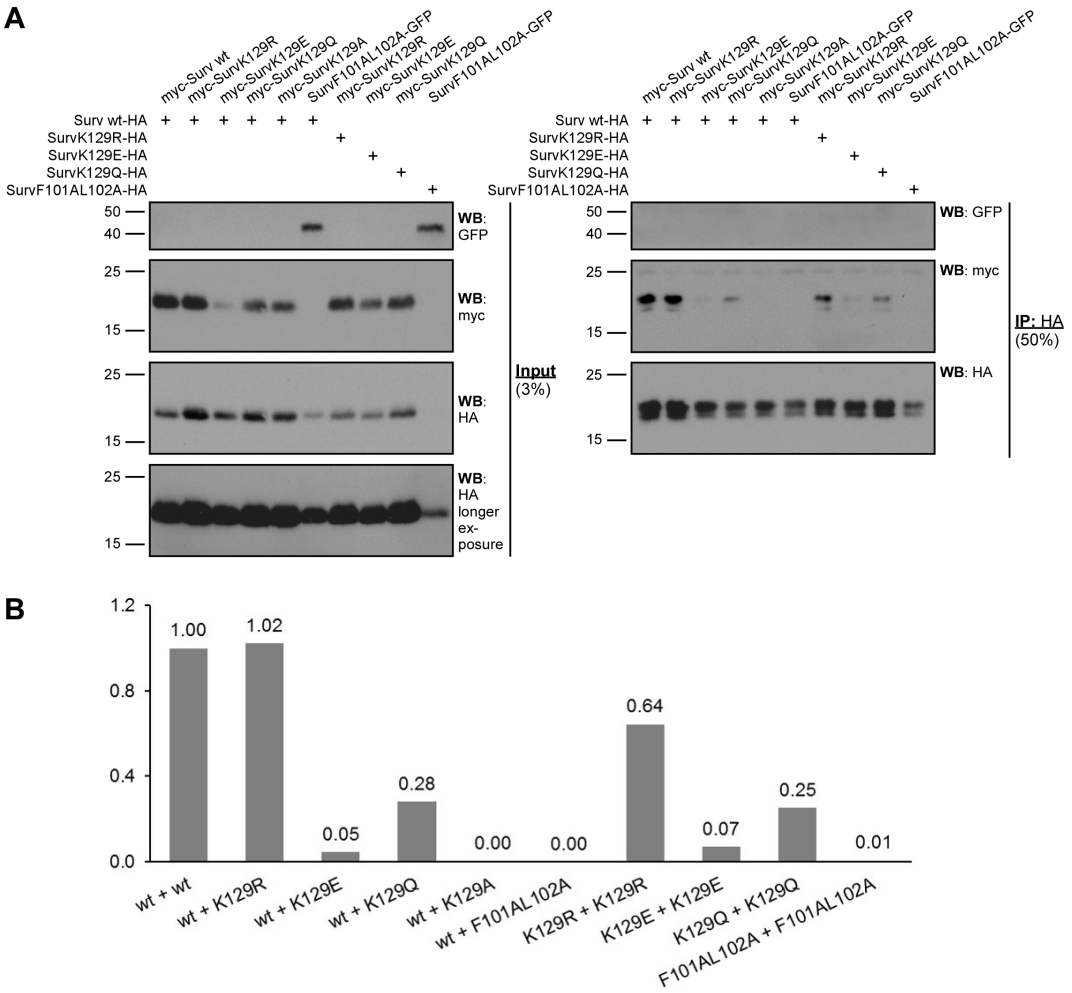

Figure 3.7: Dimerization of myc-tagged Survivin K129 mutants. A) Lysates from 293T cells transiently transfected with myc-, HA- or GFP-tagged Survivin mutants were immunoprecipitated (IP) with magnetic beads coupled to an HA-specific antibody and immunoblotted (WB). Membranes were probed with antibodies specific for GFP, myc or HA. B) Quantification of the immunoblot shown in A.

strength was found for the acetylation mimicking mutants SurvK129Q and SurvK129A. While no dimerization of SurvK129A with wt Survivin was evident, the dimerization of SurvK129Q with Survivin wt or with itself was enhanced (28 % and 25 %, respectively, compared to Survivin wt with wt).

To verify the results obtained by IP experiments, gel filtration analyses were performed. For recombinant expression in bacteria, the Survivin mutants were integrated into the pET41-GST-PreSc vector system. The advantage of this system is that proteins can be expressed with an N-terminal GST tag followed by the PreScission protease cleavage site allowing to purify the proteins from bacterial lysates with Sepharose-GSH beads, and subsequently, use PreScission protease to remove the tag. The expression of GST-tagged Survivin wt in *E.coli* SoluBL21 bacteria (Genlantis) was tested under different

conditions. Finally, expression at 30 °C for 7 h resulted in the highest yield of soluble protein. Consequently, the expression of Survivin wt and the mutants was performed under these conditions.

The purified, tag-free Survivin proteins were then analyzed in PBS containing 2.5 mM β-mercaptoethanol using a Superdex 75 10/300 GL column (GE Healtcare Life Sciences) (Figure 3.8A). The dimerization-deficient SurvF101AL102A mutant was again used as negative control.

The gel filtration analysis revealed that for SurvF101AL102A (gray) indeed only one peak was detectable at an elution volume of 10.4 mL, indicative for a monomer. In contrast, the profiles of Survivin wt (green) and the mutants SurvK129R (dark blue) and SurvK129Q (red) also showed a low monomer peak at approx. 10.3 mL, but the major peak appeared at an elution volume of 9.5 mL indicating a Survivin dimer. The profile of SurvK129E (blue) resembled that of Survivin wt and the other K129 mutants, but both peaks eluted 0.1 mL earlier, at 9.4 and 10.2 mL, respectively. SurvK129A was not included in this analysis. Gel filtration was repeated (data not shown), this time including the K129A mutant.

As it was not possible to draw conclusions on the dimerization properties of the mutants only by comparing their elution profiles due to the different height of the peaks, the dimer and monomer peaks of each profile were integrated separately to obtain the amount of dimer or momomer. The sum of both integrals was set to 100 %. Figure 3.8B shows the results of both gel filtration analyses. As already apparent from its gel filtration profile, SurvF101AL102A did not form homodimers. The quantification revealed an amount of 84 % monomeric protein. The results for Survivin wt and the SurvK129 mutants differed from the distribution obtained for the dimerization-deficient variant. With percentages of 75 % for Survivin wt, SurvK129R and SurvK129E, 76 % for SurvK129Q and even 85 % for SurvK129A, the dimeric form was clearly predominant.

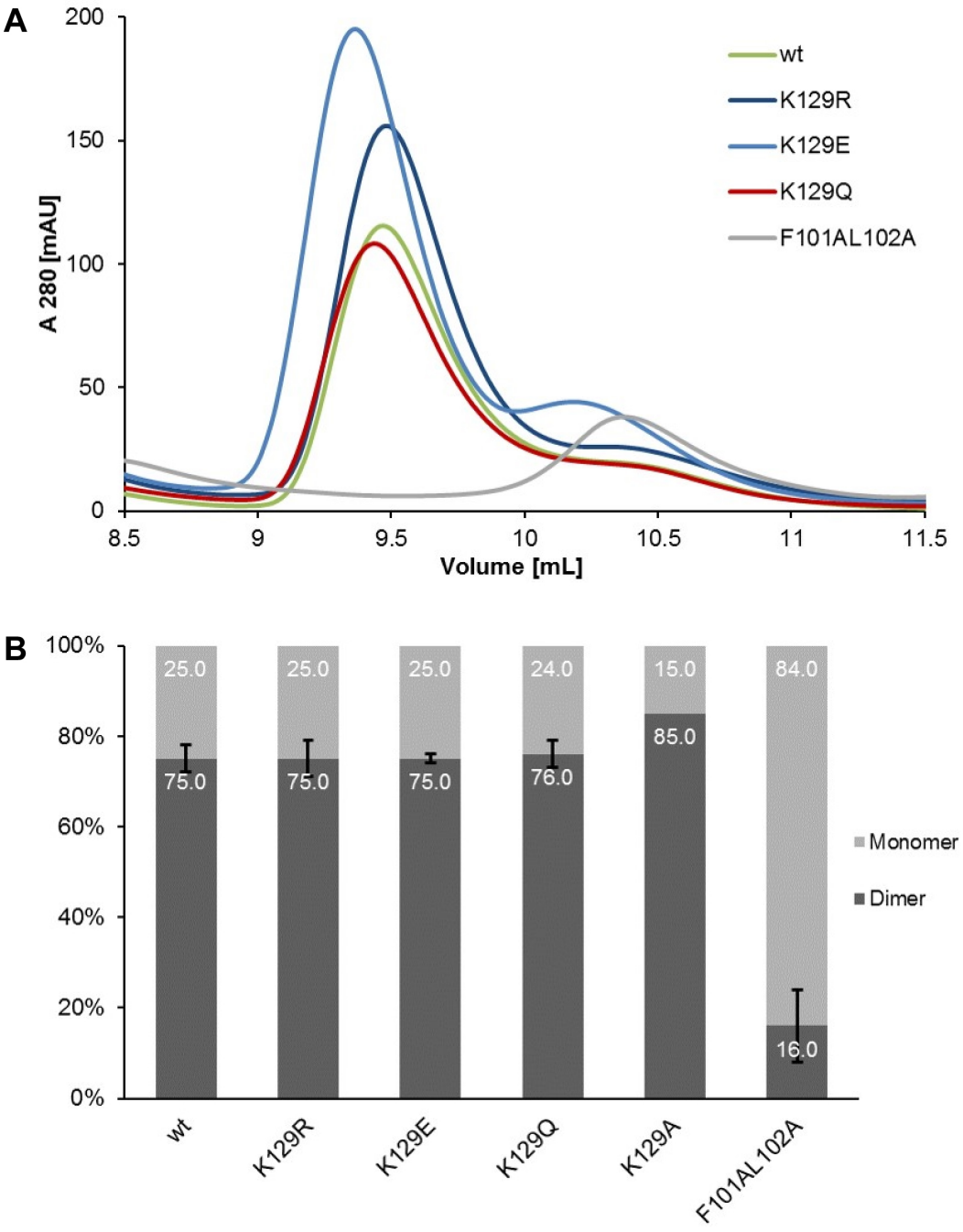

Figure 3.8: Dimerization of recombinant, untagged Survivin K129 mutants. A) Gel filtration profiles of purified, tag-free Survivin mutants in PBS containing 2.5 mM β-mercaptoethanol. Only the elution range between 8.5 and 11.5 mL is shown. A 280: absorption at 280 nm; AU: absorption units. B) Quantification of Survivin dimerization. Monomer and dimer peaks of the gel filtration profiles shown in A were integrated and the sum of both integrals was set to 100 %. The data are means of two experiments, except for SurvK129A (n=1). The error bars represent s.d.

3.2.4 Effect of Survivin acetylation on its interaction with the export receptor CRM1

As also shown by Wang *et al.* (2010b), the SurvK129E mutant exhibited an altered subcellular localization compared to the other mutants (Figure 3.6), which indicates differences in their nucleo-cytoplasmic transport and their interaction patterns with the export receptor CRM1. In order to investigate whether the nuclear export of the Survivin variants is indeed CRM1-dependent, a cellular CRM1 inhibition assay was performed. To this end, HeLa K cells transfected with the myc-Survivin variants were treated with 10 nM leptomycin B (LMB) for 3.5 h. LMB irreversibly inhibits CRM1 by alkylating C528 in its NES binding pocket, thus preventing the binding of NES-containing proteins (Kudo *et al.*, 1999). Then the cells were fixed, permeabilized, and immunostained with a myc-specific antibody (Figure 3.9).

In the untreated control cells, myc-tagged Survivin wt and the different mutants showed the same localization as already described in subsection 3.2.2 (Figure 3.6). Again, only SurvK129E did not localized to the nucleus, but was exclusively found in the cytoplasm. The SurvF101AL102A mutant, for which a stronger binding to CRM1 was described (Engelsma *et al.*, 2007), localized like Survivin wt in the untreated cells. SurvNESmut-GFP, in contrast, exhibited a prominent nuclear accumulation. After LMB treatment, all SurvK129 variants showed an increased nuclear localization, but still more protein was detectable in the cytoplasm than in the nucleus. An equal protein distribution in both compartments could be observed for the dimerization-deficient mutant. SurvNESmut-GFP accumulated in the nucleus as before the treatment with LMB.

The CRM1 inhibition assay was accompanied by IP experiments in order to evaluate the differences of the SurvK129 mutants in CRM1 binding reported by Wang *et al.* (2010b). Therefore, 293T cells were transfected with CRM1-HA and the different myc-SurvK129 mutants. The lysates were incubated for 20 min at 37 °C before adding the microbeads coupled to an HA-specific antibody. CRM1-HA (125 kDa) was then immunoprecipitated from the lysates, and the co-IP of the Survivin variants was analyzed by western blot (Figure 3.10).

Indeed, differences between the acetylation abolishing mutants K129R and K129E could be observed. While the binding affinity of SurvK129R to CRM1 was reduced by 16 % compared to wt Survivin, the interaction of SurvK129E with CRM1 was even stronger than that of Survivin wt (1.11). The acetylation mimicking mutants SurvK129Q and SurvK129A exhibited a 28 % and 48 % decreased binding affinity, respecticely, compared to Survivin wt. A binding of Surv1-119-GFP, a truncated variant of Survivin missing the C-terminal part of the helix in which Rodriguez *et al.* (2002) hypothesized a

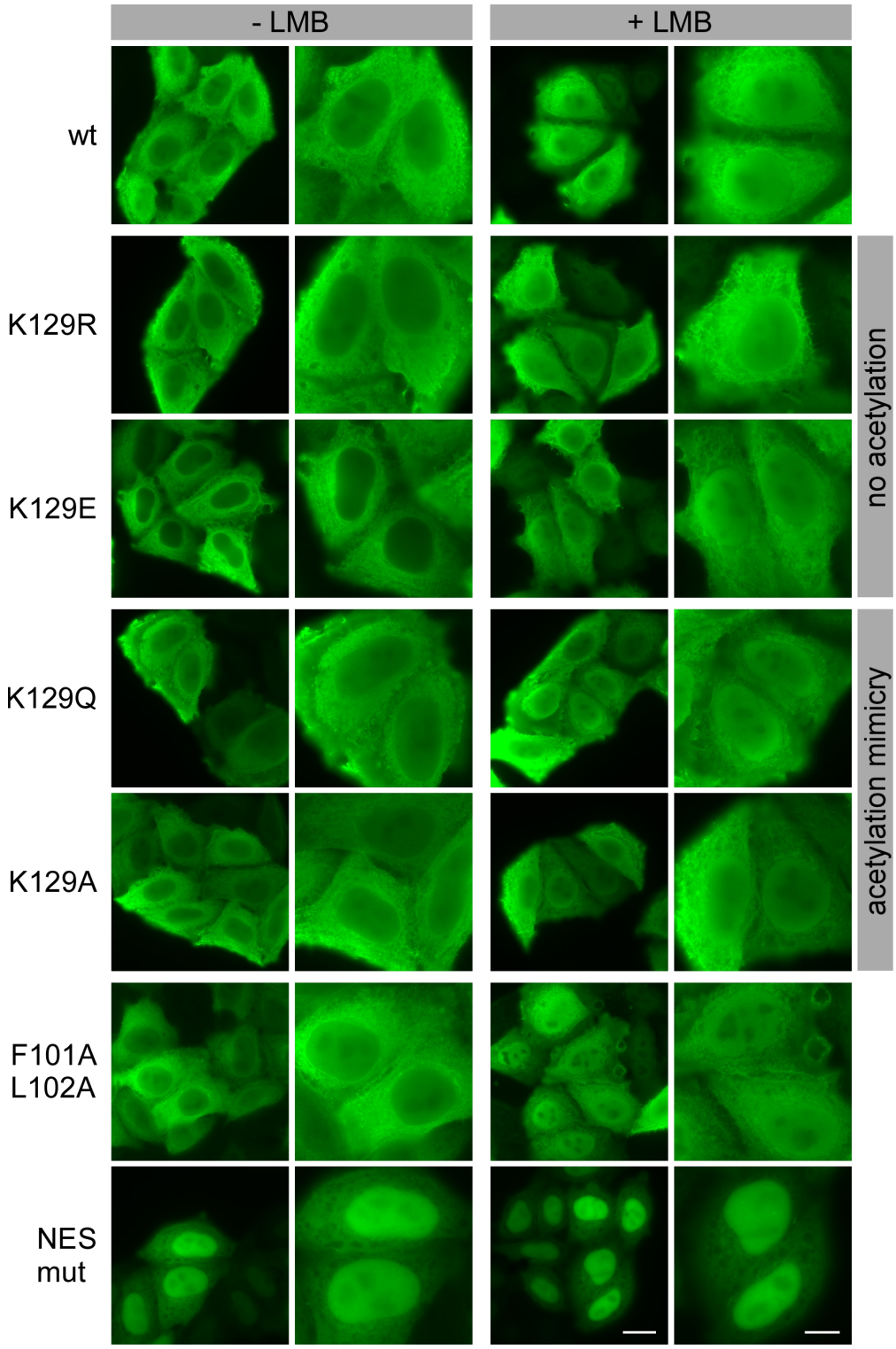

Figure 3.9: Effect of CRM1 inhibition on the cellular localization of myc-tagged Survivin mutants. HeLa K cells were transiently transfected with myc-Survivin variants (green) or SurvNESmut-GFP. 24 h later they were treated with 10 nM LMB for 3.5 h. After permeabilization, cells were immunostained with a myc-specific antibody. Untreated cells were used as control. Images were taken with a Zeiss Axiovert epifluorescence microscope. Scale bar, 20 µm (overview) and 10 µm (zoom), respectively.

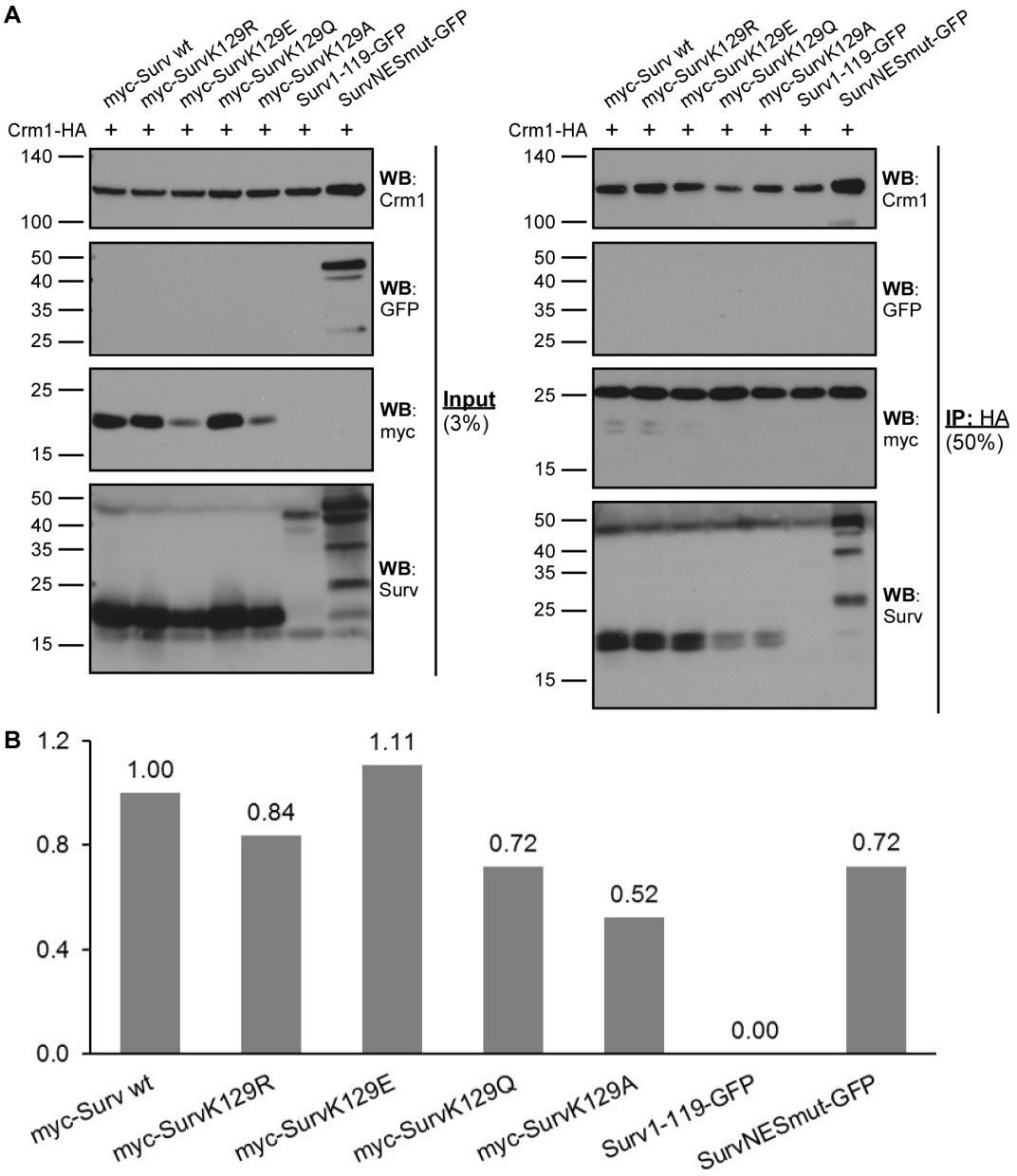

Figure 3.10: Interaction of myc-tagged Survivin K129 mutants with CRM1. A) Lysates from 293T cells transiently transfected with HA-tagged CRM1 and myc- or GFP-tagged Survivin mutants were immunoprecipitated (IP) with magnetic beads coupled to an HA-specific antibody and immunoblotted (WB). Membranes were probed with antibodies specific for CRM1, GFP, myc or Surv. B) Quantification of the immunoblot shown in A.

non-classical CRM1-dependent export motif, could not be detected. For SurvNESmut-GFP, where the interaction with CRM1 is abolished by mutating two essential leucine residues within the export signal (Knauer *et al.*, 2006), an only 28 % reduced interaction with CRM1 was observed, however.

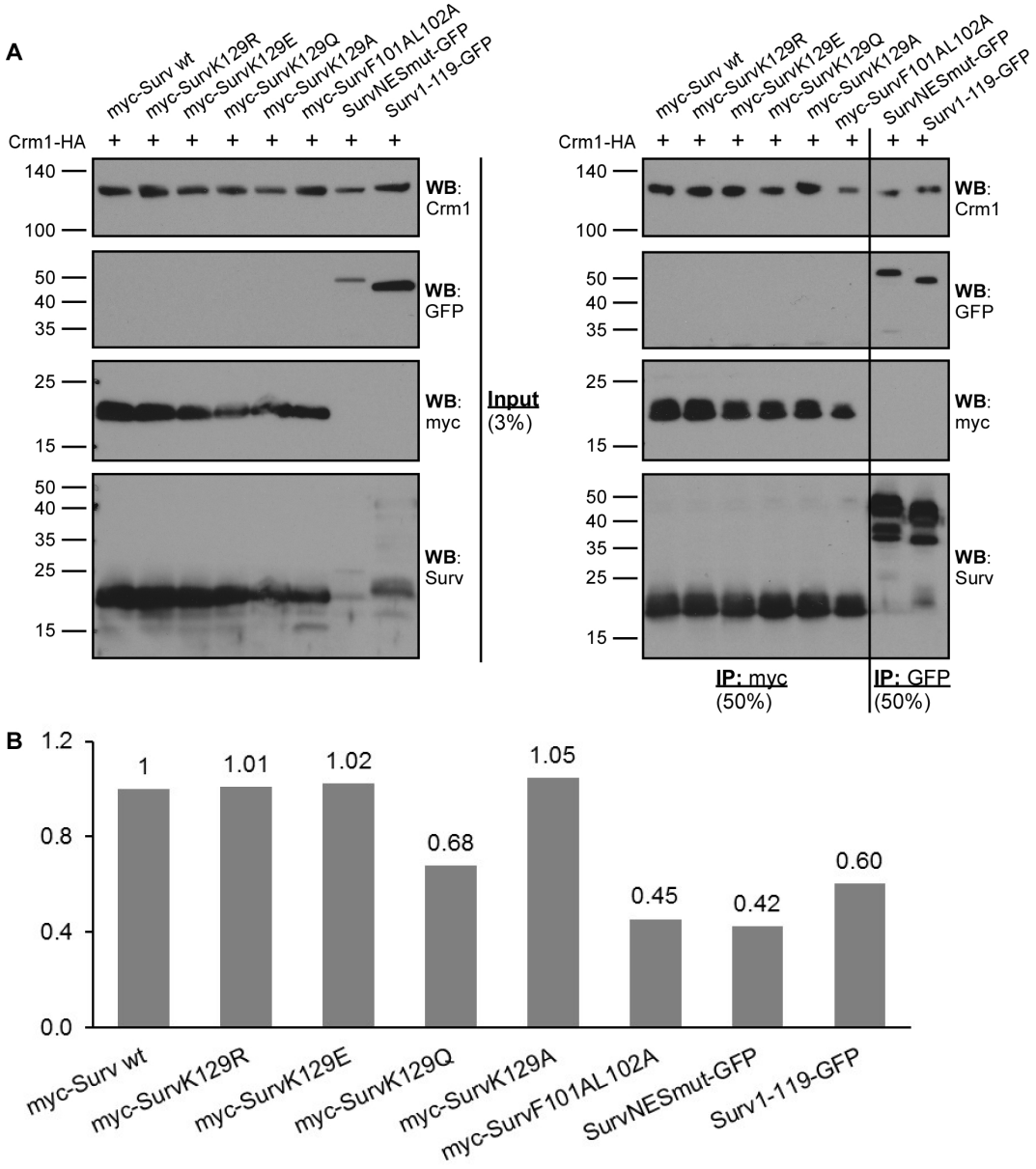

Figure 3.11: Interaction of CRM1 with myc-tagged Survivin K129 mutants. A) Lysates from 293T cells transiently transfected with HA-tagged CRM1 and myc- or GFP-tagged Survivin mutants were immunoprecipitated (IP) with magnetic beads coupled to antibodies specific for myc or GFP and immunoblotted (WB). Membranes were probed with antibodies specific for CRM1, GFP, myc or Surv. B) Quantification of the immunoblot shown in A.

In a further experiment, microbeads coupled to a myc- or GFP-specific antibody were

used, so the Survivin mutants were precipitated from the lysates instead of CRM1-HA (Figure 3.11). As positive control the dimerization-deficient myc-SurvF101AL102A mutant was included, as Engelsma *et al.* (2007) reported an increased binding to CRM1.

For SurvK129E and SurvK129Q, the quantification of the western blot revealed results similar to those shown in Figure 3.10 (1.02 and 0.68, respectively). For SurvK129R and SurvK129A, however, a binding affinity comparable to Survivin wt was determined. The interaction strength of SurvNESmut to CRM1 was reduced to 42 %. Even an interaction of Surv1-119 with CRM1 could be observed, which was only decreased by 40 % compared to Survivin wt. SurvF101AL102A, the positive control for an increased binding to CRM1, showed a 55 % lower binding affinity compared to wt Survivin.

3.2.5 Analysis of the secondary structure of Survivin K129 mutants

The introduction of a mutation into a protein can cause conformational changes due to different biochemical properties of the amino acids. To evaluate whether amino acid substitutions introduced in the Survivin protein caused alterations in the protein secondary structure, far-UV CD spectroscopy was applied. CD spectroscopy allows to draw conclusions on the conformation of peptide bonds from their optical activity, thus providing insight into the secondary structure of proteins. The far-UV CD spectra of the recombinant Survivin variants were recorded in phosphate buffer containing 10 µM Zn^{2+} at 20 °C (Figure 3.12).

The spectra of all SurvK129 mutants showed a similar progression with one maximum of the specific ellipticity at approx. 191 nm and two minima at 207 and 225 nm. All spectra intersected the x-axis at approx. 200 nm. SurvF101AL102A (gray), however, exhibited a spectrum clearly different from those of the other mutants. The specific ellipticity decreased earlier with the curve intersecting the x-axis already at approx. 197 nm. Also the first minimum was slightly shifted to lower wavelengths, and a second minimum at 225 nm could not be observed.

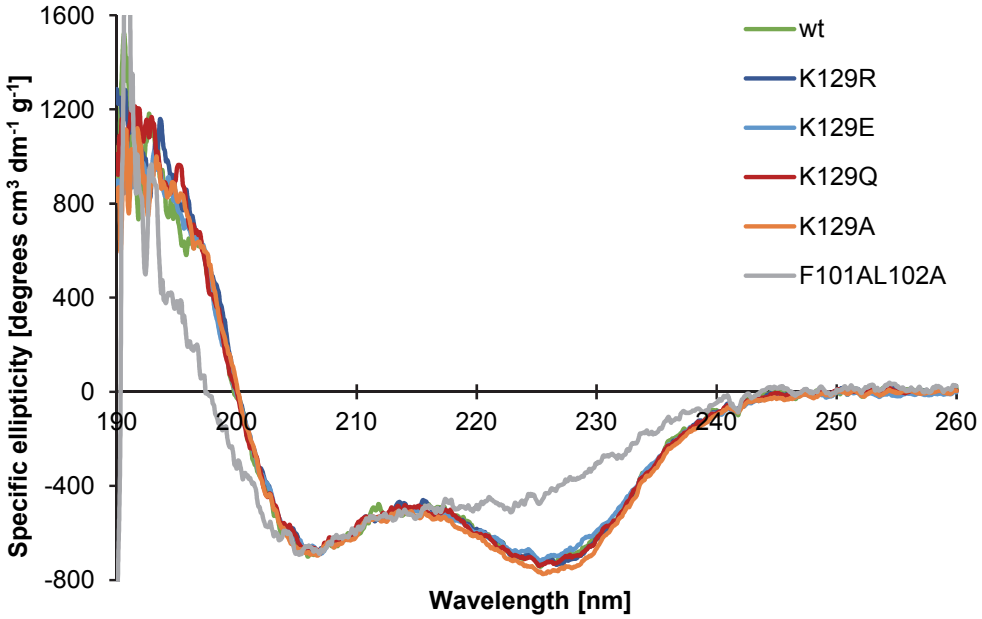

Figure 3.12: CD spectra of recombinant, untagged Survivin K129 mutants. Far-UV circular dichroism spectra of purified, tag-free Survivin mutants in 20 mM phosphate buffer containing 10 µM Zn^{2+} at 20 °C.

3.2.6 Involvement of acetylated Survivin in mitosis

Survivin, besides its role as an apoptosis inhibitor, is an essential regulator of cell division since it is a member of the CPC (Lens *et al.*, 2006). The CPC consists of a kinase module comprising Aurora B and INCENP's C-terminus, and a regulatory module composed of Survivin, Borealin and the N-terminus of INCENP. These three proteins interact with each other forming a helix bundle which stabilizes the complex. The two modules are linked together by INCENP. A direct interaction of Survivin with Aurora B occurs only temporarily, when Aurora B phosphorylates Survivin at T117 (Wheatley *et al.*, 2007). For the formation and the proper localization of the CPC, Survivin's dimerization state as well as its interaction with the export receptor CRM1 are of particular importance: on the one hand Survivin is present as a monomer in the CPC since Borealin and INCENP occupy its dimer interface (Jeyaprakash *et al.*, 2007), and on the other hand the interaction of Survivin with CRM1 is essential for targeting the CPC to centromers (Knauer *et al.*, 2006). Since Wang *et al.* (2010b) proposed that Survivin K129 acetylation regulates both, the protein's dimerization as well as its interaction with CRM1, we aimed to analyze the involvement of Survivin acetylated at lysine 129 (SurvK129Ac) in mitosis.

For this purpose, a primary antibody specific for SurvK129Ac, also described by Wang *et al.* (2010b), was tested. This antibody offers the possibility to directly gain insight into the functions of SurvK129Ac without having to use a mimicking mutant. First tests with GFP-tagged Survivin wt and mutants showed that the antibody was only able to detect endogenous Survivin in western blot, but not the overexpressed variants (Figure 3.13).

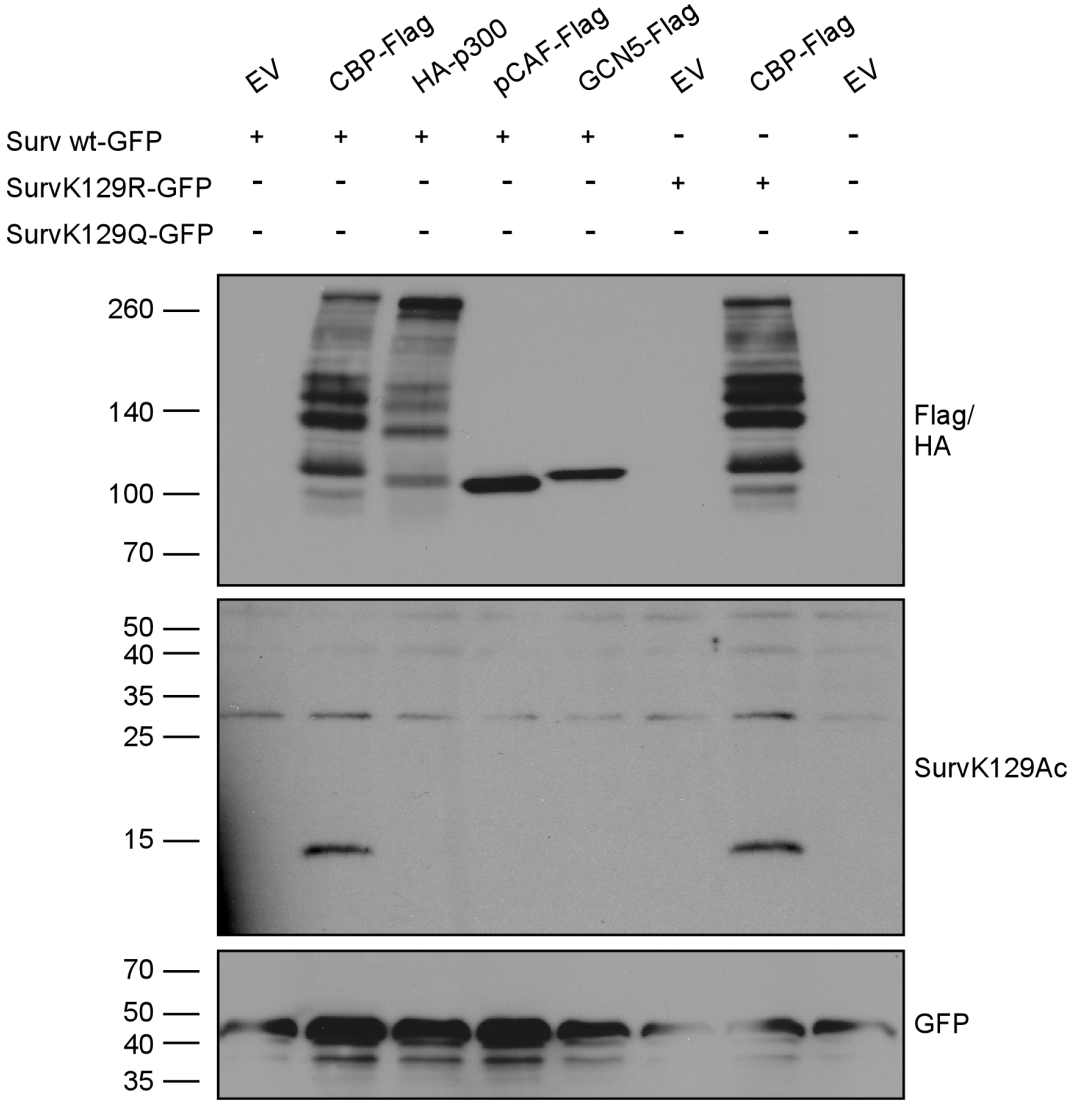

Figure 3.13: Detection of Survivin K129 acetylation by a specific antibody. Lysates from 293T cells transiently co-transfected with GFP-tagged Survivin mutants and Flag- or HA-tagged acetyltransferases or empty vector (EV) were immunoblotted. Membranes were probed with antibodies specific for Flag, HA, GFP or SurvK129Ac.

The SurvK129Ac antibody only detected specific bands at a molecular weight of approx. 15 kDa indicating endogenous Survivin. These bands only occurred when CBP-

Flag was co-transfected. A transfection of other lysine acetyltransferases like p300, PCAF or GCN5 did not result in a detectable Survivin K129 acetylation. In addition, three unspecific bands were visible at approx. 30, 42 and 60 kDa, but no specific band could be observed at 43 kDa, the molecular weight of the Survivin-GFP fusion protein.

To exclude that the C-terminal GFP tag (27 kDa), which is considerably bigger than Survivin (16.5 kDa), disturbed the binding of the antibody, the experiment was repeated comparing Survivin-GFP to Survivin constructs with small C-terminal expression tags (Figure 3.14).

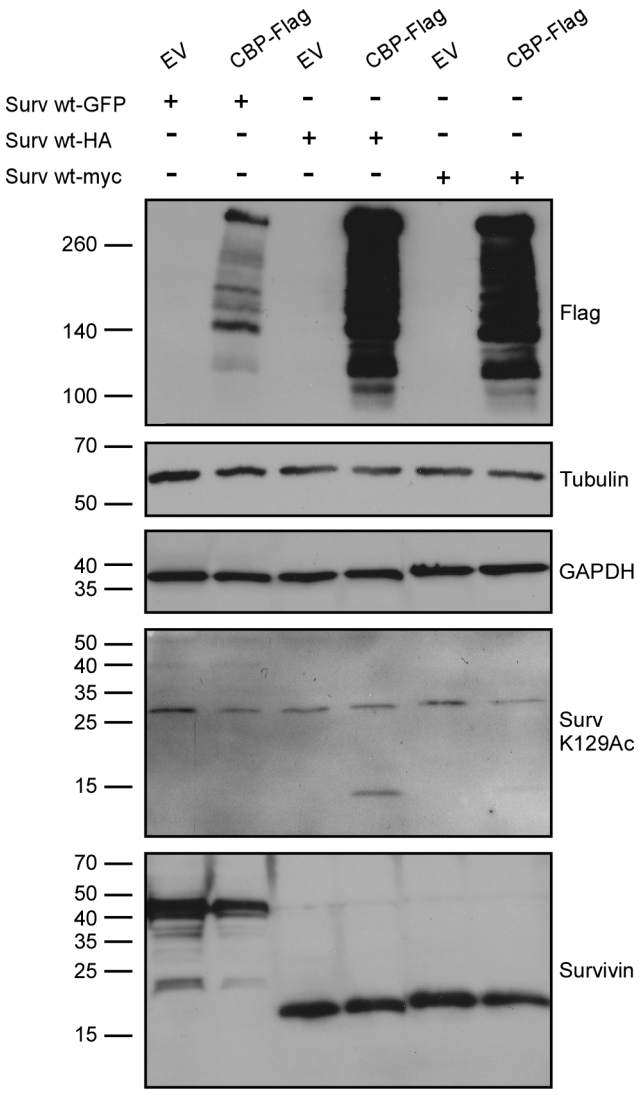

Figure 3.14: Influence of different C-terminal tags on Survivin K129 acetylation. Lysates from 293T cells transiently co-transfected with GFP-, HA- or myc-tagged Survivin and the Flag-tagged acetyltransferase CBP or empty vector (EV) were immunoblotted. Membranes were probed with antibodies specific for Flag, Tubulin, SurvK129Ac, Surv or GAPDH.

The SurvK129Ac antibody only detected bands in samples containing Survivin wt-HA or Survivin wt-myc co-transfected with CBP-Flag at a molecular weight of approx. 15 kDa indicating that the detected protein was again endogenous Survivin and not the transfected Survivin wt-HA (17.5 kDa) or Survivin wt-myc (17.7 kDa). In the sample containing Survivin wt-GFP co-transfected with CBP, no band was visible.

Next, it was tested whether the antibody could detect overexpressed Survivin with an N-terminal myc tag (Figure 3.15).

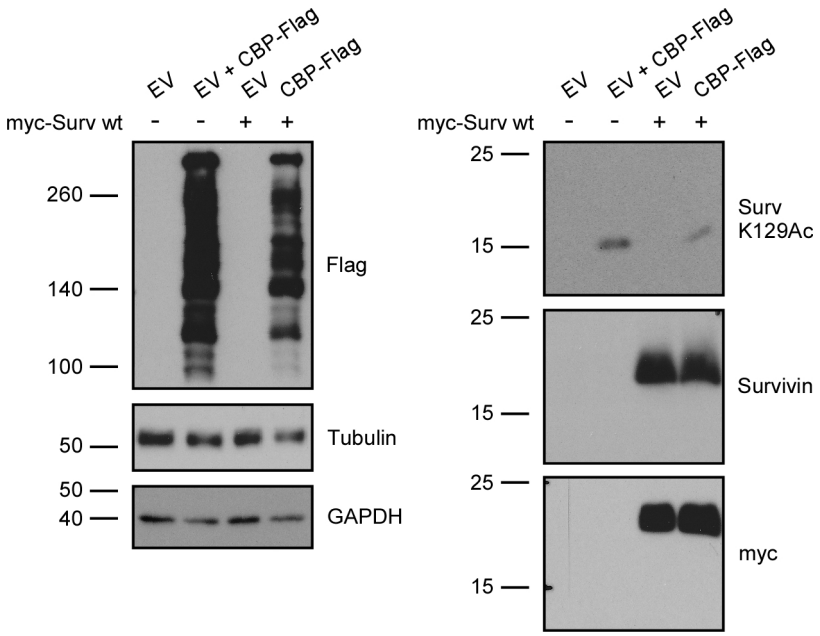

Figure 3.15: Detection of N-terminally tagged Survivin K129 acetylation. Lysates from 293T cells transiently co-transfected with myc-tagged Survivin and Flag-tagged CBP or empty vector (EV) were immunoblotted. Membranes were probed with antibodies specific for Flag, Tubulin, GAPDH, SurvK129Ac, Surv or myc.

In both samples in which CBP-Flag was overexpressed, the SurvK129Ac antibody detected a band of a molecular weight of approx. 15 kDa irrespective of whether myc-Survivin wt had been transfected or not.

The antibody was also tested in IF stainings of HeLa K cells (Figure 3.16).

In untransfected HeLa K cells, the SurvK129Ac antibody revealed a weak and heterogeneous nuclear staining. After transfection with myc-Survivin wt, the staining was more prominent and still mainly nuclear, but also a weak cytoplasmic staining could be observed.

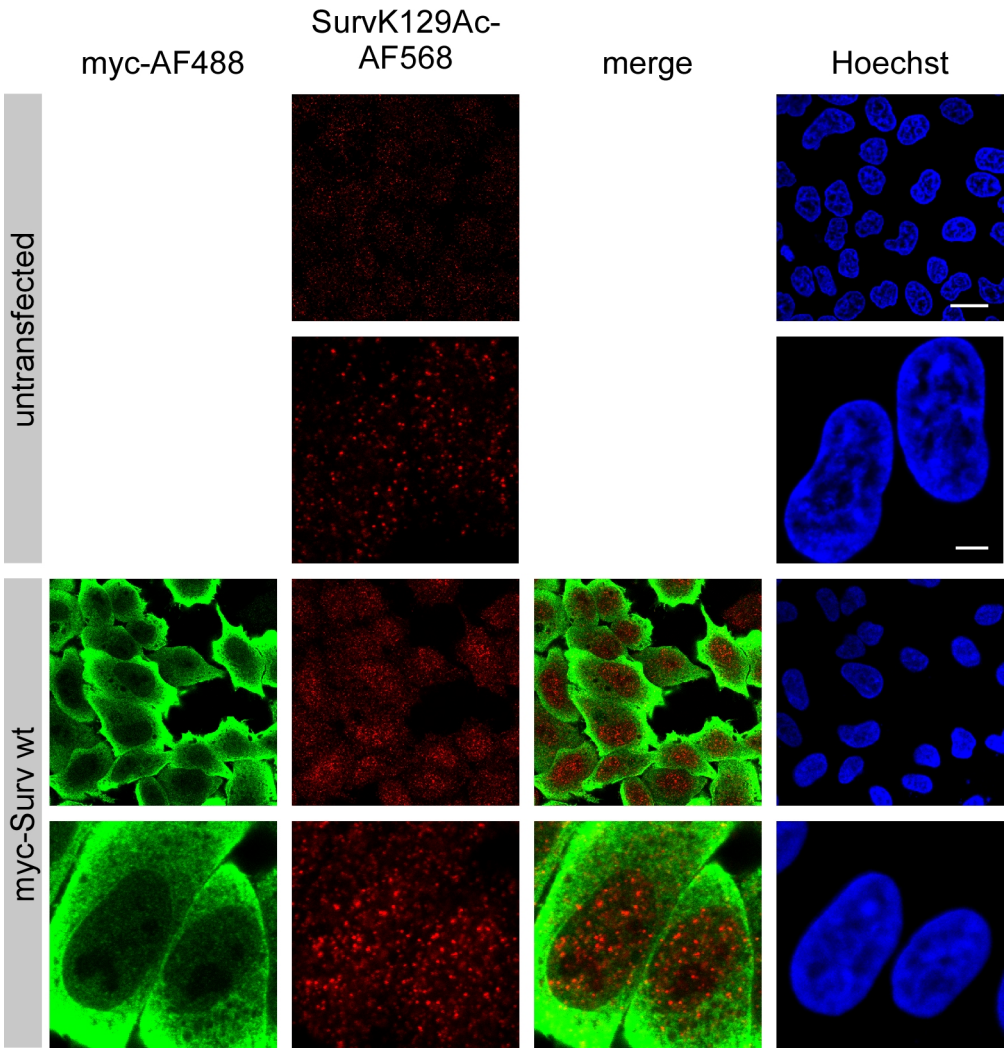

Figure 3.16: Cellular localization of K129 acetylated Survivin. HeLa K cells were transiently transfected with myc-Survivin wt or left untransfected and fixed 24 h later. After permeabilization, they were immunostained with antibodies specific for SurvK129Ac (red) and myc (green). DNA was stained with Hoechst (blue). Images were taken with a Leica SP5 confocal microscope. Scale bar, 20 µm (overview) and 5 µm (zoom), respectively.

As mentioned before, the correct localization and function of Survivin during mitosis is dependent on its physical interaction with the other CPC members. To analyze this binding biochemically by IP, 293T cells were co-transfected with Survivin wt-myc and Borealin- or Aurora B-GFP, and the GFP-tagged proteins were immunoprecipitated (Figure 3.17). CBP-Flag was co-transfected to enhance acetylation in general.

Co-transfection with GFP or empty vector serving as negative control demonstrated that there was no unspecific binding of GFP microbeads alone or precipitated GFP to Surv-myc. Borealin-GFP and Aurora B-GFP both could be precipitated, but overexpressed Surv-myc as well as endogenous SurvK129Ac were only co-immunoprecipitated with Borealin.

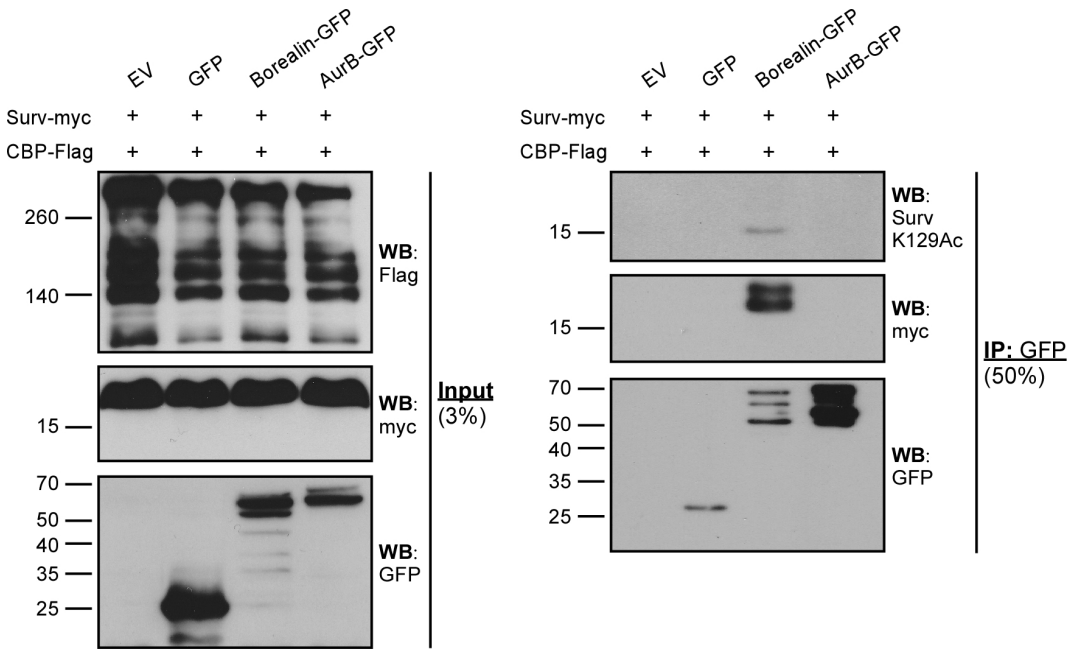

Figure 3.17: Interaction of endogenous K129 acetylated Survivin with Borealin. Lysates from 293T cells transiently co-transfected with cDNAs encoding myc-tagged Survivin wt, Flag-tagged CBP and the GFP-tagged CPC proteins Borealin or Aurora B (AurB) or with empty vector (EV) were immunoprecipitated with magnetic beads coupled to a GFP antibody and immunoblotted. Membranes were probed with antibodies specific for Flag, myc, GFP and SurvK129Ac.

Next, the lysine deacetylase inhibitor TSA was used to enhance the general acetylation level instead of overexpressing CBP. Moreover, the lysate containing Surv-myc and Aurora B-GFP was incubated at 37 ℃ for 20 min before adding the antibody-coupled microbeads. Also myc-tagged INCENP was included in the analysis (Figure 3.18).

As already shown before (Figure 3.17), Survivin was precipitated with Borealin-GFP, but also with Aurora B-GFP and INCENP-myc. In the sample in which Aurora B-GFP, INCENP-myc and Survivin-myc were expressed together, only INCENP, but not Survivin was recovered. In contrast to the results depicted in Figure 3.17, no interaction of endogenous SurvK129Ac with Borealin or any other CPC member could be shown.

In a further experiment, cDNAs encoding GFP-tagged CPC proteins were co-transfected again with CBP-Flag to enhance acetylation. As the SurvK129Ac antibody only detects the endogenous protein, overexpression of tagged Survivin was set aside in this experiment. All lysates were incubated at 37 ℃ for 20 min before adding the antibody-coupled microbeads. To accumulate mitotic cells, and thus, increase the amount of assembled chromosomal passenger complexes, cells were treated with nocodazole, which arrests them in prometaphase (Figure 3.19).

Endogenous Survivin precipitated with Borealin-, Aurora B- and INCENP-GFP. In asyn-

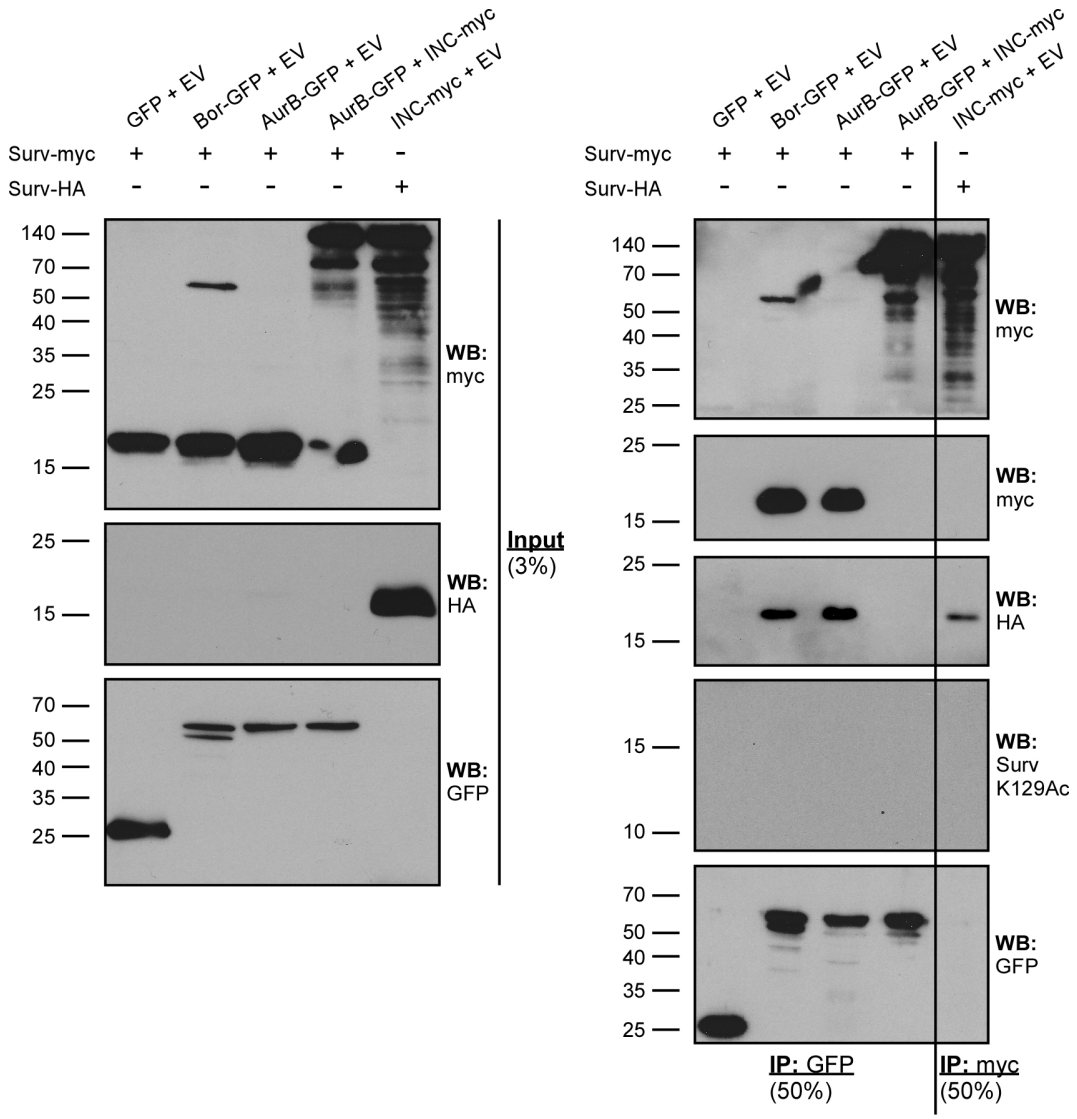

Figure 3.18: Impact of TSA-enforced acetylation on SurvK129Ac interaction with members of the CPC. 293T cells were transiently co-transfected with empty vector (EV) or with cDNAs encoding myc- or HA-tagged Survivin and the GFP- or myc-tagged CPC proteins Borealin (Bor), Aurora B (AurB) or INCENP (INC). 24 h after transfection, cells were treated with 100 nM TSA for 16 h. Lysates were immunoprecipitated (IP) with magnetic beads coupled to a GFP- or myc-specific antibody and immunoblotted (WB). Membranes were probed with antibodies specific for myc, HA, GFP and SurvK129Ac.

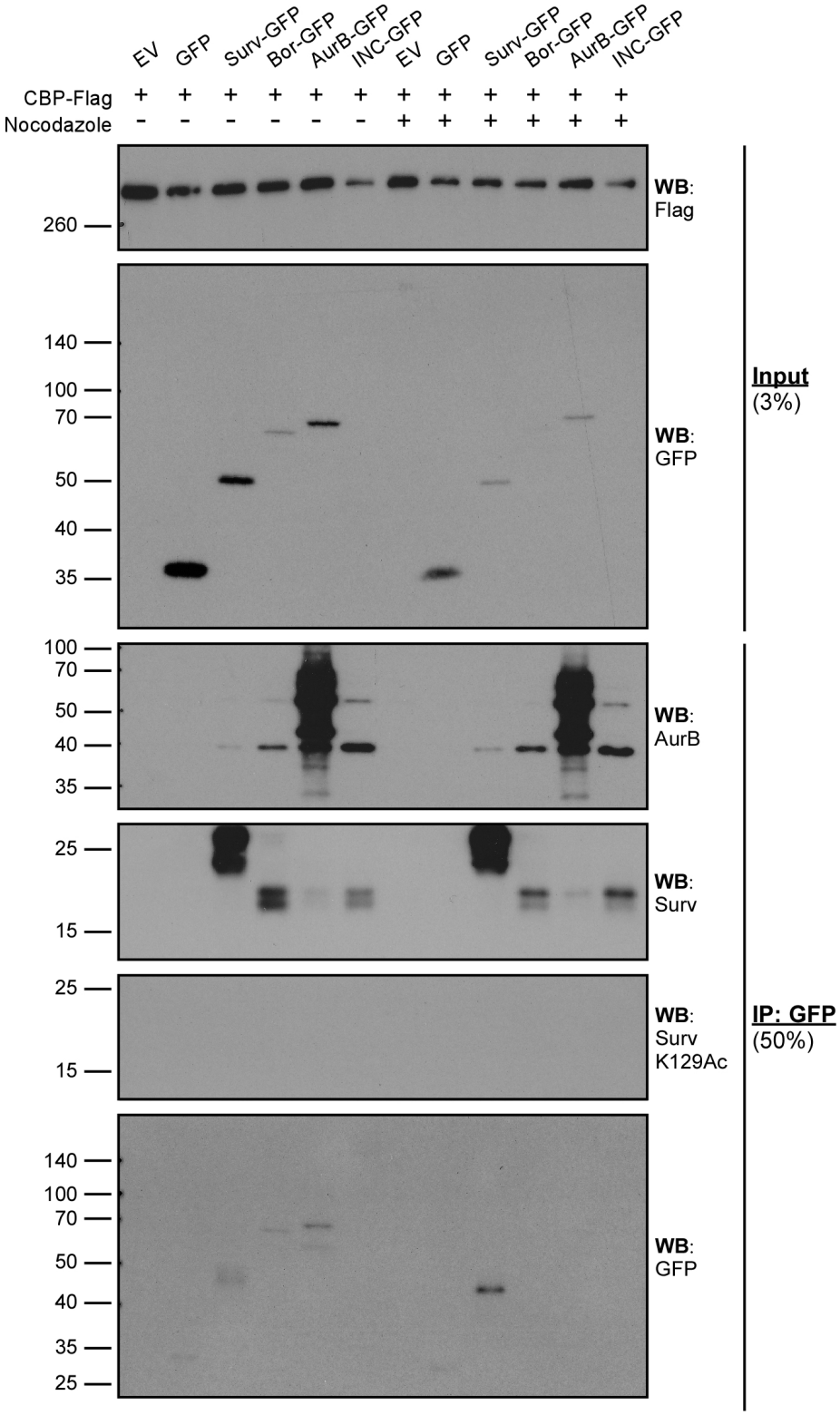

Figure 3.19: Interaction of SurvK129Ac with members of the CPC in cells arrested in mitosis. 293T cells were transiently co-transfected with empty vector (EV) or with cDNAs encoding the GFP-tagged CPC proteins Survivin (Surv), Aurora B (AurB), Borealin (Bor) and INCENP (INC) and with CBP-Flag. 8 h after transfection, cells were treated with 50 ng/mL nocodazole for 16 h. Lysates were immunoprecipitated (IP) with magnetic beads coupled to a GFP-specific antibody and immunoblotted (WB). Membranes were probed with antibodies specific for Flag, GFP, AurB, Surv and SurvK129Ac.

chronous as well as in mitotically arrested cells, the strongest interaction with Survivin was found for Borealin-GFP, the weakest for Aurora B-GFP. Although an interaction of Survivin with these CPC proteins as well as the expression of CBP-Flag was observed, no SurvK129Ac was detected in the eluates. A dimerization of Survivin-GFP with the endogenous protein was could not be detected.

IF stainings were performed to test for co-localization of SurvK129Ac with members of the CPC. HeLa K cells were fixed, permeabilized, and immunostained with antibodies specific for Survivin or SurvK129Ac and Aurora B, Borealin, INCENP or α-Tubulin (Figure 3.20).

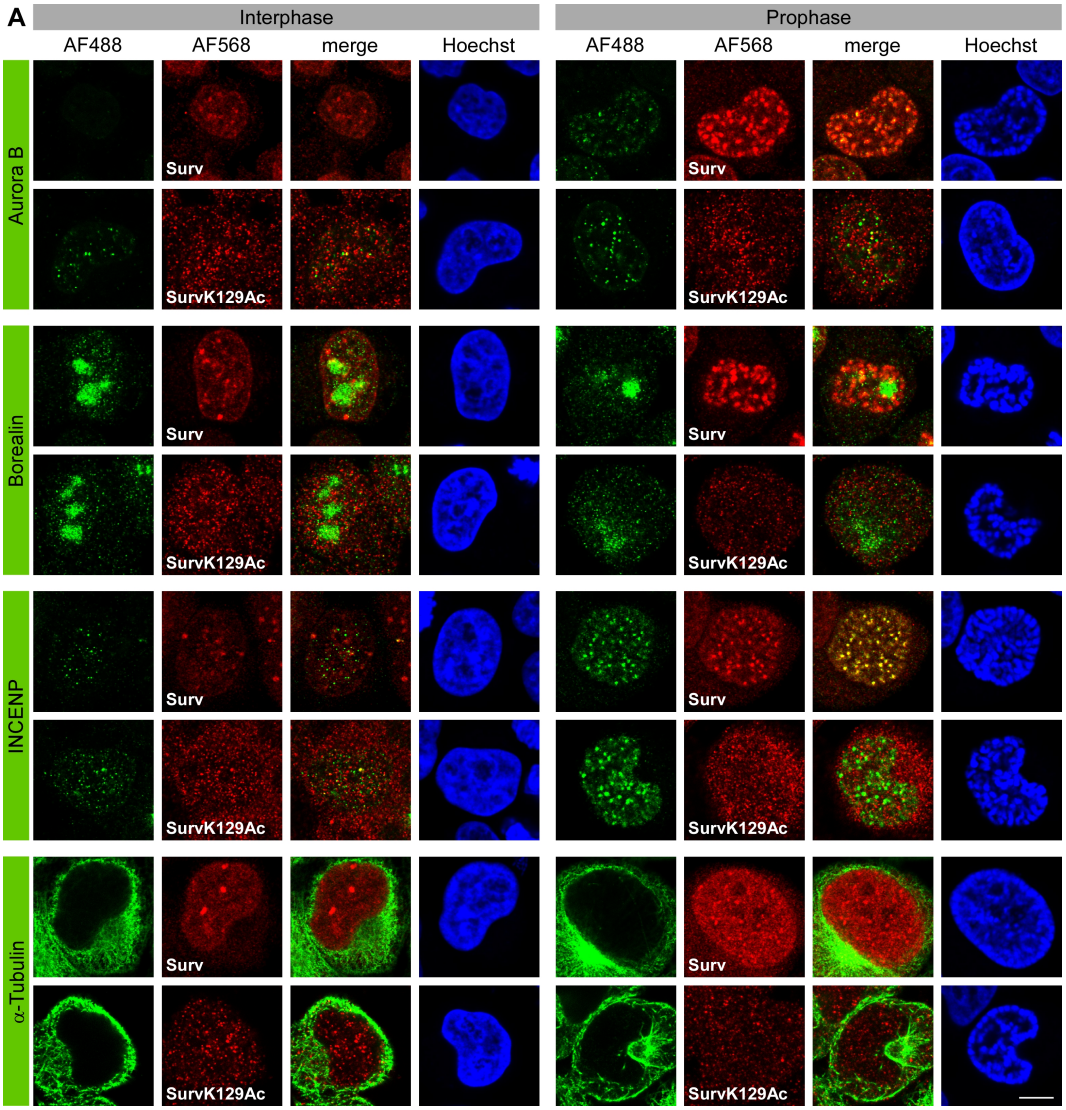

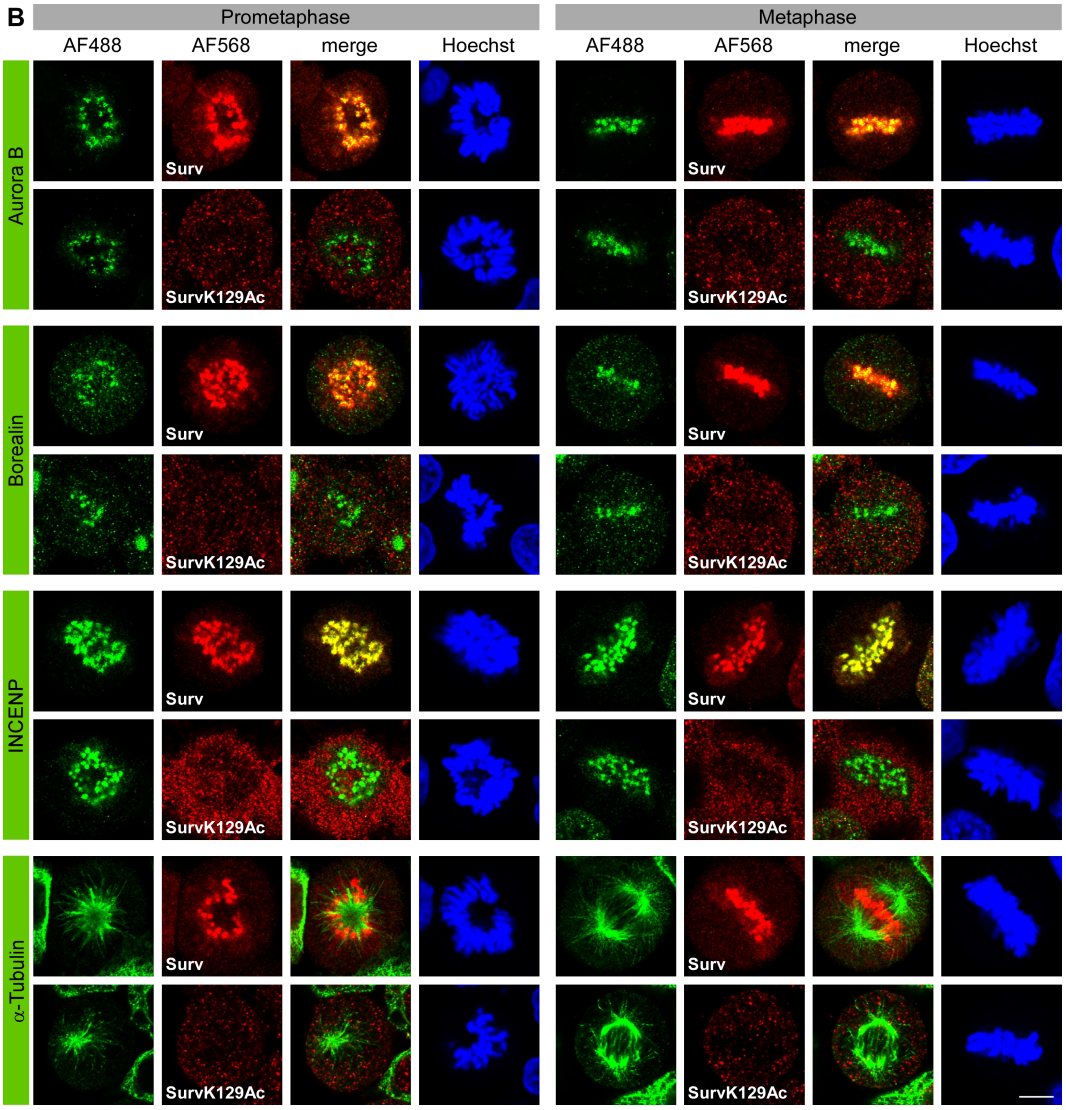
B
Prometaphase
Metaphase
AF488
AF568
merge
Hoechst
Aurora B
Borealin
INCENP
α-Tubulin
Surv
SurvK129Ac

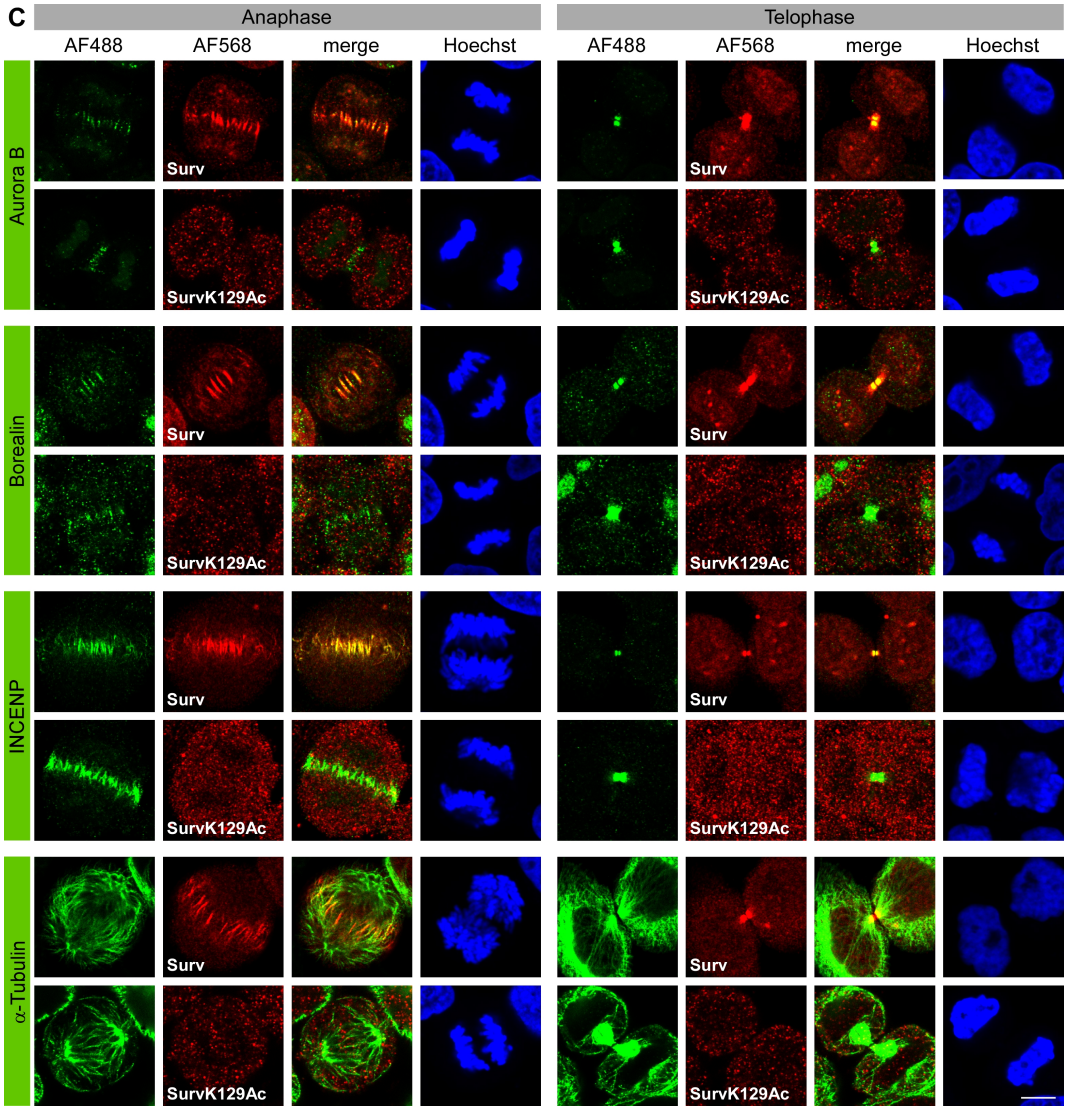

Figure 3.20: Localization of endogenous K129 acetylated Survivin in mitosis. HeLa K cells were fixed, permeabilized and immunostained with antibodies specific for Survivin or SurvK129Ac (red) and Aurora B, Borealin, INCENP or α-Tubulin (green). DNA was stained with Hoechst (blue). A) Interphase and prophase. B) Prometaphase and metaphase. C) Anaphase and telophase. Images were taken with a Leica SP5 confocal microscope. Scale bar, 10 µm.

Survivin localized primarily to the nucleus in interphase. During mitosis, the typical chomosomal passenger staining pattern was observed: In prophase, when the chromatin condenses to form chromosomes, the CPC is initially found on chromosome arms, but starts to accumulate at centromeres. It persists at centromeres in prometaphase and also in metaphase, when chomosomes align on the spindle equator forming the characteristic metaphase plate. When the sister chromatids are pulled to opposite spindle poles in anaphase, the CPC is no longer attached to centromeres, but translocates to the spindle midzone and the cortex. In telophase, the CPC accumulates at the cleavage furrow, and subsequently, at the midbody, which is located between the separated and again partly decondensed chromatin. The staining of the other CPC members Aurora B, Borealin and INCENP showed an exact co-localization with Survivin in all phases of mitosis. For SurvK129Ac, however, no such localization typical for CPC proteins was observed.

To gain further insight into the role of Survivin acetylated at lysine 129 in mitosis, the SurvK129 mutants were transfected in HeLa K cells and their localization in mitosis was assessed by IF staining (Figure 3.21). It was observed that all of the Survivin mutants, like wt Survivin, showed a staining typical for CPC proteins in all phases of mitosis.

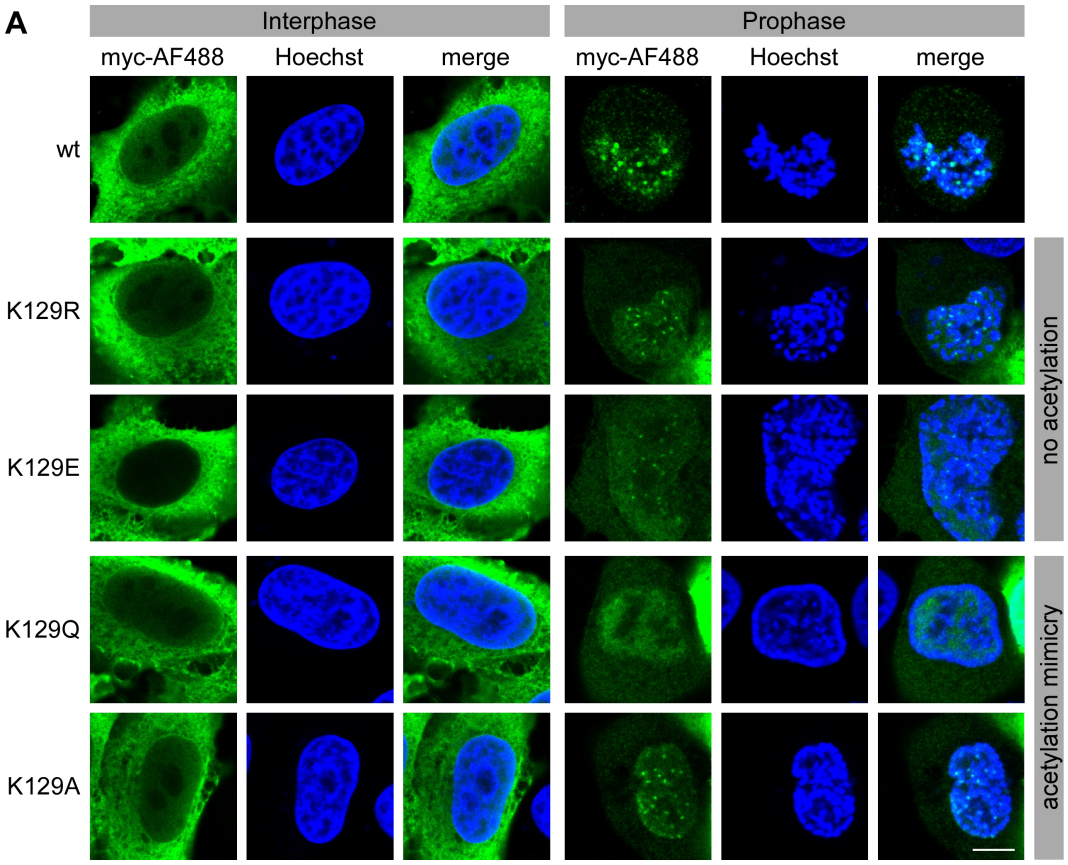

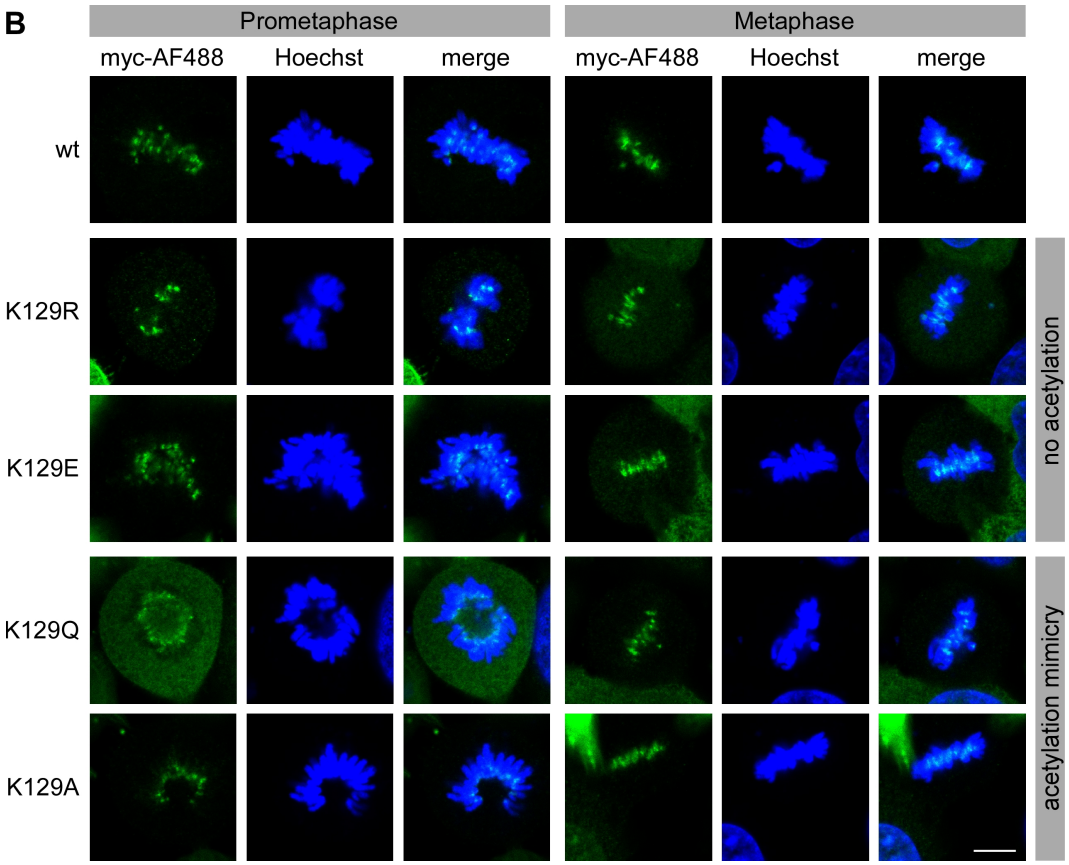
B
Prometaphase
Metaphase
myc-AF488
Hoechst
merge
myc-AF488
Hoechst
merge
wt
K129R
K129E
K129Q
K129A
no acetylation
acetylation mimicry

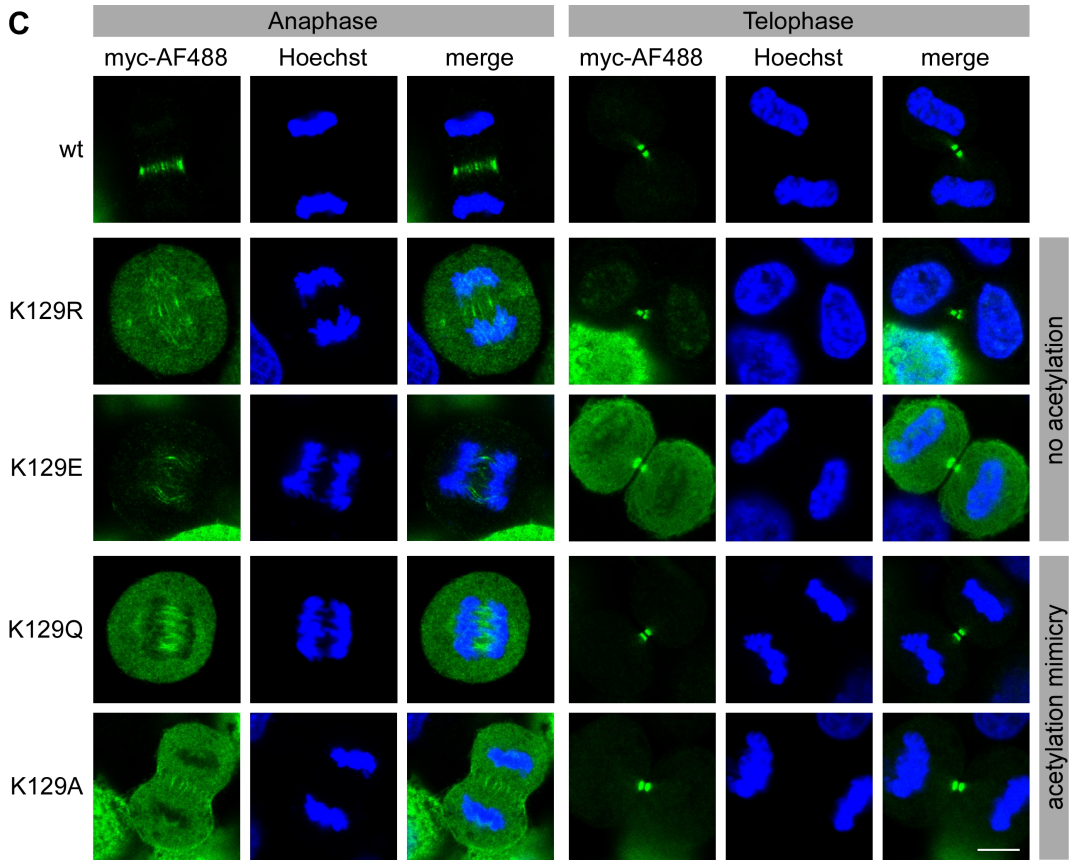

Figure 3.21: Localization of myc-tagged Survivin K129 mutants in mitosis. HeLa K cells transiently transfected with myc-tagged Survivin variants were fixed, permeabilized and immunostained with a myc-specific antibody (green). DNA was stained with Hoechst (blue). A) Interphase and prophase. B) Prometaphase and metaphase. C) Anaphase and telophase. Images were taken with a Leica SP5 confocal microscope. Scale bar, 10 µm.

3.3 Characterization of Survivin acetylation at other lysine residues

3.3.1 Prediction of acetylation sites in Survivin

Lysine acetylation has emerged as a major post-translational modification comparable to phosphorylation targeting not only histones and other nuclear proteins, but all types of proteins throughout the cell. Multiple effects of acetylation on target proteins have been reported including the regulation of protein interaction, function and localization (Close *et al.*, 2010; Sadoul *et al.*, 2011). Therefore, we aimed to investigate whether further of Survivin's 16 lysine residues become acetylated, and which effects a possible acetylation might have on the divers functions of the protein.

Table 3.1: Results of the prediction of acetylated lysine residues in Survivin. The most promising values are emphasized.

Source	**Wang et al. (2010)**	**PAIL**	**ASEB**	**ASEB**
Acetylated by	CBP		CBP/p300	GCN5/PCAF
Position				
15			0.0186	0.4180
23	x		0.1761	0.7494
78		0.50	**0.0015**	**0.0899**
79		0.69	0.3426	0.6256
90	x	**1.82**	0.2429	0.3626
91		0.69		
103		0.46		0.6145
110	x	0.86	0.1740	
112	x	**1.09**	**0.0001**	0.3798
115	x	**1.22**	0.0551	**0.0694**
120	x			
121	x		0.0376	0.6780
122	x	0.53	0.0836	0.8724
129	x	0.56		
130	x			

To address this questions, first, an *in silico* analysis was performed using two acetylation prediction online tools, the PAIL tool and the ASEB tool, which allows KAT-specific

prediction of acetylation sites (http://bioinfo.bjmu.edu.cn/huac/; Wang *et al.*, 2012). Table 3.1 summarizes the respective lysine residues from both predictions together with the lysines Wang *et al.* (2010b) reported to be acteylated.

As the prediction tools are based on different mathematical algorithms, the results of the analysis are by some means divergent. The score put out by PAIL increases with rising probability for a lysine residue to be acetylated. In contrast, ASEB puts out P-values which means that low values indicate a high acetylation probability. Unexpectedly, there were no values for lysine 129 in both ASEB predictions. This results from the fact that ASEB prediction only works if the exact sequence coded by the Swiss-Prot accession number is entered. In case of Survivin, this is a natural variant of the canonical sequence which contains the aforementioned K129E mutation. Thus, the analysis of the amino acid sequence containing a lysine at position 129, which is referred to as Survivin wt in this thesis, was not possible. The predictions revealed that lysines 78, 90, 112 and 115 are promiment candidates for further analyses. In addition, some of the lysine residues suggested to be acetylated by Wang *et al.* (2010b), especially those located in vicinity to other potentially acetylated lysines, were also included in further experiments. Since lysine to arginine and lysine to glutamine mutations are typically used in studies analyzing protein acetylation, as already mentioned in section 3.1, only these mutations were introduced. Mutations modifying acetylation at K90 were of particular interest as it is located in the NES and the overlapping dimer interface of Survivin. Therefore, also a K90E and a K90,91R double mutant were generated. Figure 3.22 gives an overview on all myc-Survivin mutants cloned.

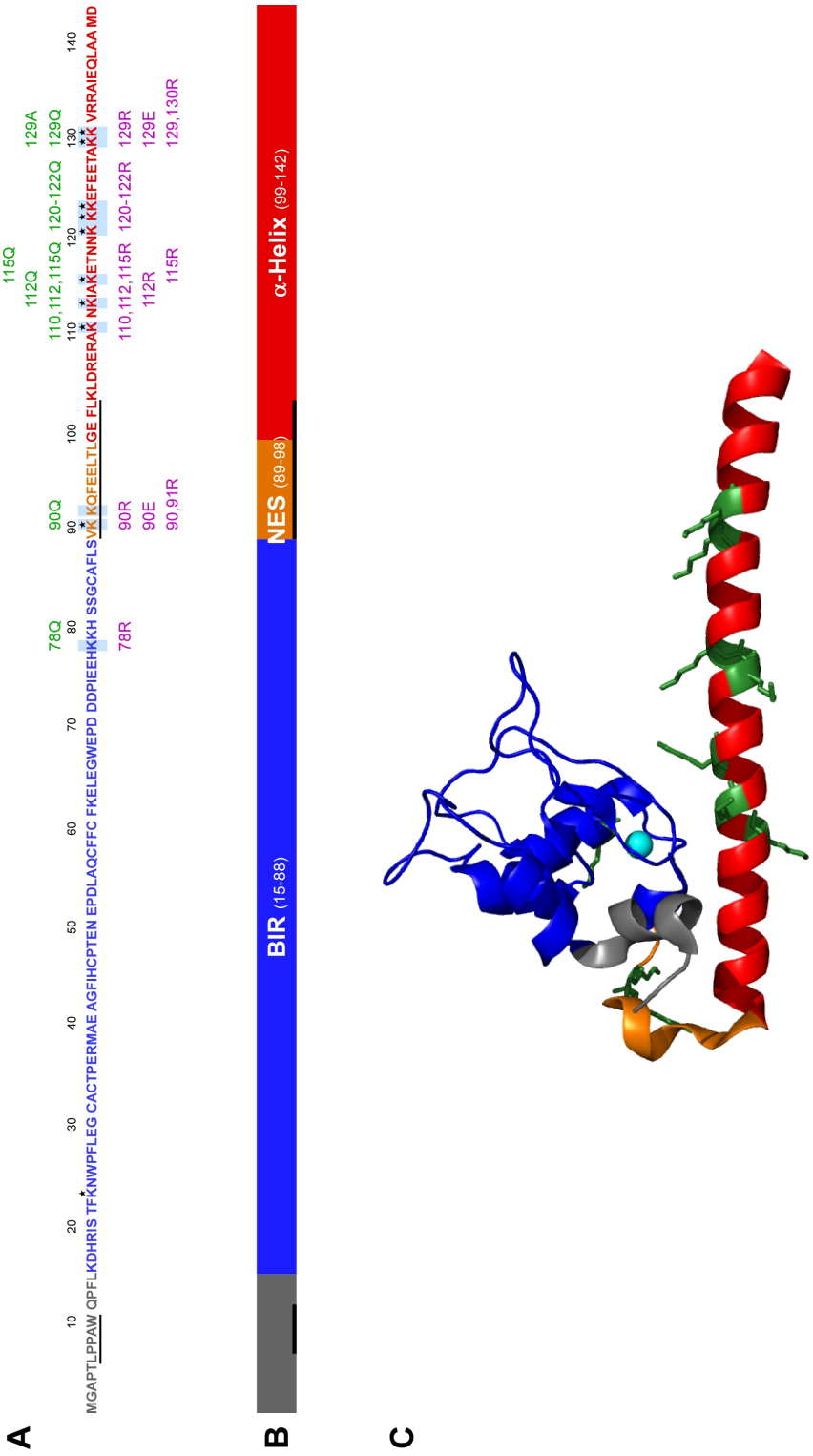

Figure 3.22: Overview on the primary and secondary structure of Survivin illustrating the positions of mutated lysine residues. The N-terminal BIR domain is depicted in blue, the NES in orange and the C-terminal α-helix in red. The black line indicates the position of the dimer interface. A) Amino acid sequence of Survivin wt. Mutated lysine residues are highlighted with a light blue box. Acetylation mimicking mutations are indicated in green, mutations preventing acetylation are indicated in purple. Lysine residues Wang *et al.* (2010b) found to be acetylated are marked with an asterisk. B) Domain organization of Survivin. C) Ribbon representation of the Survivin monomer (Chantalat *et al.*, 2000; PDB ID: 1E31). Mutated lysine residues are depicted in stick representation in green. The Zn^{2+}ion is shown as a cyan shpere.

3.3.2 Effect of Survivin acetylation on its cellular localization

With the new myc-tagged Survivin mutants available, the analysis of their different properties was carried out analogously to the examination of the SurvK129 mutants.

First of all, in order to investigate their cellular localization, the Survivin mutants were expressed in HeLa K cells, and their localization was assessed by IF staining (Figure 3.23). All Survivin mutants exhibited the same localization: the bulk of overexpressed protein resided in the cytoplasm of the cells, a minor amount was present in the nucleus and the nucleoli were completely spared. No clear difference appeared in the ratio of cytoplasmic to nuclear protein between the Survivin variants. Only the SurvK90E mutant (Figure 3.23A) showed a slightly decreased amount of nuclear protein compared to Survivin wt.

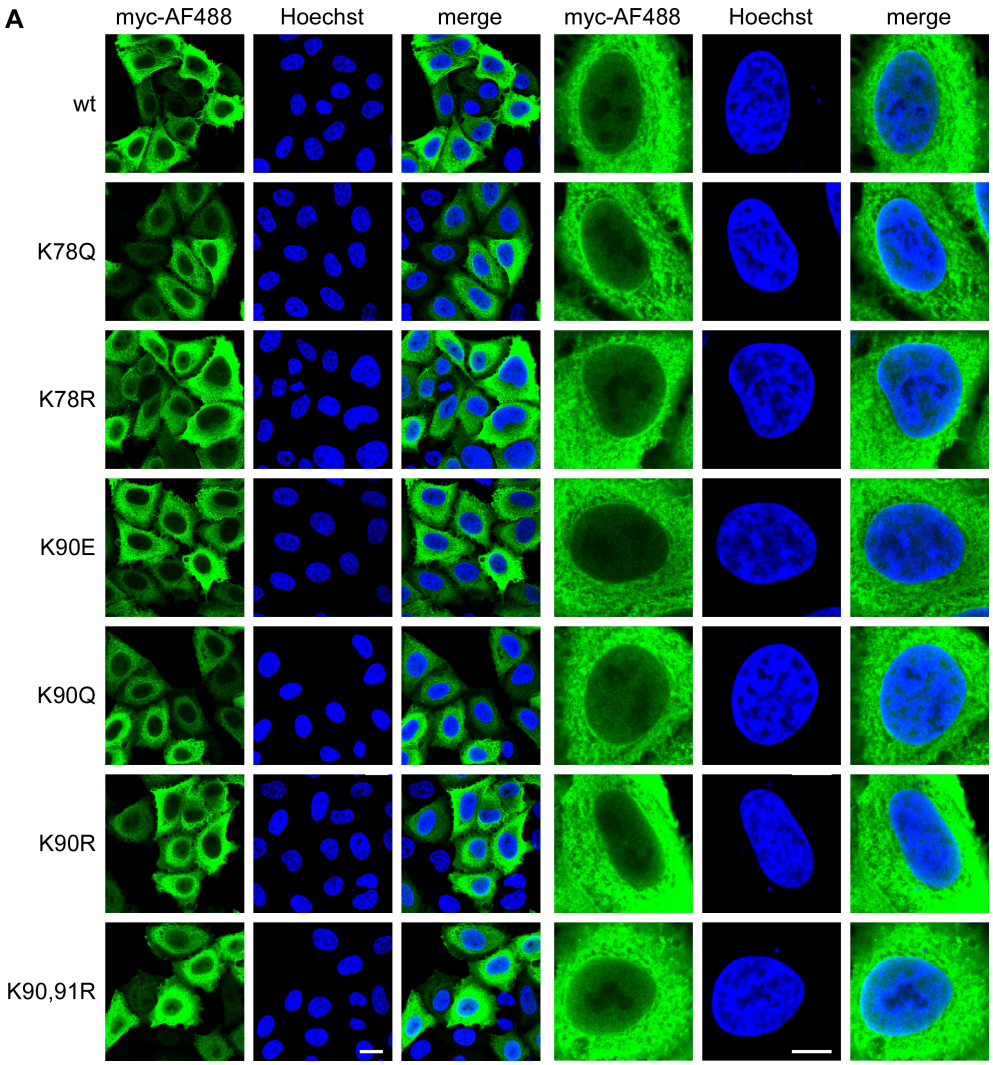

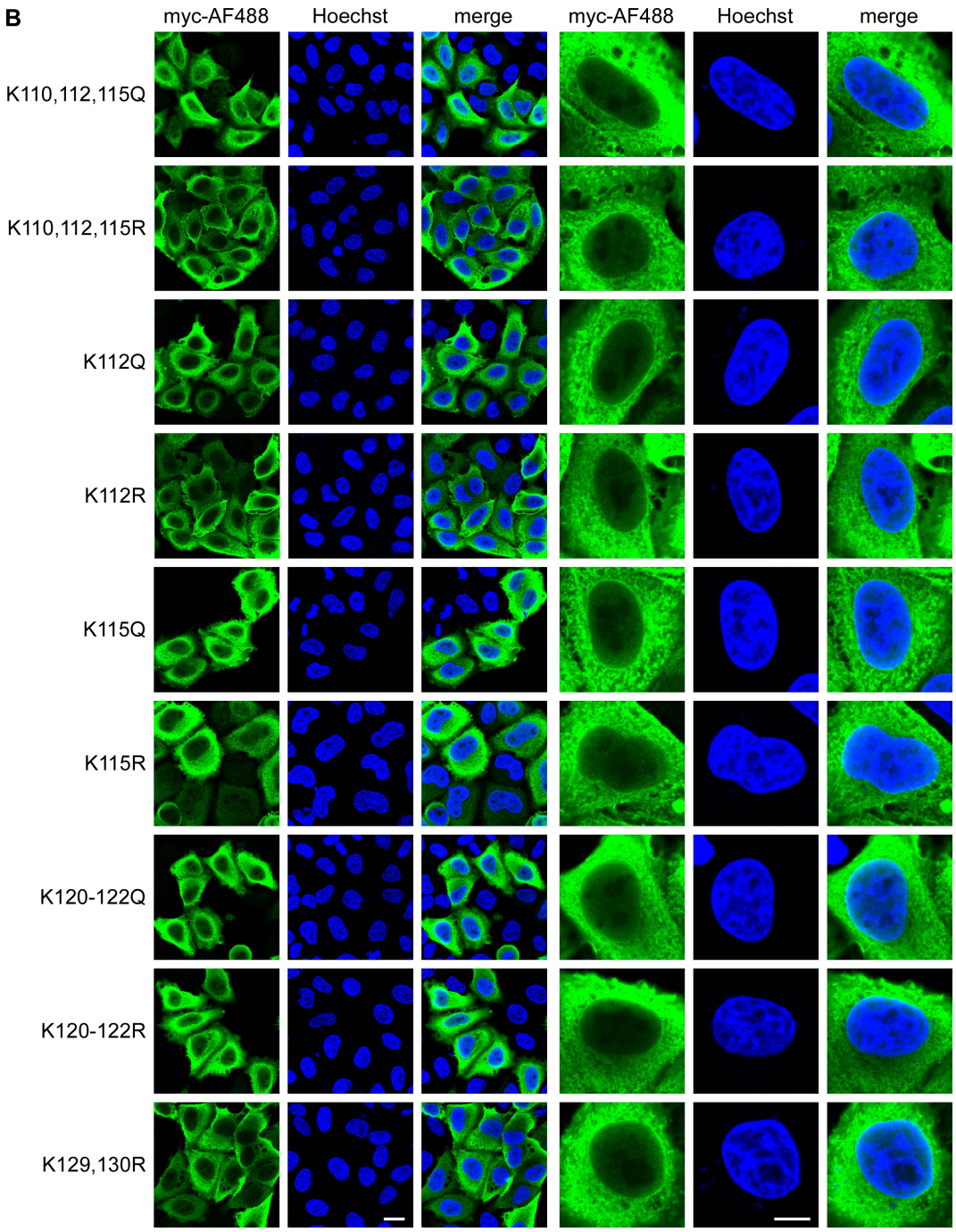

Figure 3.23: Cellular localization of myc-tagged Survivin mutants. HeLa K cells transiently transfected with myc-tagged Survivin variants were fixed, permeabilized and immunostained with a myc-specific antibody (green). DNA was stained with Hoechst (blue). A) IF staining of Survivin wt and the mutants SurvK78Q to SurvK90,91R. B) IF staining of the mutants SurvK110,112,115Q to SurvK129,130R. Images were taken with a Leica SP5 confocal microscope. Scale bar, 20 µm (overview) and 10 µm (zoom), respectively.

3.3.3 Involvement of acetylated Survivin in mitosis

Proper localization and function of Survivin and the CPC during the different phases of mitosis is essential for accurate control and progression of cell division. Survivin, as a part of the localization and regulation module of the CPC together with Borealin and INCENP, forms numerous protein-protein interactions crucial for the localization and stability of the complex. Some of the lysine residues which were identified as potential acetylation sites have been shown to form electrostatic interactions within the CPC. According to Jeyaprakash *et al.* (2007), lysine residues 110, 112, 120 and 121 are critical for the stability of the CPC as K110 and K121 form electrostatic interactions with amino acids in the helix of Borealin, while K112 and K120 build salt bridges with amino acids in the helix of INCENP. The helices of Survivin, Borealin and INCENP get in contact when the CPC assembles, forming a tight three-helical bundle, the core complex of the CPC (Figure 3.24).

K78 has not been shown to form direct interactions with amino acids of other proteins, but it is located within a region of Survivin's BIR domain responsible for binding and recognition of the N-terminus of histone H3 phosphorylated at threonine 3 (H3T3Ph) (Jeyaprakash *et al.*, 2011; Du *et al.*, 2012). This interaction is necessary to recruit the CPC to centromers (Kelly *et al.*, 2010; Wang *et al.*, 2010a). As already mentioned, K90 is located within Survivin's classical NES. The binding of Survivin to CRM1 via its NES does not only allow Survivin to shuttle between nucleus and cytoplasm, but is also necessary for the proper localization and function of the CPC (Knauer *et al.*, 2006).

To evaluate their localization in mitosis, the new myc-tagged Survivin variants were transiently expressed in HeLa K cells, and their localization was assessed by IF staining (Figure 3.25).

The microscopic analysis revealed no differences in the mitotic localization between the Survivin mutants and Survivin wt. Of note, for some mutants, no cells in pro- and/or anaphase were found, although the experiment was repeated several times.

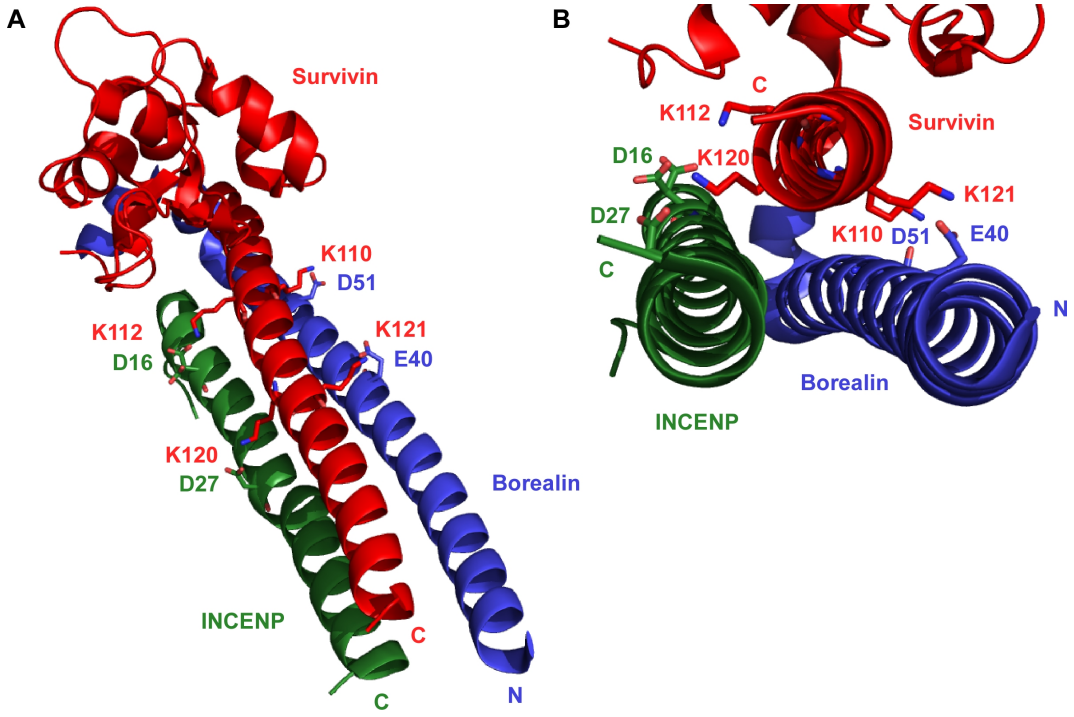

Figure 3.24: Schematic representation of the three-helix bundle essential for stable CPC formation. Ribbon representation of the three-helical bundle formed by Survivin (red), Borealin (blue) and INCENP (green)(Jeyaprakash *et al.*, 2007; PDB ID: 2QFA). Amino acids forming salt bridges with residues of one of the other proteins are depicted in stick representation (in the same color as the protein). A) View on the helix bundle perpendicular to the helix axis. B) View from the C-terminus of Survivin parallel to the helix axis.

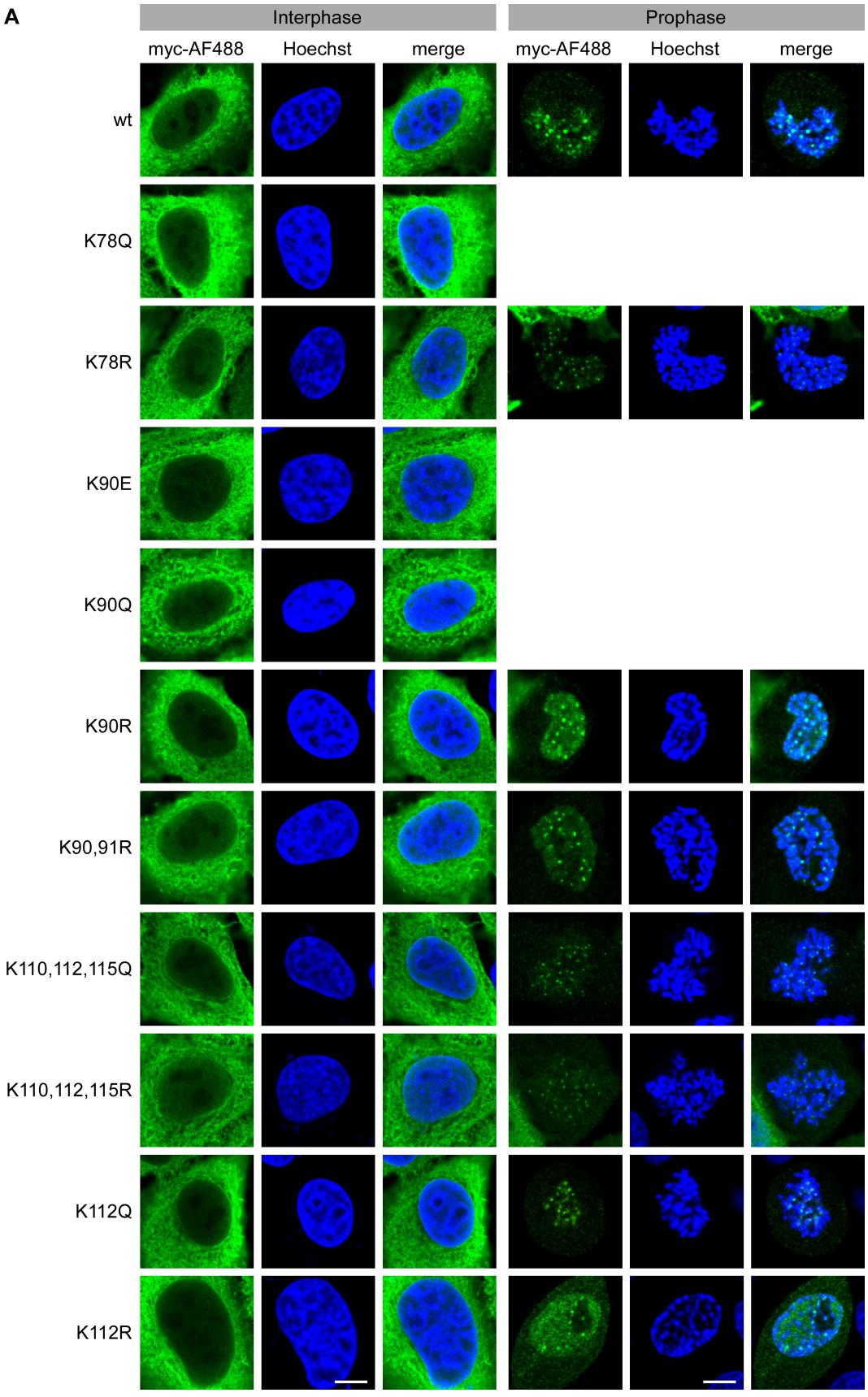
A
Interphase
Prophase
myc-AF488
Hoechst
merge
myc-AF488
Hoechst
merge
wt
K78Q
K78R
K90E
K90Q
K90R
K90,91R
K110,112,115Q
K110,112,115R
K112Q
K112R

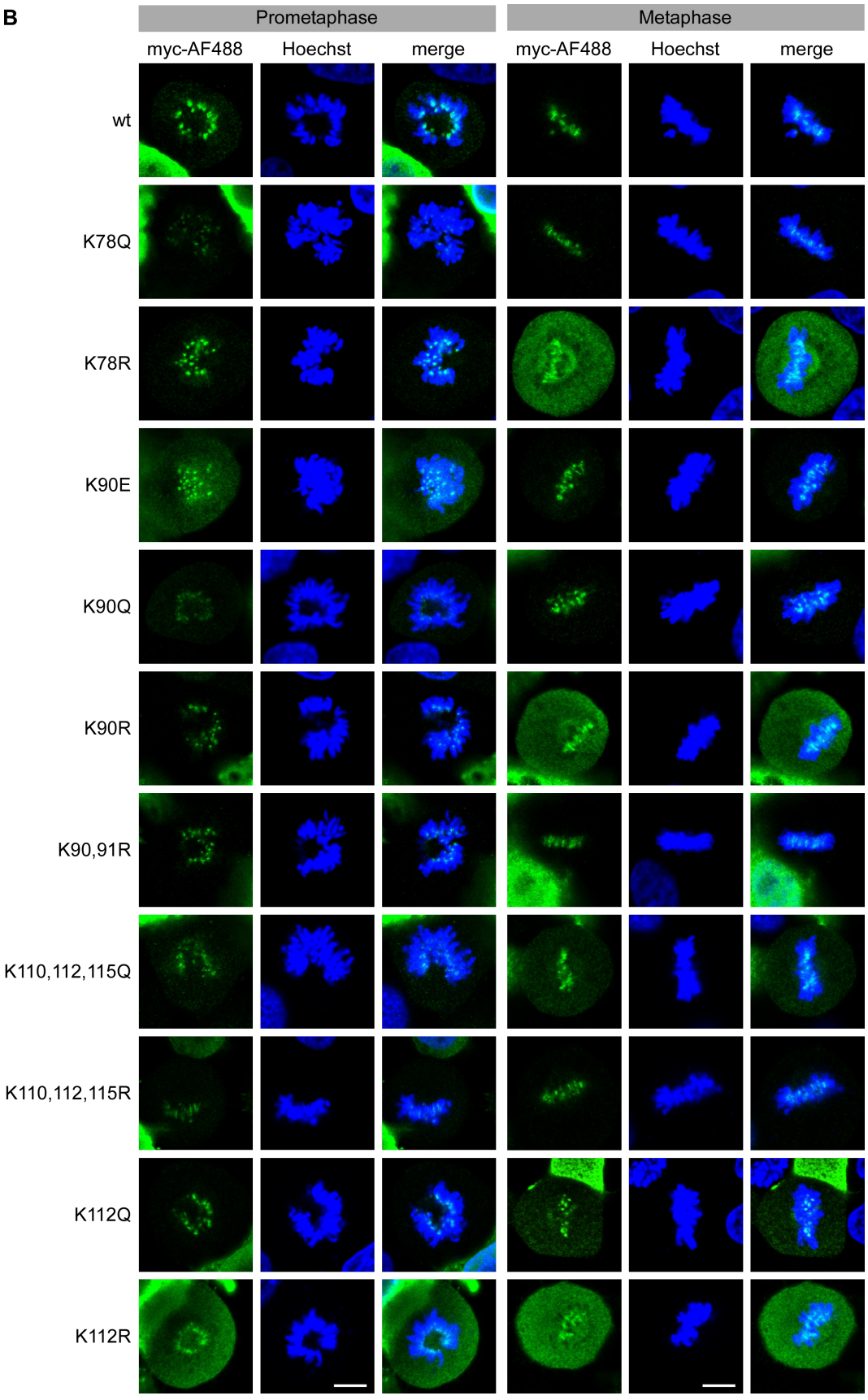
B
Prometaphase
Metaphase
myc-AF488
Hoechst
merge
myc-AF488
Hoechst
merge
wt
K78Q
K78R
K90E
K90Q
K90R
K90,91R
K110,112,115Q
K110,112,115R
K112Q
K112R

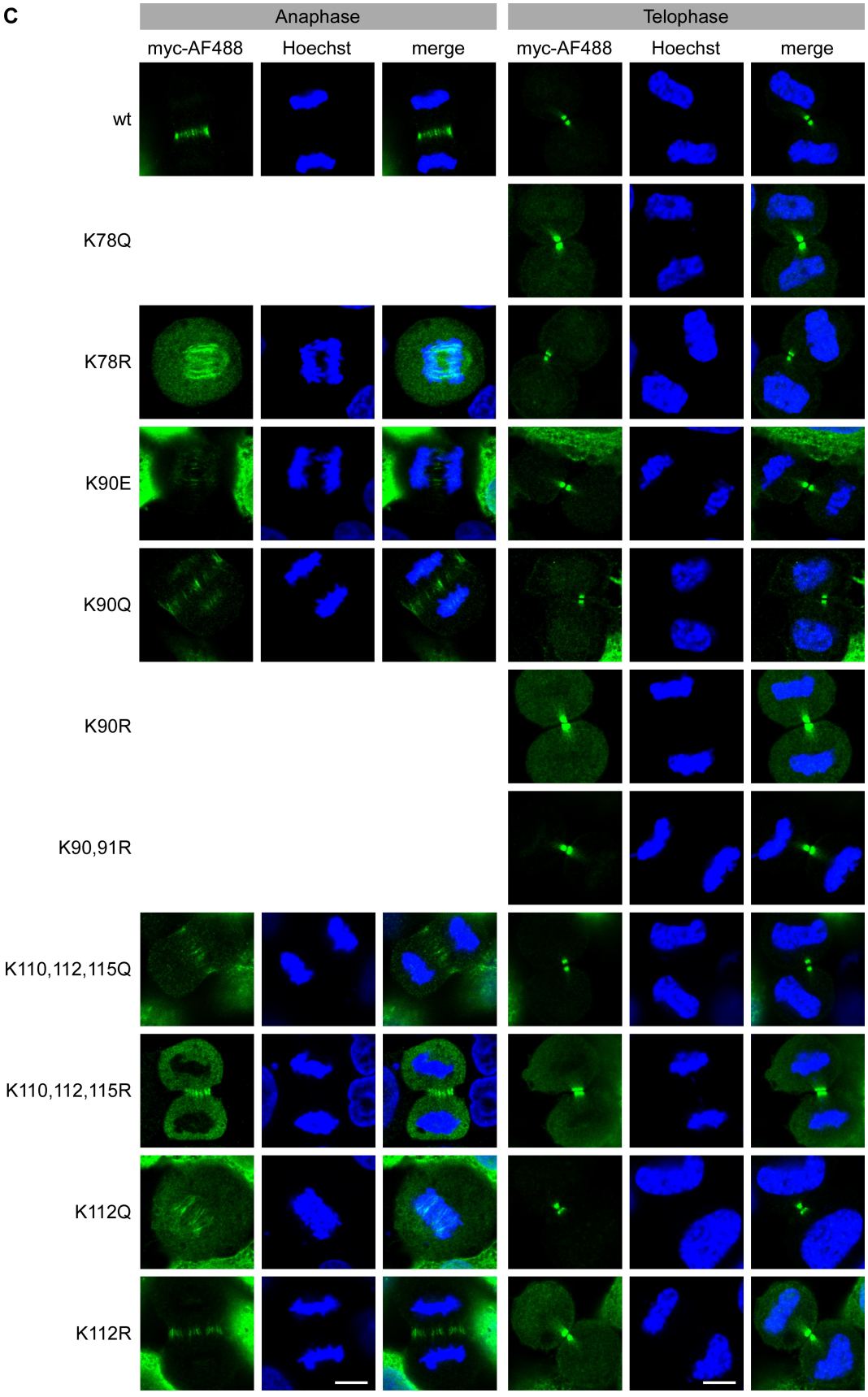
C
Anaphase
Telophase
myc-AF488
Hoechst
merge
myc-AF488
Hoechst
merge
wt
K78Q
K78R
K90E
K90Q
K90R
K90,91R
K110,112,115Q
K110,112,115R
K112Q
K112R

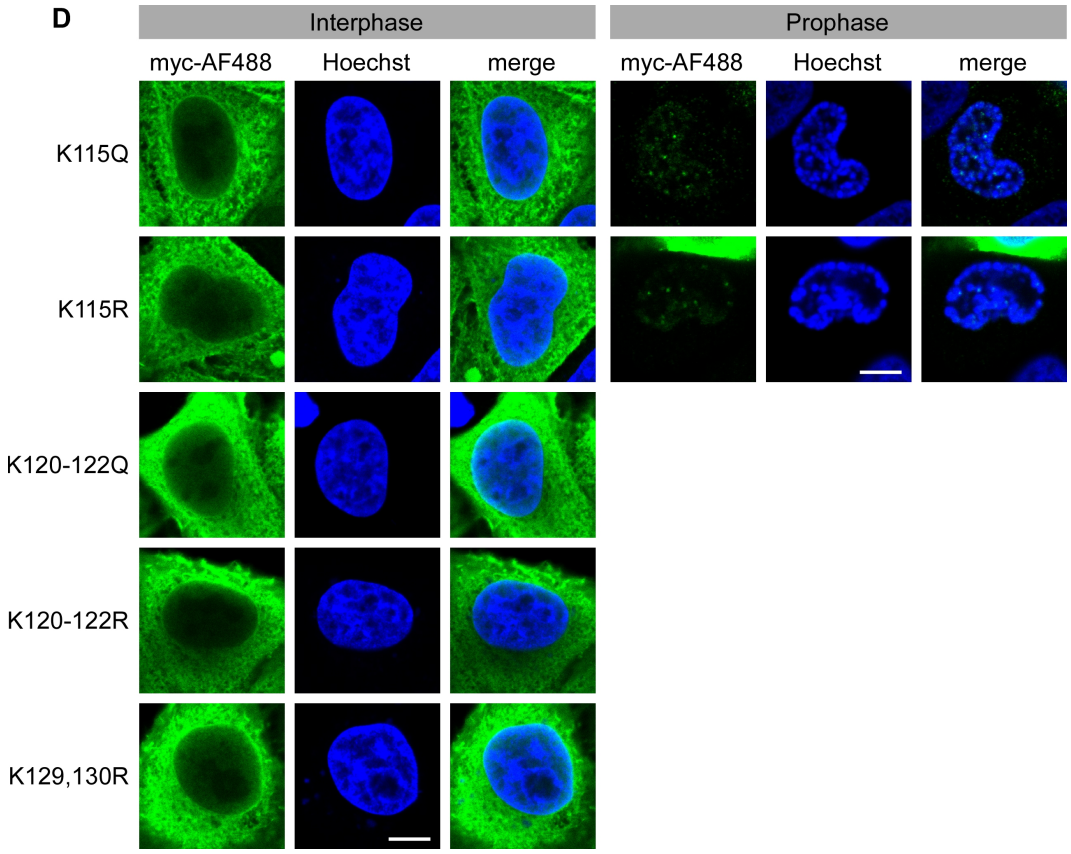
D
Interphase
Prophase
myc-AF488
Hoechst
merge
myc-AF488
Hoechst
merge
K115Q
K115R
K120-122Q
K120-122R
K129,130R

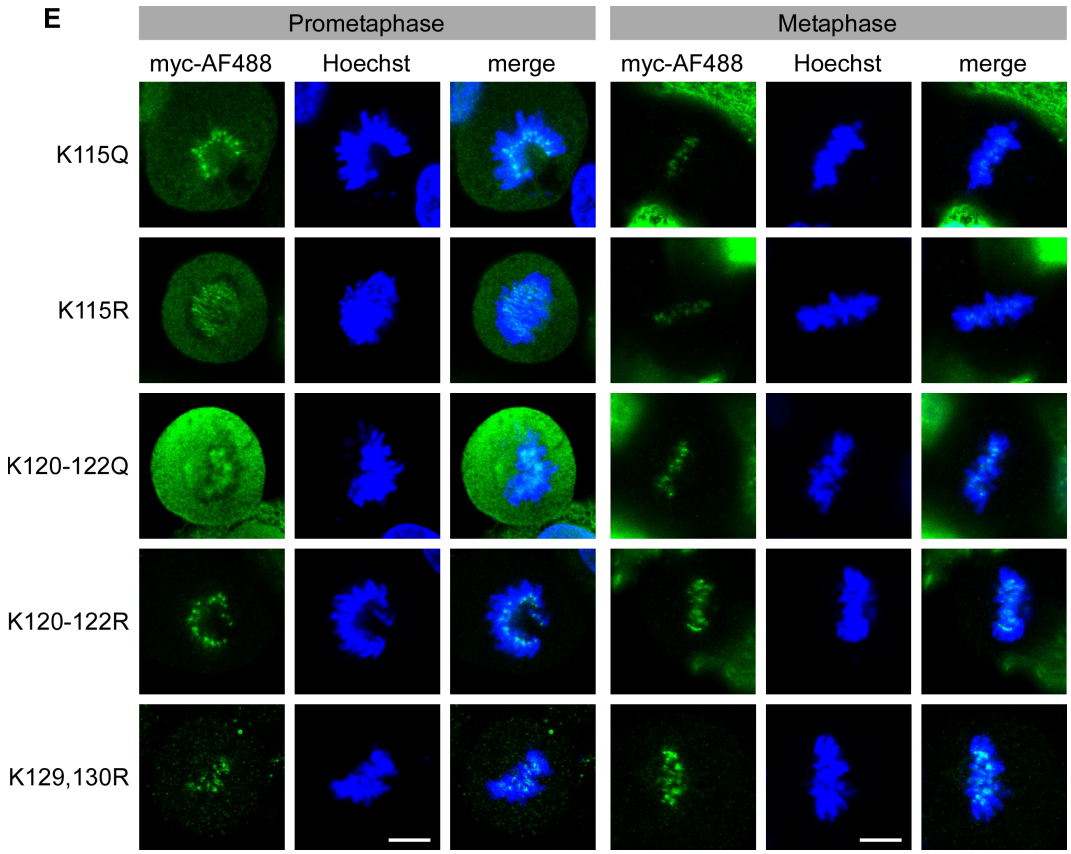
E
Prometaphase
Metaphase
myc-AF488
Hoechst
merge
myc-AF488
Hoechst
merge
K115Q
K115R
K120-122Q
K120-122R
K129,130R

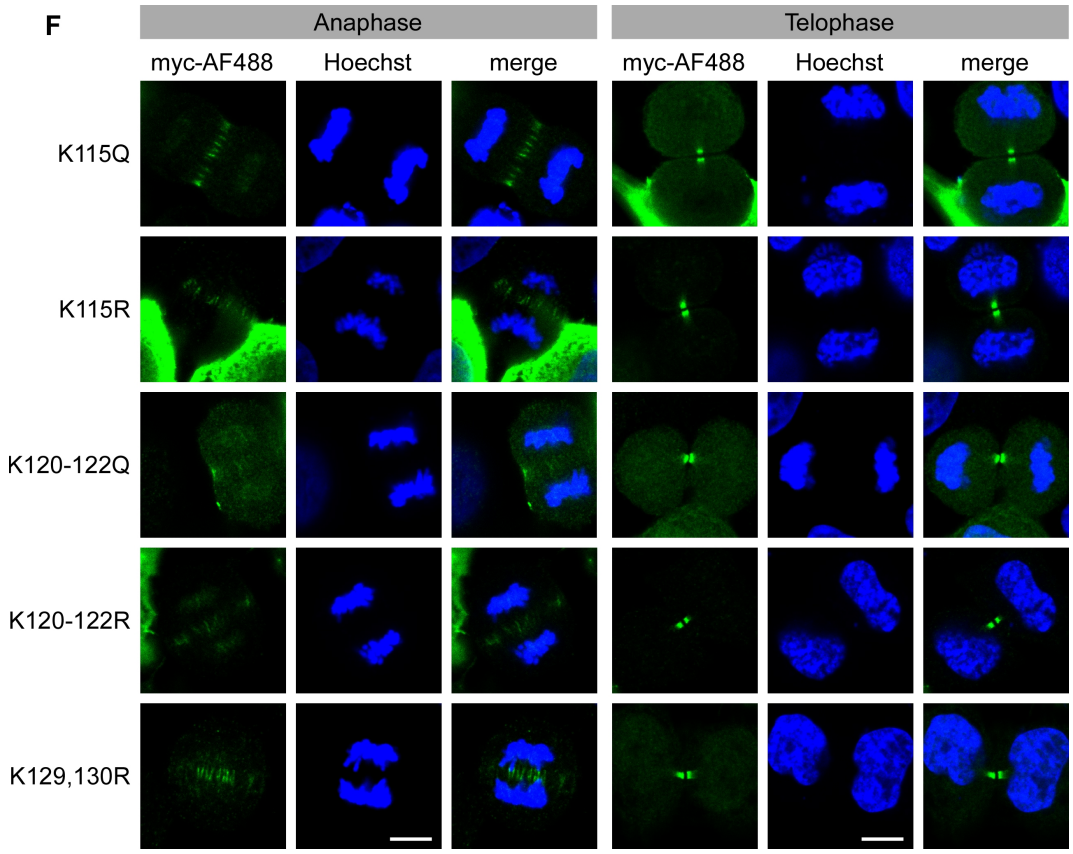

Figure 3.25: Localization of myc-tagged Survivin mutants in mitosis. HeLa K cells transiently transfected with myc-tagged Survivin variants were fixed, permeabilized, and immunostained with a myc-specific antibody (green). DNA was stained with Hoechst (blue). A) IF staining of Survivin wt and the mutants SurvK78Q to SurvK112R in interphase and prophase. B) IF staining of Survivin wt and the mutants SurvK78Q to SurvK112R in prometaphase and metaphase. C) IF staining of Survivin wt and the mutants SurvK78Q to SurvK112R in anaphase and telophase. D) IF staining of the mutants SurvK115Q to SurvK129,130R in interphase and prophase. E) IF staining of the mutants SurvK115Q to SurvK129,130R in prometaphase and metaphase. F) IF staining of the mutants SurvK115Q to SurvK129,130R in anaphase and telophase. Images were taken with a Leica SP5 confocal microscope. Scale bar, 10 µm.

3.3.4 Effect of Survivin acetylation on its dimerization

While for a long time Survivin was considered to be existing and functioning only as a dimer (Muchmore *et al.*, 2000; Song *et al.*, 2004), more recent studies demonstrated that monomeric Survivin plays crucial roles in diverse cellular processes. It has been shown that only the Survivin monomer can be part of the CPC (Jeyaprakash *et al.*, 2007), interact with CRM1 for its nuclear export (Engelsma *et al.*, 2007), and that it is also involved in the inhibition of caspase-dependent and -independent apoptosis (Pavlyukov *et al.*, 2011). Although important functions for monomeric as well as dimeric Survivin in the nucleus and the cytoplasm have been reported, the mechanisms regulating its dimerization and subcellular localization are still not completely understood. As mentioned before, Wang *et al.* (2010b) suggested that the acetylation of Survivin at K129 functions as a switch between the momoneric and dimeric state of the protein.

To investigate whether a potential acetylation at lysine residues different from K129 is also able to influence Survivin dimerization, the dimerization of the Survivin variants was assessed by gel filtration using a Superdex 75 10/300 GL column (GE Healthcare Life Sciences) (Figure 3.26A). Initially, the SurvK90R and SurvK90Q mutants were analyzed since, as already mentioned, K90 is located in the dimer interface of Survivin, thus mutations altering the biochemical properties of K90 could possibly interfere with Survivin's dimerization. For gel filtration experiments, recombinant, tag-free proteins were produced as described in subsubsection 2.2.3.1 and subsection 3.2.3. Again, the dimerization-deficient SurvF101AL102A mutant was used as negative control.

The elution profile of SurvK90R (red) mostly resembled that of Survivin wt (green) with the dimer peak eluting at 9.5 mL and the monomer peak eluting at approx. 10.3 mL. Only the height of the dimer peak was slightly lower than that of Survivin wt. The peaks of SurvK90Q (orange) were both higher than that of Survivin wt, and their elution volumes were slightly lower.

Again, the peaks were integrated and the monomer and dimer populations were determined (Figure 3.26B). The quantification revealed 76.5 % dimeric protein in case of SurvK90Q in comparison to 75 % in case of Survivin wt. With a percentage of 79.5 % an increased dimerization was observed for SurvK90R.

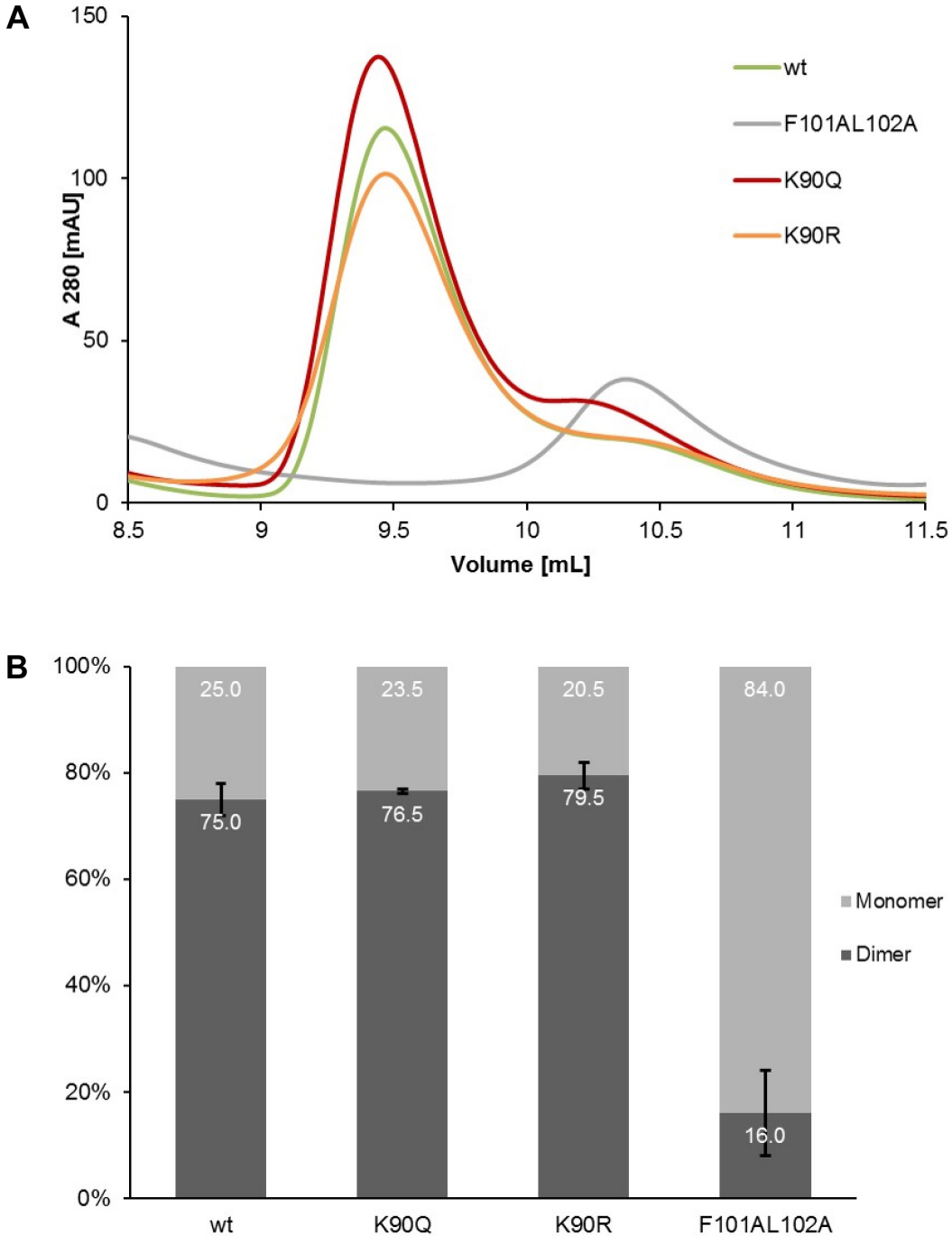

Figure 3.26: Dimerization of recombinant, untagged Survivin K90 mutants. A) Gel filtration profiles of purified, tag-free Survivin mutants in PBS containing 2.5 mM β-mercaptoethanol. Only the elution range between 8.5 and 11.5 mL is shown. A 280: absorption at 280 nm; AU: absorption units. B) Quantification of Survivin dimerization. Monomer and dimer peaks of the gel filtration profiles shown in A were integrated, and the sum of both integrals was set to 100 %. n = 2; the error bars represent s.d.

3.3.5 Analysis of the secondary structure of Survivin K90 mutants

The secondary structure of the SurvK90 mutants was also surveyed by CD spectroscopy (Figure 3.27) as already performed for the SurvK129 mutants. Both spectra were similar to that of Survivin wt, with one maximum of the specific ellipticity at approx. 191 nm and two minima at 207 and 225 nm.

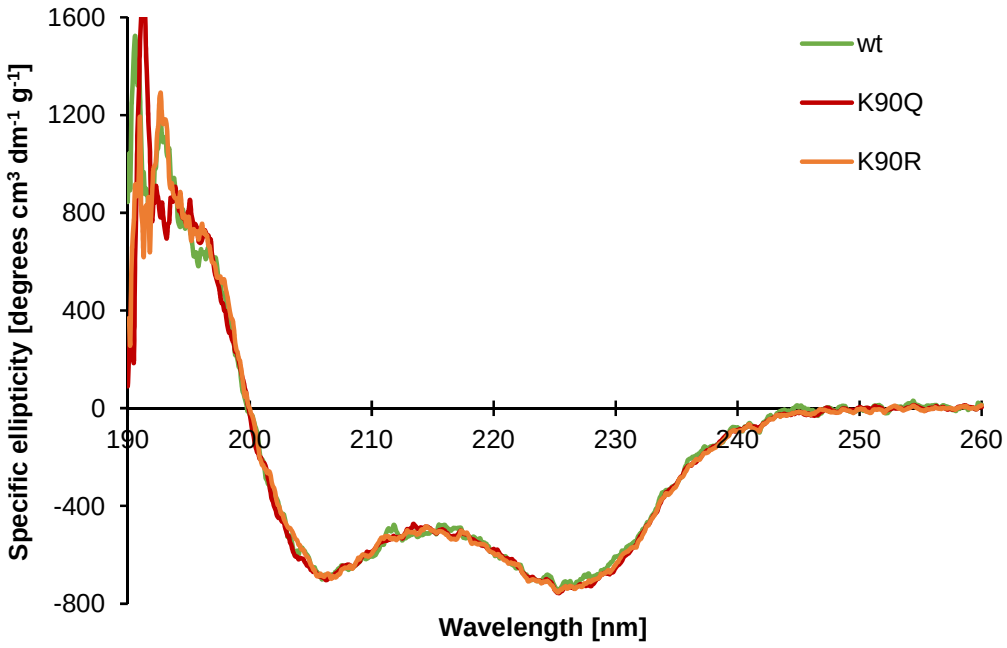

Figure 3.27: CD spectra of recombinant, untagged Survivin K90 mutants. Far-UV circular dichroism spectra of purified, tag-free Survivin mutants in 20 mM phosphate buffer containing 10 µM Zn^{2+} at 20 °C.

4 Discussion

Survivin plays crucial roles in various cellular processes. While some of its functions are conducted by the Survivin monomer, others require the homodimer. However, the mechanisms regulating Survivin dimerization are not understood yet. As Wang *et al.* have claimed that the dimerization as well as the nuclear export of Survivin is regulated by its acetylation at lysine 129, in this study, we first wanted to verify their results. While we could confirm their findings concerning the SurvK129E mutant, for example its exclusively cellular localization as well as its reduced tendency to form dimers, we could not verify their assumption that the results obtained for SurvK129E can be conferred to wt Survivin unmodified at K129. Furthermore, we aimed to investigate the role of Survivin acetylated at K129 in mitosis. Here, we found indications that acetylated Survivin might be incorporated into the chromosomal passenger complex.

As lysine acetylation has emerged as a major post-translational modification capable of altering the functions and interactions of proteins, we intended to identify further acetylation sites within Survivin and the effects of a potential acetylation on Survivin's divers functions. However, the investigation of 15 Survivin mutants in which one to three probably acetylated lysine residues were mutated to arginine or glutamine could not identify potential candidates.

4.1 Characterization of Survivin acetylation at lysine 129

4.1.1 Influence of the size and and position of different expression tags on the cellular localization of the SurvivinK129 mutants

As lysine to arginine and lysine to glutamine mutations are conventionally used to mimic an unmodified or acetylated lysine residue, respectively, initially, we decided to only analyze Survivin wt and the SurvK129R and SurvK129Q mutants. Additionally, Wang *et al.* (2010b) have reported that SurvK129R exhibited the same cellular localization as SurvK129E, while SurvK129Q localized similar to SurvK129A. Thus, the typical mutants should have been sufficient to analyze the effect of K129 acetylation. The GFP tag was chosen as fluorescent fusion proteins can be easily examined for their expression level and cellular localization without cell fixation and immunostaining. Additionally, previous experiments revealed that GFP-tagged Survivin is able to rescue the functions of endogenous Survivin depleted with siRNA indicating that, despite its size, the GFP tag does not compromise Survivin's functionality.

First analyses of the overall acetylation of GFP, GFP-tagged Survivin wt and both mutants revealed that, in accordance to Wang *et al.* (2010b), acetylation of Surv wt-GFP increased upon co-expression of the lysine acetyltransferases p300 and CBP (Figure 3.3). However, acetylated lysine residues were also detected in the isolated GFP tag raising the question whether the increased acetylation levels were due to Survivin or GFP acetylation, or both. Thus, for analyses of the general acetylation level using an AcK antibody, Survivin variants with a lysine-free tag would be required.

Surprisingly, the analysis of the cellular localization of SurvK129R and SurvK129Q in HeLa cells showed no differences between the GFP-tagged Survivin variants (Figure 3.4). Whereas Wang *et al.* (2010b) reported a nuclear localization for Survivin wt and SurvK129Q and a cytoplasmic localization for SurvK129E, we observed that Survivin wt as well as both mutants predominantly localized to the cytoplasm. In contrast to Wang *et al.* (2010b), who used Survivin mutants with an N-terminal myc tag, our mutants were C-terminally tagged with GFP. Hence, the predominantly cytoplasmic localization of the Survivin-GFP variants could be due to the larger size of the proteins compared to the myc-tagged variants. Nevertheless, LMB treatment of HeLa cells expressing the Survivin-GFP variants led to a nuclear accumulation of the proteins (data not shown), demonstrating that Survivin-GFP can passively diffuse into the nucleus. In

addition, a huge protein like GFP fused to the C-terminus of Survivin might mask the α-helix, thus affecting the normal function and localization of Survivin. Due to the aforementioned reasons and the finding that GFP itself is acetylated, Survivin wt and both mutants were cloned with smaller C-terminal expression tags (myc and HA). However, the cellular localization of the Survivin variants with smaller tags (Figure 3.5 and data not shown) was comparable to that observed for the GFP-tagged proteins with the only difference that the nuclear proportion of protein was slightly increased. This demonstrates that the GFP tag was not the reason for the deviant results. Nevertheless, even a small C-terminal tag could interfere with a mutational effect at position 129.

Therefore, Survivin wt as well as the SurvK129R and SurvK129Q mutant was finally cloned with an N-terminal myc tag in order create the same conditions as reported in the study by Wang *et al.* (2010b), although acetylation prediction revealed that the lysine within the myc tag is likely to be acetylated if the tag is placed at the N-terminus of the protein. Also the unconventional SurvK129E and SurvK129A mutants were included in our study. To avoid staining artifacts as observed in Figure 3.5, an optimized IF protocol including an extended permeabilization step was applied. In addition, a different strain of HeLa cells, HeLa Kyoto, was used for subsequent microscopic analyses, as these cells have a larger cell body, they form an ordered monolayer and no staining artifacts like membrane straining occur in IF experiments.

However, as discussed in subsection 4.1.2, the N-terminally myc-tagged mutants SurvK129R and SurvK129Q exhibited an identical cellular localization as the mutants with C-terminal myc or HA expression tags implying that the C-terminal tags were not the reason why no differences could be observed in the cellular localization of the acetylation mimicking (SurvK129Q) and the acetylation preventing (SurvK129R) mutant.

4.1.2 Transferability of the results obtained for SurvivinK129E to Survivin unmodified at lysine 129

The microscopic analysis of HeLa K cells expressing the myc-Survivin variants revealed a predominantly cytoplasmic localization of Survivin wt, SurvK129R and SurvK129Q (Figure 3.6). The second acetylation mimicking mutant, SurvK129A, also exhibited a similar cellular distribution. Only SurvK129E, representing a natural variant of Survivin in which the positively charged lysine at position 129 is exchanged by a negatively charged glutamate, exhibited a clearly different localization as it was detected exclusively in the cytoplasm. This hints towards a facilitated export of SurvK129E by

the nuclear export receptor CRM1 as suggested by Wang *et al.* (2010b). However, the contradictory findings for SurvK129E and SurvK129R were surprising since Wang *et al.* (2010b) reported a predominantly cytoplasmic localization for SurvK129E, but also for SurvK129R, arguing that this is caused by their acetylation abolishing function. Our results, however, indicate that SurvK129E is not comparable to SurvK129R. In contrast, our findings suggest that the effect observed for SurvK129E might not be due to the inhibition of acetylation by the mutation as in that case the same effect should be detectable for SurvK129R. The results obtained by IF experiments could be verified by western blot analyses of lysates prepared from nuclear and cytoplasmic fractions of cells expressing the Survivin variants.

Because Wang *et al.* (2010b) argued that SurvK129E forms less stable dimers than wt Survivin, the homodimerization of the Survivin variants was investigated by IP experiments in 293T cells (Figure 3.7). Again, contradictory results were obtained for the acetylation abolishing mutants. While SurvK129R exhibited a dimerization capability similar to Survivin wt, SurvK129E preferentially existed as a monomer like the dimerization-deficient SurvF101AL102A mutant. These findings again suggest that the effects observed for SurvK129E are not based on a lack of acetylation at position 129. Instead, they suggest that the presence of a negatively charged glutamate instead of a positively charged lysine at this position alters protein-protein interactions, for instance with CRM1. This impression is confirmed by the reduced dimerization tendency found for SurvK129Q and SurvK129A. According to Wang *et al.* (2010b), acetylation at K129 facilitates the formation of Survivin dimers. Thus, the acetylation mimicking mutants were supposed to preferentially exist as dimers like Survivin wt instead of exhibiting a decreased dimerization. The SurvK129R mutant, which mimics Survivin unacetylated at K129, however, formed dimers comparable to Survivin wt. Hence, contrary to the findings of Wang *et al.* (2010b), our results suggest that acetylation at K129 impairs Survivin dimerization rather than facilitating it.

IP experiments were accompanied by gel filtration analyses of recombinant, tag-free Survivin variants. This allows to test in a cell-free background whether the introduced mutations directly affect the homodimerization of the proteins (Figure 3.8). Due to different protein concentrations of the samples, the peaks of the elution profiles reached different heights which impeded their comparison. Thus, the dimer and the monomer peaks were integrated in order to obtain the percentage of dimeric and monomeric Survivin. The quantitative analysis revealed that all Survivin variants predominantly existed as homodimers, except for the dimerization-deficient mutant SurvF101AL102A serving as negative control. The monomer and dimer ratio was equal in all samples. Only for SurvK129A, a slightly higher proportion of dimeric protein was determined,

but in contrast to the other Survivin mutants, the protein was only analyzed once. As expected, none of the mutations at position 129 directly interfered with the formation of Survivin homodimers, as they are not positioned within the dimer interface (aa 6-10 and 89-102). Thus, the different dimerization capabilities of the mutants observed in cell-based IP experiments are likely to be mediated by altered interactions with other proteins, for example CRM1.

As Wang *et al.* (2010b) proposed that SurvK129E is exported from the nucleus more efficiently than Survivin wt due to its enhanced interaction with CRM1, first of all, we investigated whether all myc-Survivin variants are exported in a CRM1-dependent manner (Figure 3.9). Therefore, HeLa K cells expressing the myc-Survivin variants were either treated with the CRM1 inhibitor leptomycin B, or left untreated, and the localization of the Survivin variants was investigated microscopically. As expected, in untreated cells, all Survivin variants, except for SurvK129E, predominantly localized to the cytoplasm as already depicted in Figure 3.6. LMB treatment led to a nuclear accumulation of Survivin wt as well as all SurvivinK129 variants demonstrating that their export from the nucleus is mediated by CRM1. However, less protein accumulated in the nucleus than in case of the positive control SurvNESmut-GFP, which exhibited a strong nuclear enrichment already prior to CRM1 inhibition. This might be due to the fact that, with their small molecular weight of 17.9 kDa, the myc-Survivin variants can more easily exit the nucleus by passive diffusion than SurvNESmut-GFP (43 kDa). Thus, to achieve a more distinct effect upon CRM1 inhibition not hampered by passive diffusion as well as a better comparability, Survivin-GFP variants should be used for this assay. SurvF101AL102A, which again served as positive control, exhibited a cellular distribution similar to that of Survivin wt in untreated cells, although Engelsma *et al.* (2007) have shown that it undergoes enhanced CRM1 binding. This indicates that the enhanced interaction of a Survivin mutant with CRM1 via its classical NES (aa 89-98) does not seem to be sufficient for its complete exclusion from the nucleus as observed in case of SurvK129E.

In order to quantify the interaction of the Survivin variants with CRM1, we performed IP experiments in 293T cells. In a first approach, CRM1 was directly precipitated from the lysates by its HA tag, and the co-immunoprecipitation of the myc- or GFP-tagged Survivin variants was analyzed (Figure 3.10). In a second experiment, the Survivin mutants were precipitated from the lysates, and the CRM1 co-IP was analyzed (Figure 3.11). The experiments did not provide consistent results. In addition, the results have to be assessed as not meaningful as the positive as well as negative control did not exhibit the expected results. SurvF101AL102A was used as positive control as Engelsma *et al.* (2007) have demonstrated an enhanced binding to CRM1. However, our

interaction analysis showed a 55 % reduction in the interaction of SurvF101AL102A with CRM1 compared to Survivin wt. In contrast, the negative control SurvNESmut, which is unable to bind CRM1 due to mutations of two essential leucine residues within its NES (Knauer *et al.*, 2006), exhibited an only 28 % and 58 %, respectively, reduced interaction with CRM1 compared to Survivin wt. The results indicate that either the IP protocol or the quantification method have to be optimized in order to gain reliable results concerning the interaction of CRM1 with Survivin mutants. Perhaps the additional incubation of the lysates for 20 min at 37 °C prior to the addition of antibody-coupled microbeads should be omitted, though it improved the results for Survivin dimerization IPs. Quantification could be improved by using secondary antibodies coupled to near-infrared fluorescence dyes for western blotting allowing the direct detection and quantification of protein bands with the Odyssey System (LI-COR Biotechnology). Another possibility to examine the CRM1-Survivin binding is an *in vitro* pulldown assay using purified Survivin proteins and either purified or *in vitro* translated CRM1.

In order to exclude that conformational changes caused by the introduced mutation are the reason for the altered behavior of the SurvK129E mutant, the secondary structure of the recombinant, tag-free Survivin variants was examined by CD spectroscopy (Figure 3.12). Identical CD spectra were recorded for Survivin wt and the other variants showing one maximum of the specific ellipticity at approx. 191 nm and two minima at 207 and 225 nm characteristic for proteins containing a high proportion of α-helical structures. These results demonstrate that the facilitated nuclear export as well as the reduced dimerization of SurvK129E are not due to an altered secondary structure of the mutant. Only the spectrum of the dimerization-deficient SurvF101AL102A mutant differed from the others as the negative peak at 225 nm was missing. This indicates a reduced amount of α-helical structures probably due to a partial unwinding of the C-terminal α-helix caused by the double mutation. CD measurements at a constant wavelength of 209 nm (the wavelength at which one of the minima appears in the CD spectrum of a protein α-helix) over a distinct temperature range (melting curves) could reveal potential stability problems in the helix.

4.1.3 Emergence of a potential high-affinity export signal in the C-terminus of Survivin as an explanation for the unique behavior of the SurvivinK129E mutant

In summary, contrary to Wang *et al.* (2010b) who reported a predominatly cytoplasmic localization of SurvK129E and SurvK129R, we observed this localization for the

SurvK129E mutant only. SurvK129R, however, exhibited a cellular localization comparable to Survivin wt and the mutants SurvK129Q and SurvK129A. Furthermore, we could confirm that SurvK129E preferentially exists as a monomer, but again, different results were obtained for SurvK129R which was shown to form dimers like Survivin wt. The different results for SurvK129E and SurvK129R indicate that the facilitated export and reduced dimerization of SurvK129E are unlikely to be caused by a lack of acetylation at position 129 because if that was the case, the effects should also be detectable for SurvK129R. While the direct inhibition of dimerization as well as the disruption of correct protein folding by the K129E mutation could be excluded as reasons for the different results obtained for SurvK129E, an increased interaction with CRM1 could provide a potential explanation. However, the comparison of the cellular localization of SurvK129E with that of SurvF101AL102A, which, despite its enhanced interaction with CRM1, localized like Survivin wt, suggests that the increased export of SurvK129E leading to a complete absence of the protein from the nucleus is probably not mediated by its classical NES, but occurs either NES-independently via adapter proteins, or is mediated by a second, non-classical export motif. In fact, Rodriguez *et al.* (2002) have reported that Surv119-142, which lacks the classical NES, is as efficiently exported by CRM1 as Surv89-136 containing the NES. Nevertheless, full-length Survivin was exported even more efficiently. Rodriguez *et al.* (2002) argued that the nuclear export of Surv119-142 is likely to be mediated by NES containing adapter proteins confirming the hypothesis that the K129E mutation could alter, and thus enhance the interaction with such a protein leading to an increased export.

However, analysis of the amino acid sequence of Survivin's C-terminus revealed the presence of a cluster of hydrophobic amino acids between F124 and M141 hinting at a potential export signal (Figure 4.1D). NESs are peptides of 8 to 15 amino acids containing clusters of hydrophobic residues separated by spacers of other amino acids. The classical consensus sequence is Φ1-$X_{2,3}$-Φ2-$X_{2,3}$-Φ3-X-Φ4, where Φ represents a hydrophobic amino acid like leucine, valine, isoleucine, phenylalanine, or methionine, and X can be any amino acid (Xu *et al.*, 2012). However, the NES consensus is continuously updated and refined as recently by Güttler *et al.* (2010) or Xu *et al.* (2012). Güttler *et al.* (2010), for example, redefined the NES consensus by analyzing structures of PKI-type and Rev-type NESs bound to CRM1. They proposed that, in addition to the classical four hydrophobic residues Φ1 to Φ4, a fifth hydrophobic residue, Φ0, can contribute to CRM1 binding as the NES binding site of CRM1 comprises five hydrophobic pockets. Furthermore, they stated characteristics for PKI-class as well as for Rev-class export signals summarized in Figure 4.1A and B.

Taking these characteristics into account, a potential 5Φ PKI-class export motif can be

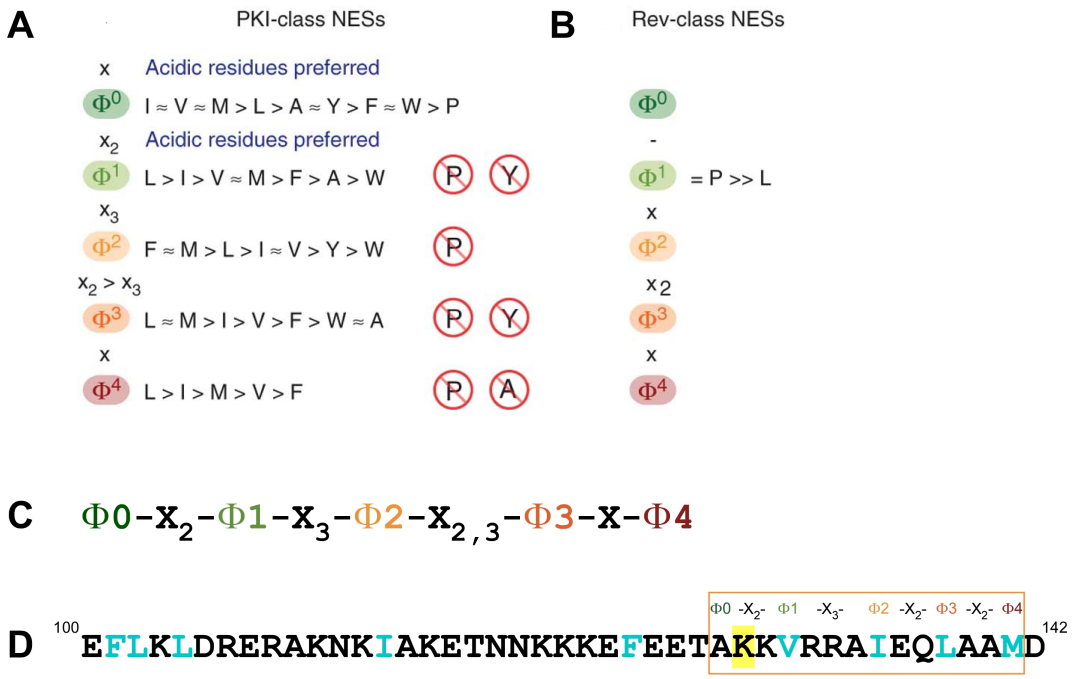

Figure 4.1: Identification of a potential NES in the Survivin C-terminus. A) and B) Characteristics of PKI-class and Rev-class NESs (modified after Güttler *et al.*, 2010). C) Consensus sequence for PKI-class NESs (Güttler *et al.*, 2010). D) Amino acid sequence of the Survivin C-terminus (aa 100-142) indicating hydrophobic amino acids (light blue). K129 is highlighted in yellow. The position of the hypothesized NES is indicated by an orange box. Colors and annotations were selected according to A.

located within Survivin's C-terminus between A128 and M141 revealing a Φ0-X_2-Φ1-X_3-Φ2-X_2-Φ3-X_2-Φ4 sequence (Figure 4.1D). Hence, except for the spacer between Φ3 and Φ4, which is too long by one amino acid, this identified potential NES is consistent with the consensus for PKI-class NESs (Figure 4.1C) defined by Güttler *et al.* (2010). However, the proper composition and spacing of amino acids in the C-terminus of a NES are critical for CRM1 binding. The mutation of the Φ3 and Φ4 positions to alanine, for example, is sufficient to completely abolish the export activity of a NES (Knauer *et al.*, 2006; Güttler *et al.*, 2010). In addition to the requirements for the Φ-positions, Güttler *et al.* (2010) found that acidic residues are preferred in the spacer between Φ0 and Φ1 as they engage in electrostatic interactions with K522 and K560 of the CRM1 NES binding pocket. In Survivin wt this is not the case as two lysine residues are located in this position likely to undergo electrostatic repulsion with K522 and K560 of CRM1. The K129E mutation, however, alters this unfavorable condition by exchanging at least one positively charged lysine residue with negatively charged glutamate. Thus, a possible explanation for the observed facilitated CRM1-dependent export of SurvK129E could be the conversion of a low-affinity NES in Survivin wt to a high-affinity NES due to the exchange of lysine with glutamate. Similar effects elicited

by the exchange of neutral residues with acidic amino acids within the Φ0-Φ1 spacer have been reported by Güttler *et al.* (2010). Of course, this hypothesis has to be further validated, for example by investigating the cellular localization as well as CRM1 interaction of SurvK129 mutants lacking amino acids 1-98 by IF and IP experiments. Furthermore, microinjection of recombinant proteins consisting of the potential NES flanked by an N-terminal GST and a C-terminal GFP tag into the nucleus of adherent, mammalian cells would provide deeper insight into the functionality of the hypothesized export signal.

The presence of a high-affinity NES in the C-terminal α-helix of Survivin, however, does not *per se* explain the preferentially monomeric state of SurvK129E as this potential export signal does not overlap with Survivin's dimer interface (aa 6-10 and 89-102). However, enhanced CRM1 binding to this site could probably sterically hamper dimerization. One has also to take into consideration that the hydrophobic amino acids representing the Φ positions of the potential C-terminal NES are the same as those engaging in hydrophobic contacts with Borealin and INCENP within the three-helical bundle that stabilizes the CPC (Figure 4.2). Hence, an enhanced CRM1 binding to this site could probably interfere with CPC assembly. SurvK129E, though, localized correctly in all phases of mitosis. However, the competition of CRM1 and Borealin/INCENP for Survivin binding also occurs at the classical NES as Borealin and INCENP bind to Survivin's dimer interface. This suggests that the binding of CRM1 and Borealin/INCENP, although being mediated by the same amino acids, are temporally and/or spatially separated processes that do not affect each other.

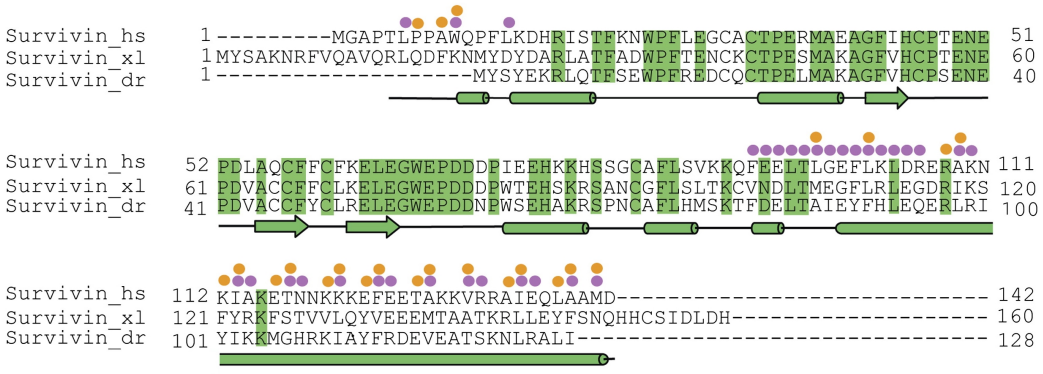

Figure 4.2: Interactions of Survivin in the CPC core. Structure-based-sequence alignments indicating amino acid conservation and interactions of Survivin with Borealin and INCENP. The secondary structure elements are shown below the sequences. Conserved residues are highlighted in green. Above the sequences, colored circles identify residues involved in interactions with Borealin (magenta circles) and INCENP (orange circles). hs: *Homo sapiens*, xl: *Xenopus laevis*, dr: *Danio rerio* (modified after Jeyaprakash *et al.*, 2007).

4.1.4 Involvement of Survivin acetylated at lysine 129 in CPC formation

In order to investigate the involvement of Survivin acetylated at K129 in mitosis, a topic which has not been addressed in the study by Wang *et al.* (2010b), we intended to utilize a commercially available primary antibody specific for SurvK129Ac, which had also been used by Wang *et al.* (2010b). We assumed the SurvK129Ac antibody would offer advantages over the aforementioned SurvK129Ac mimicking mutants since it directly detects acetylated Survivin. Thus, it does not have to be considered whether any findings are due to acetylation or simply to the introduced mutation as discussed above. Wang *et al.* (2010b) could detect overexpressed acetylated myc-Survivin wt in western blot, and an intense nuclear staining of endogenous SurvK129Ac in IF experiments. Our tests of the SurvK129Ac antibody, however, revealed that overexpressed, tagged Survivin is not recognized in western blot irrespective of the expression tag or its position (Figure 3.13 - Figure 3.15). Only endogenous SurvK129Ac could be detected upon CBP co-expression. Moreover, in IF stainings of untransfected HeLa K cells, or cells transfected with myc-Survivin wt, only a weak, heterogeneous, predominantly nuclear staining was detected (Figure 3.16), which, however, was more intense in transfected cells indicating that the antibody might recognize overexpressed Survivin under native conditions.

The antibody was first applied in IP analyses in 293T cells aiming to find out whether SurvK129Ac engages in interactions with members of the chromosomal passenger complex (Figure 3.17). We found that Borealin, which together with Survivin and INCENP's N-terminus belongs to the localization module of the CPC, interacts with Survivin-myc as well as with endogenous SurvK129Ac. This was surprising as on the one hand it is known that Survivin is a monomer within the CPC as Borealin and INCENP occupy its dimer interface (Jeyaprakash *et al.*, 2007), but on the other hand Wang *et al.* (2010b) have claimed that SurvK129Ac preferentially exists as a dimer. Our results, however, suggest that at least one portion of Survivin acetylated at K129 is present in a monomeric state and can be incorporated into the CPC. Together with Aurora B, neither Survivin-myc nor SurvK129Ac could be co-precipitated. In case of overexpressed Survivin-myc, this was unexpected. Though a direct interaction of both proteins occurs only temporarily when Aurora B phosphorylates Survivin at T117, the proteins are linked by INCENP within the CPC . However, this indirect interaction does not seem to be sufficient to co-precipitate Survivin with Aurora B under the applied conditions. Based on findings by Honda *et al.* (2003) who suggested that in mitosis, the CPC is only stable if all members are present, a possible explanation could be that the expression of endogenous Borealin and INCENP in this sample was not suffi-

cient to form a detectable amount of assembled CPCs. Recent work by the Musacchio group (personal communication), however, has shown that the CPC core comprising Survivin, Borealin and INCENP's N-terminus is also stable in the absence of Aurora B. This suggests that Aurora B is possibly not only present and functional as a member of the CPC, which might explain why Survivin could not be precipitated with the kinase.

With a further IP experiment, we wanted to verify the finding that Borealin interacts with SurvK129Ac, and also wanted to include INCENP in the study (Figure 3.18). As for this experiment the cells had to be transfected with three different plasmids, we decided to enhance acetylation by treating the cells with TSA instead of transfecting them with cDNA coding for CBP. Survivin was co-immunoprecipitated with Borealin and INCENP, and the additional incubation for 20 min at 37 °C prior to the IP allowed the precipitation of Survivin also with Aurora B. However, we could neither confirm the interaction of Borealin with SurvK129Ac, nor could we detect an interaction of Aurora B or INCENP with acetylated Survivin.

Thus, in another IP experiment, the conditions were changed again (Figure 3.19). As the SurvK129Ac antibody only detects the endogenous protein, overexpression of tagged Survivin was set aside. Additionally, transfection of CBP-encoding cDNA was again applied to enhance acetylation, and all lysates were incubated for 20 min at 37 °C before adding the micro beads. In order to arrest cells in prometaphase, thus increasing the amount of assembled CPCs, cells were treated with nocodazole. While the analysis of the IP with a GFP-specific antibody suggested a low IP efficiency, the analysis with antibodies specific for Survivin and Aurora B showed intense bands for Survivin-GFP and Aurora B-GFP, which hints towards a problem with the GFP-specific antibody. For Borealin and INCENP, this was not tested due to the lack of specific antibodies working in western blot. The IP revealed that, although endogenous wt Survivin co-precipitated with Borealin, Aurora B and INCENP, SurvK129Ac does not seem to interact with these CPC members. Dimerization of endogenous Survivin with Survivin-GFP could not be detected. This is not surprising as Survivin-GFP homodimerization is likely to outbalance the formation of heterodimers of Survivin-GFP with endogenous Survivin. The results were similar in mitotically arrested and asynchronous cells.

In summary, the interaction of Borealin with Survivin acetylated at K129 could not be verified. It has to be noted that the SurvK129Ac antibody used in the experiments depicted in Figure 3.18 and Figure 3.19 was of a different lot than that used in the first IP experiment (Figure 3.17). With the new lot, no SurvK129Ac could be detected in any western blot analysis performed, not even in test experiments where cells were only transfected with CBP, or treated with TSA. In addition, at the same time, the production of the PVDF membrane used for western blotting was discontinued. Thus, for the latter

IP experiments, a new membrane with a lower protein binding capacity had to be used. It is therefore unclear whether the lack of a signal from the SurvK129Ac antibody is due to a lack of interaction of Survivin acetylated at K129 with other CPC proteins, or if this is caused by a technical problem with the new antibody lot or the PVDF membrane. Hence, as a direct investigation of SurvK129Ac is not possible, IP analyses of the interaction of CPC proteins with the SurvK129R and SurvK129Q mutants could provide further insight into the involvement of SurvK129Ac in mitosis.

IP experiments were accompanied by IF stainings in order to analyze the localization of SurvK129Ac in mitotic HeLa K cells and its co-localization with CPC members (Figure 3.20). This was again performed using the SurvK129Ac-specific antibody. While Survivin showed a staining pattern typical for CPC proteins, and exhibited an exact co-localization with Aurora B, Borealin and INCENP, for SurvK129Ac no such localization could be observed. In interphase cells, the aforementioned weak, heterogeneous, predominantly nuclear staining was visible, whereas in mitotic cells, the staining was detected in the whole cell, but DNA was spared. These findings indicate that SurvK129Ac is not a part of the CPC, but as mentioned above, it is not clear whether the antibody specific for SurvK129Ac yields reliable results.

In order to avoid using the SurvK129Ac antibody, but, nevertheless, obtain more information on a potential role of SurvK129Ac in mitosis, we analyzed the mitotic localization of the myc-SurvK129 mutants in HeLa K cells (Figure 3.21). The experiment revealed that all mutants localized like myc-Survivin wt. Concerning the SurvK129Q mutant, which is supposed to mimic Survivin acetylated at K129, this suggests that SurvK129Ac can be incorporated into the CPC. However, this finding is contradictory to the results gained using the SurvK129Ac antibody and also to the theory by Wang *et al.* (2010b) that SurvK129Ac predominantly exists as a dimer. In addition, as we found the dimerization of SurvK129Q to be clearly reduced, it is not unlikely that SurvK129Q or SurvK129Ac, respectively, can be a member of the CPC.

To verify this, IF experiments should be performed in the absence of endogenous Survivin as it might undo the effects of the mutants. To this end, endogenous Survivin should be depleted with siRNA. As siRNA also has to be transfected into HeLa K cells, and a simultaneous as well as a successive transient transfection of plasmid DNA and siRNA dramatically reduces the transfection efficiency and viability of the cells, this should be done in HeLa K cells stably expressing the Survivin variants. One way to generate stably expressing HeLa K cells is via the Flp-In system (Life Technologies). Here, the gene of interest is introduced into the cell genome with the help of the *Saccharomyces cerevisiae* DNA recombinase Flp. Another way to achieve a constitutive expression of Survivin variants in HeLa K cells would be by lentiviral transduction tak-

ing advantage of the ability of lentiviruses like HIV to stably integrate their own genome into that of host cells.

4.2 Characterization of Survivin acetylation at other lysine residues

We also aimed to investigate whether further of Survivin's 16 lysine residues are acetylated, and which effects a possible acetylation might have on Survivin's functions. To this end, we performed acetylation predictions with two different online tools, and compared the results with those obtained by mass spectrometric analyses performed by Wang *et al.* (2010b) (Table 3.1). Furthermore, we wanted to identify acetylated lysine residues by own mass spectrometric measurements. However, due to problems with sample preparation this approach has not yet yielded any results. The Survivin proteins to be analyzed were isolated from 293T lysates with antibody-coupled magnetic micro beads using µMACS Isolation kits (Miltenyi Biotec). Precipitated proteins can be efficiently eluted from the micro beads with a denaturing buffer containing DTT and SDS. These substances have to be removed from the sample prior to mass spectrometric measurements. However, sample purification could not be achieved without a loss of the protein. Another way to elute precipitated proteins from the columns is with a non-denaturing solution of triethylamine inducing a pH shift. This elution method, however, did not yield a sufficient amount of protein. Therefore, sample preparation as well as purification have to be improved.

Based on the findings of the *in silico* analysis, 15 new myc-tagged Survivin mutants were cloned. Since lysine to arginine and lysine to glutamine mutations are typically used in studies analyzing protein acetylation, only these mutations were introduced with the exception of SurvK90E. We believed it would be interesting to analyze the effect of a lysine to glutamate exchange within Survivin's classical NES as it could, at least to some extent, resemble the effect of the K129E mutation.

First of all, the cellular localization of the mutants was examined by IF stainings in HeLa K cells (Figure 3.23). The experiments revealed that, except for SurvK90E, which exhibited a reduced nuclear localization, the localization of all Survivin mutants resembled that of Survivin wt. The finding that SurvK90E also showed a reduced nuclear localization, albeit to a lesser extend than SurvK129E, confirms that the exchange of a positively charged lysine with a negatively charged glutamate within a spacer sequence of a NES can indeed lead to facilitated CRM1 binding and nuclear export. As

already argued concerning the the cellular localization of the SurvK129 mutants, the results could be verified by performing fractionation experiments . In addition, the nuclear export of SurvK90E must be further analyzed to validate this theory. To test for a facilitated export of SurvK90E, its NES could be expressed as a recombinant fusion protein with GST and GFP, and microinjected into the nucleus of adherent cells. Its interaction with CRM1 could be investigated on the one hand in cells by performing IP experiments. On the other hand, the binding of recombinant SurvK90E or its NES to *in vitro* translated or recombinant CRM1 could be analyzed by performing pull-down assays.

As almost all of the newly cloned Survivin variants contained mutations possibly affecting CPC localization as well as stability (see subsection 3.3.3) we aimed to examine their mitotic localization by IF experiments in HeLa K cells (Figure 3.25). The analysis revealed that all Survivin mutants exhibited the same localization as Survivin wt. This was especially unexpected for the mutants SurvK110,112,115Q, SurvK112Q, and SurvK120-122Q as they contain lysine to glutamine mutations at positions which have been demonstrated to engage in electrostatic interactions with aspartate or glutamate residues of the helices of Borealin and INCENP (Jeyaprakash *et al.*, 2007) (Figure 3.24). Thus, hampering these contacts either by removing lysine's positive charge by acetylation, or by exchanging lysine with glutamine, could likely lead to a destabilization, or even disassembly of the three-helix bundle. However, only one electrostatic contact to INCENP is lost in case of SurvivinK112Q, and one contact to INCENP as well one to Borealin is abolished in case of SurvK110,112,115Q and SurvK120-122Q. This might not be sufficient to destabilize the three-helical bundle as it is additionally stabilized by hydrophobic interactions of other amino acids. Nevertheless, it would be interesting to analyze the effect of a multiple K110,112,120,121Q mutation, which would abrogate all of Survivin's salt bridges to Borealin and INCENP within the three-helix bundle. As mentioned above, effects which could be hidden by endogenous Survivin could become more obvious when Survivin is depleted with siRNA.

Survivin plays crucial roles in divers cellular processes, for example in mitosis and apoptosis. In some of these processes, Survivin is involved as a monomer, whereas other functions are exerted by the dimer. However, it is still not completely understood how the dimerization of Survivin is regulated. As PTMs can function as regulators of protein-protein interactions, we aimed to test whether any of the new Survivin mutants shows an altered dimerization due to the inhibition of post-translational modifications, or the mimicry of acetylated lysine. Since mutations within the dimer interface could most likely affect Survivin dimerization, initially, the SurvK90R and SurvK90Q mutants were analyzed by gel filtration (Figure 3.26). SurvK90E was not analyzed as, at that

point in time, the mutant had not been cloned into the GST-PreSc vector. The determination of the dimeric and monomeric proportion within the samples revealed that both mutants predominantly form dimers like Survivin wt. An 1.5 % and 4.5 % increased proportion of dimeric protein was found for SurvK90Q and SurvK90R, respectively, compared to the wt protein. However, the differences were not significant. From these results, it can be concluded that acetylation of Survivin at K90, as mimicked by the SurvK90Q mutant, does not directly affect Survivin dimerization. In order to determine its indirect effect on dimerization, which could be mediated by an alteration in CRM1 binding, IP analyses have to be performed.

The secondary structure of SurvK90R and SurvK90Q was analyzed by CD spectroscopy (Figure 3.27). Both mutants exhibited CD spectra identical to that of Survivin wt indicating that the introduced mutations do not hamper the folding of the proteins. The stability of the mutants could be further investigated by recording CD melting curves, for example at 209 nm.

In summary, concerning the SurvK129 mutants, we could not verify the findings reported by Wang *et al.* (2010b). In contrast, our results indicate that the effect observed for the SurvK129E mutant is not due to a lack of acetylation at K129, but is rather caused by the emergence of a high-affinity NES in Survivin's C-terminal α-helix. Furthermore, our experiments suggest that acetylation at K129 rather impairs Survivin dimerization than facilitating it. We have also found indications that Survivin acetylated at K129 could be involved in mitosis. The investigations conducted in order to discover further acetylation sites regulating Survivin's localization or function could not identify potential candidates. We could only show that, although K90 is located within Survivin's NES, its acetylation is unlikely to affect the protein's dimerization. However, in order to validate the obtained results and to gain a deeper understanding of how Survivin is regulated by acetylation, further studies have to be performed as discussed in detail above.

References

Adams, R. R., Wheatley, S. P., Gouldsworthy, A. M., Kandels-Lewis, S. E., Carmena, M., Smythe, C., Gerloff, D. L., and Earnshaw, W. C. (2000). Incenp binds the aurora-related kinase airk2 and is required to target it to chromosomes, the central spindle and cleavage furrow. *Curr Biol*, 10(17):1075–1078.

Adida, C., Crotty, P. L., McGrath, J., Berrebi, D., Diebold, J., and Altieri, D. C. (1998). Developmentally regulated expression of the novel cancer anti-apoptosis gene survivin in human and mouse differentiation. *Am J Pathol*, 152(1):43–49.

Adida, C., Haioun, C., Gaulard, P., Lepage, E., Morel, P., Briere, J., Dombret, H., Reyes, F., Diebold, J., Gisselbrecht, C., Salles, G., Altieri, D. C., and Molina, T. J. (2000). Prognostic significance of survivin expression in diffuse large b-cell lymphomas. *Blood*, 96(5):1921–1925.

Agromayor, M. and Martin-Serrano, J. (2013). Knowing when to cut and run: mechanisms that control cytokinetic abscission. *Trends Cell Biol*, 23(9):433–441.

Ainsztein, A. M., Kandels-Lewis, S. E., Mackay, A. M., and Earnshaw, W. C. (1998). Incenp centromere and spindle targeting: identification of essential conserved motifs and involvement of heterochromatin protein hp1. *J Cell Biol*, 143(7):1763–1774.

Alajez, N. M., Lenarduzzi, M., Ito, E., Hui, A. B. Y., Shi, W., Bruce, J., Yue, S., Huang, S. H., Xu, W., Waldron, J., O'Sullivan, B., and Liu, F.-F. (2011). Mir-218 suppresses nasopharyngeal cancer progression through downregulation of survivin and the slit2-robo1 pathway. *Cancer Res*, 71(6):2381–2391.

Allfrey, V. G., Faulkner, R., and Mirsky, A. E. (1964). Acetylation and methylation of histones and their possible role in the regulation of rna synthesis. *Proc Natl Acad Sci U S A*, 51:786–794.

Altieri, D. C. (2006). The case for survivin as a regulator of microtubule dynamics and cell-death decisions. *Current opinion in cell biology*, 18(6):609–15.

Altieri, D. C. (2010). Survivin and iap proteins in cell-death mechanisms. *Biochem J*, 430(2):199–205.

Alvarez-Fernández, M. and Malumbres, M. (2014). Preparing a cell for nuclear envelope breakdown: Spatio-temporal control of phosphorylation during mitotic entry. *Bioessays*, 36(8):757–765.

Ambrosini, G., Adida, C., and Altieri, D. C. (1997). A novel anti-apoptosis gene, survivin, expressed in cancer and lymphoma. *Nat Med*, 3(8):917–921.

Arif, M., Senapati, P., Shandilya, J., and Kundu, T. K. (2010). Protein lysine acetylation in cellular function and its role in cancer manifestation. *Biochim Biophys Acta*, 1799(10-12):702–16.

Arnaoutov, A., Azuma, Y., Ribbeck, K., Joseph, J., Boyarchuk, Y., Karpova, T., McNally, J., and Dasso, M. (2005). Crm1 is a mitotic effector of ran-gtp in somatic cells. *Nat Cell Biol*, 7(6):626–632.

Arora, V., Cheung, H. H., Plenchette, S., Micali, O. C., Liston, P., and Korneluk, R. G. (2007). Degradation of survivin by the x-linked inhibitor of apoptosis (xiap)-xaf1 complex. *J Biol Chem*, 282(36):26202–26209.

Atassi, G. and Tagnon, H. J. (1975). R17934-nsc 238159: a new antitumor drug–i. effect on experimental tumors and factors influencing effectiveness. *Eur J Cancer*, 11(9):599–607.

Barrett, R. M. A., Colnaghi, R., and Wheatley, S. P. (2011). Threonine 48 in the bir domain of survivin is critical to its mitotic and anti-apoptotic activities and can be phosphorylated by ck2 in vitro. *Cell Cycle*, 10(3):538–548.

Barrett, R. M. A., Osborne, T. P., and Wheatley, S. P. (2009). Phosphorylation of survivin at threonine 34 inhibits its mitotic function and enhances its cytoprotective activity. *Cell Cycle*, 8(2):278–283.

Birnboim, H. C. and Doly, J. (1979). A rapid alkaline extraction procedure for screening recombinant plasmid dna. *Nucleic Acids Res*, 7(6):1513–1523.

Bishop, J. D. and Schumacher, J. M. (2002). Phosphorylation of the carboxyl terminus of inner centromere protein (incenp) by the aurora b kinase stimulates aurora b kinase activity. *J Biol Chem*, 277(31):27577–27580.

Boidot, R., Végran, F., Jacob, D., Chevrier, S., Cadouot, M., Feron, O., Solary, E., and Lizard-Nacol, S. (2010). The transcription factor gata-1 is overexpressed in breast carcinomas and contributes to survivin upregulation via a promoter polymorphism. *Oncogene*, 29(17):2577–2584.

Bradford, M. M. (1976). A rapid and sensitive method for the quantitation of microgram quantities of protein utilizing the principle of protein-dye binding. *Anal Biochem*, 72:248–254.

Capalbo, G., Dittmann, K., Weiss, C., Reichert, S., Hausmann, E., Rödel, C., and Rödel, F. (2010). Radiation-induced survivin nuclear accumulation is linked to dna damage repair. *Int J Radiat Oncol Biol Phys*, 77(1):226–234.

Capalbo, G., Rodel, C., Stauber, R. H., Knauer, S. K., Bache, M., Kappler, M., and Rodel, F. (2007). The role of survivin for radiation therapy. prognostic and predictive factor and therapeutic target. *Strahlenther Onkol*, 183(11):593–9.

Capalbo, L., Montembault, E., Takeda, T., Bassi, Z. I., Glover, D. M., and D'Avino, P. P. (2012). The chromosomal passenger complex controls the function of endosomal sorting complex required for transport-iii snf7 proteins during cytokinesis. *Open Biol*, 2(5):120070.

Carlton, J. G., Caballe, A., Agromayor, M., Kloc, M., and Martin-Serrano, J. (2012). Escrt-iii governs the aurora b-mediated abscission checkpoint through chmp4c. *Science*, 336(6078):220–225.

Carmena, M., Ruchaud, S., and Earnshaw, W. C. (2009). Making the auroras glow: regulation of aurora a and b kinase function by interacting proteins. *Curr Opin Cell Biol*, 21(6):796–805.

Carmena, M., Wheelock, M., Funabiki, H., and Earnshaw, W. C. (2012). The chromosomal passenger complex (cpc): from easy rider to the godfather of mitosis. *Nature reviews. Molecular cell biology*, 13(12):789–803.

Ceballos-Cancino, G., Espinosa, M., Maldonado, V., and Melendez-Zajgla, J. (2007). Regulation of mitochondrial smac/diablo-selective release by survivin. *Oncogene*, 26(54):7569–7575.

Chantalat, L., Skoufias, D. A., Kleman, J. P., Jung, B., Dideberg, O., and Margolis, R. L. (2000). Crystal structure of human survivin reveals a bow tie-shaped dimer with two unusual alpha-helical extensions. *Molecular cell*, 6(1):183–9.

Cheerambathur, D. K. and Desai, A. (2014). Linked in: formation and regulation of microtubule attachments during chromosome segregation. *Curr Opin Cell Biol*, 26:113–122.

Cheeseman, I. M., Chappie, J. S., Wilson-Kubalek, E. M., and Desai, A. (2006). The conserved kmn network constitutes the core microtubule-binding site of the kinetochore. *Cell*, 127(5):983–997.

Chen, P., Zhu, J., Liu, D.-Y., Li, H.-Y., Xu, N., and Hou, M. (2014). Over-expression of survivin and vegf in small-cell lung cancer may predict the poorer prognosis. *Med Oncol*, 31(1):775.

Chircop, M. (2014). Rho gtpases as regulators of mitosis and cytokinesis in mammalian cells. *Small GTPases*, 5.

Chu, Y., Yao, P. Y., Wang, W., Wang, D., Wang, Z., Zhang, L., Huang, Y., Ke, Y., Ding, X., and Yao, X. (2011). Aurora b kinase activation requires survivin priming phosphorylation by plk1. *J Mol Cell Biol*, 3(4):260–267.

Close, P., Creppe, C., Gillard, M., Ladang, A., Chapelle, J. P., Nguyen, L., and Chariot, A. (2010). The emerging role of lysine acetylation of non-nuclear proteins. *Cell Mol Life Sci*, 67(8):1255–64.

Collette, K. S., Petty, E. L., Golenberg, N., Bembenek, J. N., and Csankovszki, G. (2011). Different roles for aurora b in condensin targeting during mitosis and meiosis. *J Cell Sci*, 124(Pt 21):3684–3694.

Colnaghi, R. and Wheatley, S. P. (2010). Liaisons between survivin and plk1 during cell division and cell death. *J Biol Chem*, 285(29):22592–22604.

Colotta, F., Allavena, P., Sica, A., Garlanda, C., and Mantovani, A. (2009). Cancer-related inflammation, the seventh hallmark of cancer: links to genetic instability. *Carcinogenesis*, 30(7):1073–1081.

Conte, M. S. and Altieri, D. C. (2006). Survivin regulation of vascular injury. *Trends Cardiovasc Med*, 16(4):114–117.

Cosgrave, N., Hill, A. D. K., and Young, L. S. (2006). Growth factor-dependent regulation of survivin by c-myc in human breast cancer. *J Mol Endocrinol*, 37(3):377–390.

Costa, A., Hood, I. V., and Berger, J. M. (2013). Mechanisms for initiating cellular dna replication. *Annu Rev Biochem*, 82:25–54.

Daelemans, D., Costes, S. V., Lockett, S., and Pavlakis, G. N. (2005). Kinetic and molecular analysis of nuclear export factor crm1 association with its cargo in vivo. *Mol Cell Biol*, 25(2):728–739.

Delacour-Larose, M., Thi, M.-N. H., Dimitrov, S., and Molla, A. (2007). Role of survivin phosphorylation by aurora b in mitosis. *Cell Cycle*, 6(15):1878–1885.

DeLuca, J. G., Gall, W. E., Ciferri, C., Cimini, D., Musacchio, A., and Salmon, E. D. (2006). Kinetochore microtubule dynamics and attachment stability are regulated by hec1. *Cell*, 127(5):969–982.

DeNardo, D. G., Andreu, P., and Coussens, L. M. (2010). Interactions between lymphocytes and myeloid cells regulate pro- versus anti-tumor immunity. *Cancer Metastasis Rev*, 29(2):309–316.

Deveraux, Q. L. and Reed, J. C. (1999). Iap family proteins–suppressors of apoptosis. *Genes Dev*, 13(3):239–252.

Ditchfield, C., Johnson, V. L., Tighe, A., Ellston, R., Haworth, C., Johnson, T., Mortlock, A., Keen, N., and Taylor, S. S. (2003). Aurora b couples chromosome alignment with anaphase by targeting bubr1, mad2, and cenp-e to kinetochores. *J Cell Biol*, 161(2):267–280.

Dobrynin, G., Popp, O., Romer, T., Bremer, S., Schmitz, M. H. A., Gerlich, D. W., and Meyer, H. (2011). Cdc48/p97-ufd1-npl4 antagonizes aurora b during chromosome segregation in hela cells. *J Cell Sci*, 124(Pt 9):1571–1580.

Dohi, T., Okada, K., Xia, F., Wilford, C. E., Samuel, T., Welsh, K., Marusawa, H., Zou, H., Armstrong, R., Matsuzawa, S.-i., Salvesen, G. S., Reed, J. C., and Altieri, D. C. (2004). An iap-iap complex inhibits apoptosis. *J Biol Chem*, 279(33):34087–34090.

Dohi, T., Xia, F., and Altieri, D. C. (2007). Compartmentalized phosphorylation of iap by protein kinase a regulates cytoprotection. *Mol Cell*, 27(1):17–28.

Douglas, M. E., Davies, T., Joseph, N., and Mishima, M. (2010). Aurora b and 14-3-3 coordinately regulate clustering of centralspindlin during cytokinesis. *Curr Biol*, 20(10):927–933.

Du, J., Kelly, A. E., Funabiki, H., and Patel, D. J. (2012). Structural basis for recognition of h3t3ph and smac/diablo n-terminal peptides by human survivin. *Structure*, 20(1):185–95.

Dvorak, H. F. (1986). Tumors: wounds that do not heal. similarities between tumor stroma generation and wound healing. *N Engl J Med*, 315(26):1650–1659.

Eckelman, B. P., Salvesen, G. S., and Scott, F. L. (2006). Human inhibitor of apoptosis proteins: why xiap is the black sheep of the family. *EMBO Rep*, 7(10):988–994.

Engels, K., Knauer, S. K., Metzler, D., Simf, C., Struschka, O., Bier, C., Mann, W., Kovacs, A. F., and Stauber, R. H. (2007). Dynamic intracellular survivin in oral squamous cell carcinoma: underlying molecular mechanism and potential as an early prognostic marker. *J Pathol*, 211(5):532–40.

Engelsma, D., Rodriguez, J. A., Fish, A., Giaccone, G., and Fornerod, M. (2007). Homodimerization antagonizes nuclear export of survivin. *Traffic*, 8(11):1495–502.

Federal Statistical Office Germany (2014).

Finlay, C. A., Hinds, P. W., and Levine, A. J. (1989). The p53 proto-oncogene can act as a suppressor of transformation. *Cell*, 57(7):1083–1093.

Foley, E. A. and Kapoor, T. M. (2013). Microtubule attachment and spindle assembly checkpoint signalling at the kinetochore. *Nat Rev Mol Cell Biol*, 14(1):25–37.

Foley, E. A., Maldonado, M., and Kapoor, T. M. (2011). Formation of stable attachments between kinetochores and microtubules depends on the b56-pp2a phosphatase. *Nat Cell Biol*, 13(10):1265–1271.

Fornerod, M., Ohno, M., Yoshida, M., and Mattaj, I. W. (1997). Crm1 is an export receptor for leucine-rich nuclear export signals. *Cell*, 90(6):1051–1060.

Fortugno, P., Beltrami, E., Plescia, J., Fontana, J., Pradhan, D., Marchisio, P. C., Sessa, W. C., and Altieri, D. C. (2003). Regulation of survivin function by hsp90. *Proc Natl Acad Sci U S A*, 100(24):13791–13796.

Frey, S., Richter, R. P., and Görlich, D. (2006). Fg-rich repeats of nuclear pore proteins form a three-dimensional meshwork with hydrogel-like properties. *Science*, 314(5800):815–817.

Fuller, B. G., Lampson, M. A., Foley, E. A., Rosasco-Nitcher, S., Le, K. V., Tobelmann, P., Brautigan, D. L., Stukenberg, P. T., and Kapoor, T. M. (2008). Midzone activation of aurora b in anaphase produces an intracellular phosphorylation gradient. *Nature*, 453(7198):1132–1136.

Fung, H. Y. J. and Chook, Y. M. (2014). Atomic basis of crm1-cargo recognition, release and inhibition. *Semin Cancer Biol*, 27C:52–61.

Gelder, J., Raeymaekers, A., and Roevens, L. (1972). Benzimidazole carbamates. US Patent 3,657,267.

Ghosh, J. C., Dohi, T., Kang, B. H., and Altieri, D. C. (2008). Hsp60 regulation of tumor cell apoptosis. *J Biol Chem*, 283(8):5188–5194.

Glotzer, M. (2009). The 3ms of central spindle assembly: microtubules, motors and maps. *Nat Rev Mol Cell Biol*, 10(1):9–20.

Glover, D. M., Leibowitz, M. H., McLean, D. A., and Parry, H. (1995). Mutations in aurora prevent centrosome separation leading to the formation of monopolar spindles. *Cell*, 81(1):95–105.

Goldfarb, D. S., Gariépy, J., Schoolnik, G., and Kornberg, R. D. (1986). Synthetic peptides as nuclear localization signals. *Nature*, 322(6080):641–644.

Goubran, H. A., Kotb, R. R., Stakiw, J., Emara, M. E., and Burnouf, T. (2014). Regulation of tumor growth and metastasis: the role of tumor microenvironment. *Cancer Growth Metastasis*, 7:9–18.

Grivennikov, S. I., Greten, F. R., and Karin, M. (2010). Immunity, inflammation, and cancer. *Cell*, 140(6):883–899.

Grossman, E., Medalia, O., and Zwerger, M. (2012). Functional architecture of the nuclear pore complex. *Annu Rev Biophys*, 41:557–584.

Güttler, T., Madl, T., Neumann, P., Deichsel, D., Corsini, L., Monecke, T., Ficner, R., Sattler, M., and Görlich, D. (2010). Nes consensus redefined by structures of pki-type and rev-type nuclear export signals bound to crm1. *Nat Struct Mol Biol*, 17(11):1367–1376.

Hamamoto, T., Seto, H., and Beppu, T. (1983). Leptomycins a and b, new antifungal antibiotics. ii. structure elucidation. *J Antibiot (Tokyo)*, 36(6):646–650.

Hanahan, D. and Weinberg, R. A. (2000). The hallmarks of cancer. *Cell*, 100(1):57–70.

Hanahan, D. and Weinberg, R. A. (2011). Hallmarks of cancer: the next generation. *Cell*, 144(5):646–674.

Hirota, T., Lipp, J. J., Toh, B.-H., and Peters, J.-M. (2005). Histone h3 serine 10 phosphorylation by aurora b causes hp1 dissociation from heterochromatin. *Nature*, 438(7071):1176–1180.

Hodel, M. R., Corbett, A. H., and Hodel, A. E. (2001). Dissection of a nuclear localization signal. *J Biol Chem*, 276(2):1317–1325.

Hoebeke, J., Van Nijen, G., and De Brabander, M. (1976). Interaction of oncodazole (r 17934), a new antitumoral drug, with rat brain tubulin. *Biochem Biophys Res Commun*, 69(2):319–324.

Hoffman, W. H., Biade, S., Zilfou, J. T., Chen, J., and Murphy, M. (2002). Transcriptional repression of the anti-apoptotic survivin gene by wild type p53. *J Biol Chem*, 277(5):3247–3257.

Honda, R., Körner, R., and Nigg, E. A. (2003). Exploring the functional interactions between aurora b, incenp, and survivin in mitosis. *Mol Biol Cell*, 14(8):3325–3341.

Hu, M. and Polyak, K. (2008). Microenvironmental regulation of cancer development. *Curr Opin Genet Dev*, 18(1):27–34.

Hümmer, S. and Mayer, T. U. (2009). Cdk1 negatively regulates midzone localization of the mitotic kinesin mklp2 and the chromosomal passenger complex. *Curr Biol*, 19(7):607–612.

Iouk, T., Kerscher, O., Scott, R. J., Basrai, M. A., and Wozniak, R. W. (2002). The yeast nuclear pore complex functionally interacts with components of the spindle assembly checkpoint. *J Cell Biol*, 159(5):807–819.

Jeyaprakash, A. A., Basquin, C., Jayachandran, U., and Conti, E. (2011). Structural basis for the recognition of phosphorylated histone h3 by the survivin subunit of the chromosomal passenger complex. *Structure*, 19(11):1625–34.

Jeyaprakash, A. A., Klein, U. R., Lindner, D., Ebert, J., Nigg, E. A., and Conti, E. (2007). Structure of a survivin-borealin-incenp core complex reveals how chromosomal passengers travel together. *Cell*, 131(2):271–85.

Jiang, Y., Saavedra, H. I., Holloway, M. P., Leone, G., and Altura, R. A. (2004). Aberrant regulation of survivin by the rb/e2f family of proteins. *J Biol Chem*, 279(39):40511–40520.

Kaitna, S., Mendoza, M., Jantsch-Plunger, V., and Glotzer, M. (2000). Incenp and an aurora-like kinase form a complex essential for chromosome segregation and efficient completion of cytokinesis. *Curr Biol*, 10(19):1172–1181.

Kastan, M. B. and Bartek, J. (2004). Cell-cycle checkpoints and cancer. *Nature*, 432(7015):316–323.

Kawajiri, A., Yasui, Y., Goto, H., Tatsuka, M., Takahashi, M., Nagata, K.-I., and Inagaki, M. (2003). Functional significance of the specific sites phosphorylated in desmin at cleavage furrow: Aurora-b may phosphorylate and regulate type iii intermediate filaments during cytokinesis coordinatedly with rho-kinase. *Mol Biol Cell*, 14(4):1489–1500.

Kawashima, S. A., Tsukahara, T., Langegger, M., Hauf, S., Kitajima, T. S., and Watanabe, Y. (2007). Shugoshin enables tension-generating attachment of kinetochores by loading aurora to centromeres. *Genes Dev*, 21(4):420–435.

Kelly, A. E., Ghenoiu, C., Xue, J. Z., Zierhut, C., Kimura, H., and Funabiki, H. (2010). Survivin reads phosphorylated histone h3 threonine 3 to activate the mitotic kinase aurora b. *Science*, 330(6001):235–239.

Kelly, A. E., Sampath, S. C., Maniar, T. A., Woo, E. M., Chait, B. T., and Funabiki, H. (2007). Chromosomal enrichment and activation of the aurora b pathway are coupled to spatially regulate spindle assembly. *Dev Cell*, 12(1):31–43.

Kelly, T. J. and Brown, G. W. (2000). Regulation of chromosome replication. *Annu Rev Biochem*, 69:829–880.

Kim, S. and Yu, H. (2011). Mutual regulation between the spindle checkpoint and apc/c. *Semin Cell Dev Biol*, 22(6):551–558.

Kinzler, K. W. and Vogelstein, B. (1997). Cancer-susceptibility genes. gatekeepers and caretakers. *Nature*, 386(6627):761, 763.

Knauer, S. K., Bier, C., Habtemichael, N., and Stauber, R. H. (2006). The survivin-crm1 interaction is essential for chromosomal passenger complex localization and function. *EMBO Rep*, 7(12):1259–65.

Kolupaeva, V. and Janssens, V. (2013). Pp1 and pp2a phosphatases–cooperating partners in modulating retinoblastoma protein activation. *FEBS J*, 280(2):627–643.

Kudo, N., Matsumori, N., Taoka, H., Fujiwara, D., Schreiner, E. P., Wolff, B., Yoshida, M., and Horinouchi, S. (1999). Leptomycin b inactivates crm1/exportin 1 by covalent modification at a cysteine residue in the central conserved region. *Proc Natl Acad Sci U S A*, 96(16):9112–9117.

Kutay, U. and Güttinger, S. (2005). Leucine-rich nuclear-export signals: born to be weak. *Trends Cell Biol*, 15(3):121–124.

Laemmli, U. K. (1970). Cleavage of structural proteins during the assembly of the head of bacteriophage t4. *Nature*, 227(5259):680–685.

Lampson, M. A. and Cheeseman, I. M. (2011). Sensing centromere tension: Aurora b and the regulation of kinetochore function. *Trends Cell Biol*, 21(3):133–140.

Lan, W., Zhang, X., Kline-Smith, S. L., Rosasco, S. E., Barrett-Wilt, G. A., Shabanowitz, J., Hunt, D. F., Walczak, C. E., and Stukenberg, P. T. (2004). Aurora b phosphorylates centromeric mcak and regulates its localization and microtubule depolymerization activity. *Curr Biol*, 14(4):273–286.

Landskron, G., De la Fuente, M., Thuwajit, P., Thuwajit, C., and Hermoso, M. A. (2014). Chronic inflammation and cytokines in the tumor microenvironment. *J Immunol Res*, 2014:149185.

Lee, S. H., Sterling, H., Burlingame, A., and McCormick, F. (2008). Tpr directly binds to mad1 and mad2 and is important for the mad1-mad2-mediated mitotic spindle checkpoint. *Genes Dev*, 22(21):2926–2931.

Lee, W. H. (1989). The molecular basis of cancer suppression by the retinoblastoma gene. *Princess Takamatsu Symp*, 20:159–170.

Lens, S. M. A., Vader, G., and Medema, R. H. (2006). The case for survivin as mitotic regulator. *Curr Opin Cell Biol*, 18(6):616–622.

Levine, A. J., Finlay, C. A., and Hinds, P. W. (2004). P53 is a tumor suppressor gene. *Cell*, 116(2 Suppl):S67–9, 1 p following S69.

L'Hernault, S. W. and Rosenbaum, J. L. (1985). Chlamydomonas alpha-tubulin is post-translationally modified by acetylation on the epsilon-amino group of a lysine. *Biochemistry*, 24(2):473–478.

Li, A., Xue, Y., Jin, C., Wang, M., and Yao, X. (2006). Prediction of nepsilon-acetylation on internal lysines implemented in bayesian discriminant method. *Biochem Biophys Res Commun*, 350(4):818–824.

Li, F., Ambrosini, G., Chu, E. Y., Plescia, J., Tognin, S., Marchisio, P. C., and Altieri, D. C. (1998). Control of apoptosis and mitotic spindle checkpoint by survivin. *Nature*, 396(6711):580–4.

Lim, R. Y. H., Fahrenkrog, B., Köser, J., Schwarz-Herion, K., Deng, J., and Aebi, U. (2007). Nanomechanical basis of selective gating by the nuclear pore complex. *Science*, 318(5850):640–643.

Lippert, B. M., Knauer, S. K., Fetz, V., Mann, W., and Stauber, R. H. (2007). Dynamic survivin in head and neck cancer: molecular mechanism and therapeutic potential. *Int J Cancer*, 121(6):1169–74.

Liu, R. and Mitchell, D. A. (2010). Survivin as an immunotherapeutic target for adult and pediatric malignant brain tumors. *Cancer Immunol Immunother*, 59(2):183–193.

Liu, X., Song, Z., Huo, Y., Zhang, J., Zhu, T., Wang, J., Zhao, X., Aikhionbare, F., Zhang, J., Duan, H., Wu, J., Dou, Z., Shi, Y., and Yao, X. (2014). Chromatin protein hp1α interacts with the mitotic regulator borealin protein and specifies the centromere localization of the chromosomal passenger complex. *J Biol Chem*, 289(30):20638–20649.

Luo, X. and Yu, H. (2008). Protein metamorphosis: the two-state behavior of mad2. *Structure*, 16(11):1616–1625.

Ma, Q., Wang, X., Li, Z., Li, B., Ma, F., Peng, L., Zhang, Y., Xu, A., and Jiang, B. (2013). microrna-16 represses colorectal cancer cell growth in vitro by regulating the p53/survivin signaling pathway. *Oncol Rep*, 29(4):1652–1658.

Malumbres, M. and Barbacid, M. (2001). To cycle or not to cycle: a critical decision in cancer. *Nat Rev Cancer*, 1(3):222–231.

Marusawa, H., Matsuzawa, S.-I., Welsh, K., Zou, H., Armstrong, R., Tamm, I., and Reed, J. C. (2003). Hbxip functions as a cofactor of survivin in apoptosis suppression. *EMBO J*, 22(11):2729–2740.

Massagué, J. (2004). G1 cell-cycle control and cancer. *Nature*, 432(7015):298–306.

Meadows, J. C., Shepperd, L. A., Vanoosthuyse, V., Lancaster, T. C., Sochaj, A. M., Buttrick, G. J., Hardwick, K. G., and Millar, J. B. A. (2011). Spindle checkpoint silencing requires association of pp1 to both spc7 and kinesin-8 motors. *Dev Cell*, 20(6):739–750.

Mirza, A., McGuirk, M., Hockenberry, T. N., Wu, Q., Ashar, H., Black, S., Wen, S. F., Wang, L., Kirschmeier, P., Bishop, W. R., Nielsen, L. L., Pickett, C. B., and Liu, S. (2002). Human survivin is negatively regulated by wild-type p53 and participates in p53-dependent apoptotic pathway. *Oncogene*, 21(17):2613–2622.

Monecke, T., Güttler, T., Neumann, P., Dickmanns, A., Görlich, D., and Ficner, R. (2009). Crystal structure of the nuclear export receptor crm1 in complex with snurportin1 and rangtp. *Science*, 324(5930):1087–1091.

Moore, J. D. (2013). In the wrong place at the wrong time: does cyclin mislocalization drive oncogenic transformation? *Nat Rev Cancer*, 13(3):201–208.

Mor, A., White, M. A., and Fontoura, B. M. A. (2014). Nuclear trafficking in health and disease. *Curr Opin Cell Biol*, 28:28–35.

Muchmore, S. W., Chen, J., Jakob, C., Zakula, D., Matayoshi, E. D., Wu, W., Zhang, H., Li, F., Ng, S. C., and Altieri, D. C. (2000). Crystal structure and mutagenic analysis of the inhibitor-of-apoptosis protein survivin. *Mol Cell*, 6(1):173–182.

Murray, A. W. (2004). Recycling the cell cycle: cyclins revisited. *Cell*, 116(2):221–234.

Musacchio, A. and Salmon, E. D. (2007). The spindle-assembly checkpoint in space and time. *Nat Rev Mol Cell Biol*, 8(5):379–393.

Nishimura, Y. and Yonemura, S. (2006). Centralspindlin regulates ect2 and rhoa accumulation at the equatorial cortex during cytokinesis. *J Cell Sci*, 119(Pt 1):104–114.

Niu, T.-K., Cheng, Y., Ren, X., and Yang, J.-M. (2010). Interaction of beclin 1 with survivin regulates sensitivity of human glioma cells to trail-induced apoptosis. *FEBS Lett*, 584(16):3519–3524.

O'Connor, D. S., Grossman, D., Plescia, J., Li, F., Zhang, H., Villa, A., Tognin, S., Marchisio, P. C., and Altieri, D. C. (2000a). Regulation of apoptosis at cell division

by p34cdc2 phosphorylation of survivin. *Proc Natl Acad Sci U S A*, 97(24):13103–13107.

O'Connor, D. S., Schechner, J. S., Adida, C., Mesri, M., Rothermel, A. L., Li, F., Nath, A. K., Pober, J. S., and Altieri, D. C. (2000b). Control of apoptosis during angiogenesis by survivin expression in endothelial cells. *Am J Pathol*, 156(2):393–398.

Ono, T., Losada, A., Hirano, M., Myers, M. P., Neuwald, A. F., and Hirano, T. (2003). Differential contributions of condensin i and condensin ii to mitotic chromosome architecture in vertebrate cells. *Cell*, 115(1):109–121.

Pavin, N. and Tolić-Nørrelykke, I. M. (2014). Swinging a sword: how microtubules search for their targets. *Syst Synth Biol*, 8(3):179–186.

Pavlyukov, M. S., Antipova, N. V., Balashova, M. V., Vinogradova, T. V., Kopantzev, E. P., and Shakhparonov, M. I. (2011). Survivin monomer plays an essential role in apoptosis regulation. *J Biol Chem*, 286(26):23296–307.

Peserico, A. and Simone, C. (2011). Physical and functional hat/hdac interplay regulates protein acetylation balance. *J Biomed Biotechnol*, 2011:371832.

Peters, J.-M. (2006). The anaphase promoting complex/cyclosome: a machine designed to destroy. *Nat Rev Mol Cell Biol*, 7(9):644–656.

Petsalaki, E., Akoumianaki, T., Black, E. J., Gillespie, D. A. F., and Zachos, G. (2011). Phosphorylation at serine 331 is required for aurora b activation. *J Cell Biol*, 195(3):449–466.

Powers, A. F., Franck, A. D., Gestaut, D. R., Cooper, J., Gracyzk, B., Wei, R. R., Wordeman, L., Davis, T. N., and Asbury, C. L. (2009). The ndc80 kinetochore complex forms load-bearing attachments to dynamic microtubule tips via biased diffusion. *Cell*, 136(5):865–875.

Prasanth, S. G., Méndez, J., Prasanth, K. V., and Stillman, B. (2004). Dynamics of pre-replication complex proteins during the cell division cycle. *Philos Trans R Soc Lond B Biol Sci*, 359(1441):7–16.

Qian, J., Lesage, B., Beullens, M., Van Eynde, A., and Bollen, M. (2011). Pp1/repoman dephosphorylates mitotic histone h3 at t3 and regulates chromosomal aurora b targeting. *Curr Biol*, 21(9):766–773.

Ramadan, K., Bruderer, R., Spiga, F. M., Popp, O., Baur, T., Gotta, M., and Meyer, H. H. (2007). Cdc48/p97 promotes reformation of the nucleus by extracting the kinase aurora b from chromatin. *Nature*, 450(7173):1258–1262.

Reichert, S., Rödel, C., Mirsch, J., Harter, P. N., Tomicic, M. T., Mittelbronn, M., Kaina, B., and Rödel, F. (2011). Survivin inhibition and dna double-strand break repair: a molecular mechanism to overcome radioresistance in glioblastoma. *Radiother Oncol*, 101(1):51–58.

Riedl, S. J. and Shi, Y. (2004). Molecular mechanisms of caspase regulation during apoptosis. *Nat Rev Mol Cell Biol*, 5(11):897–907.

Riolo, M. T., Cooper, Z. A., Holloway, M. P., Cheng, Y., Bianchi, C., Yakirevich, E., Ma, L., Chin, Y. E., and Altura, R. A. (2012). Histone deacetylase 6 (hdac6) deacetylates survivin for its nuclear export in breast cancer. *The Journal of biological chemistry*, 287(14):10885–93.

Robert Koch Institute and the Association of Population-based Cancer Registries in Germany, editors (2014). *Cancer in Germany 2009/2010*. Berlin, 9th edition.

Rodriguez, J. A., Span, S. W., Ferreira, C. G. M., Kruyt, F. A. E., and Giaccone, G. (2002). Crm1-mediated nuclear export determines the cytoplasmic localization of the antiapoptotic protein survivin. *Exp Cell Res*, 275(1):44–53.

Roux, K. J. and Burke, B. (2006). From pore to kinetochore and back: regulating envelope assembly. *Dev Cell*, 11(3):276–278.

Ruchaud, S., Carmena, M., and Earnshaw, W. C. (2007). Chromosomal passengers: conducting cell division. *Nat Rev Mol Cell Biol*, 8(10):798–812.

Sadoul, K., Wang, J., Diagouraga, B., and Khochbin, S. (2011). The tale of protein lysine acetylation in the cytoplasm. *J Biomed Biotechnol*, 2011:970382.

Sanger, F. and Coulson, A. R. (1975). A rapid method for determining sequences in dna by primed synthesis with dna polymerase. *J Mol Biol*, 94(3):441–448.

Saurin, A. T., van der Waal, M. S., Medema, R. H., Lens, S. M. A., and Kops, G. J. P. L. (2011). Aurora b potentiates mps1 activation to ensure rapid checkpoint establishment at the onset of mitosis. *Nat Commun*, 2:316.

Scholey, J. M., Brust-Mascher, I., and Mogilner, A. (2003). Cell division. *Nature*, 422(6933):746–752.

Schooley, A., Vollmer, B., and Antonin, W. (2012). Building a nuclear envelope at the end of mitosis: coordinating membrane reorganization, nuclear pore complex assembly, and chromatin de-condensation. *Chromosoma*, 121(6):539–554.

Sears, R. C. and Nevins, J. R. (2002). Signaling networks that link cell proliferation and cell fate. *J Biol Chem*, 277(14):11617–11620.

Sessa, F., Mapelli, M., Ciferri, C., Tarricone, C., Areces, L. B., Schneider, T. R., Stukenberg, P. T., and Musacchio, A. (2005). Mechanism of aurora b activation by incenp and inhibition by hesperadin. *Mol Cell*, 18(3):379–391.

Shin, S., Sung, B. J., Cho, Y. S., Kim, H. J., Ha, N. C., Hwang, J. I., Chung, C. W., Jung, Y. K., and Oh, B. H. (2001). An anti-apoptotic protein human survivin is a direct inhibitor of caspase-3 and -7. *Biochemistry*, 40(4):1117–1123.

Smallwood, A., Estève, P.-O., Pradhan, S., and Carey, M. (2007). Functional cooperation between hp1 and dnmt1 mediates gene silencing. *Genes Dev*, 21(10):1169–1178.

Song, Z., Liu, S., He, H., Hoti, N., Wang, Y., Feng, S., and Wu, M. (2004). A single amino acid change (asp 53 –> ala53) converts survivin from anti-apoptotic to pro-apoptotic. *Molecular biology of the cell*, 15(3):1287–96.

Song, Z., Yao, X., and Wu, M. (2003). Direct interaction between survivin and smac/diablo is essential for the anti-apoptotic activity of survivin during taxol-induced apoptosis. *J Biol Chem*, 278(25):23130–23140.

Srinivasula, S. M. and Ashwell, J. D. (2008). Iaps: what's in a name? *Mol Cell*, 30(2):123–135.

Steigemann, P., Wurzenberger, C., Schmitz, M. H. A., Held, M., Guizetti, J., Maar, S., and Gerlich, D. W. (2009). Aurora b-mediated abscission checkpoint protects against tetraploidization. *Cell*, 136(3):473–484.

Stevaux, O. and Dyson, N. J. (2002). A revised picture of the e2f transcriptional network and rb function. *Curr Opin Cell Biol*, 14(6):684–691.

Strambio-De-Castillia, C., Niepel, M., and Rout, M. P. (2010). The nuclear pore complex: bridging nuclear transport and gene regulation. *Nat Rev Mol Cell Biol*, 11(7):490–501.

Tajiri, T., Tanaka, S., Shono, K., Kinoshita, Y., Fujii, Y., Suita, S., Ihara, K., and Hara, T. (2001). Quick quantitative analysis of gene dosages associated with prognosis in neuroblastoma. *Cancer Lett*, 166(1):89–94.

Tamm, I., Wang, Y., Sausville, E., Scudiero, D. A., Vigna, N., Oltersdorf, T., and Reed, J. C. (1998). Iap-family protein survivin inhibits caspase activity and apoptosis induced by fas (cd95), bax, caspases, and anticancer drugs. *Cancer Res*, 58(23):5315–5320.

Touré, A., Mzali, R., Liot, C., Seguin, L., Morin, L., Crouin, C., Chen-Yang, I., Tsay, Y.-G., Dorseuil, O., Gacon, G., and Bertoglio, J. (2008). Phosphoregulation of mgcracgap in mitosis involves aurora b and cdk1 protein kinases and the pp2a phosphatase. *FEBS Lett*, 582(8):1182–1188.

Tran, E. J., King, M. C., and Corbett, A. H. (2014). Macromolecular transport between the nucleus and the cytoplasm: Advances in mechanism and emerging links to disease. *Biochim Biophys Acta*, 1843(11):2784–2795.

Tran, J., Master, Z., Yu, J. L., Rak, J., Dumont, D. J., and Kerbel, R. S. (2002). A role for survivin in chemoresistance of endothelial cells mediated by vegf. *Proc Natl Acad Sci U S A*, 99(7):4349–4354.

Tsuji, N., Kobayashi, M., Nagashima, K., Wakisaka, Y., and Koizumi, K. (1976). A new antifungal antibiotic, trichostatin. *J Antibiot (Tokyo)*, 29(1):1–6.

Turner, J. G., Dawson, J., and Sullivan, D. M. (2012). Nuclear export of proteins and drug resistance in cancer. *Biochem Pharmacol*, 83(8):1021–1032.

Verdecia, M. A., Huang, H., Dutil, E., Kaiser, D. A., Hunter, T., and Noel, J. P. (2000). Structure of the human anti-apoptotic protein survivin reveals a dimeric arrangement. *Nature structural biology*, 7(7):602–8.

Vigneron, S., Prieto, S., Bernis, C., Labbé, J.-C., Castro, A., and Lorca, T. (2004). Kinetochore localization of spindle checkpoint proteins: who controls whom? *Mol Biol Cell*, 15(10):4584–4596.

Vong, Q. P., Cao, K., Li, H. Y., Iglesias, P. A., and Zheng, Y. (2005). Chromosome alignment and segregation regulated by ubiquitination of survivin. *Science*, 310(5753):1499–504.

Wang, F., Dai, J., Daum, J. R., Niedzialkowska, E., Banerjee, B., Stukenberg, P. T., Gorbsky, G. J., and Higgins, J. M. G. (2010a). Histone h3 thr-3 phosphorylation by haspin positions aurora b at centromeres in mitosis. *Science*, 330(6001):231–235.

Wang, H., Holloway, M. P., Ma, L., Cooper, Z. A., Riolo, M., Samkari, A., Elenitoba-Johnson, K. S., Chin, Y. E., and Altura, R. A. (2010b). Acetylation directs survivin nuclear localization to repress stat3 oncogenic activity. *J Biol Chem*, 285(46):36129–37.

Wang, L., Du, Y., Lu, M., and Li, T. (2012). Aseb: a web server for kat-specific acetylation site prediction. *Nucleic Acids Res*, 40(Web Server issue):W376–W379.

Wang, Q., Chen, Z., Diao, X., and Huang, S. (2011). Induction of autophagy-dependent apoptosis by the survivin suppressant ym155 in prostate cancer cells. *Cancer Lett*, 302(1):29–36.

Weinberg, R. (2013). *The biology of cancer*. Garland Science.

Welburn, J. P. I., Vleugel, M., Liu, D., Yates, 3rd, J. R., Lampson, M. A., Fukagawa, T., and Cheeseman, I. M. (2010). Aurora b phosphorylates spatially distinct targets to differentially regulate the kinetochore-microtubule interface. *Mol Cell*, 38(3):383–392.

Wente, S. R. and Rout, M. P. (2010). The nuclear pore complex and nuclear transport. *Cold Spring Harb Perspect Biol*, 2(10):a000562.

Wheatley, S. P., Barrett, R. M., Andrews, P. D., Medema, R. H., Morley, S. J., Swedlow, J. R., and Lens, S. M. A. (2007). Phosphorylation by aurora-b negatively regulates survivin function during mitosis. *Cell Cycle*, 6(10):1220–1230.

Wheatley, S. P., Henzing, A. J., Dodson, H., Khaled, W., and Earnshaw, W. C. (2004). Aurora-b phosphorylation in vitro identifies a residue of survivin that is essential for its localization and binding to inner centromere protein (incenp) in vivo. *J Biol Chem*, 279(7):5655–5660.

Winey, M. (1999). Cell cycle: driving the centrosome cycle. *Curr Biol*, 9(12):R449–R452.

Xu, C., Yamamoto-Ibusuki, M., Yamamoto, Y., Yamamoto, S., Fujiwara, S., Murakami, K., Okumura, Y., Yamaguchi, L., Fujiki, Y., and Iwase, H. (2014). High survivin mrna expression is a predictor of poor prognosis in breast cancer: a comparative study at the mrna and protein level. *Breast Cancer*, 21(4):482–490.

Xu, D., Farmer, A., Collett, G., Grishin, N. V., and Chook, Y. M. (2012). Sequence and structural analyses of nuclear export signals in the nesdb database. *Mol Biol Cell*, 23(18):3677–3693.

Xu, Y., Fang, F., Ludewig, G., Jones, G., and Jones, D. (2004). A mutation found in the promoter region of the human survivin gene is correlated to overexpression of survivin in cancer cells. *DNA Cell Biol*, 23(9):527–537.

Yamagishi, Y., Honda, T., Tanno, Y., and Watanabe, Y. (2010). Two histone marks establish the inner centromere and chromosome bi-orientation. *Science*, 330(6001):239–243.

Yang, X. J. and Seto, E. (2008). Lysine acetylation: codified crosstalk with other post-translational modifications. *Mol Cell*, 31(4):449–61.

Yoneda, Y. (2000). Nucleocytoplasmic protein traffic and its significance to cell function. *Genes Cells*, 5(10):777–787.

Yoshida, M., Kijima, M., Akita, M., and Beppu, T. (1990). Potent and specific inhibition of mammalian histone deacetylase both in vivo and in vitro by trichostatin a. *J Biol Chem*, 265(28):17174–17179.

Zeng, W., Ball, Jr, A. R., and Yokomori, K. (2010). Hp1: heterochromatin binding proteins working the genome. *Epigenetics*, 5(4):287–292.

Zhao, J., Tenev, T., Martins, L. M., Downward, J., and Lemoine, N. R. (2000). The ubiquitin-proteasome pathway regulates survivin degradation in a cell cycle-dependent manner. *J Cell Sci*, 113 Pt 23:4363–4371.

Zou, H. (2011). The sister bonding of duplicated chromosomes. *Semin Cell Dev Biol*, 22(6):566–571.

APPENDIX

Vector maps

The following figures depict the position of the Survivin cDNA in the pc3 or pET41-GST-PreSc expression vectors.

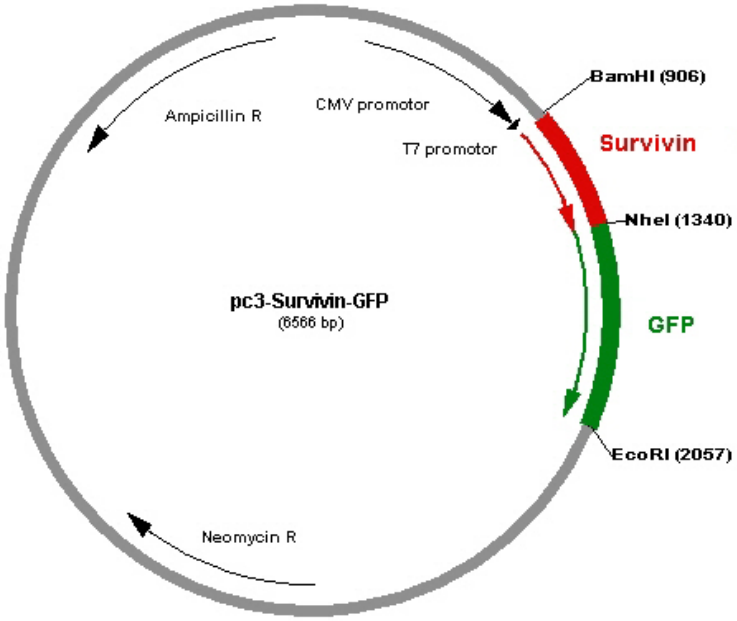

Figure A.1: pc3-Survivin-GFP.

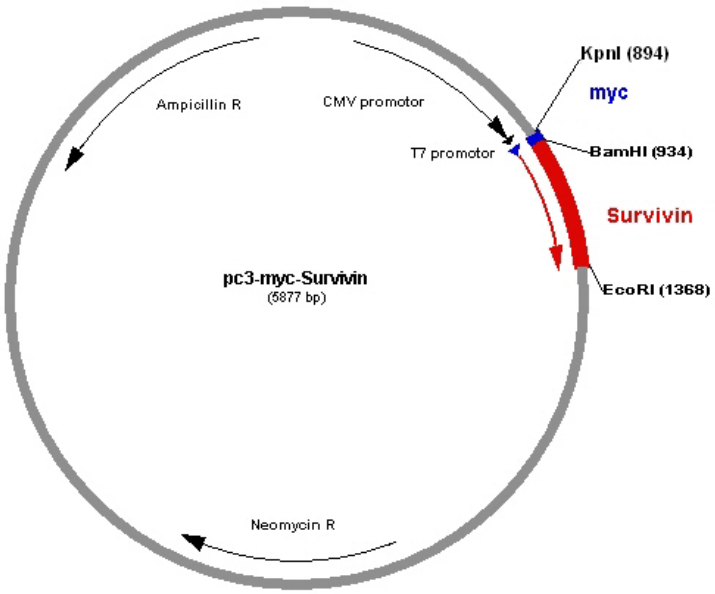

Figure A.2: pc3-myc-Survivin.

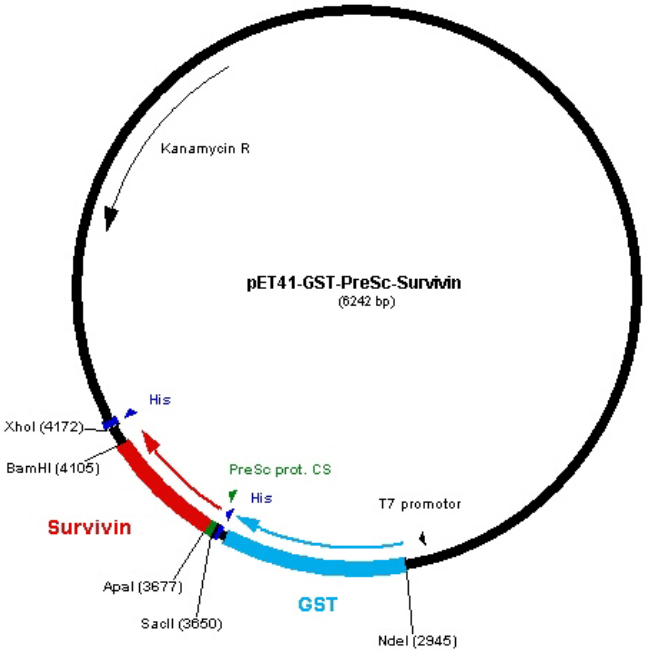

Figure A.3: pET41-GST-PreSc-Survivin.

Acknowledgment

First of all, I would like to thank my supervisor Prof. Shirley Knauer for giving me the opportunity to work on the exciting topic of post-translational Survivin regulation. I appreciate your scientific advice as well as your personal support, and I am grateful for your comments on the thesis manuscript.

I also thank all the former and present “Shirley’s girlies” and Rouven (the members of the Knauer group) for the stimulating scientific discussions, and especially for the great working atmosphere and all the fun we had together in the lab and outside.

Special thanks go to Leonel, Karolin and Cecilia who supported me a lot in the laboratory. I would also like to thank Rouven, the only guy in our lab, who sometimes really had to suffer, but nevertheless, always created a good atmosphere due to his great sense of humor. Elisabeth also deserves special mention as she has been a helpful, reliable and very entertaining colleague who has become a real friend. You are the best concert mate one could wish for.

Thanks to all the people from the Meyer and Bayer groups who provided scientific input as well as technical assistance.

I am especially grateful to my parents who supported me in every possible way.

Last, but not least, I would like to thank my fiancé for his enduring motivation, positive thinking and his endless support. I am grateful our paths have crossed.

Publications, talks and poster presentations

Publications

Feb 2013	Knauer SK, **Unruhe B**, Karczewski S, Hecht R, Fetz V, Bier C, Friedl S, Wollenberg B, Pries R, Habtemichael N, Heinrich UR, Stauber RH (2013). Functional characterization of novel mutations affecting survivin (BIRC5)-mediated therapy resistance in head and neck cancer patients. *Hum Mutat*, 34(2):395-404.
Jan 2012	Stauber RH, Knauer SK, Habtemichael N, Bier C, **Unruhe B**, Weisheit S, Spange S, Nonnenmacher F, Fetz V, Ginter T, Reichardt S, Liebmann C, Schneider G, Krämer OH (2012). A combination of a ribonucleotide reductase inhibitor and histone deacetylase inhibitors downregulates EGFR and triggers BIM-dependent apoptosis in head and neck cancer. *Oncotarget*, 3(1):31-43.
Dec 2010	Habtemichael N, Wünsch D, Bier C, Tillmann S, **Unruhe B**, Frauenknecht K, Heinrich UR, Mann WJ, Stauber RH, Knauer SK (2010). Cloning and functional characterization of the guinea pig apoptosis inhibitor protein Survivin. *Gene*, 469(1-2):9-17.

Talks

Jun 2012	**Unruhe B**, Habtemichael N, Bier C, Fetz V, Krämer OH, Stauber RH, Knauer SK (2012). Drug-induced head and neck cancer cell killing by downregulating EGFR and triggering BIM-induced apoptosis. CESAR Annual Meeting 2012, Essen.

Posters

Nov 2012	**Unruhe B**, Knauer SK (2012). Regulation of the function and localization of Survivin by acetylation. BIOME Annual Retreat 2012, Tumour and Signalling, Hamminkeln.

Curriculum vitae

For reasons of data protection, the curriculum vitae is not included in the online version.

Erklärungen

Erklärung:

Hiermit erkläre ich, gem. § 7 Abs. (2) d) + f) der Promotionsordnung der Fakultät für Biologie zur Erlangung des Dr. rer. nat., dass ich die vorliegende Dissertation selbstständig verfasst und mich keiner anderen als der angegebenen Hilfsmittel bedient, bei der Abfassung der Dissertation nur die angegeben Hilfsmittel benutzt und alle wörtlich oder inhaltlich übernommenen Stellen als solche gekennzeichnet habe.

Essen, den

Britta Unruhe

Erklärung:

Hiermit erkläre ich, gem. § 7 Abs. (2) e) + g) der Promotionsordnung der Fakultät für Biologie zur Erlangung des Dr. rer. nat., dass ich keine anderen Promotionen bzw. Promotionsversuche in der Vergangenheit durchgeführt habe und dass diese Arbeit von keiner anderen Fakultät/Fachbereich abgelehnt worden ist.

Essen, den

Britta Unruhe

Erklärung:

Hiermit erkläre ich, gem. § 6 Abs. (2) g) der Promotionsordnung der Fakultät für Biologie zur Erlangung der Dr. rer. nat., dass ich das Arbeitsgebiet, dem das Thema “Relevance of Survivin acetylation for its biological function” zuzuordnen ist, in Forschung und Lehre vertrete und den Antrag von Britta Unruhe befürworte und die Betreuung auch im Falle eines Weggangs, wenn nicht wichtige Gründe dem entgegenstehen, weiterführen werde.

Essen, den

Prof. Dr. Shirley Knauer